



U.S. DEPARTMENT OF
ENERGY

PNNL- 19229

Prepared for the U.S. Department of Energy
under Contract DE-AC05-76RL01830

Analysis Methodology for Balancing Authority Cooperation in High Penetration of Variable Generation

FINAL REPORT

YV Makarov	R Diao
PV Etingov	S Malhara
N Zhou	RT Guttromson
J Ma	P Du
NA. Samaan	C Sastry

February 2010



Pacific Northwest
NATIONAL LABORATORY

*Proudly Operated by **Battelle** Since 1965*

DISCLAIMER

This report was prepared as an account of work sponsored by an agency of the United States Government. Neither the United States Government nor any agency thereof, nor Battelle Memorial Institute, nor any of their employees, makes **any warranty, express or implied, or assumes any legal liability or responsibility for the accuracy, completeness, or usefulness of any information, apparatus, product, or process disclosed, or represents that its use would not infringe privately owned rights.** Reference herein to any specific commercial product, process, or service by trade name, trademark, manufacturer, or otherwise does not necessarily constitute or imply its endorsement, recommendation, or favoring by the United States Government or any agency thereof, or Battelle Memorial Institute. The views and opinions of authors expressed herein do not necessarily state or reflect those of the United States Government or any agency thereof.

PACIFIC NORTHWEST NATIONAL LABORATORY

operated by

BATTELLE

for the

UNITED STATES DEPARTMENT OF ENERGY

under Contract DE-AC05-76RL01830

Printed in the United States of America

Available to DOE and DOE contractors from the
Office of Scientific and Technical Information,

P.O. Box 62, Oak Ridge, TN 37831-0062;

ph: (865) 576-8401

fax: (865) 576-5728

email: reports@adonis.osti.gov

Available to the public from the National Technical Information Service,
U.S. Department of Commerce, 5285 Port Royal Rd., Springfield, VA 22161

ph: (800) 553-6847

fax: (703) 605-6900

email: orders@ntis.fedworld.gov

online ordering: <http://www.ntis.gov/ordering.htm>



This document was printed on recycled paper.

(9/2003)

Analysis Methodology for Balancing Authority Cooperation in High Penetration of Variable Generation

FINAL REPORT

YV Makarov¹ R Diao²
PV Etingov³ S Malhara⁴
N. Zhou⁵ RT Guttromson⁶
J Ma⁷ P Du⁸
NA Samaan⁹ C Sastry¹⁰

Subcontractors:

Prof. Gerald Heydt, Arizona State University
Prof. Vijay Vittal, Arizona State University

February 2010

Prepared for
U.S. Department of Energy (DOE)
Under Contract DE-AC05-76RL01830

Pacific Northwest National Laboratory
Richland, Washington 99352

¹ Principal Investigator, Chief Scientist – Power Systems

² Research Engineer

³ Project Lead, Senior Research Engineer

⁴ Research Engineer

⁵ Project Manager, Senior Research Engineer

⁶ Program Manager, Renewables Integration

⁷ Research Engineer

⁸ Research Engineer

⁹ Senior Research Engineer

¹⁰ Senior Engineer

Abstract

The work described in this report was performed by Pacific Northwest National Laboratory (PNNL) and funded by the Office of the Energy Efficiency and Renewable Energy, U.S. Department of Energy (EERE DOE). This project is a joint project with National Renewable Energy Laboratory (NREL).

With the rapidly growing penetration level of wind and solar generation, the challenges of managing variability and the uncertainty of intermittent renewable generation become more and more significant. The problem of power variability and uncertainty gets exacerbated when each balancing authority (BA) works locally and separately to balance its own subsystem. The virtual BA concept is based on various forms of collaboration between individual BAs to manage power variability and uncertainty. The virtual BA will have a wide area control capability in managing its operational balancing requirements in different time frames. This coordination results in the improvement of efficiency and reliability of power system operation while facilitating the high level integration of green, intermittent energy resources.

Several strategies for virtual BA implementation, such as Area Control Error (ACE) diversity interchange (ADI), wind only BA, BA consolidation, dynamic scheduling, regulation and load following sharing, extreme event impact study are discussed in this report. The objective of such strategies is to allow individual BAs within a large power grid to help each other deal with power variability. Innovative methods have been developed to simulate the balancing operation of BAs. These methods evaluate the BA operation through a number of metrics — such as capacity, ramp rate, ramp duration, energy and cycling requirements — to evaluate the performance of different virtual BA strategies.

The report describes a systematic framework for evaluating BA consolidation and coordination. Results for case studies show that significant economic and reliability benefits can be gained. The merits and limitation of each virtual BA strategy are investigated. The report provides guidelines for the power industry to evaluate the coordination or consolidation method. Several related projects are underway to work with regional BAs to evaluate the strategies defined in this report.

Executive Summary

The work described in this report was performed by the Pacific Northwest National Laboratory (PNNL) and funded by the Office of the Energy Efficiency and Renewable Energy, U.S. Department of Energy (EERE DOE). This project is conducted jointly with the National Renewable Energy Laboratory (NREL).

Renewable variable generation (VG) will penetrate the power grid at a high level, as required by different state's Renewable Portfolio Standards (RPS). Twenty four states' RPSs establish the goal of reaching 10-40% of renewable energy integrated into the grid by 2015-2030. The DOE has modeled an energy scenario in which wind would provide 20% of U.S. electricity by 2030. Because of the variability and uncertainty of wind and solar generation, the high penetration of renewable generation makes it more difficult for balancing authorities (BAs) to maintain balance between their load, interchange and generation. Operating separately and locally, individual BAs would have to purchase more expensive balancing reserves to accommodate the variability and uncertainty from high penetration of VG in the future. Cooperation and consolidation between BA's has been identified as one of the most important strategies to facilitate high-level VG penetration while limiting requirement for generation reserves.

Consolidation of BA processes already takes place in the industry. For example, an actual consolidation of 26 BAs in the Midwest Independent System Operator (ISO) area into a single BA took place on January 6, 2009. In 2006-2007, four BAs¹ formed a new cooperation by combining their area control error (ACE) in the Pacific Northwest. Later, the ACE diversity initiative (ADI) was extended over a larger geographical region in the Western interconnection, by including 8 more BAs². Similar processes take place elsewhere in the world. In 2005, two Danish transmission system operators³ (TSOs) merged forming a consolidated TSO called Energinet.dk. All wind power production and its deviations in Germany are combined virtually, and then distributed to each of four transmission system operators⁴.

To support these processes there is a need to develop a systematic and comprehensive framework in order to evaluate the benefits and problems with current BA cooperation approaches. This report describes such a framework and a set of essential tools which can be used to quantify the benefits and limitations of different BA cooperation/consolidation approaches.

The goal of this work is to equip industry with tools and methodologies helping to select the most appropriate BA cooperation methods and, by doing so, to facilitate high penetration of VG required by RPSs without creating control performance, or reliability problems. To demonstrate the performance and the usefulness of the tools and methodologies proposed in this work, they have been applied to real system analyses, including the ones conducted for industry.

The project directly supports the EERE's mission of "Bringing clean, reliable and affordable energy technologies to the marketplace." The project helps to achieve the national goal of having 20% of our energy supply from renewable resources and possibly to exceed that goal by reaching a target of 33%.

¹ British Columbia Transmission Corporation, Idaho Power, PacifiCorp East, PacifiCorp West and Northwest Energy.

² Arizona Public Service, Nevada Power/Sierra Pacific Power, Public Service Company of New Mexico, Salt River Project, Seattle City Light, Bonneville Power Administration (BPA), Public Service Colorado/Excel Energy and Glacier Wind Farm (Naturener).

³ Eltra and Elkraft.

⁴ Amprion GmbH, 50Hetz Transmission Europe GmbH, Transpower Stromuebertragungs GmbH and EnBW Transportnetze AG.

Challenges Facing Individual Balancing Authorities at High VG Penetration Levels

In an electric power grid generation and load must remain balanced all the time. Significant imbalances could result in significant interconnection frequency deviations, transmission system violations, stability problems and so on. Ultimately, those problems could cause widespread system blackouts. The load varies with time and is in large extent not controllable. Generation must be dispatched to follow the load variation to ensure an adequate balance of supply and demand. To accommodate the variability and uncertainty of the load, some generation must be reserved for reliable grid operation.

High penetration of VG increases the challenges of maintaining power system balance. VGs are not dispatchable resources in the traditional manner. Wind power can only be produced when the wind blows. Likewise, solar power can only be produced when the sun shines. Wind and solar generators usually supply “must take” energy for BAs, which have little to no control over their power output. Quite often the power generation from these resources is treated as negative load, so that the remaining generators are committed and dispatched to balance against so called “net load,” which is the difference between the BA’s load, interchange and the variable generation. Renewable power resources increase the power variability and uncertainty which has to be balanced. Specific problems with system reliability and control performance, which may occur because of the increasing VG, include increasing risk of system imbalances potentially harming BA control performance, over-generation, fast unpredicted ramps, unpredicted transmission overloads and loop flows, voltage deviations, decreasing system frequency response and inertia, stability issues, adverse impact on conventional generators (including increasing cycling, wear-and-tear and emissions and decreasing efficiency), and others.

Challenges of maintaining the load-generation balance become more significant when an interconnected power grid is operated locally and separately by each individual BA. In North America, power grids are divided into many balancing areas to allow autonomy in operation. For example, the U.S. Western Interconnection is a large integrated and interconnected power system. Organizationally, it is divided into 37 BAs. Within each BA, operators are responsible for maintaining the balance between load and generation within their territory, as well as for following interchange schedules between BAs. Metrics (e.g., area control errors and control performance standards) are used to evaluate the performance of each BA in maintaining the balance. BAs that do not meet the balancing requirements could jeopardize system reliability and are thus penalized financially. It has been proven that the impact of intermittency and uncertainty caused by VGs becomes relatively smaller if these resources are lumped together over a large geographical area and if they are more dispersed over a territory. The existing BA structure is limiting the potential of wide-area integration of VGs because the BAs have to deal with their own local variable generation individually. In addition, each BA must maintain balance with its own, sometimes limited resources. A BA with limited balancing reserves and high wind and solar power penetration will face significant problems. To maintain the balance, it frequently may have to resort to more expensive resources. Sometimes, it may even run out of resources to maintain balance. Associated economic and reliability concerns may create hurdles to high level penetration of VG under the existing BA structure and operational practices.

Some additional problems associated with the operation of individual BAs are:

- Control area operators do not have a broad view of the system.
- Individual BAs do not have the authority or mechanisms to achieve maximum efficiency on a system-wide basis.

- Independent decisions by individual BAs may generate negative impacts on other control areas.
- Transmission system flexibility becomes increasingly insufficient to accommodate all variability of power transfers.
- There is an increasing difficulty managing unscheduled flows on the transmission system, leading to reliability risks.

Motivations for BA Cooperation

More VG can be integrated into the current power grid through the cooperation of BAs. BA cooperation is, perhaps, the least expensive option among the other possible solutions helping to achieve the RPS objectives. A recent General Electric Energy (GE) study, conducted for NREL, states explicitly that to integrate 35% of wind and solar resources in the area served by the WestConnect group of utilities and 25% of these resources in the rest of the WECC system, BA cooperation and consolidation is required among the other measures. When BAs cooperate with each other in one form or another, the total variability will be less due to the geographical diversity. Wind and solar generation as well as the associated forecasts errors are generally not strongly correlated with each other over a wide geographic area. Thus, the combined large-area power variation is smaller than the sum of variations for individual BAs. Such variability reduction can be shared among the participating BAs. Problems with balancing the system can be also mitigated through BA collaboration. The balancing generation resources in participating areas can be shared and more effectively used to manage power variations through coordination. Working together, BAs can balance reduced power variance with shared resources. This approach benefits power system operation from both economic and reliability perspectives. In addition, with the rapid development of information technology in the power industry, cooperation among individual BAs is becoming more viable.

Benefits from BA Cooperation

Numerous benefits from the cooperation of individual BAs can be identified and evaluated:

- Reducing regulation requirements in terms of its required upward and downward reserved capacity, actual use (energy), reduced impact on the regulation units (wear and tear, efficiency) and cost.
- Reducing load following requirements in terms of its required upward and downward capacity, actual use (energy)
- Reducing ramping requirements. Fast and continuous ramps, especially unexpected, create problems for grid operators. The ramping capability of the most thermal generators is limited, so to follow fast ramps, more generators need to be used, which means more online capacity.
- Improving BA performance (Control performance standard (CPS1/2) indices).

The benefits of BA cooperation and consolidation increase when renewable generation penetration increases.

Major BA Cooperation Strategies

Balancing authorities have been developing various measures to mitigate VG integration problems including improved day-ahead, hour-ahead and real-time wind and solar forecasting systems (and wind ramp forecasting systems); incorporating these forecasts into power markets, scheduling and real time processes; increasing operating reserve requirements; grid codes requiring at least partial dispatchability

from wind generators; additional energy storage; demand response programs; new regional markets for the intra-hour balancing services; coordinated wide-area real-time; congestion management; building special control centers for wind; transmission system enhancements; adding more flexible generation to the system; increasing operating reserves (especially, intra-hour balancing reserves); dynamic scheduling and pseudo-tie options to deliver more ancillary services from the neighboring BAs; and other measures. Many of these methods are expensive options. BA cooperation and consolidation options are, perhaps, among the least expensive measures to mitigate the impacts of wind and solar power variability, poor predictability and uncertainty.

BA cooperation can be implemented using different strategies. Each strategy has its own advantages and disadvantages. There is a minimum set of requirements that needs to be adopted by BAs to have successful cooperation. The objective of such strategies is to reduce the overall variability and uncertainty of the net load so that individual BAs within a large power grid can accommodate more VG without a significant increase of generation reserves. The major cooperation strategies are briefly described below (a more comprehensive list is provided and discussed in the report's body):

BA Consolidation

The consolidation of individual BAs is the integration of two or more BAs into a single consolidated balancing authority (CBA). There are multiple ways and cooperation levels that can be used to consolidate BAs, e.g., full actual consolidation and virtual or partial consolidation.

The full actual consolidation implies the actual merging of BAs into a single CBA. Under this option, the former BAs stop scheduling their individual interchanges except for the one between the common CBA and the rest of interconnection, they introduce common unit commitment and dispatch procedures, procure common operating reserves, common automatic generation control (AGC), and so on. The full actual consolidation helps to maximally exploit the benefits of consolidation.

The virtual or partial consolidation option generally implies that the existing BAs and their certain functions are preserved in the consolidated BA and remain separated from the corresponding other BAs functions. For instance, participating BAs may select to schedule and dispatch their own generators and provide intra-day and intra-hour balancing functions individually, based on sharing certain reduced collective CBA requirements. For the partial consolidation option, it is important to underline which features of the consolidated BA are important to fully exploit potential benefits of consolidated operation..

Area Control Error (ACE) Diversity Interchange (ADI)

The laws of physics requires the balance between load and generation to be achieved at the whole power grid level (unless it causes transmission system violations). But the reality is that, working separately, each BA needs to achieve local balance within its territory. Area control error is used to check how well a BA balances its generation against the native net load and interchange schedule. Automatic generation control systems are used to adjust special generation resources to achieve balance on a minute-to-minute basis. There are times when a BA instructs its AGC-connected generators to produce more power than the original schedule, while another BA in the same grid instructs its AGC-connected generators reduce their output.. When the excessive power generated in one BA is equal to the excessive power consumed in another BA, the whole power grid is well balanced. But, if there is no cooperation between BAs, each BA still has to adjust its regulation generation to achieve local balance.

Regulation reserve is an expensive resource. The main idea of ADI is to let all participating BAs pool excessive generation and consumption together to net out some collective adjustment requirement. The

goal is to reduce the regulation required to balance the system. Relaxed control can be achieved because of the ACE diversity.

Wind-only BA

Unlike a traditional BA — which includes generating units and load — wind-only BA includes only variable generation (VG) resources. Wind-only BAs do not have to stay in one concentrated location. VGs, which are distributed over a larger geographical region, can still be put together to form a wind-only BA in order to benefit from the geographical diversity factor. The wind-only BA is responsible for controlling the interchange of its control area with the other BAs following a pre-determined interchange schedule. BAs' control performance is mandated by North American Electric Reliability Corporation (NERC) and Western Electricity Coordinating Council (WECC) Control Performance Standards. Generators participating in the wind-only BA will be required to provide their own balancing reserves or purchase those services from external resources.

Dynamic Scheduling

Through telemetry, dynamic scheduling is a service which allows load or generation to be virtually transferred from one BA to another BA. Dynamic scheduling allows the receiving BA to control the generation or load in the sending BA as if the generation or load was physically located in that BA. Dynamic scheduling could be used to bring more external renewable resources into a control area to meet the RPS requirements while exploiting the geographic diversity factor. On the other hand, dynamic schedules can be used to incorporate external balancing resources helping to deal with VG variability.

Methodologies to Evaluate BA Cooperation

Currently, there is no systematic way to evaluate the benefits and problems with different BA cooperation approaches. It is hard for industry to determine which approach is better for their specific situations. This report introduces new methodologies to evaluate BA cooperation approaches. The methodologies include:

- Two sets of metrics to quantify the benefits of BA collaboration. Each set of metrics is defined by a performance envelope.
 - The first performance envelope represents BA balancing operations, hence it includes capacity, ramp rate, ramp duration, and energy requirements for regulation, load following and scheduling.
 - The second performance envelope represents the cycling of generating and storage units within the BA to perform the needed balancing operations. It reflects the nature of using such units to meet the variation of load and the output of intermittent generation resources.
- A methodology for building an incremental power flow model has been developed. It has been used to evaluate the impact of various wide area wind integration options. It is also used in investigating transmission congestions that can limit BA cooperation. The method has been implemented and validated with WECC models.
- A method has been developed for evaluating the power system security region has been applied to quantify the transmission system congestion with better accuracy. That results in improving the usage of transmission system and minimizing the congestion cost under different wide area wind integration options.
- Several strategies for BAs collaboration have been investigated such as ACE diversity interchange, wind only BA, BA consolidation, dynamic scheduling, and regulation and load following sharing.

- Two methods to optimize the advanced ACE diversity interchange have been developed. These methods show improved performance compared with the current ADI method used in the western interconnection.
- An analytical method has been developed to assess the benefits of the consolidation of individual BAs. The method used the developed tools to determine the savings in regulation, load following and scheduling requirements for the consolidated BA in comparison with individual BAs.
- A preliminary approach for dynamic scheduling evaluation is given. The main concept is to connect external wind farms to specific balancing authorities and to provide ancillary services from external resources.
- An optimization method for regulation and load following sharing amongst individual BAs has been developed.
- A method for evaluating the benefits of creating a wind only BA has been investigated. A wind-only BA is responsible for controlling the interchange of its control area with the other balancing authorities following a pre-determined interchange schedule.
- An extreme event analysis method has been developed to evaluate the expectation of an extreme event in the future and its impact on the operating reserves and transmission congestion.
- A procedure for loop flow analysis has been developed to be able to estimate the unplanned additional power transfers caused by VGs as well as by BA cooperation options used.
- Two methodologies for cycling analysis have been proposed. The methodologies will help to evaluate the impacts of VGs and BA consolidation options on conventional generators, evaluate the need in flexible generation resources and energy storage.
- The virtual energy storage concept was proposed and proven through experiments. The concept creates an opportunity to detect, predict, and use the unplanned randomly occurring cyclic exchanges of energy between BAs as a virtual energy storage naturally existing in the system. By using this idea, participating BA could reduce their cycling balancing requirement without investing in additional generation or energy storage..

The Impact of the Project

This project showed the potential for the current electric power grid to accommodating more renewable generation through BA cooperation. This project identifies viable cooperation options between BAs by analyzing the benefits and implementation challenges with each option so that individual BAs can choose the most suitable cooperation strategy that fits their regional circumstances. Innovative metrics were developed to quantify BA cooperation benefits. In depth analysis for different BA cooperation techniques is introduced with conclusions about the pros and cons of each strategy. Consequently, the benefits of BA consolidation can be quantified and recognized. The significant economic and reliability benefits from BA cooperation were revealed. The results have stimulated strong interest from industry. PNNL has been contacted by its industrial partners (including WECC, Bonneville Power Administration (BPA), California Independent System Operator (CAISO), Constellation Energy and Columbia Grid) to extend the BA cooperation studies for some specific systems in subsequent projects.

Conclusion and Future Work

Through BA cooperation, more VG can be integrated into the U.S. electric power grid reliably and efficiently. High renewable penetration will significantly increase power variability and uncertainty in

power grid. More generation reserves are required to maintain balance if BAs work separately. Working together, BAs only need to manage the netted out variability and uncertainty with shared resources. Consequently, more VG can be integrated into the power grid with the same amount of resources. The benefits of BA cooperation become more significant with higher VG penetration.

There are several BA cooperation approaches proposed in the power industry. Each approach has its advantages and disadvantages. This report provides an overview and a systematic way of evaluating these approaches. It helps individual BAs choose the most appropriate approach for their cooperation.

The project is an initial attempt to evaluate the benefits of BA cooperation in high renewable generation penetration. It has generated significant interest in industry and paves the way for selection and implementation of BA cooperation for specific industrial systems. The innovative methodologies developed make it possible to compare the differences of BA cooperation strategies. Consequently, the benefits of BA consolidation can be quantified and recognized.

Future studies aim to evaluate BA cooperation benefits in terms of reducing generation production cost with high renewable generation penetration. Funded by DOE, PNNL, in cooperation with NREL and the WECC variable generation subcommittee, has started a project to analyze the BA consolidation benefits for the entire US Western Interconnection. The study will quantify the benefits of BA consolidation at different levels of renewable generation penetration up to 30%. It will also evaluate the effects of transmission congestion and the benefits of intra-hour scheduling.

Acknowledgements

The Pacific Northwest National Laboratory project team would like to thank the following people and organizations for their support on the project.

U.S. Department of Energy, Office of Energy Efficiency and Renewable Energy (EERE)

Megan McCluer, Program Manager, Wind and Hydropower Technologies Program
Stan Calvert, Manager, Technology Application

California Institute of Energy Environment (CIEE)

Merwin Brown, Director of Transmission Research
Larry Miller, Senior Research Advisor
Jim Cole, Senior Advisor

California Independent System Operator (CAISO)

Grant Rosenblum, Manager, Renewables Integration
Clyde Loutan, Senior Advisor, Planning and Infrastructure Development
Tim VanBlaricom, Manager, Floor Operations

Bonneville Power Administration (BPA)

Bart A. McManus, Senior Electrical Engineer, technical lead at BPA Transmission for wind integration.
John H. Pease, Manager, Technology Innovation

National Renewable Energy Laboratory (NREL)

Michael Milligan

Consult Kirby

Brendan Kirby, Consultant

Pacific Northwest National Laboratory (PNNL)

Kristy Huston, Technician
Susan J. Arey, Project Specialist
Sheena Kanyid, Contracting Officer
Evan O. Jones, Product Line Manager
Carl H. Imhoff, Market Sector Manager, Energy Infrastructure
Mark P. Morgan, Manager, Energy Technology Development
Kim A. Chamberlin, Administrator

Acronyms and Abbreviations

ACE	Area Control Error
ADI	ACE Diversity Interchange
AGC	Automatic Generation Control
BA	Balancing Authority
BPA	Bonneville Power Administration
CA	Contingency Analysis
CAISO	California Independent System Operator
CEC	California Energy Commission
CIEE	California Institute of Energy Environment
COI	California–Oregon Intertie
CPS	Control Performance Standard
DCS	Disturbance Control Standard
DOE	U.S. Department of Energy
DS	Dynamic Schedule or Dynamic Interchange Schedule
EERE	Energy Efficiency and Renewable Energy
EMS	Energy Management System
FRS	Frequency Response Standard
IEEE	Institute of Electrical and Electronics Engineers
ISO	Independent System Operator
MAPE	Mean Absolute Percent Error
MATLAB	MATLAB™
MRTU	Market Redesign and Technology Upgrade
NERC	North America Electric Reliability Corporation
NREL	National Renewable Energy Laboratory
PDF	Probability Density Function

PNNL	Pacific Northwest National Laboratory
PTDF	Power Transfer Distribution Factors
RSG	Reserve Sharing Group
RTO	Regional Transmission Organization
TND	Truncated Normal Distribution
TSO	Transmission System Operators
WECC	Western Electricity Coordinating Council

Glossary

Term	Meaning
Area Control Error	The instantaneous difference between a Balancing Authority's net actual and scheduled interchange, taking into account the effects of frequency bias and correction for meter error.
ACE Diversity Interchange	ADI or ACE Diversity Interchange is the pooling of area control errors (ACE) to take advantage of control error diversity (momentary imbalances of generation and load).
Automatic Generation Control	Equipment that automatically adjusts generation in a balancing authority area from a central location to maintain the balancing authority's interchange schedule plus frequency bias. AGC may also accommodate automatic inadvertent payback and time error correction.
Balancing Authority	The responsible entity that integrates resource plans ahead of time, maintains load-interchange-generation balance within a balancing authority area, and supports Interconnection frequency in real time.
Bonneville Power Administration	The Bonneville Power Administration, headquartered in Portland, Oregon, is a federal agency under the U.S. Department of Energy. BPA serves the Pacific Northwest through operating an extensive electricity transmission system and marketing wholesale electrical power at cost from federal dams, one non-federal nuclear plant and other nonfederal hydroelectric and wind energy generation facilities.
Contingency Analysis	Contingency Analysis (CA) runs automatically on a real-time basis to determine which branch and generator outages pose the most severe threat to the system. CA supports complex contingencies (more than one device outage) and cascaded relay actions, providing an accurate representation of the power system following the outage. Outages can be ranked and branch overloads and voltage limit violations are listed, along with identification of associated contingencies.
California Independent System Operator	The California ISO is a nonprofit public benefit corporation charged with operating the majority of California's high-voltage wholesale power grid. Balancing the demand for electricity with an equal supply of megawatts, the ISO is the impartial link between power plants and the utilities that serve more than 30 million consumers.
California Energy Commission	The California Energy Commission is the state's primary energy policy and planning agency. The Commission responsibilities include: 1) Forecasting future energy needs and keeping historical energy data. 2) Licensing thermal power plants 50 megawatts or larger. 3) Promoting energy efficiency by setting the state's appliance and building efficiency standards and working with local government to enforce those standards. 4) Supporting public interest energy research that advances energy science and technology through research, development, and demonstration programs. 5) Supporting renewable energy by providing market support to existing, new, and emerging renewable technologies; providing incentives for small wind and fuel cell electricity systems; and providing incentives for solar electricity systems in new home construction. 6) Implementing the state's Alternative and Renewable Fuel and Vehicle Technology Program. 7) Planning for and directing state response to energy emergencies.
California Institute of Energy Environment	A University of California partnership of energy agencies, utilities, building industry, non-profits, and research entities designed to advance energy efficiency science and technology for the benefit of California and other energy consumers and the environment. CIEE is a branch of the University of California Energy Institute.

California–Oregon Intertie	Path 66 (also called the California Oregon Intertie or abbreviated COI) is the name of several 500 kV power lines. It is the northern half of a set of three 500 kV lines that makes up the Pacific AC Intertie which is the AC portion of a greater project linking power grids in the Southwest with the grids in the Pacific Northwest. Also, this is the larger and older of the two segments of the Pacific AC Intertie, the other is the Los Banos-Gates third 500 kV wire of Path 15. The set of three 500 kV wires is mostly located in the Modoc Plateau.
Control Performance Standard	The NERC reliability standard that sets the limits of a Balancing Authority's Area Control Error over a specified time period.
Disturbance Control Standard	The reliability standard that sets the time limits following a Disturbance within which a Balancing Authority must return its Area Control Error to within a specified range.
the U.S. Department of Energy	The United States Department of Energy (DOE) is a Cabinet-level department of the United States government concerned with the United States' policies regarding energy and safety in handling nuclear material. Its responsibilities include the nation's nuclear weapons program, nuclear reactor production for the United States Navy, energy conservation, energy-related research, radioactive waste disposal, and domestic energy production. DOE also sponsors more basic and applied scientific research than any other US federal agency; most of this is funded through its system of United States Department of Energy National Laboratories.
Dynamic Schedule or Dynamic Interchange Schedule	A telemeter reading or value that is updated in real time and used as a schedule in the AGC/ACE equation and the integrated value of which is treated as a schedule for interchange accounting purposes.. Commonly used for scheduling jointly owned generation to or from another balancing authority area.
The office of Energy Efficiency and Renewable Energy	The Office of Energy Efficiency and Renewable Energy (EERE) is an office within the United States Department of Energy that invests in high-risk, high-value research and development in the fields of energy efficiency and renewable energy technologies. The Office of EERE is led by the Assistant Secretary of Energy Efficiency and Renewable Energy, who manages several internal EERE offices and ten programs that support research, development, and outreach efforts.
Energy Management System	A computer control system used by electric utility dispatchers to monitor the real time performance of the various elements of an electric system and to control generation and transmission facilities.
Frequency Response Standard	(Equipment) The ability of a system or elements of the system to react or respond to a change in system frequency. (System) The sum of the change in demand, plus the change in generation, divided by the change in frequency, expressed in megawatts per 0.1 Hertz (MW/0.1 Hz).
Institute of Electrical and Electronics Engineers	An international non-profit, professional organization for the advancement of technology related to electricity. IEEE is the world's largest professional association advancing innovation and technological excellence for the benefit of humanity.
Independent System Operator	An Independent System Operator (ISO) is an organization formed at the direction or recommendation of the Federal Energy Regulatory Commission (FERC). In the areas where an ISO is established, it coordinates controls and monitors the operation of the electrical power system, usually within a single US State, but sometimes encompassing multiple states.
Mean Absolute Percent Error	Mean absolute percentage error (MAPE) is measure of accuracy in a fitted time series value in statistics, specifically trending. It usually expresses accuracy as a

	<p>percentage.</p> $\text{MAPE} = \frac{1}{n} \sum_{t=1}^n \left \frac{A_t - F_t}{A_t} \right $ <p>where A_t is the actual value and F_t is the forecast value. The difference between A_t and F_t is divided by the actual value A_t again. The absolute value of this calculation is summed for every fitted or forecast point in time and divided again by the number of fitted points n. This makes it a percentage error so one can compare the error of fitted time series that differ in level.</p>
MATLAB™	<p>MATLAB is a numerical computing environment and fourth generation programming language. Developed by The MathWorks, MATLAB allows matrix manipulation, plotting of functions and data, implementation of algorithms, creation of user interfaces, and interfacing with programs in other languages. Although it is numeric only, an optional toolbox uses the MuPAD symbolic engine, allowing access to computer algebra capabilities. An additional package, Simulink, adds graphical multidomain simulation and model-based design for dynamic and embedded systems.</p>
Market Redesign and Technology Upgrade	<p>Market Redesign and Technology Upgrade, a program owned by the California Independent System Operation (CAISO). MRTU is a comprehensive redesign and upgrade of the ISO market structure and its supporting technology. MRTU was fully implemented on 1st April, 2009.</p>
North America Electric Reliability Corporation	<p>NERC's mission is to improve the reliability and security of the bulk power system in North America. To achieve that, NERC develops and enforces reliability standards; monitors the bulk power system; assesses future adequacy; audits owners, operators, and users for preparedness; and educates and trains industry personnel. NERC is a self-regulatory organization that relies on the diverse and collective expertise of industry participants. As the Electric Reliability Organization, NERC is subject to audit by the U.S. Federal Energy Regulatory Commission and governmental authorities in Canada.</p>
National Renewable Energy Laboratory	<p>The National Renewable Energy Laboratory (NREL), located in Golden, Colorado, as part of the U.S. Department of Energy, is the United States' primary laboratory for renewable energy and energy efficiency research and development.</p>
Probability Density Function	<p>A real-valued function whose integral over any set gives the probability that a random variable has values in this set. Also known as density function; frequency function.</p>
Pacific Northwest National Laboratory	<p>U.S. Department of Energy Laboratory located in the Pacific Northwest. The Laboratory is run by Battelle Memorial Institution.</p>
Power Transfer Distribution Factors	<p>In the pre-contingency configuration of a system under study, a measure of the responsiveness or change in electrical loadings on transmission system facilities due to a change in electric power transfer from one area to another, expressed in percent (up to 100%) of the change in power transfer.</p>
Reserve Sharing Group	<p>A group whose members consist of two or more balancing authorities that collectively maintain, allocate, and supply operating reserves required for each balancing authority's use in recovering from contingencies within the group. Scheduling energy from an adjacent balancing authority to aid recovery need not constitute reserve sharing provided the transaction is ramped in over a period the supplying party could reasonably be expected to load generation in (e.g., ten minutes). If the transaction is ramped in quicker (e.g., between zero and ten minutes) then, for the purposes of disturbance control performance, the areas become a Reserve Sharing Group.</p>
Regional Transmission	<p>A Regional Transmission Organization (RTO) in the United States is an</p>

<p>Organization</p>	<p>organization that is responsible for moving electricity over large interstate areas. Like a Transmission system operator (TSO), an RTO coordinates controls and monitors an electricity transmission grid that is larger with much higher voltages than the typical power company's distribution grid. TSO's in Europe cross state and provincial borders like RTOs.</p>
<p>Truncated Normal Distribution</p>	<p>In probability and statistics, the truncated normal distribution is the probability distribution of a normally distributed random variable whose value is either bounded below or above (or both).</p>
<p>Transmission System Operators</p>	<p>In electrical power business, a transmission system operator (TSO) is an operator that transmits electrical power from generation plants to regional or local electricity distribution operators.</p>
<p>Western Electricity Coordinating Council</p>	<p>WECC is responsible for coordinating and promoting electric system reliability in the Western Interconnection. WECC supports efficient competitive power markets, assure open and non-discriminatory transmission access among members, provide a forum for resolving transmission access disputes, and provide an environment for coordinating the operating and planning activities of its members as set forth in the WECC Bylaws.</p>

Contents

1.0	Background and Introduction	1.1
2.0	BA’s Responsibility and Resources in Maintaining Balance	2.1
2.1	Metrics to Measure BA’s Performance and Capability to Maintain Power Balance	2.2
2.1.1	Area Control Error (ACE).....	2.2
2.1.2	Control Performance Standards (CPS).....	2.3
2.1.3	Balancing Authorities ACE Limit.....	2.4
2.1.4	Disturbance Control Standard	2.5
2.1.5	Proposed Performance Metrics	2.5
2.2	Imbalance Caused by Load or Generation Variation and Uncertainty.....	2.9
2.2.1	Load variation, Predictability, and Prediction Errors.....	2.9
2.2.2	Wind and Solar Variation, Predictability and Prediction Errors	2.11
2.3	Scheduling Procedure to Maintain Balance	2.17
2.3.1	Scheduling Process.....	2.17
2.3.2	Load Following	2.20
2.3.3	Regulation	2.21
2.3.4	Frequency Response.....	2.21
2.3.5	Governor Speed Droop Compensation.....	2.23
2.3.6	Inertial Responses	2.23
2.4	Structure of System Reserves.....	2.24
2.5	Dynamic Scheduling and Pseudo-Ties.....	2.25
3.0	Methods of BA Cooperation.....	3.1
3.1	Approaches Used for BA Consolidation	3.2
3.2	Potential Benefits of BA Cooperation.....	3.3
3.2.1	Reduction in Balancing Burdens.....	3.3
3.2.2	Meeting Renewable Portfolio Standards’ Goals	3.5
3.2.3	Security and Reliability Enhancement	3.6
3.3	Potential Challenges	3.6
3.3.1	Congestion Problem	3.6
3.3.2	Loop flows.....	3.7
3.3.3	Inadvertent Interchange.....	3.8
3.4	Methodologies Developed to Evaluate and Compare the Performance of BA Cooperation Methods	3.8
3.4.1	Load Following and Regulation Assessment	3.8
3.4.2	Forecast Error Modeling	3.9
3.4.3	Power Flow Incremental Model.....	3.17
4.0	Analysis Methodologies for BA Cooperation Approaches	4.1
4.1	Area Control Error (ACE) Sharing	4.1
4.1.1	ACE Diversity Interchange (ADI)	4.1
4.1.2	ADI Philosophy.....	4.1

4.1.3	ADI Limitations	4.3
4.2	Dynamic Scheduling	4.4
4.2.1	Background of the Study	4.4
4.2.2	Available Options for Dynamic Transfers	4.4
4.2.3	Benefits and Main Issues.....	4.5
4.2.4	Proposed Methodology and Outcomes.....	4.6
4.2.5	Example Study Scenarios.....	4.12
4.3	Regulation and Load Following Sharing.....	4.13
4.3.1	Regulation Sharing.....	4.13
4.4	Wind Only BA	4.16
4.4.1	Wind Only BA Basic Idea.....	4.16
4.4.2	Wind Only BA Simplified Mathematical Model	4.16
4.5	BA Consolidation.....	4.18
4.5.1	The Concept of BA Consolidation	4.18
4.5.2	Motivation for BA Consolidation.....	4.19
4.5.3	Benefits of BA Consolidation	4.19
4.5.4	Case Study.....	4.21
4.5.5	Future Work:	4.31
5.0	Development and Evaluation on Some New BA Cooperation Approaches.....	5.1
5.1	Advanced ADI Methodology	5.1
5.2	Virtual Energy Storage to Partially Mitigate Unscheduled Interchange Caused by Wind Power.....	5.5
5.2.1	Background and Basic Principle	5.6
5.2.2	Performance Evaluation	5.7
5.2.3	Technical and Operation Implications	5.11
5.2.4	Summary	5.14
6.0	Extreme Event Analysis	6.1
6.1	Objective of the Analysis	6.1
6.2	Impact on Operating Reserve	6.1
6.2.1	Introduction to Gumbel’s Theory.....	6.1
6.2.2	Probability Model for Wind Forecast Error Exceedences.....	6.2
6.2.3	Application to Wind Forecasts	6.3
6.2.4	Implications on Reserve Margin Calculations	6.5
6.3	Impact on the Transmission Congestion	6.5
6.3.1	The Problem:	6.6
6.3.2	Methodology to Estimate Congestion in Case of Extreme Events.....	6.7
6.4	Future work on the Extreme Events	6.12
7.0	Conclusions and Future Work	7.1
8.0	Summary of Project Contributions	8.1
9.0	References	9.1
	Appendix A Balancing Reserve Needs Calculation Methodology	A.1

Appendix B ACE Diversity Interchange	B.1
Appendix C Regulation Sharing Model.....	C.1
Appendix D Load Following Sharing Model	D.1
Appendix E Incremental Power Flow Model	E.1
Appendix F Alternative Representation of the WECC Automatic Time Error Correction Term....	F.1
Appendix G Load, Wind, Solar Forecast Errors	G.1

Figures

2.1	Traditional Operation and the Raw ACE	2.3
2.2	Schematic Illustration for the Four Performance Metrics	2.6
2.3	Cycling Analysis for a Time-Domain Signal	2.8
2.4	Load Fluctuation and Uncertainty	2.10
2.5	Wind Generation Forecast Statistical Characteristic for Different Look-Ahead Period:.....	2.12
2.6	Hypothetical Distribution of the Standard Deviation of Solar Forecast Error Depending on the CI	2.15
2.7	Distribution of Solar Forecast Error in a Very Cloudy Day and a Very Sunny Day.....	2.16
2.8	CAISO Generation Schedule.....	2.18
2.9	CAISO Day-Ahead Market Flowchart.....	2.19
2.10	CAISO Real-Time Scheduling Process Flowchart.....	2.20
2.11	CAISO Real-Time Economic Dispatch Process.....	2.21
2.12	An illustration of Primary and Secondary Frequency Responses.....	2.22
2.13	An Illustration of Generator Droops.....	2.23
2.14	Structure of System Reserves	2.24
2.15	Allocation of Generation Unit Capacity	2.25
3.1	Example of Variability of Aggregated ACE	3.2
3.2	Benefits in System Scheduling Process.....	3.4
3.3	Benefits for Load Following Capacity	3.4
3.4	Benefits for Regulation Capacity	3.5
3.5	Load Following Ramp Rate Savings	3.5
3.6	Idea of BA Cooperation.....	3.6
3.7	Congestion Problem Illustration.....	3.7
3.8	Loop Flow Problem Illustration	3.8
3.9	Separation of Regulation From Load Following Based on Simulated Hour-Ahead Schedule	3.9
3.10	Doubly Truncated Normal Distribution Model for Forecast Errors	3.10
3.11	Hour-Ahead Load Forecast Error Distribution.....	3.11
3.12	Simulated Hour-Ahead Load Schedule	3.14
3.13	Probability Density Function of the Load Forecast Function	3.15
3.14	Simulated Real-Time Load Forecast	3.16
3.15	Zonal Structure of the WECC System.....	3.19
3.16	WECC Key Transmission Lines and Paths	3.20
4.1	ADI Operation and ADI ACE	4.3
4.2	Concept of Dynamic Scheduling.....	4.4
4.3	Concept of a Pseudo-Tie	4.5
4.4	Example of 1 Hour Ahead Scheduling Curve	4.7

4.5	Example of Load Following Curve	4.7
4.6	Example of Regulation Curve in a Month.....	4.8
4.7	Example of the Scheduling Capacity Requirement for 24 Operating Hours	4.9
4.8	Example of Load Following Capacity for 24 Operating Hours	4.9
4.9	Example of Regulation Capacity for 24 Operating Hours.....	4.10
4.10	Example of Max & Min Regulation Ramp Rate for 24 Operating Hours.....	4.10
4.11	Incremental Zonal Model for WECC Wystem.....	4.12
4.12	A Diagram of Source BA and Sink BA.....	4.14
4.13	Regulation Capacity Probability Distribution Function for BA 1	4.15
4.14	Regulation Capacity PDF for BA 2	4.15
4.15	Regulation Capacity PDF for BA 3	4.16
4.16	Three Conventional Bas and One Wind Generation Only BA Example.....	4.17
4.17	An Example of Results Comparison for Load Following Incremental/ Decremental Capacity Requirement.....	4.21
4.18	Actual load L_{actual} and Real-Time Load Schedule $L_{schedule}$	4.22
4.19	Actual Wind W_{actual} and Real-Time Wind Schedule $W_{schedule}$	4.22
4.20	Calculated Load Following Requirements Curve.....	4.23
4.21	Calculated Regulation Requirement Curve	4.23
4.22	Min/Max Capacity Requirement Comparison for Scheduling	4.24
4.23	Incremental Capacity Saving Comparison for Load Following	4.26
4.24	Decremental Capacity Saving Comparison for Load Following.....	4.27
4.25	Incremental Capacity Saving Comparison for Regulation	4.27
4.26	Decremental Capacity Saving Comparison for Regulation.....	4.27
4.27	Ramp Rate Saving Comparison for Inc/Up Load Following	4.28
4.28	Ramp Rate Saving Comparison for Dec/Down Load Following	4.28
4.29	Ramp Rate Saving Comparison for Inc/Up Regulation	4.29
4.30	Ramp Rate Saving Comparison for Dec/Down Regulation	4.29
4.31	Percentage Energy Saving Comparison for Load Following	4.30
4.32	Percentage Energy Saving Comparison for Regulation	4.30
5.1	ACE Adjustments	5.1
5.2	BPA Regulating Energy: Without ADI, ADI With 25MW Limit, ADI, ADI With Congestion Model	5.2
5.3	CAISO Regulating Energy: Without ADI, ADI With 25MW Limit, ADI, ADI With Congestion Model	5.3
5.4	BPA ACE Distribution: With ADI, Without ADI.....	5.3
5.5	CAISO ACE Distribution: With ADI, Without ADI.....	5.4
5.6	BPA Ramp Rate Requirements Distribution: With ADI, Without ADI.....	5.4
5.7	CAISO Ramp Rate Requirements Distribution: With ADI, Without ADI.....	5.5
5.8	Illustration of Virtual Energy Storage Concept.....	5.6

5.9	COI Power Deviation from Scheduled.....	5.7
5.10	Characteristics of the Band-Pass Filter.....	5.8
5.11	Filtered Power and Residue of COI Power Deviation.....	5.9
5.12	Histogram of COI Power Deviation, Filtered Power and Residue.....	5.10
5.13	Predication of Filtered COI Power Deviation by LMS Filter.....	5.11
5.14	Charge Profile of Virtual Energy Storage.....	5.11
5.15	Illustration of Loop Flow.....	5.12
6.1	Wind Power Forecast and Actual Wind Power Values, for One Day, in 5 Minute Intervals.....	6.4
6.2	Ranked Wind Power Forecast Error ξ for a Day at 5 Minute Intervals.....	6.4
6.3	Exceedance Level Versus Expected Number of Exceedances in the Next 5N Minutes.....	6.5
6.4	Problem of Transmission Congestion and Extreme Wind Forecast Errors.....	6.6
6.5	Forecast Error Histogram for a Month.....	6.7
6.6	Ranked Forecast Error.....	6.7
6.7	Expectancy vs. Exceedance Level of Forecast for Two BAs in Next 30 Hours.....	6.8
6.8	Zonal and Interface PTDFs.....	6.9
6.9	Incremental Power Flow – Methodology 1.....	6.11
6.10	Hourly Instantaneous Incremental Power Flow and Hourly Ranked Incremental Power Flow.....	6.12
6.11	Incremental Power Flow – Methodology 2.....	6.12

Tables

1.1. Various BA Consolidation Options	1.3
2.1. Standard Deviations of Solar Forecast Errors Based on CI Levels.....	2.17
3.1. Zonal Information	3.18
3.2. Interface PTDFs (%).....	3.21
3.3. Interface Power Flow Validation	3.22
4.1. Analyzed Scenarios in the Study Case.....	4.26
5.1. Statistics of COI Power Deviation, Filtered Power and Residue.....	5.10
6.1. Zonal PTDF for the Balancing Areas	6.9
6.2. Interface PTDF for the Transmission Path 1-2 Joining BA1 and BA2.....	6.9
6.3. PTDFs for Different Interfaces Connected to BAs	6.10

1.0 Background and Introduction

A successful power grid must maintain the balance between its generation, net load and interchange schedule. Significant imbalances can result in significant interconnection frequency deviations, transmission system violations, stability problems and other problems that could disrupt service, and ultimately result in wide-spread system blackouts. Dispatchable generators must be committed and dispatched ahead of time and controlled in real time to follow the load variation and ensure an adequate balance of supply and demand. They constitute additional balancing reserve and so called flexibility characteristics including the available maneuverable capacity, ramping capability, start up time, cycling characteristics (number of available start ups and shut downs during a day), and others. The task of balancing systems becomes more difficult with increasing penetration of intermittent resources, such as solar and wind generation, which produce variable and hardly predictable power.

Traditionally, the system balance is achieved through the balancing efforts of multiple balancing authorities (BAs), which are responsible for controlling their areas, or parts of interconnection. For example, the U.S. Western Interconnection is operated by 37 balancing authorities. Each BA is responsible to maintain the balance within its territory so that the combined effort of all BAs will keep the entire Western Interconnection balanced. Various metrics (e.g., Area Control Error [ACE], Control Performance Standards [CPS1 and CPS 2], Disturbance Control Standard [DCS], Frequency Response Standard [FRS], Balancing Authority ACE Limit [BAAL], frequency deviation limits) are introduced by NERC as standards to check how well a BA balances generation against load, wind and solar generation and interchange [36]. Generation reserves are needed to achieve the control performance objectives. The generation reserves are expensive and may be limited. BAs, which do not meet these requirements, could jeopardize the system reliability and are thus penalized financially.

Renewable variable generation (VG) will penetrate the power grid at a high level, as required by different state's Renewable Portfolios Standard (RPS). Twenty four states' RFPs establish the goal of reaching 10-40% of renewable energy to be integrated into the grid by 2015-2030 [49]. The DOE has analyzed a modeled energy scenario in which wind would provide 20% of U.S. electricity by 2030 [50]. Because of the variability and uncertainty of the wind and solar generation, the high penetration of renewable generation makes it more difficult for balancing authorities (BAs) to maintain balance between their load, interchange and generation. Operating separately and locally, individual BAs would have to purchase more expensive balancing reserves to accommodate the variability and uncertainty from high penetration of VG in the future. It has been observed that additional balancing requirements, caused by renewable intermittent resources, could be reduced, if their collective impact is accumulated over a large geographic area, taken from multiple distributed resources, and for all sources of variability and intermittency (including system load). BA's cooperation and consolidation are identified as one of the most important strategies to facilitate high-level VG penetration while limiting the requirement of generation reserves [44], [33]. A recent General Electric Energy (GE) study, conducted for NREL, states explicitly that to integrate 35% of wind and solar resources in the area served by WestConnect group of utilities and 25% of these resources in the rest of the WECC system, BA cooperation and consolidation is required among the other measures [33].

Balancing authorities have been developing various measures to mitigate VG integration problems including improved day-ahead, hour-ahead and real-time wind and solar forecasting systems (and wind ramp forecasting systems); incorporating these forecasts into the market, scheduling and real time processes; subhourly schedules, increasing operating reserve requirements; grid codes requiring at least partial dispatchability from wind generators; additional energy storage; demand response programs; new regional markets for the intra-hour balancing services; coordinated wide-area real-time; congestion

management; building special control centers for wind; transmission system enhancements; adding more flexible generation to the system; increasing operating reserves (especially, intra-hour balancing reserves); dynamic scheduling and pseudo-tie options to deliver more ancillary services from the neighboring BAs; and other measures. Many of these methods are expensive options. BA cooperation and consolidation options are, perhaps, among the least expensive measures to mitigate the impacts of wind and solar power variability, poor predictability and uncertainty.

Consolidation processes already take place in the industry. For example, an actual consolidation of 26 BAs in the Midwest Independent System Operator (ISO) area into a single BA took place on January 6, 2009 [18]. In 2006-2007, four BAs¹ formed a new cooperation by combining their area control error (ACE) in the Pacific Northwest [48]. Later on, the ACE diversity initiative (ADI) was extended over a larger geographical region in the Western interconnection, by including 8 more BAs² [12]. Similar processes take place elsewhere in the world. In 2005, two Danish transmission system operators³ (TSOs) merged forming a consolidated TSO called Energinet.dk. All wind power production and its deviations in Germany are combined virtually, and then distributed to each of four transmission system operators⁴ [2].

PNNL is running a study for several BAs in the Western Interconnection who are willing to evaluate the benefits of creating one single BA. Funded by DOE, PNNL, in cooperation with NREL and the WECC Variable Generation Subcommittee (VGS), has started a project to analyze the consolidation benefits for the entire U.S. Western Interconnection. Nevertheless, essentially, most of the approaches are trying to find ways of consolidating intermittency impacts, balancing efforts, and reserves to solve this problem without creating a single supper balancing authority. This can be done through different approaches shown and analyzed in Table 1.1.

¹ British Columbia Transmission Corporation, Idaho Power, PacifiCorp East, PacifiCorp West and Northwest Energy.

² Arizona Public Service, Nevada Power/Sierra Pacific Power, Public Service Company of New Mexico, Salt River Project, Seattle City Light, Bonneville Power Administration (BPA), Public Service Colorado/Excel Energy and Glacier Wind Farm (Naturener).

³ Eltra and Elkraft.

⁴ Amprion GmbH, 50Hetz Transmission Europe GmbH, Transpower Stromuebertragungs GmbH and EnBW Transportnetze AG.

Table 1.1. Various BA Consolidation Options

Category	Explanation	Options	Explanation	Comments
Actual BA consolidation in a single Balancing Authority in WECC	Participating BAs form a single Balancing Authority	Full actual consolidation	BAs merge and all balancing functions are centralized	Example: Actual consolidation of 26 BAs in the MISO area into a single BA on January 6, 2009 [12].
		Virtual or partial consolidation	Participating BAs or utilities perform some or all balancing functions individually based on certain sharing agreements	
Wind only BA	Wind power producers form their own BA			Example :Glacier Wind [29].
Sharing or globalization of some of the balancing functions	Participating BA share some of the balancing functions, but do not form a single Balancing Authority	Primary reserve (frequency response) sharing and coordination	BAs determine and provide frequency response based on the system wide standard and share the amount of response provided by each BA based on certain sharing agreement	European transmission system operators use this option for primary reserves (frequency response) [2].
		ACE sharing (or ADI)	Participating BAs calculate a common ACE in real time and share the ACE diversity based on certain sharing principles	Examples: (1) Simple ADI (like in WECC [12]). (4) ADI with globalized use of regulation resources (like in Germany [2]). Some possible variants: (1) Bilateral market or agreements (e.g., using dynamic schedules) (2) Spot market

Table 1.1. (contd) Various BA Consolidation Options

Category	Explanation	Options	Explanation	Comments
		Flexibility market or other similar globalization options for load following services (intra-hour balancing)	Participating BA use market or other mechanisms to provide wide area intra-hour balancing service	Some possible variants: (1) Bilateral market or agreements (e.g., using dynamic schedules) (2) Spot market
		Coordinated scheduling process	Participating BAs build and optimize their generation and interchange schedules in a coordinated fashion based on their load, wind and solar generation forecasts	
Sharing balancing services and resources	The balancing services can be provided by resources outside of the BA that needs these services. Also, the same resource could provide services to multiple BAs.	Dynamic schedules	A balancing resource is scheduled and/or controlled from an outside BA. Its output is telemetered to the BA where this resource is accounted for.	Currently, this is a widely used option.
		Globalization of balancing services in a wide area	BAs have access and can use balancing resources outside their Balancing Authority	Example: regulation (secondary reserve) market and globalization in Germany
		Regulation resource sharing	A regulation resource provide regulation services for 2 or more BAs	PNNL project funded by BPA and CEC
Globalization and sharing of unscheduled deviations	Participating BAs agree to globalize unscheduled deviations and balance only against some share of these deviations	Globalization and sharing of unscheduled deviations of wind and solar resources	The arrangement covers only wind and solar station errors	Example: Germany

Table 1.1. (contd) Various BA Consolidation Options

Category	Explanation	Options	Explanation	Comments
		Globalization includes all deviations including load deviations		Note differences with sharing the balancing functions
		The sharing goes below the BAs' level to the level of specific resources	The resources get only a fraction of their own balancing responsibility	Resources have a choice between self-provided regulation, buying regulation service from some other resources or using services provided by BAs. The option is currently under discussion at BPA
Sub-hour scheduling within each participating BA	Participating BAs' scheduling process is conducted for sub-hour time intervals for all resources within the BA	The arrangement is done for participating BAs only, with the external BAs, the one hour schedules are used		Used in MISO, ERCOT, PJM, ISO-NE, NYISO, IESO, NYISO, CAISO, ...
Sub-hour scheduling within and among participating BAs	Participating BAs' scheduling process is conducted for sub-hour time intervals among BAs	The arrangement is done for participating BAs only, with the external BAs, the one hour schedules are used All interconnection is using sub-hour schedules		Used in Germany, Being implemented between NYISO, ISO-NE, IESO

There is a need to have a systematic look and formal comparison of benefits and problems associated with different consolidation options. Using the ADI as an example, there is a need to quantify the advantages of this form of cooperation using certain performance metrics. Calculating the performance metrics used in real life operations (such as ACE, CPS1 and CPS 2, DCS, FRS, BAAL, frequency deviation limits) requires a comprehensive system model. These models would be precise tools, used to deal with extremely uncertain system situations. Building such a model needs multi-million dollar investment, In this regard, developing a simplified set of performance metrics (performance envelopes) which is connected to the NERC performance standards is important. In this study, our target is to develop performance envelopes, which help to achieve that goal. By implementing those metrics, one could run multi-variant studies and evaluate the benefits of BA cooperation by robustly covering uncertainties in the system model without investing major resources and man power. Methodologies developed could be widely used in the U.S. and abroad for making informed decisions on the possible consolidation schemes.

The next problem we are addressing in this report concerns possible disadvantages, restrictions and other aspect of wide area BA consolidation. For example, when implementing the ACE diversity interchange (ADI) in the Western Interconnection, it has been noticed that the ADI could create congestion problem in the heavily loaded path of the system. Because of the potential congestion problem, it has been decided to restrict the ADI adjustment by 25MW. It is of course a restriction, which decreases the efficiency of the ADI. Another example can be found in Germany, there is a large amount of wind and solar energy resources in the system and the instantaneous trade of wind and solar energy between four transmission system operator results in major unpredicted loop flows through neighboring systems. So additional problems which can be caused by BA consolidations are congestions, major imbalances (tail events), inadvertent interchanges, unauthorized use of third party transmission systems and other problems. As discussed, along with possible negative reliability impacts, economical issues, transmission utilization rights, these problems can also limit the number and efficiency of BA consolidation options.

Along with analysis of existing consolidation schemes, there is a need to propose improvements or ideas on possible consolidation framework. Currently, we are dealing with new areas and non-traditional system behaviors that cannot be considered traditional anymore. Out-of-the-box thinking could result in suggestions which significantly improve the existing consolidation ideas or in completely fresh and new ideas. For example, dynamic scheduling has been successfully applied to not only bring more flexible balancing resources into system with high penetration of wind energy, but also to meet the RPS requirements by adding more renewable resources into the system. In this study, we suggest several completely new ideas. They are advanced ADI, capable of controlling congestion problems, virtual energy storage, loop flow analysis and monitoring schemes, and others. In our opinion, results of this study will benefit the power industry, and currently we have been contacted by our industrial partners, who are interested in our innovative ideas. We have already several projects materialize with industry partners, which incorporate solutions developed in this work:

- Investigation of consolidation benefits in terms of the savings in regulation, load following, and scheduling requirements for a group of BAs.
- Several WECC BAs, such as Bonneville Power Administration (BPA) who have joined the current ADI program, show strong interest in the optimized ADI method and are going to evaluate it. In particular, BPA is helping test the method by providing field measurement data.
- A study on the needed energy storage capacity in all three interconnections in the US to minimize the cycling of generating units.
- Several Bas, such as Constellation Energy Group, Inc. have shown interest in the developed approach for wind only BA. The current intention is to incorporate this analysis in the next phase of the study.
- The methodology of regulation and load following sharing has been applied in two of PNNL's projects with BPA and the California Energy Commission (CEC).
- Work is underway to start a project with BPA on dynamic scheduling. The objective is to develop a methodology for quantifying the benefits of using dynamic scheduling. The California ISO has also expressed interest in using the results of this study.
- A larger-scale study to investigate potential collaboration between more than thirty WECC BAs to overcome transmission congestion problems and to be able to meet the challenges associated with the rapid growth of wind energy that is expected to reach a penetration level of 20% within a decade.

Approaches considered in this report have been extensively discussed with National Renewable Energy Laboratory (NREL)partners (Dr. Michael Milligan, and Brendan Kirby). Innovative solutions for

wide-area coordination using event analysis have been developed in collaboration with professors Gerald Heydt and Vijay Vittal of Arizona State University (ASU).

The results of the study have been decimated extensively through papers and reports. One paper is submitted and successfully accepted to the Institute of Electrical and Electronics Engineers (IEEE) T&D conference; another paper was recently submitted to IEEE General meeting. A paper for IEEE transaction - in collaboration with V. Vittal and G. Heydt - is in the pipeline.

2.0 BA's Responsibility and Resources in Maintaining Balance

Traditionally, each balancing authority (BA) works independently and separately to maintain balance between generation and load, wind, solar and other intermittent resources and interchange within its area. Each BA needs sufficient balancing reserves and proper procedures to comply with North America Electric Reliability Corporation (NERC) control performance standards [36]. To operate a power system reliably, operational procedures and automatic systems are created in each BA to use generation reserves and other ancillary services to maintain power grid balance. Reserves should be sufficient enough to compensate predicted and unpredicted load and wind solar generation changes. Significant imbalances caused by insufficient reserves, deficient characteristic of these reserves (i.e., insufficient ramping capability, system inertia or frequency response) could result in significant interconnection frequency deviations, transmission system violations, stability problems and so on. Ultimately those problems could result in wide spread system blackouts. The task of balancing the system becomes more difficult with increasing penetration of intermittent resource of the systems, such as solar and wind generation. The balancing service and reserves are expensive and each BA is trying to minimize these requirements without compromising system reliability and control performance.

Traditionally, the system balance is achieved through the balancing efforts of multiple balancing authorities, which are responsible for controlling their areas (parts of interconnection). For example, Western Interconnection is operated by 37 BAs. Each BA is responsible to maintain balance within its territory so that the combined effort of all BAs will keep the entire Western Interconnection balanced. Various metrics (e.g., area control error ACE, control performance standarts CPS1 and CPS 2, disturbance control standart DCS, frequency response standart FRS, balancing authority ACE limit BAAL, Frequency deviation limits [36]) are introduced by NERC as standards used to monitor how well a BA balances generation against load, wind generation, solar generation and interchange. Generation reserves needed to achieve the control performance objectives are expensive and may be limited. BAs that do not meet the requirements, could jeopardize the system reliability and are thus penalized financially.

This chapter explains what types of reserves are needed and how BA determines minimum reserve requirements to maintain the balance with existing BA structure which are not employing BA cooperation options. The following questions are addressed in the text.

- What cause the problem in maintaining balance?
- What metrics are applicable to check whether a balance is maintained?
- How the problem is handled?
- What kinds of reserves are needed to maintain balance?
- How can the amount of reserves be determined?
- Why additional reserves are required for high level penetration of variable generations?

Finally, a detailed modeling procedure developed in the study for calculating reserves is given in the Section 3.4. Those procedures have been developed before by PNNL for projects conducted by California System Operator (CAISO) and the Bonneville Power Administration (BPA). The procedure was updated in this work as described below in this chapter, and in the updated form, the procedure has already been used in an offshoot project aiming to quantify benefits of possible actual consolidation of BAs in the

Western Electricity Coordinating Council (WECC) system. Information provided in the chapter is to help readers better understand approaches used and results obtained in this study.

2.1 Metrics to Measure BA's Performance and Capability to Maintain Power Balance

2.1.1 Area Control Error (ACE)

Area control error (ACE) index has been used for many years to reflect the control area power balance. ACE signal includes the interconnection frequency error and the interchange power error with neighboring BAs. ACE signal value is used as an input of Automatic Generation Control (AGC) system. Most of BAs have their own AGC systems. An AGC system automatically controls generation units, which participate in regulation process. The regulation process is a real-time process and ACE is calculated every several seconds.

2.1.1.1 NERC Definition of ACE

Area control error (ACE) plays an important role in power system generation control to reflecting the balance of generation, load and interchange [60]. ACE values help to determine how much a balancing authority needs to move its regulating units to meet the mandatory control performance standard requirements [36].

ACE of BA i is defined as¹:

$$ACE_i = \Delta P - 10B_i\Delta F, \quad (2.1)$$

where: ΔF is the interconnection frequency error in Hz

ΔP is the interchange power error in MW

B_i is the control area frequency bias in MW/0.1Hz

Each BA is required to keep its ACE within certain statistical limits established by the NERC Control Performance Standards [40]. As shown in Figure 2.1, traditionally, ACE is calculated independently for each BA, and the AGCs are operated accordingly to reduce individual BA ACEs.

¹ Expression (2.1) is a simplified representation of the ACE equation. The full expression contains additional terms such as metering error term, inadvertent interchange pay back term, and automatic time error correction term (in WECC).

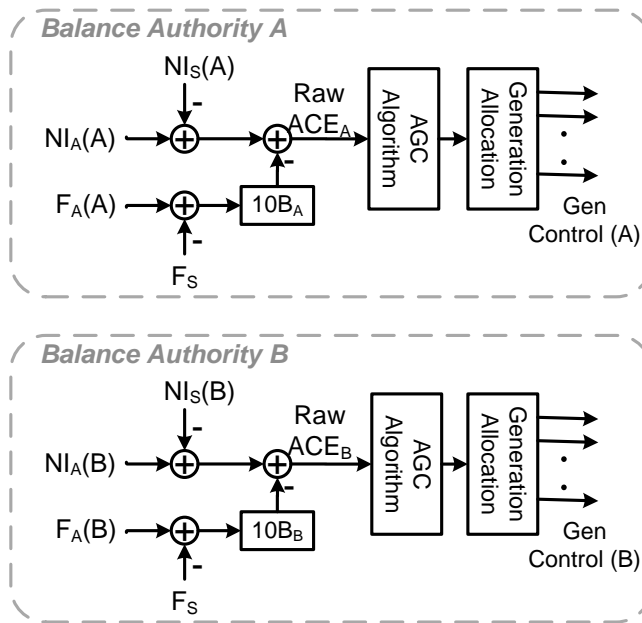


Figure 2.1. Traditional Operation and the Raw ACE

2.1.1.2 WECC Differences

Details and mathematical models of alternative representation of the WECC Automatic Time Error Correction Term are given in the Appendix F.

2.1.2 Control Performance Standards (CPS)

To evaluate the quality of the balancing process, control performance standards (CPSs) are used. Control performance standards are introduced by the NERC. There are two standards: CPS1 and CPS2 [24].

CPS1 assesses the impact of individual ACEs on interconnection frequency variations over a 12-month sliding window using 1-minute average compliance factors. CPS2 is a monthly measure that a BA must report to NERC, and is calculated by averaging the ACE for each 10-minute period within a month. CPS2 is the percentage calculated by dividing the number of averages, which are less than the BA's CPS2 limit by the total number of averages. A CPS2 score of 90% or more is considered as acceptable.

2.1.2.1 CPS1

Each BA shall achieve, as a minimum, CPS1 compliance of 100% [40].

CPS1 is calculated by converting a compliance ratio to a compliance percentage as follows [16], [24]:

$$CPS1 = (2 - CF) \cdot 100\% > 100\% , \quad (2.2)$$

Where CF is a compliance factor and it can be calculated as:

$$CF = AVG_{12-month} [CF_1] \quad (2.3)$$

$$CF_1 = \left[\left(\frac{ACE}{-10B} \right)_1 \left(\frac{\Delta F}{\varepsilon_1^2} \right)_1 \right], \quad (2.4)$$

where: ε_1 is the targeted frequency bound for CPS1

ΔF is the interconnection frequency error

B_i is the frequency bias of the i th control area

$(\cdot)_1$ is the clock -1-min average.

2.1.2.2 CPS2

Each BA shall operate such that its average ACE is within a specific limit, (referred to as L10) for at least 90% of clock-ten-minute periods (six non-overlapping periods per hour) during a calendar month.

$$AVG_{10\text{-min}}(ACE_i) \leq L_{10} \quad (2.5)$$

$$L_{10} = 1.65\varepsilon_{10}\sqrt{(-10B_i)(-10B_s)} \quad (2.6)$$

$$CPS2 = \left[1 - \frac{\text{violations}_{month}}{\text{total periods} - \text{unavailable periods}} \right] \times 100 > 90\% \quad (2.7)$$

ε_{10} is the targeted frequency bound.

B_s is the sum of the frequency bias settings of the balancing authority areas in the respective interconnection.

2.1.3 Balancing Authorities ACE Limit

The balancing authority ACE limit standard is a part of a new set of control performance standards currently under development at NERC [55]. BAAL is designed to replace CPS2 and Disturbance Control Standart. It establishes frequency-dependent ACE limits.

The new Balance Resources and Demand Standards are [55]:

BAL-007-1, Balance of Resources and Demand,

BAL-008-1, Frequency and Area Control Error,

BAL-009-1, Actions to Return Frequency to within Frequency Trigger Limits,

BAL-010-1, Frequency Bias Settings, and

BAL-011-1, Frequency Limits.

These new proposed standards are a major change from the existing control performance metrics calling for an elimination of CPS2 [55]. The new standards require BAs to maintain interconnection scheduled frequency within a wide, predefined frequency profile under all conditions (i.e., normal and abnormal). They are designed to prevent unwarranted load shedding and to prevent frequency-related cascading collapse of the interconnected grid.

The standard has been designed so that the BA ACE Limits (BAALs) become frequency sensitive and can be used by the system operators as performance indicators in real-time. The balancing authority can monitor its own performance against its BAAL target and take corrective actions before one of its BAAL limits is exceeded [55].

The following important considerations outlining potential impacts of the BAAL standard on the value of fast regulation resources can be foreseen at this moment:

- A control that opposes frequency deviation always improves area performance against the BAAL. This means that the new standard will not have potential problems with compliance if the regulating resources are controlled, based on the local frequency signals rather than AGC signals.
- Distributed resources that react to local frequency signals will contribute to BAAL compliance without being connected to the BA control signal. This would dramatically increase opportunities for distributed resources demand side control and decrease associated costs (as a result of eliminating telemetry systems connecting the AGC system with distributed resources and loads).
- BAAL is designed to replace CPS2 standard ; therefore, no controversy is expected from interaction of local frequency-based controls with the CPS2 requirements.
- Unlike the CPS2 standard formulated for 10-minute averages of ACE, the BAAL standard is formulated for instantaneous values of the area control error.
- Expectation is that the BAAL standard will relax the area regulation needs and reduce the regulation burden.

2.1.4 Disturbance Control Standard

The purpose of the Disturbance Control Standard (DCS) is to ensure the BA is able to utilize its contingency reserve to return interconnection frequency within its defined limits following a reportable disturbance [38]. Because generator failures are far more common than significant losses of load and because contingency reserve activation does not typically apply to the loss of load, the DCS applies to the loss of supply only and it does not apply to the loss of load.

2.1.5 Proposed Performance Metrics

Control performance standard (CPS) scores CPS1 and CPS2 (or BAAL) are appropriate indices to evaluate a BA performance. At the same time, to derive these indices from a study based on a system model, much more detailed information is needed than is usually available. For instance, the load following, AGC regulation and generators' response to controls should be simulated in details. Moreover, the CPS scores are not giving essential information on more detailed characteristics required from generators performing the balancing service, such as the capacity, ramping, energy, cycling, and other metrics.

Wind and solar generation is variable and non-dispatchable source of energy. It causes additional unscheduled deviations of power balance and complicates the problem of system balancing. For instance, BAs need to procure more regulation capacity to met CPS requirements. However increasing in regulation capacity requirements is not the only problem which could be caused by variable generation. Another important issue is ramping capability of the units evolved in regulation process. Due to the lack of fast response units, while slow units are not capable of following fast ramping events, more units should be committed and an even greater capacity must be involved in regulation process.

To assess the new challenges caused by the growth of intermittent generation resources we propose to use two sets of performance criteria (performance envelopes). The first performance envelope allows evaluating the capacity, ramping and energy requirements of the system. It includes: capacity, ramp rate, ramp duration and energy criteria. Second performance envelope evaluates cycling characteristics of the generation system and includes: half-cycle magnitude, half-cycle duration and half-cycle frequency.

2.1.5.1 Performance Envelope I

The key technical metrics or indices proposed to compare BAs operational performance are explained in this section.

Potential benefits of BA coordination or consolidation can be demonstrated through four basic metrics, which we refer to as the “first performance envelope,” and relate to the evaluation of capacity, ramp duration, ramp rate and energy of ramps. These four metrics are schematically illustrated in Figure 2.2 and defined below.

The regulating unit ramping capability can directly influence the required regulation and load following capacity. If the ramping capability is insufficient, more units and more capacity must be involved in regulation to follow the ramps. Hence, a simultaneous evaluation is necessary to determine the true balancing requirements. The required ramping capability can be derived from the shape of the regulation/load following requirement curve.

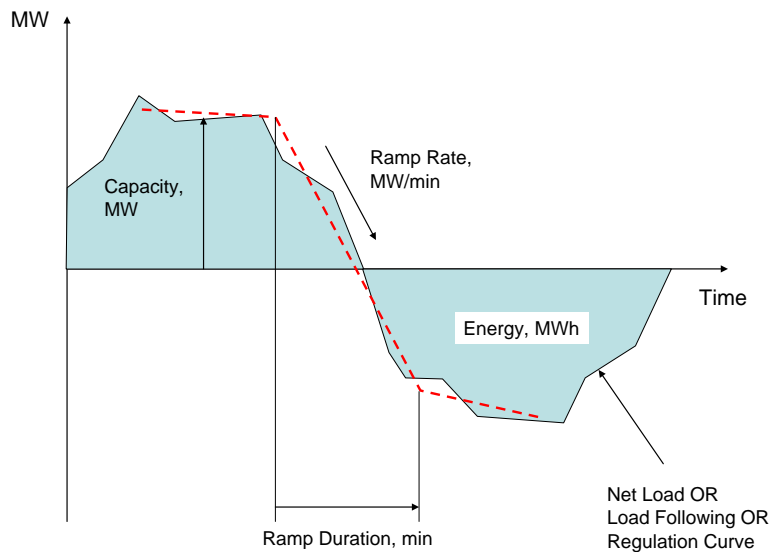


Figure 2.2. Schematic Illustration for the Four Performance Metrics

Capacity

Capacity (π) indicates the required minute-to-minute amount of generation or change in generation output, either up or down, to meet variations in net load/load following/regulation requirements. The capacity requirement metric is calculated separately for positive and negative generation changes needed to balance the system.

Ramp rate

Ramp rate (ρ) is the slope of the ramp. This indicates the needed ramping capability of on-line generating units to meet the net load/load following/regulation requirements. If the ramping capability is insufficient, extra generating units are needed to be online.

Ramp duration

Ramp duration (δ) is the duration of a curve's ramp along the time axis. The ramp duration shows how long the generators should be able to change their output at a specific ramp rate.

Energy

Energy (ϵ) is the integration of capacity over time and can be calculated as the area between the analyzed curve and the time axis. This indicates the energy needed to meet the net load/load following/regulation requirements (either positive or negative).

2.1.5.2 Performance Envelope II

Concept of a “Half-Cycle”

For time-domain signals with large ramps (either up/down), such as load following/regulation processes (Figure 2.3), the concept of a ‘half-cycle’ is first introduced in this work. In Figure 2.3, the curve consists of a series of data points with time stamps, including points 1,2,3...,8,9,...,20,...,30,...,36,... It can be observed that points 1, 8, 20, 30 and 36 are “turning points” representing either local maximum or local minimum in the curve. Half-cycle can be defined as a portion of curve starting from the current turning point to the next turning point. The idea of cycling analysis is designed to discover curve cycling characteristics. Cycling analysis can be performed yearly, monthly, daily or even hourly. By applying statistical analysis, similar patterns (e.g., ramping or capacity requirement) can be identified. This information can be used to assess the cycling cost, wear and tear, equipment life span, etc.

Half-cycle can contain many data points. Half-cycle can be determined by analyzing the sign of ramp (slope) at each point. If two subsequent points have the same ramp sign, they belong to one half-cycle. In Figure 2.3, points 1–8 have different ramping requirements, but the ramps at these points are all positive. Therefore points 1–8 belong to the same half-cycle (half-cycle 1). Similarly, points 9, ..., 20 belong to another half-cycle (half-cycle 2).

Let α be the ramp at a data point and the parameter ψ denote the half-cycle number. If point i belongs to half cycle Ψ_j , then at the next point ($i+1$) the following rules can be applied:

$$\text{if } \text{sign}(\alpha_{i+1}) = \text{sign}(\alpha_i) \text{ then } \{i, i+1\} \in \Psi_j, \psi_{i+1} = j \quad (2.8)$$

$$\text{if } \text{sign}(\alpha_{i+1}) \neq \text{sign}(\alpha_i) \text{ then } \{i+1\} \in \Psi_{j+1}, \psi_{i+1} = j+1 \quad (2.9)$$

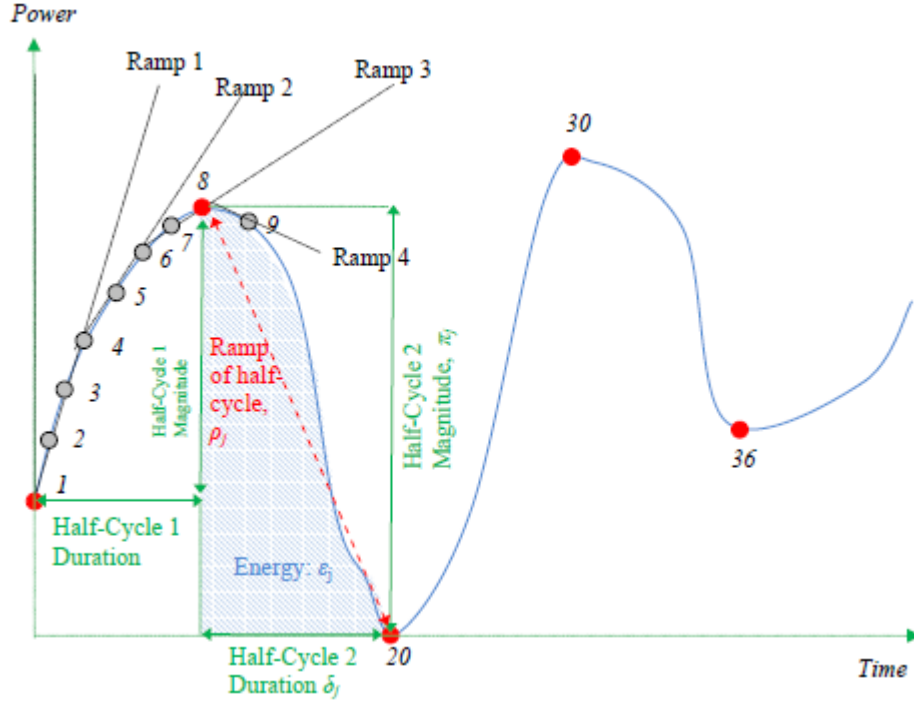


Figure 2.3. Cycling Analysis for a Time-Domain Signal

Features of a Half-Cycle

Half-cycle Ψ_j can be characterized by 5 important parameters:

Magnitude – π_j , ramp – ρ_j , duration – δ_j , energy – ϵ_j and frequency – θ_j

The magnitude π_j of half-cycle j can be calculated as:

$$\pi_j = P_j^{end} - P_j^{beg} \quad (2.10)$$

where P_j^{beg} is the capacity at the beginning of half-cycle j ;

P_j^{end} is the capacity at the end of half-cycle j ;

The duration δ_j of half-cycle j can be calculated as:

$$\delta_j = t_j^{end} - t_j^{beg} \quad (2.11)$$

where t_j^{beg} is the time stamp at the beginning of half-cycle j ;

t_j^{end} is the time stamp at the end of half-cycle j ;

The ramp ρ_j of half-cycle j can be calculated as:

$$\rho_j = \frac{\pi_j}{\delta_j} \quad (2.12)$$

The energy ε_j of half-cycle j can be calculated as:

$$\varepsilon_j = \int_{t_j^{beg}}^{t_j^{end}} p_j dt \quad (2.13)$$

where p_j is the power function of half-cycle j

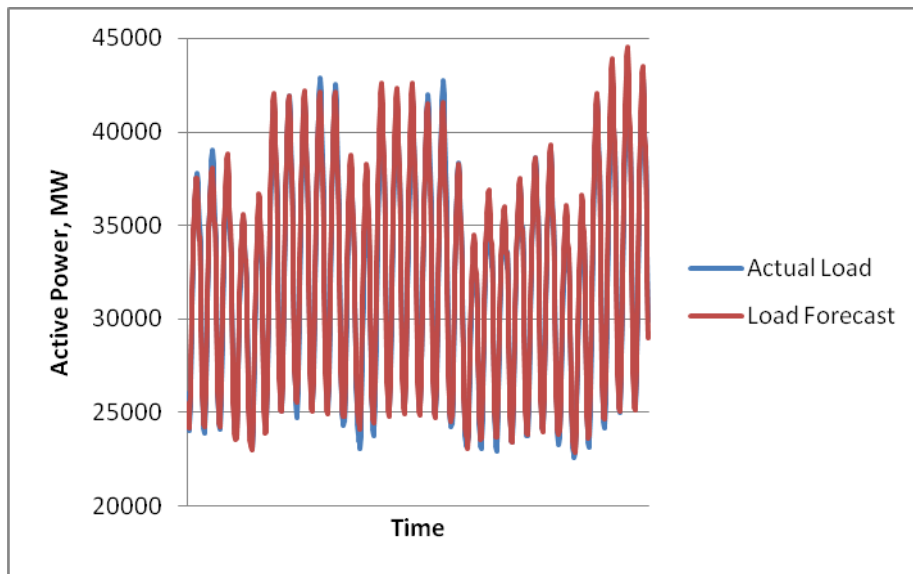
Half-cycle frequency θ_j is the main feature to be estimated over a period of time through statistical analysis, because it contains important information regarding how many times similar half-cycles can occur.

2.2 Imbalance Caused by Load or Generation Variation and Uncertainty

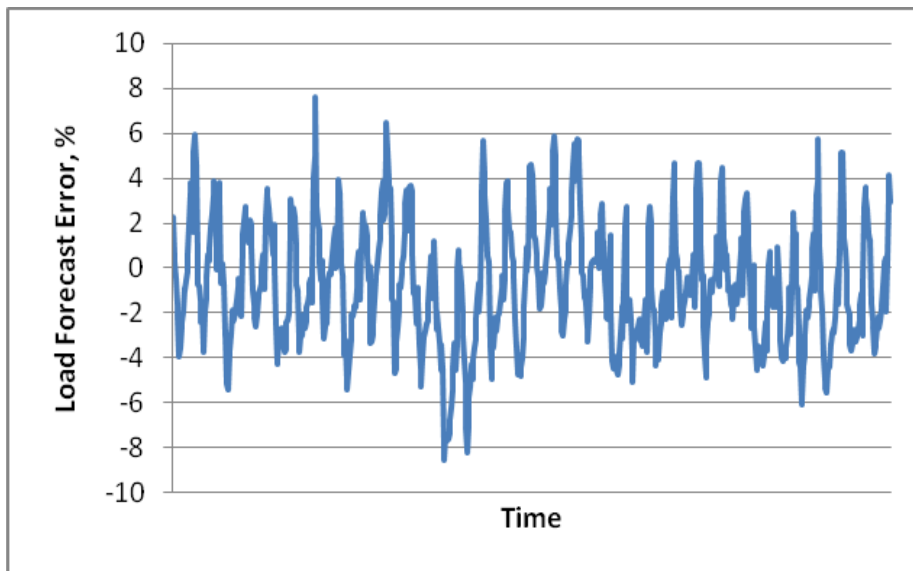
To be integrated with the unit commitment and economic dispatch processes, wind generation and load demand are assumed to be forecasted in three different time frames, i.e., day-ahead (DA), hour-ahead (HA), and real-time (RT). The DA forecast is produced for the 24 1-hour intervals of the following day. The HA forecast is updated each hour and the RT forecast is updated within the hour (e.g., every five minutes). In this subsection, variations associated with the load, wind and solar forecast and their forecast errors are analyzed.

2.2.1 Load variation, Predictability, and Prediction Errors

One of the most influential factors affecting the resulting uncertainty is the uncertainty associated with the load forecast. In Figure 2.4, the load forecast uncertainty and load forecast errors for one of the balancing authorities is shown. In Figure 2.4(a), the solid blue curve represents hourly demand over one month, while the red curve shows the day-ahead load forecast for the same time period. The load forecast error is illustrated in Figure 2.4(b). One can see that day-ahead load forecast errors vary within the $\pm 8\%$ range (Figure 2.4(b)). System load is normally more significant than wind or solar generation, therefore even if the load forecast is more accurate than the forecast for intermittent resources (in terms of percentage error), the MW values of the MW forecast errors can be quite comparable.



a)



b)

Figure 2.4. Load Fluctuation and Uncertainty: a) Load Forecast vs. Actual Load; b) Load Forecast Error

DA, HA and RT load forecast errors have the following characteristics. The distribution of the load forecast errors is usually “bell-shaped” and in this regards is similar to the Gaussian distribution. Significant autocorrelation exists in DA, HA and RT load forecast errors series between the t and $t-1$ values. There are cross-correlations between DA and HA load forecast errors and between HA and RT load forecast errors. RT load forecast errors are very highly concentrated near zero, with a few high error occurrences. The load forecast errors do not have “natural” bounds as the wind forecast errors, which are bounded by the wind farm capacity and zero. However, load forecast errors should be bounded using a fixed percentage, for example, $\pm 15\%$, which represents the maximum error to vary with the load. High load periods tend to have larger MW error because of the sensitivity of load forecasts to temperature forecasts.

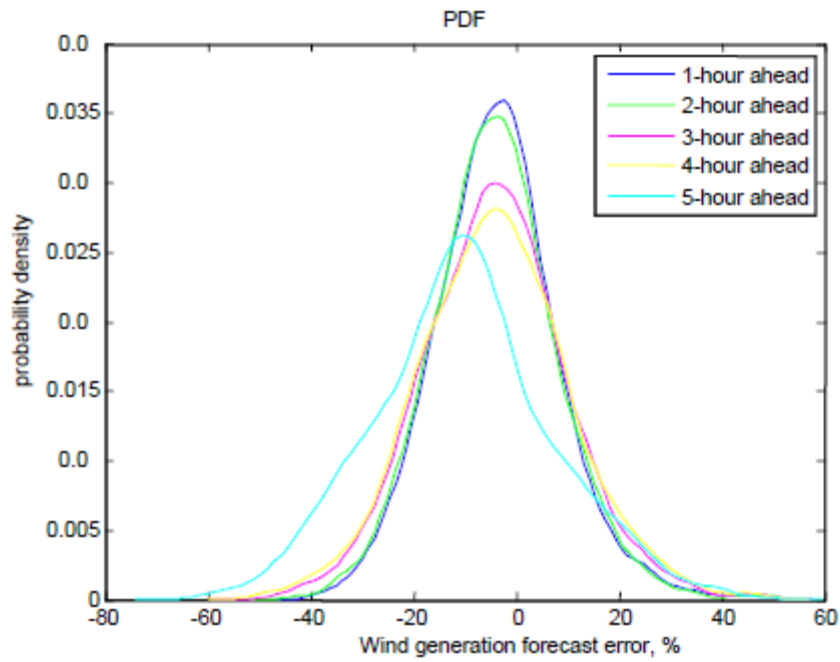
2.2.2 Wind and Solar Variation, Predictability and Prediction Errors

Wind/solar generation and load demand share a number of similar features such as:

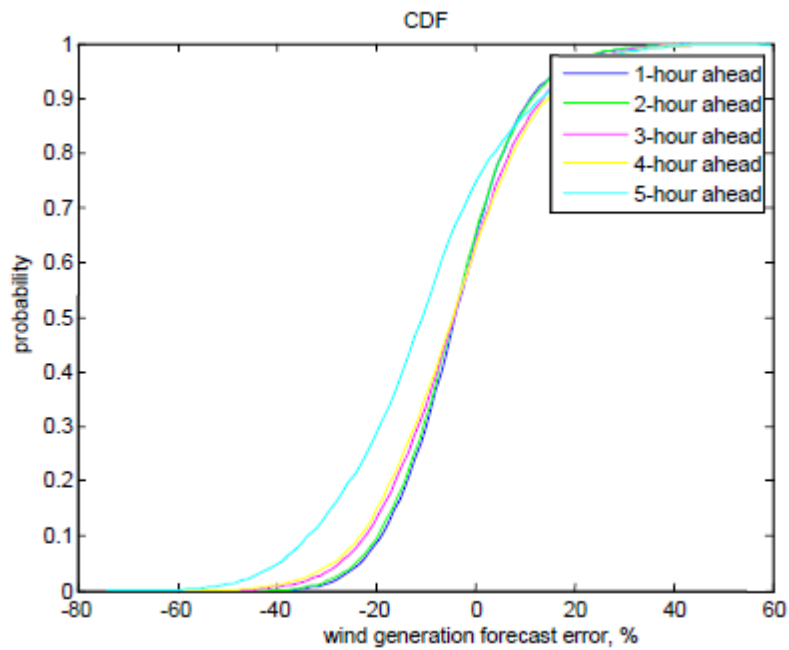
- Wind/solar generation and most of the load are non-dispatchable resources,
- They both have cycling behaviors,
- They both depend on weather conditions, and
- They deviate from the forecast.

2.2.2.1 Wind Forecast Errors

Actually, wind and solar generation has more in common with electrical load than with traditional (dispatchable) generation. Therefore, wind and solar generation can be considered as negative load. An example of wind generation forecast statistical characteristics for different look-ahead dispatch intervals (1, 2, 3, 4, and 5 hours ahead) for a real power system is presented in Figure 2.5. Figure 2.5 (a) shows the empirical PDF of the wind generation forecast errors and Figure 2.5 (b) shows the empirical CDF of the wind generation forecast errors.



a)



b)

Figure 2.5. Wind Generation Forecast Statistical Characteristic for Different Look-Ahead Period: a) PDF; b) Empirical CDF

Similar to the load forecast errors, the autocorrelation between t and $t-1$ time intervals and cross-correlation of the HA with RT and DA with HA wind forecast error time series are also significant. The RT wind forecast errors tend to have many very small errors and a few large errors. The DA and HA wind forecast error PDFs tend to be asymmetrical. The wind forecast errors are constrained by the available wind generation range. A reasonable forecast for wind generation must stay between zero and the capacity of the wind farms. At lower generation levels, the forecast errors tend to be positive, while they are more negative at higher production levels. Electrical load and wind/solar generation cannot be considered as independent statistical variables. The cross-correlation between load and wind generation forecast errors is shown in [30], [32]. The net load concept is commonly used in wind integration studies to assess the impact of load and wind generation variability on the power system operation. The net load has the following definition: net load is total electrical load minus total wind generation output minus total solar generation output plus the interchange, i.e.,

$$\begin{aligned} \text{Net Load} = & \text{Total Load} - \text{Total Wind Generation} - \text{Total Solar Generation} \\ & + \text{Interchange} \end{aligned} \quad (2.14)$$

Actual measured generation output from wind farms usually deviates from its forecast. Therefore, wind forecast error is usually calculated from the difference between the wind generation forecast and the measured actual wind generation. Typical wind forecast errors for single wind farm can vary quite significantly. Wind forecast error may also have offsetting effects on load demand forecast error by lessening or exacerbating the impacts of demand forecast error. In addition, wind forecast error could also have significant effect on the scheduling of intertie transactions, the spinning reserve generation, and day-ahead scheduling process [23].

To simulate forecast errors impacts, the actual forecast error is not always available. A simulated error should be used instead to evaluate its impacts on system performance characteristics.

The assumption used in this project is that the hour-ahead wind and solar generation forecast error distribution is an unbiased Truncated Normal Distribution (TND) (see Section 3.4.2 for details). A detailed description on the derivative of the PDF of the TND is provided in Appendix G.2.

The error limits used in the TND reflects the maximum and minimum wind or solar generation values. If the actual wind or solar generation P_a is limited by $P_{\min} = 0$ and P_{\max} , the forecast error limits can be found as follows:

$$\begin{aligned} \varepsilon_{\min} &= P_{\min} - P_a = -P_a \\ \varepsilon_{\max} &= P_{\max} - P_a \end{aligned} \quad (2.15)$$

2.2.2.2 Solar Generation Forecast Errors

The load and wind generation have strong autocorrelation between the subsequent samples of these errors. In some extent, this may be also the case for the solar power generation forecast error. The autocorrelation, if it is positive and significant, means that the forecast error is not “zigzagging” form significantly one sample to another, and that it has certain “inertia” associated with the error’s subsequent values. To reflect this fact while simulating the solar forecast error, the autocorrelation factor must be incorporated into these simulations.

For this project, we will use statistical characteristics of the hour-ahead and real time solar generation forecast errors. These models are complex and depend on various factors including the extraterrestrial solar radiation annual and daily patterns, hour-to-hour clearness index (CI), dynamic patterns of the cloud systems, types of solar generators (photovoltaic, concentrated thermal, etc.), geographical location and spatial distribution of solar power plants, and other factors. This section reflects our best effort to build an adequate solar generation model in view of very limited information about the subject both generally and specifically to this project. A detailed description on Clearness Index is provided in Appendix G.3.

Unlike wind generation, the solar generation is limited by the extraterrestrial solar irradiance level, changing over a day. The maximum possible generation can be achieved at $CI = 1$, and this maximum value $P_{max}(t)$ also changes over a day following a similar mostly deterministic pattern (note that there is also an annual component in this process). Variances of the generation under these conditions can be only caused by diffused solar irradiance and ambient temperature variations. Assuming that these variances are also included in $P_{max}(t)$, the maximum solar generation during the daytime can be described as a function of time, and is always less than the total capacity, i.e.,

$$SG_a(t) \leq P_{max}(t) \quad (2.16)$$

where $P_{max}(t)$ is the maximum solar generation capacity, and is a function of time.

The solar forecast $f(t)$ has the relation of:

$$P_{min}(t) \leq f(t) = SG_a(t) - \varepsilon(t) \leq P_{max}(t) \quad (2.17)$$

where the minimum solar capacity $P_{min}(t)$ could be assumed to be zero; the maximum capacity of solar farm generation $P_{max}(t)$ is a function of time. During the night time,

$$f(t) = SG_a(t) = \varepsilon(t) = 0 \quad (2.18)$$

From (2.17) we have,

$$SG_a(t) - P_{max}(t) \leq \varepsilon(t) \leq SG_a(t) \quad (2.19)$$

where $SG_a(t) - P_{max}(t)$ may be negative or zero.

Different patterns of solar generation in day time and night time need to be considered in the prediction of solar forecast errors. The solar forecast errors in night time are zero because there are no solar irradiance, thus the solar generation is zero. The sunrise and sunset time are different in different seasons at different regions, as well as the daily patterns of the CI. The previous years' information regarding this matter can be categorized and used for the solar forecast error prediction.

Depending on different time period of a day and weather conditions, the solar forecast errors can show different patterns, such as (1) the forecast error is zero, $\varepsilon = 0$, at night time; (2) the forecast error is small or close to 0, $\varepsilon \rightarrow 0$, on sunny days, that is when $CI \rightarrow 1$; and (3) the forecast error is limited or close to zero under heavily clouding conditions, that is when $CI \rightarrow 1$, and (4) the forecast error varies in a wide range for the intermediate values of CI .

Thus, the standard distribution of the solar forecast errors can be described as a function of the parameter CI , $0 \leq std_{\min} \leq std(\varepsilon) = f(CI) \leq std_{\max}$. Figure 2.6 shows possible distribution of standard deviation of solar forecast errors depending on the CI .

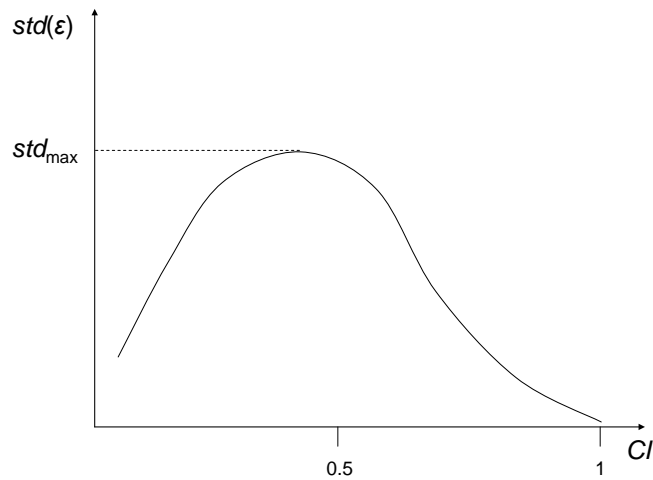


Figure 2.6. Distribution of the Standard Deviation of Solar Forecast Error Depending on the CI

In a sunny day, the variation of the forecast errors is in a shape shown in Figure 2.7(a). The forecast error can be predominantly negative. If the sky is covered with clouds, the distribution of solar forecast error could be like in Figure 2.7(b). The forecast error can be predominantly positive.

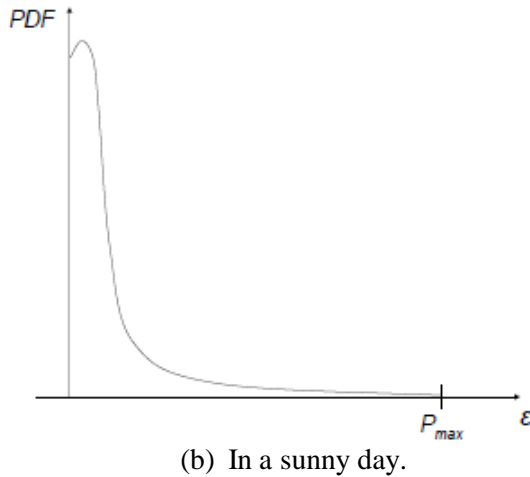
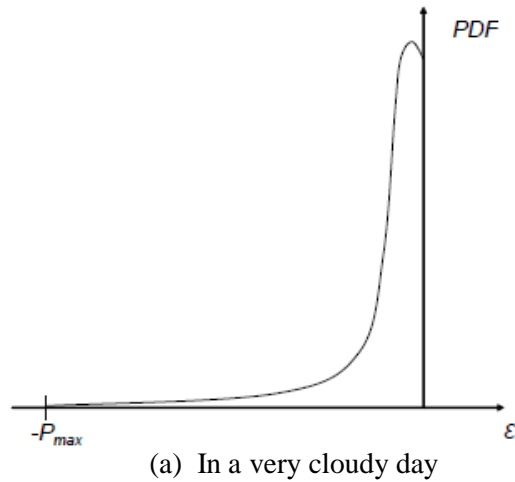


Figure 2.7. Distribution of Solar Forecast Error in a Very Cloudy Day and a Very Sunny Day

The persistence model is used for real-time wind forecast. But for solar, there are obvious incremental pattern in solar generation during morning hours just after sunrise and decremental pattern in solar generation during evening hours just before sunset. The solar generation could increase or decrease dramatically in a very short period of time in the sunrise or sunset hours. This will cause significant ramps during sunrise or sunset hours. The persistence model cannot address this concern. Therefore a new model based on the CI is proposed for real-time solar forecast errors. The detailed steps used to generation real-time solar forecast is provided in Appendix G.4.

The proposed real-time solar forecast model takes into account the solar radiation condition at $(t - 7.5)$ minute². Therefore the incremental and decremental patterns on solar generation at sunrise and sunset hours are reflected in the proposed model. The proposed real-time solar forecast model is applied to each solar generation profile, i.e., photovoltaic solar, distributed photovoltaic solar, solar thermal, and outstate solar thermal. Then the overall real-time solar generation forecast profile is calculated by accumulating all the real-time solar forecast of different solar profiles.

² The 7.5 minute lead is selected base on assumption that the RT forecast is provided 7.5 minutes before a 5-minute dispatch interval.

The hourly average CI is used in hour-ahead solar generation forecast model. The hourly average CI can be calculated by:

$$CI(h) = \frac{\overline{P}_a(h)}{\overline{P}_{\max}(h)} \quad (2.20)$$

where: $\overline{P}_a(h)$ is average actual solar generation in the h -th hour,
 $\overline{P}_{\max}(h)$ is average ideal solar generation in the h -th hour for $CI=1$.

The detailed description on the hour-ahead solar forecast model is provided in Appendix G.5. The CI is divided into different levels. For different levels of CI, different standard deviations are applied to the solar forecast errors. Table 2.1 shows an example of the standard deviations of solar forecast errors corresponding to different CI levels. The percentage number of total solar generation capacity is used to represent the standard deviations of solar forecast errors. For example, 5% means the standard deviation for the CI level in the range of (0, 0.5] is 5% of the capacity of the solar generation profile.

Table 2.1. Standard Deviations of Solar Forecast Errors Based on CI Levels

CI	σ_{HA}
$0 < CI \leq 0.5$	5%
$0.2 < CI \leq 0.5$	20%
$0.5 < CI \leq 0.8$	15%
$0.8 < CI \leq 1.0$	5%

2.3 Scheduling Procedure to Maintain Balance

Each BA is responsible to maintain generation–load balance within its balancing area, support scheduled interchange with other BAs and system frequency.

Usually, the processes of achieving the balance between generation and load demand consist of day-ahead schedule, hour-ahead schedule, real time dispatch and AGC regulation.

In order to match the supply and demand of electricity, the independent system operators (ISOs) operate several markets prior to the actual operating interval. Each market utilizes latest available information.

Different ISOs utilize somehow different operating and scheduling practices. To analyze the possible benefits of BA cooperation and consolidation options, these practices should be reflected in the analysis. To illustrate scheduling process, the CAISO market process is presented [5] as following.

2.3.1 Scheduling Process

CAISO runs different schedules in their Day Ahead Market and Real Time Market in order to make sure that the energy, reserves including regulating up and down reserves and ramp requirement are met in real time operation. The CAISO scheduling process includes Day-Ahead Market (DAM) and Real-Time Unit Commitment (RTUC), Short-Term Unit Commitment (STUC) and Real-Time Economic Dispatch (RTED).

Figure 2.8 represents the CAISO generation schedules. In the DAM, the forecast of the CAISO's hourly demand is done for three days in advance. The Day-Ahead schedule is an hourly blocked energy schedule that includes 20-minute ramps between hours. It is provided at 10 a.m. the day prior to the operating day. CAISO Day-Ahead Market flowchart is shown in Figure 2.9 [6].

The real-time schedule is based on STUC/RTUC timelines (Figure 2.10) [7]. The Real Time Market (RTM) closes 75 minutes before the actual beginning of an operating hour as shown in Figure 2.10. RTED is provided 7.5 minutes before the dispatch operating target (DOT) and is based on real-time forecasts. Symmetrical ramping is used which means that by dispatching for the average, the DOT ends in the center of the interval. In the RTM, the CAISO Automatic Load Forecasting System (ALFS) provides a load forecast for each 15-minute and 5-minute intervals.

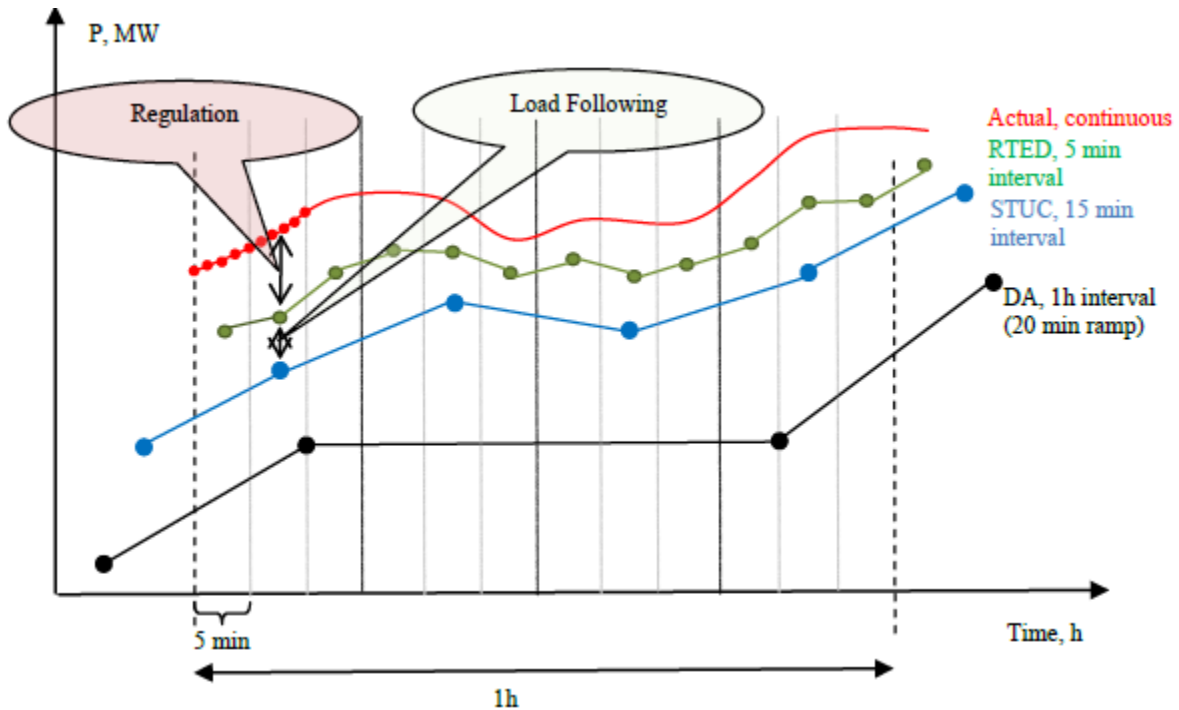
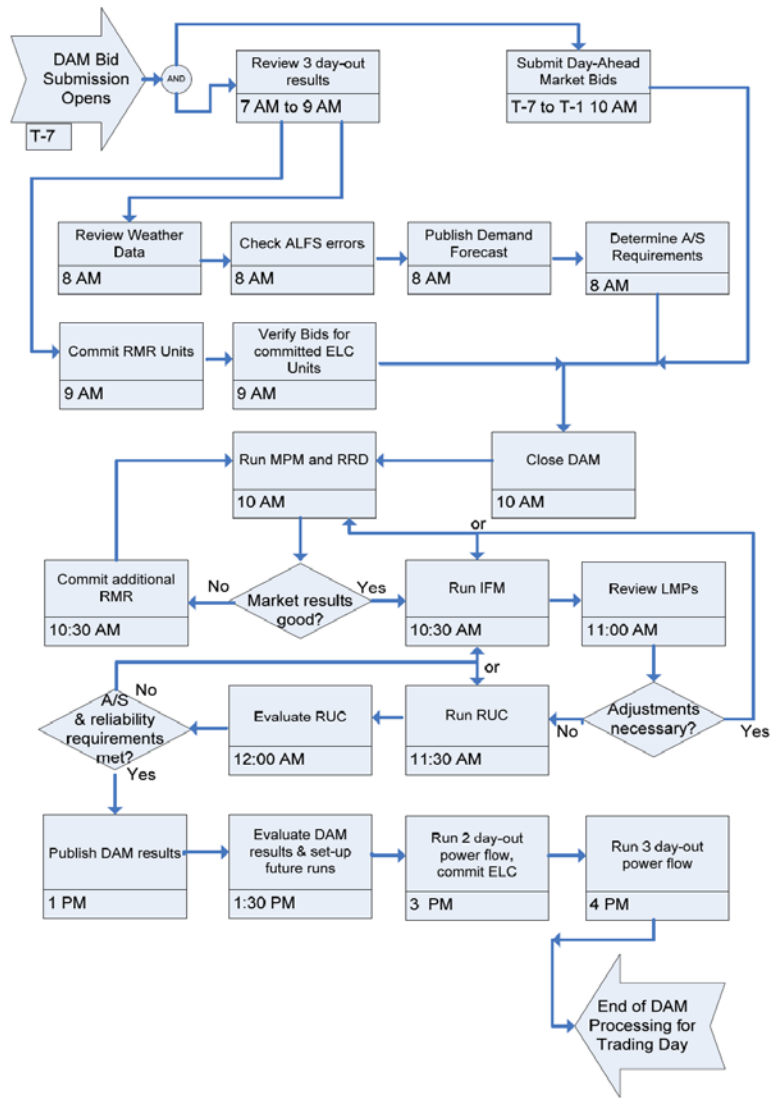
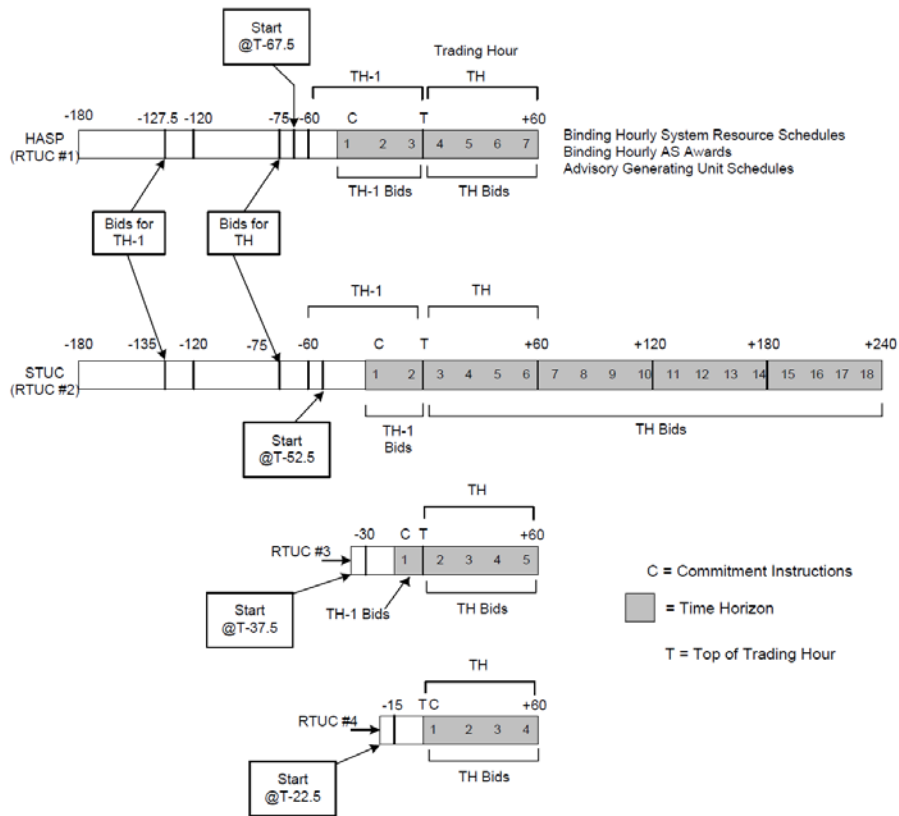


Figure 2.8. CAISO Generation Schedule



* Picture Source [6]

Figure 2.9. CAISO Day-Ahead Market Flowchart



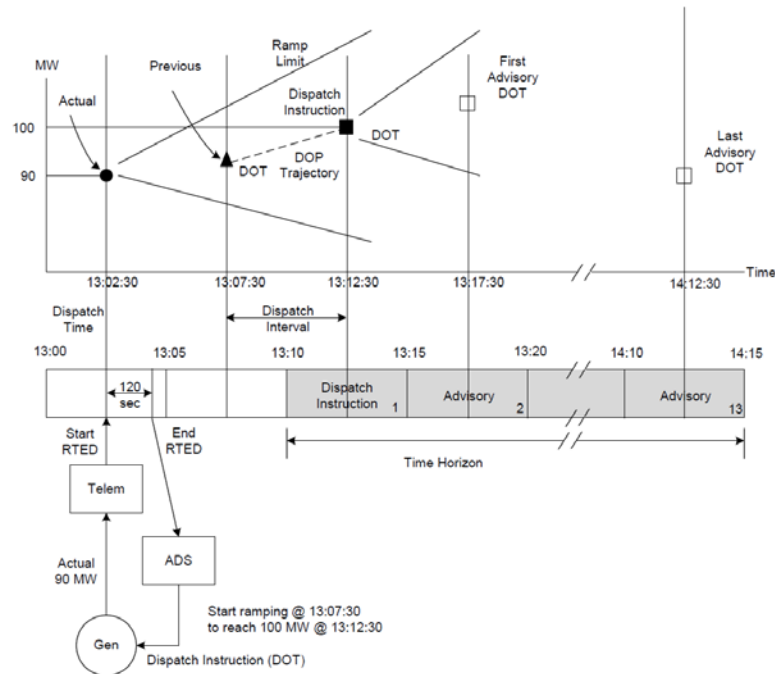
* Picture Source [7]

Figure 2.10. CAISO Real-Time Scheduling Process Flowchart

2.3.2 Load Following

Real-time dispatch is also known as load following or supplemental energy dispatch. Within each operating hour, ISO continues to adjust generator operating points every five minutes.

The CAISO real-time economic dispatch process flowchart is presented in Figure 2.11 [7]. The RTED process runs every five minutes to meet the imbalance energy requirements of the CAISO. This process looks ahead 65 minutes. RTED results are five-minute dispatch instructions and advisory notice for the look-ahead timeframe. RTED is the lowest granularity of dispatch in the ISO market, except for regulating reserves, which is procured in the RTM, but is dispatched through the EMS AGC system every 4 seconds.



* Picture Source [7]

Figure 2.11. CAISO Real-Time Economic Dispatch Process

2.3.3 Regulation

Every 4 seconds the ISO adjusts the output of specific generators based on its ACE and frequency deviation values.

AGC/Regulation is the online, synchronized, generation capacity that is available to respond to the ISO’s AGC control signals on a second-by-second basis [9]. This capacity enables continuous balance of generation and load within the ISO-controlled grid, and maintains frequency during normal operating conditions. Generating units offering regulation services must be capable of being controlled by the ISO AGC system).

2.3.4 Frequency Response

The new WECC Frequency Responsive Reserves standard is under development [56], [58].

The purpose of the Frequency Response Standard (FRS) is to assure that balancing authorities are able to arrest frequency decline and support Interconnection frequency during a frequency deviation resulting from a loss of generation [56]. Frequency Responsive Reserve is the measurement of the reserves’ quality and might be a subset of Contingency Reserve.

The frequency response is needed to prevent deviations in system frequency from nominal frequency. The deviation in system frequency is a result of the imbalance between generation and load

The frequency controls utilized by BA’s are grouped according to three criteria:

1. Primary controls are fast-acting controls that contribute to achieving an energy balance following loss of generation output. These controls are effective over the period 0 to 20 seconds. Primary frequency control (response) is achieved through:
 - a. Generating unit governor response, which includes the generator inertia — which responds instantaneously then the movement of the governor valves based on the governor settings such as set-point control. Governor response occurs in the 3 to 10 second time frame.
 - b. Frequency dependent loads (the load value will decrease due to the decrease in frequency). The time frame is within 3 to 20 seconds following the disturbance, e.g., contingency.
2. Secondary controls are synchronous resources that are available to restore the frequency to 60 Hz following the actions of the primary controls. These resources are effective over the 1 minute to 15 minute period and include regulating reserves (under AGC), spinning reserves, and dispatchable demand response. These resources should be capable of fast ramping within the 10 to 15 minute time frame. In the absence of effective secondary control, the system will operate at a new steady-state frequency that is slightly less than the system nominal frequency based on the characteristics of the primary control. That could result in unscheduled flows on the tie-lines and will lead to penalized accumulations of Area Control Error (ACE). An illustration of the primary and secondary frequency responses is shown in Figure 2.12.

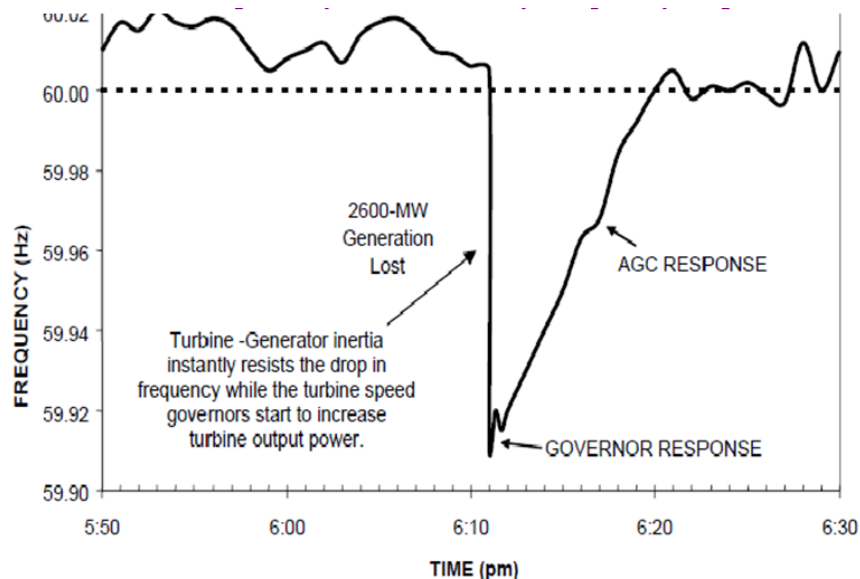


Figure 2.12. An illustration of Primary and Secondary Frequency Responses. (This graph is taken from the report “Frequency Control Concerns In The North American Electric Power System) ORNL/PNNL report December 2002)

3. Tertiary controls are those resources that are available to restore the resources used for Secondary Control. These resources can be effective over the period 15 minutes and longer and include generation redispatch, non-spinning reserves, and storage controls. If after the tertiary frequency response, the system is still experiencing low frequency, the BA may have to perform load shedding to protect the system integrity.

2.3.5 Governor Speed Droop Compensation

The control of generating unit governor is designed so that the unit speed drops as the load is increased. The relation between change in frequency (unit speed) and change in output power is known as the speed-droop characteristic as shown in Figure 2.13 where the droop characteristic is adjustable from 0% to 5%. The droop is defined as the percentage frequency change that will cause a 100% change in generator power. A 5% droop means that a 5% frequency deviation causes 100% change in output power. The relationship can be adjusted by changing the set point at which the generating unit is operated at its synchronous speed. Figure 2.13 shows three different characteristic lines. At, 60 Hz, characteristic A results in zero output power, characteristic B results in 50% output power, characteristic C results in 100% output power.

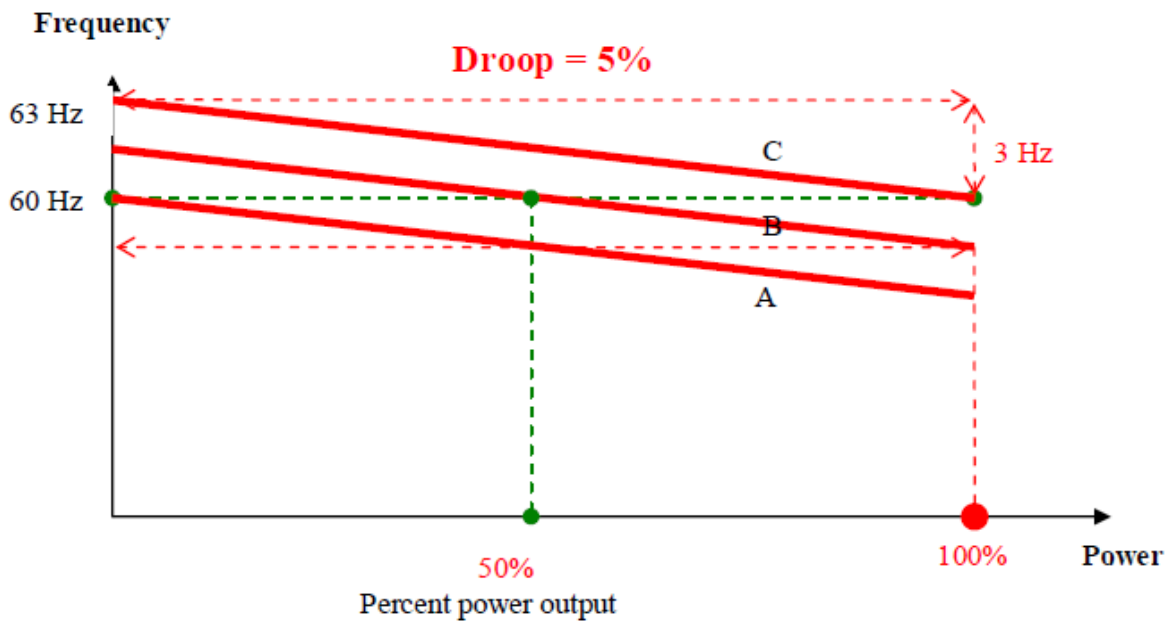


Figure 2.13. An Illustration of Generator Droops

The droop characteristic is used for local, autonomous control response to frequency variations. For example, if the load increases and all generators have the same droop setting, then each will pick up the incremental load in proportion to their nominal power ratings. That will cause a change in power output at each generator. The system dispatch center monitors frequency error and, after some time, will adjust the generators to bring the accumulated frequency error back to zero.

2.3.6 Inertial Responses

As mentioned in the frequency response section, the generating unit inertia is an important factor for primary frequency response. The energy stored in the large rotating mass will prevent the sudden change in frequency due to large mismatch between load and generating power. In other words, the large amount of rotating mass in the power system helps in keeping the system stable after disturbances.

There are currently few BAs that require generating units to have certain inertia constant. For example, HydroQuebec states that a generator may be required to have an inertia constant “compatible” with other generators on the system, as determined through the system impact study. It is expected for the

system inertial response to decline with high penetration of wind turbines where generating units mass are much smaller, distributed and in some cases buffered from the grid through full DC/AC inverters

2.4 Structure of System Reserves

To ensure the balance between generation and demand power grid must maintain the system operating reserve. Figure 2.14 shows the structure of system reserves. Operating reserve can be spinning and non-spinning. Spinning reserve is used for regulation (regulating reserve) and to ensure system reliability in case of contingency (contingency reserve). Regulating reserve units receive control signals (every 4 second) from AGC system. Contingency reserve must be at least 50% spinning and must be activated in 10 minutes.

High penetration level of renewable resources, especially, wind and solar generation increases requirements to operating reserve due to uncertainty and variability of the renewable generation. For instance, sudden wind rumps (up or down) can cause significant imbalance of the system. To handle such events system needs to have more fast-response generating units in reserve.

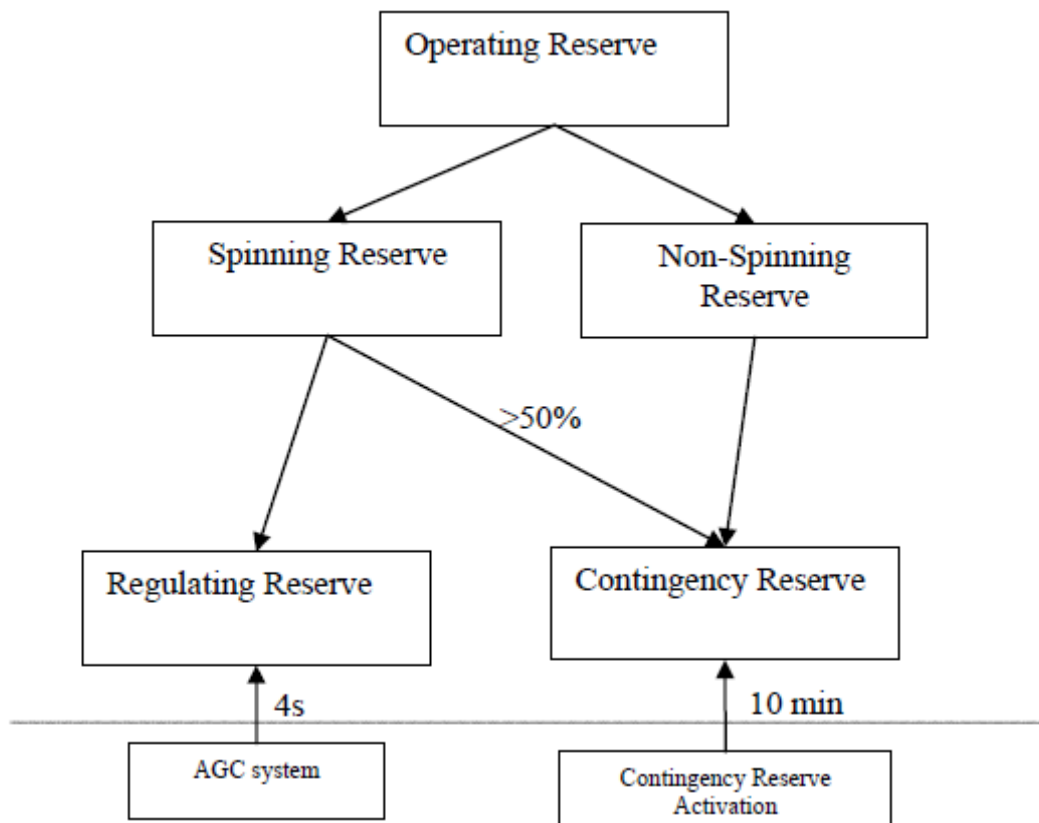


Figure 2.14. Structure of System Reserves

NERC/WECC Disturbance Control Performance Standard gives the following definitions of system reserves [38]:

Operating Reserve - That capability above firm system demand required providing for regulation, load forecasting error, equipment forced and scheduled outages, and local area protection. It consists of Spinning Reserve and Non-spinning Reserve.

Spinning Reserve - Unloaded generation that is synchronized, automatically responsive to frequency deviations and ready to serve additional demand. It consists of Regulating Reserve and Contingency Reserve.

Non-spinning Reserve – 1. That generating reserve not connected to the system but capable of serving demand within a specified time. 2. Loads or exports that can be removed from the system in a specified time.

Regulating Reserve – An amount of reserve responsive to automatic generation control, which is sufficient to provide normal regulating margin.

Contingency Reserve – The provision of capacity available to be deployed by the BA to meet the NERC and WECC contingency requirements.

Contingency reserve shall be at least greater than [38]:

- The loss of generating capacity due to forced outages of generation or transmission equipment that would result from the most severe single contingency (at least half of which must be spinning reserve); or
- Five percent of the balancing authority requirements load as calculated by the balancing authority's Energy Management System (EMS) (at least half of which must be spinning reserve).

In general, the generation capacity allocation is shown in Figure 2.15.

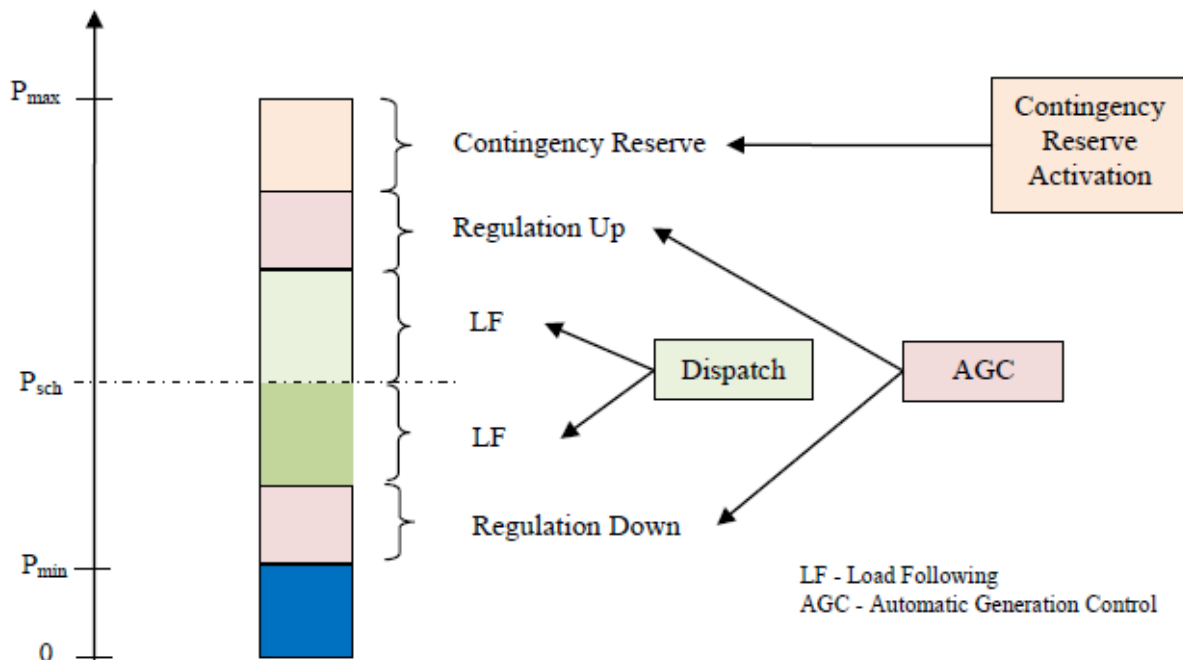


Figure 2.15. Allocation of Generation Unit Capacity

2.5 Dynamic Scheduling and Pseudo-Ties

Dynamic scheduling and pseudo-ties allow a Load Serving Entity (LSE) or generator to move via telemetry some or all of its demand and/or generation from its host BA control area and place it in

another-BA control area. Thus, the control area balances to this load and/or generation as though it was physically in that control area [59].

The electronic transfer of generation and/or a load can be implemented in one of two ways: The creation of a pseudo-tie, or by dynamic scheduling [59]:

Dynamic Scheduling is the service that provides for the real-time metering, telemetering, computer software, hardware, communications, engineering, and administration required to electronically move a portion or all of the energy services associated with generation or load out of the control area to which it is physically connected and into a different control area.

Pseudo-tie occurs when two control areas' AGC are electronically linked and the transfer of generation and/or load is treated as a new point of interconnection (pseudo-tie), but for which no physical tie or energy metering actually exists, between the two Control Areas. In this case, the actual interchange term in the ACE equation are adjusted, rather than the scheduled interchange terms. The application of a pseudo-tie is also used to replace static or manual scheduling for load and base loaded generating resources.

Dynamic schedules of generation and/or loads between two BAs are implemented when [59]:

- An entity desires automatic generation control (AGC) of its remote resources,
- The host control area for a joint ownership project cannot accommodate a significant difference between the participants actual generation entitlement versus its schedule,
- An entity desires to serve customer loads located in another control area, or
- Parties desire to move load regulation responsibilities from one control area to another.

Dynamic schedules are currently evaluated as a possible option to implement different BA consolidation and cooperation schemes. In particular, they are considered as opportunities to integrate more renewable resources in a control area or to bring more ancillary services to a control area.

3.0 Methods of BA Cooperation

This chapter describes some perspectives on how BA cooperation should be evaluated. BAs are connected by transmission lines. The transmission lines allow BA to share load and generation to maintain balance. The amount of required balancing reserves can be reduced through BA cooperation. BA cooperation allows BAs to decrease balancing requirements by averaging out some variation of loads and variable generation.

The impact of wind power on BA's operation depends on a number of factors, including wind penetration level, composition of generation fleet, size, interconnection and transmission capacity of the control area, load following interval, wind forecast accuracy, etc.

One of the most effective measures to mitigate the operational impacts of wind generation intermittency and load variability is the cooperation among BAs to make use of a broader geographical distribution of generating resources.

“Both load and wind power generation variability benefit from the statistics of large numbers, as they are aggregated over larger geographical areas. Load diversity reduces the magnitude of the peak load with respect to the installed generation. Similarly, geographical diversity of wind power is expected to reduce the magnitude and frequency of the tails on the variability distributions. As a result, the amount of engaging time and capacity needed for running expensive regulation reserves can be reduced by the cooperation among BAs” [27].

This can be illustrated through the following statistical example. Assume that there are two BAs sharing their ACEs. The ACEs can be treated as random variables, and the correlation between the ACEs is normally low. Then, the expected total ACE standard deviation before sharing can be represented as $\sigma(ACE_A) + \sigma(ACE_B)$. The expected total ACE standard deviation after sharing can be represented as $\sigma(ACE_A + ACE_B)$. Here $\sigma(\bullet)$ is the operation for calculating standard deviation. Note that

$$\begin{aligned}
 & \sigma(ACE_A + ACE_B) \\
 &= \left\{ \sigma^2(ACE_A) + \sigma^2(ACE_B) + 2\rho_{AB}\sigma(ACE_A)\sigma(ACE_B) \right\}^{1/2} \\
 &= \left\{ \left[\sigma(ACE_A) + \sigma(ACE_B) \right]^2 + 2\rho_{AB} - 1 \sigma(ACE_A)\sigma(ACE_B) \right\}^{1/2} \\
 &\leq \sigma(ACE_A) + \sigma(ACE_B)
 \end{aligned} \tag{3.1}$$

where ρ_{AB} is the correlation coefficient between ACE_A and ACE_B .

The inequality is derived based on the property that $-1 \leq \rho_{AB} \leq 1$. Assume that $\sigma(ACE_A) = 80$ MW and $\sigma(ACE_B) = 110$ MW. Figure 3.1 shows the $\sigma(ACE_A + ACE_B)$ plotted against the correlation coefficient ρ_{AB} . It can be observed that the $\sigma(ACE_A + ACE_B)$ changes from 30 to 190 MW. For $-0.2 \leq \rho_{AB} \leq 0.2$, $\sigma(ACE_A + ACE_B)$ changes from 122.4 to 148.4 MW, which is much less than $\sigma(ACE_A) + \sigma(ACE_B) = 190$ MW. This example shows that a simple ACE sharing can help reduce the expected total ACEs.

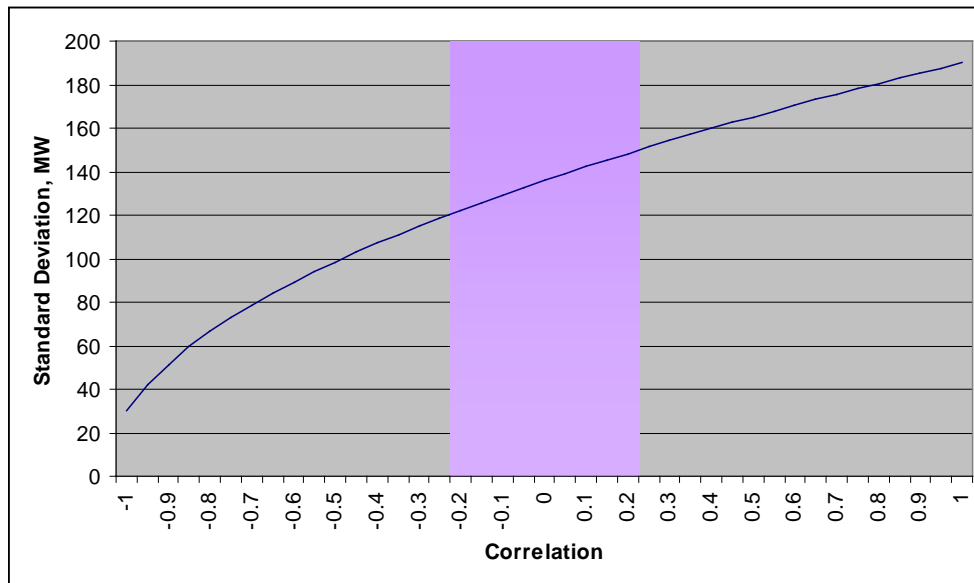


Figure 3.1. Example of Variability of Aggregated ACE

3.1 Approaches Used for BA Consolidation

Currently several different approaches regarding BAs coordination are being considered or already implemented:

- ACE sharing or ACE diversity interchange (ADI) [43], [4] and [12]

The main idea of ADI is to reduce the regulation needed to balance the system through ACE sharing among multiple BAs, compared to isolated operation. Relaxed control can be achieved because of the sign diversity (some ACEs are net positive or over-generating relative to load and some are net negative or under-generating relative to load) among area control errors.

- Regulation and Load Following sharing

Regulation (load following) sharing idea is similar to the idea of ACE sharing. Due to control action sign diversity, the relaxed control is achieved through sharing of regulation (load following) signals rather than ACEs. Another option is to provide regulation services to several BAs by single unit [30].

- Dynamic Scheduling [59]

Dynamic Scheduling is used to provide balancing services from one BA to another by telemetry, which allows the receiving BA to control the generation or load in the sending BA as if it were physically in that BA.

- Actual BA consolidation

The main idea of BA consolidation is consolidating several BAs into a single consolidated BA.

- Wind-only BA [34]

Unlike traditional BA that includes generating units and load, wind-only BA includes only wind generation. Wind-only BAs could incorporate wind generators distributed over a large geographical region to benefit from the geographical diversity factor. The wind-only BA is responsible for controlling

the interchange of its control area with the other BAs to follow a pre-determined interchange schedule. BAs' control performance is mandated by NERC and WECC Control Performance Standards. Wind-only BA is required to provide internal balancing reserves or purchase those services from external resources.

3.2 Potential Benefits of BA Cooperation

As stated above, there are several approaches to implement the cooperation between different balancing authorities. With careful design and implementation, it is expected that the geographical diversity factor across a wide area in a power system can help to achieve many potential benefits, from the perspectives of exchanging energy services, sharing balancing burdens and providing emergency support to enhance power system control performance and reliability. Such benefits can be directly reflected as the savings in the required regulation reserves, load following dispatch stack, ramping capability and so forth.

Thus, establishing cooperation among BAs potentially can bring the following benefits to electrical utilities:

- Reducing regulation reserve requirements
- Reducing load following requirements
- Reducing regulation reserve ramping requirements
- Reducing regulation energy expended for balancing process
- Improving control performance indices
- Reducing wear and tear of generating units

In general, with sufficient diversity of load and renewable characteristics, the sum of either loads or wind power outputs and associated forecast errors in different BAs can be averaged out to certain extent, resulting in less amount of balancing efforts. For example, if one BA requires 100 MW ramping up capability to meet the increasing regulation obligation, another BA can require 30 MW ramping down action for the same time period. If these two BAs cooperate with each other, the total amount of regulation will be $100-30=70$ MW, which is a great amount of savings in required ramping capability. More generally, various benefits of BA cooperation are further summarized as follows:

3.2.1 Reduction in Balancing Burdens

By enabling the intra-zonal transfers among BAs within a large geographical area, the balancing burdens of certain BAs can be easily transferred to neighboring BAs. At the same time, the total amount of system balancing burdens is also expected to be significantly reduced due to such diversity. Based on different time frames, balancing services can be further characterized as scheduling, load following and regulation, as introduced in Section 2.3. The actual balancing actions for different services include several key factors, ramp magnitude, ramp ratio, ramp duration, and energy requirement.

The following figures provide several examples of the savings for system balancing obligations after cooperation is in place (the analysis was conducted by PNNL for several real BAs in the WECC system considering opportunities of BA consolidation). Figure 3.2 shows the savings in the total amount of scheduling capacity in a system within 24 operating hours during a season. It provides insight information regarding how much generation level that a system needs to prepare in order to serve the changing loads. A very clear improvement can be observed that the generation peak is systematically

reduced and the valley is systematically higher with BA cooperation. Figure 3.3 shows huge savings in the amount of load following capacity for 24 operating hours. If different BAs are operating their system individually, the total amount of load following capacity is much higher than the case with BA cooperation. Similarly, Figure 3.4 gives the savings in system regulation obligation. It is worth to mention that the savings in system balancing services can also be applied for the ramp rate of such services, as shown in Figure 3.5. In addition, the frequency of ramping action including incremental/up and decremental/down can be reduced, which will help to reduce the tear and wear of generation units and lengthen their service life. In fact, there are several factors including the diversity of load and wind characteristics of different balancing authorities and level of forecast errors that may affect the actual savings in the above aspects. More details will be discussed in Section 4.5, where a balancing authority consolidation case study is demonstrated.

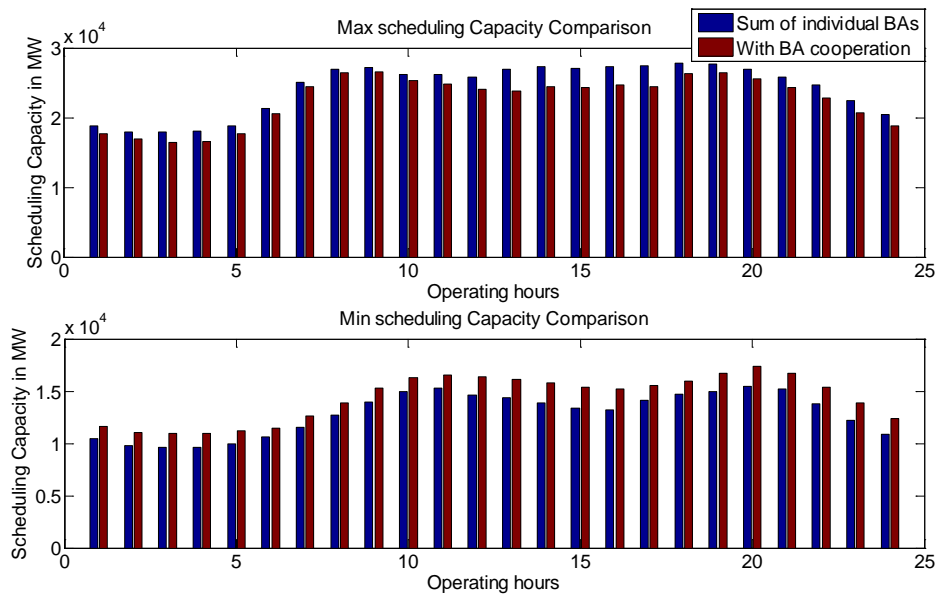


Figure 3.2. Benefits in System Scheduling Process

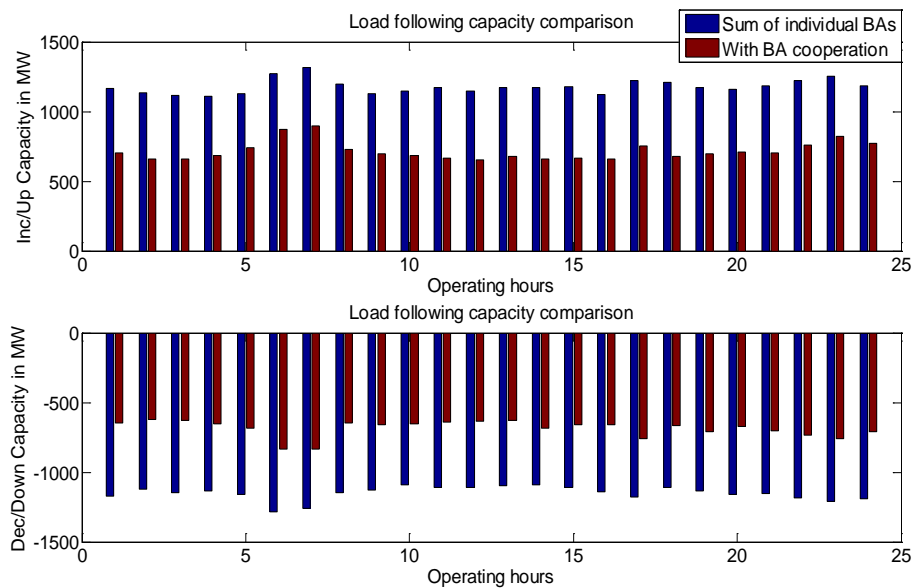


Figure 3.3. Benefits for Load Following Capacity

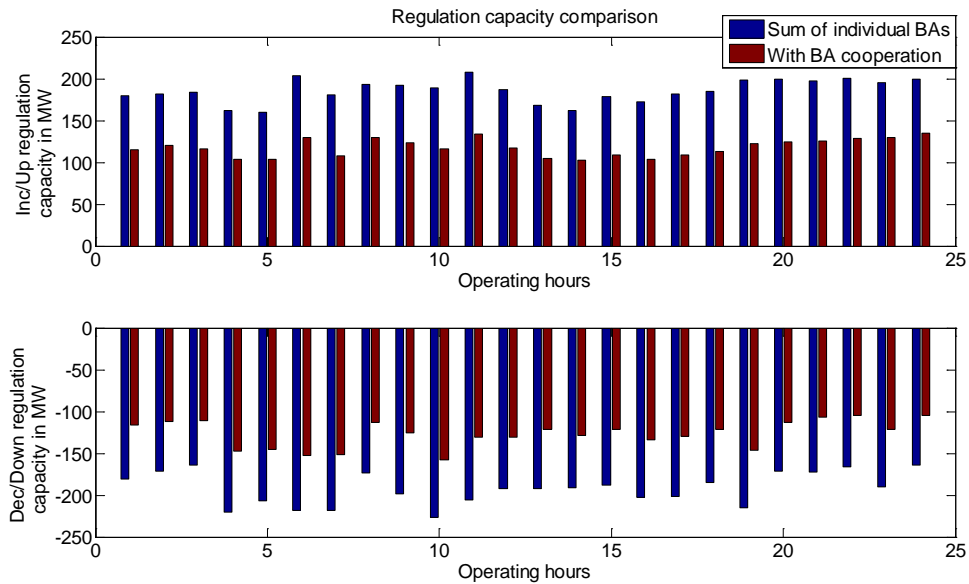


Figure 3.4. Benefits for Regulation Capacity

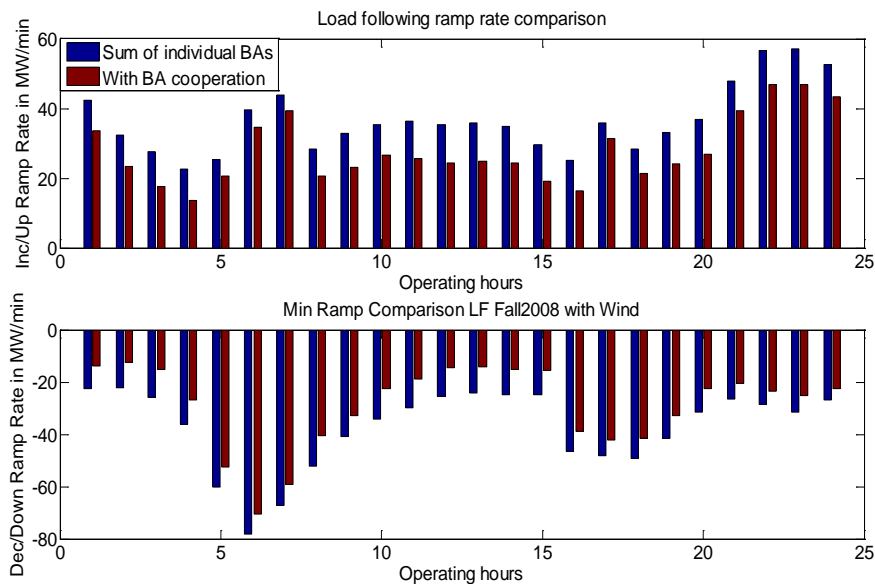


Figure 3.5. Load Following Ramp Rate Savings

3.2.2 Meeting Renewable Portfolio Standards' Goals

Establishing cooperation among BAs not only can relieve balancing burdens, but also make it possible to increase the penetration of renewable energy like wind and solar even if certain BAs have very limited renewable resources (Figure 3.6). For the past few decades, more and more focus has been placed on finding ways to increase the penetration of clean and renewable energy into power grid, according to the RFP's goals like the 33% requirement in California by 2020. However, the distribution of renewable energy resource is uneven. For some balancing authorities with insufficient renewable resources, purchasing renewable energy from external resources becomes an option to increase their renewable penetration. On the other hand, for those balancing authorities with abundant wind or solar, the system balancing burdens are also increased accordingly. In this case, such BAs may not need to provide for for

a very large additional amount of balancing services to be able to balance the system by themselves. Seeking support from outside system is also a feasible and beneficial option to accomplish this goal.

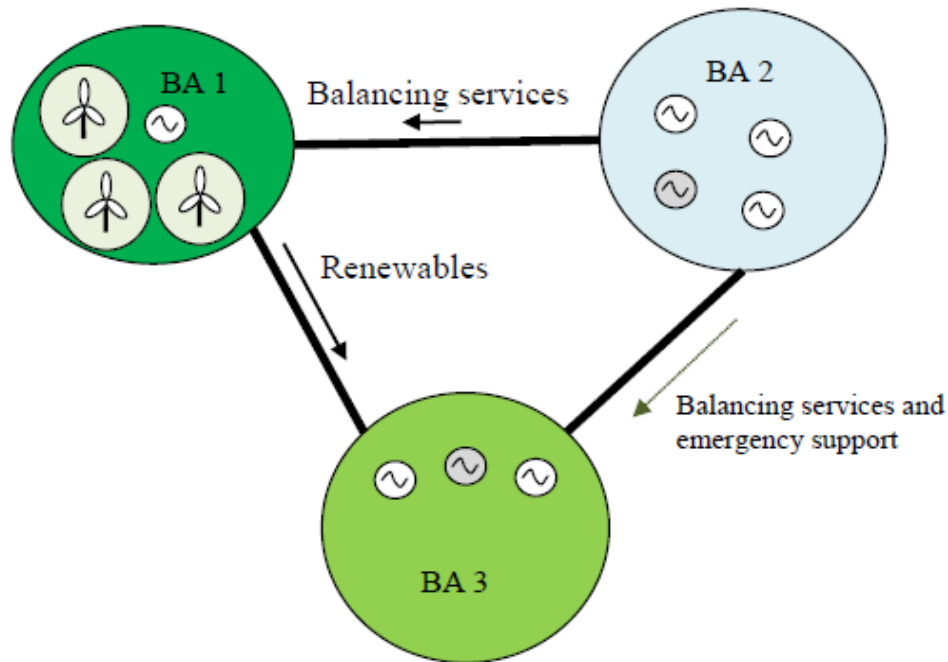


Figure 3.6. Idea of BA Cooperation

3.2.3 Security and Reliability Enhancement

The cooperation of different BAs can provide emergency support at extreme conditions, which can help to improve system stability and reliability. With efficient information exchange between BAs, it is expected to greatly reduce the possibility of large scale blackout by properly coordinating control actions. A much better view of system health will be available and it can help to handle emergency cases with great flexibility. In addition, the cooperation in unit commitment and scheduling process can help to optimize system available resources and reduce the total operating cost. System operational profiles can be improved in terms of control performance standards as well.

3.3 Potential Challenges

Establishing BA cooperation can also create some problems to the power system, especially, to the transmission network.

3.3.1 Congestion Problem

Figure 3.7 illustrates the congestion problem that can be caused by BA coordination. In case of cooperation between BA1 and BA3 through the transmission path 1–3 can flow additional unscheduled active power. If the transmission capability of transmission path 1–3 is not sufficient it can lead to unpredicted congestion problems. An example of congestion problems, created by massive amounts of wind generation, can be found in Germany, where wind generation variations in the 50 Hertz Transmission GmbH (one of four German Transmission System Operators) area cause transmission system violations on the German-Polish border [2].

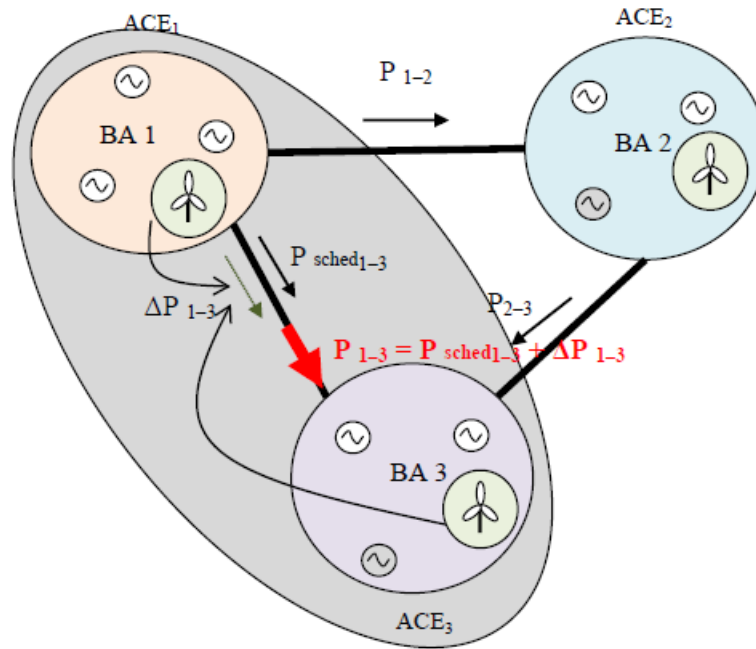


Figure 3.7. Congestion Problem Illustration

3.3.2 Loop flows

Figure 3.8 illustrates the loop flow problem that can be caused by BA coordination. For instance, consider wind generation, which geographically belongs to BA1, operated by BA3 through dynamic scheduling. It can create unscheduled power flow through neighboring BAs: ΔP_{1-2} and ΔP_{2-3} (Figure 3.8). Loop flows created by wind generation in Germany create loop flows in Poland and the Czech Republic [2]. Countries that are neighboring western Germany have protected themselves from loop flows by using phase shifting transformers.

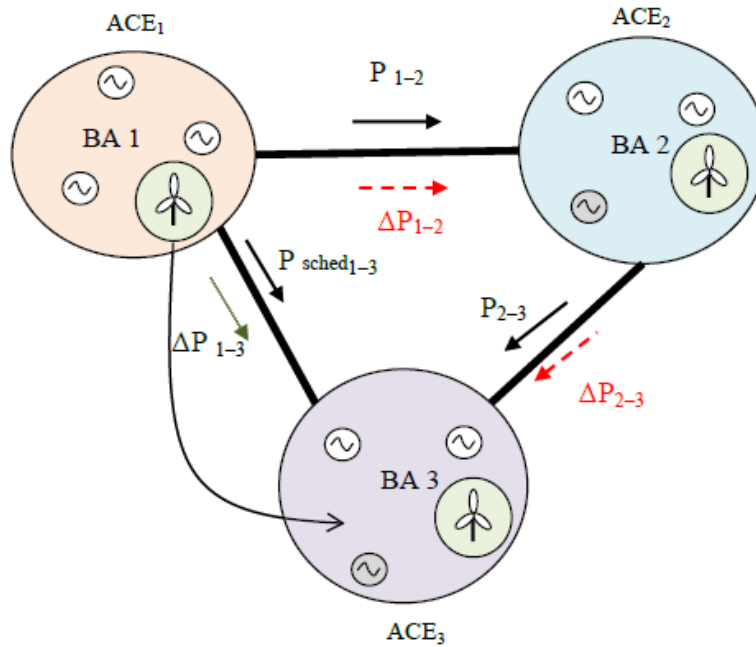


Figure 3.8. Loop Flow Problem Illustration

3.3.3 Inadvertent Interchange

Each BA in a grid conforms to a schedule that sets forth how much capacity will be allowed to pass through the area at given times of the day. These schedules are normally set a day in advance. However, a certain amount of energy will normally pass through over or below the scheduled amount. This unscheduled energy accumulation is referred to as inadvertent interchange, and less is normally considered better. [41]

Inadvertent energy balancing refers to the accounting and settlement procedures that control areas follow on a daily basis to account for these differences. When one control area is "owed" energy from another due to inadvertent interchange, the difference is usually repaid in energy, not in cash. [41]

NERC standard [37] defines a process for monitoring BAs to ensure that, over the long term, BA areas do not excessively depend on other BA areas in the interconnection for meeting their demand or interchange obligations.

3.4 Methodologies Developed to Evaluate and Compare the Performance of BA Cooperation Methods

3.4.1 Load Following and Regulation Assessment

Load Following is understood as the difference between the hourly energy schedule including 20-minute ramps (shown as the red line in Figure 3.9) and the short-term five-minute forecast/schedule and applied "limited ramping capability" function (the blue line in Figure 3.9). This difference is also shown as the blue area below the curves.

Regulation is interpreted as the difference between the actual generation requirement and the short-term 5-minute dispatch shown in Figure 3.9 as the red area between the blue and green lines.

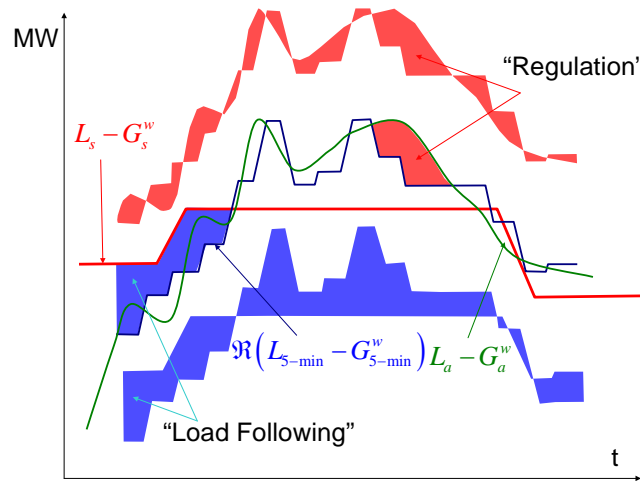


Figure 3.9. Separation of Regulation From Load Following Based on Simulated Hour-Ahead Schedule

By simulating hour-ahead and five-minute schedules for load and hour-ahead schedules for wind generation, regulation can be separated from load following. The schedule/forecast based approach uses the short-term forecasts of wind generation and load, $G_{rf,5min}^{w,y}$ and $L_{rf,5min}^y$. In this case, the following formulas can be used:

$$\Delta G^r(m) = L_a^y(m) - G_a^{w,y}(m) - L_{rf,5min}^y(m) + G_{rf,5min}^{w,y}(m) \quad (3.2)$$

$$\Delta G^{lf}(m) = L_{rf,5min}^y(m) - G_{rf,5min}^{w,y}(m) - L_{ha,1hr}^y(m) + G_{ha,1hr}^{w,y}(m) \quad (3.3)$$

3.4.2 Forecast Error Modeling

In this subsection, a methodology to model load forecast errors and wind generation forecast errors is described. The models for the forecast errors will be used whenever the actual forecast errors are not available. An approach is developed to simulate the hour-ahead and real time forecast errors based on their statistical characteristics including their standard deviation, autocorrelation, and cross-correlation between the forecasts. The approach produces time sequences for various forecast errors that mimic the real errors.

3.4.2.1 Truncated Normal Distribution

The assumption used in this approach is that the distribution of hour-ahead forecast errors is an unbiased Truncated Normal Distribution (TND) (Figure 3.10). This truncation is based on the fact that values of a normally distributed random variable can, in theory, be any value over the range from $-\infty$ to $+\infty$. Without truncation, the use of the normal distribution may lead to significant simulation errors. Meanwhile, the characteristic parameters (i.e., mean ε_0 and standard deviation σ) of a truncated normal distribution can be readily derived using basic statistical methods.

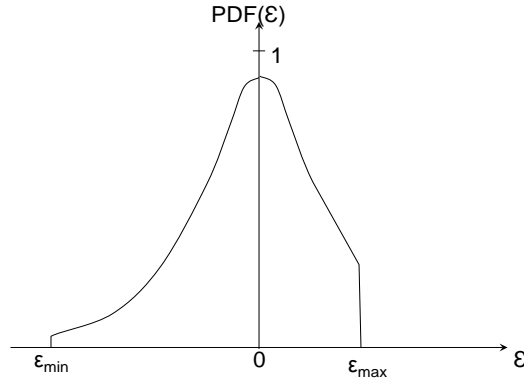


Figure 3.10. Doubly Truncated Normal Distribution Model for Forecast Errors

The Probability Density Function (PDF) of the doubly truncated normal distribution (shown in Figure 3.10) is expressed by the following formula:

$$PDF_{TND}(\varepsilon) = \begin{cases} 0, & -\infty \leq \varepsilon < \varepsilon_{\min} \\ \frac{PDF_N(\varepsilon)}{\int_{\varepsilon_{\min}}^{\varepsilon_{\max}} PDF_N(\varepsilon) d\varepsilon}, & \varepsilon_{\min} \leq \varepsilon < \varepsilon_{\max} \\ 0, & \varepsilon_{\max} \leq \varepsilon < +\infty \end{cases} \quad (3.4)$$

where ε_{\min} and ε_{\max} are the lower and the upper truncation points respectively, and $PDF_N(\varepsilon)$ denotes the PDF of the standard normal distribution, which can be specified as:

$$PDF_N(\varepsilon) = \frac{1}{\sqrt{2\pi\sigma^2}} e^{-\frac{1}{2}\left(\frac{\varepsilon-\varepsilon_0}{\sigma}\right)^2}, \quad -\infty \leq \varepsilon \leq +\infty \quad (3.5)$$

where ε_0 refers to mean and σ is standard deviation of the normal distribution.

3.4.2.2 Load Forecast Error Model

The load forecast error is modeled as a random quantity, represented by the load forecast error average value and its standard deviation.

Hour-Ahead Forecast

The hour-ahead load forecast error is the difference between the average actual load over an operating hour and the hour-ahead load schedule. This error is denoted as $\varepsilon_{L,ha}$. The hypothesis concerning the TND distribution of $\varepsilon_{L,ha}$ is confirmed by the analyses of the actual hour-ahead error similar to the one provided in Figure 3.11. The mean absolute percent error (MAPE) of the hour-ahead load forecast usually stays within 2%.

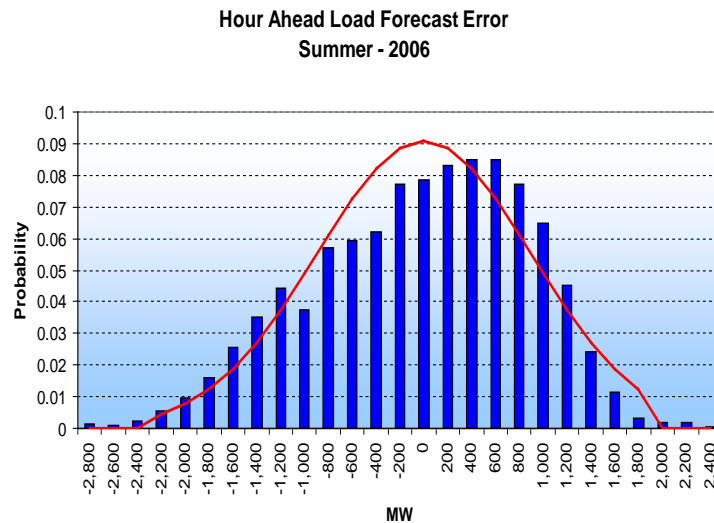


Figure 3.11. Hour-Ahead Load Forecast Error Distribution (Actual PDF vs. the Normal Distribution PDF)

By analyzing the actual data, the average, maximum, minimum values and standard deviation of the relevant variables can be obtained. It is assumed that the same statistical characteristics of the hour-ahead load forecast error will be observed in the future, including autocorrelation and cross-correlation of the forecast errors.

It was also assumed that the same statistical characteristics of the real-time load forecast error will be observed in the future years. The standard deviation of the real-time load forecast error is $\sigma_{L,rtf}$.

Real-Time Load Forecast

The real-time load forecast error is the difference between the average actual load over a five minute interval and the real-time load schedule.

For example, the CAISO utilizes a Very Short Term Load Predictor (VSTLP) program to provide an average load forecast for the interval $[t, t+5]$ 7.5 minutes before the beginning of the interval or 10 minutes before the middle point of this interval. The VSTLP program uses real-time telemetry data to generate the forecast.

After analysis, average, maximum, minimum values and standard deviation of the relevant variables are obtained. The standard deviation and autocorrelation of the real-time load forecast error is based on statistical analysis of historical data.

3.4.2.3 Wind Generation Forecast Error

Similar to load, the simulated wind generation forecast error is assumed to be a TND quantity, represented by the wind-power average error value (zero) and its standard deviation.

Hour-Ahead Forecast Error

It is assumed that the hour-ahead wind generation forecast is incorporated into the BA's scheduling system. It is assumed that the hour-ahead wind generation forecast error is distributed according to the TND law. The characteristics are obtained from statistical analysis of historical data.

Real-Time Forecast Error

Real-time wind generation forecast is neither provided nor included into the real-time dispatch process. It is assumed that the naïve persistence model is implicitly used.

3.4.2.4 Area Control Error Model

The BA's operations control objective is to minimize its Area Control Error (ACE) to the extent sufficient to comply with the NERC Control Performance Standards (see Chapter 2.0). Therefore, the ideal regulation and load following signal is the signal that opposes deviations of ACE from zero when it exceeds a certain threshold:

$$\begin{aligned} -ACE &= -(I_a - I_s) + \underbrace{10B(F_a - F_s)}_{\text{Neglected}} \\ &\approx G_s - L_s - G_a + L_a \rightarrow \min \end{aligned} \quad (3.6)$$

where I_a denotes net interchange (MW flow out of the control area); I_s refers to scheduled net interchange; B is area frequency bias constant; F_a and F_s are actual and scheduled frequency respectively. Impacts of wind generation on the interconnection frequency are neglected. This is a valid assumption given the large interconnection (>140GW peak load in the WECC system), which frequency deviates very small amounts with normal imbalances. The generation component of the ACE equation can be represented as follows:

$$G_s = G_{ha} + G_{ha}^w \quad (3.7)$$

$$G_a = G_s + \Delta G^{lf} + \Delta G^r + \Delta G^w + \Delta G^{ud} \quad (3.8)$$

where ha denotes the hour-ahead generation schedule; lf denotes instructed deviations from the hour-ahead schedule caused by generators involved into the load following process; r denotes instructed deviations caused by generators involved into the regulation process, ΔG^{lf} and ΔG^r are the deviations of the regulation and load following units from their base points, ΔG^w is the deviation of the wind generators from their schedule (wind generation real-time schedule forecast error), and ΔG^{ud} is the total deviation of generators from the dispatched instructions. ΔG^{ud} is simulated similarly to the load forecast error (random number generator based on TND).

The total deviation of generators from dispatch instructions for the conventional units that are not involved in regulation and load following can be represented as follows:

$$\Delta G^{ud} = G_a - G_{ha} \quad (3.9)$$

$$\Delta G^w = G_a^w - G_{ha}^w \quad (3.10)$$

$$\Delta L = L_a - L_{ha} \quad (3.11)$$

Since the control objective is $ACE \rightarrow 0$,

$$\Delta G^{lf} + \Delta G^r = \Delta L - \Delta G^w - \Delta G^{ud} \quad (3.12)$$

where ΔL is the deviation of the actual load from its real-time scheduled value (load forecast error).

The above equations are written for instantaneous values of ΔL , ΔG^w and ΔG^{ud} . Therefore, the statistical interaction between the load forecast error and the wind generation forecast error is fully preserved. The load and wind generation errors can vary depending on the wind generation penetration level within a BA area and the accuracy of the load forecast compared to the accuracy of the wind generation forecast. Since the percent wind generation forecast error is more significant than the percent load forecast error, the former may have a considerable impact on $\Delta G^{lf} + \Delta G^r$.

Wind generation would have no impact on regulation and load following requirements if

$$\Delta G^w = 0$$

Therefore, we have following expression for the combined load following and regulation requirement

$$\Delta G^{rlf} = \Delta G^{lf} + \Delta G^r = \Delta L - \Delta G^{ud} \quad (3.13)$$

3.4.2.5 Simulation of Future Scenarios and Data Set Generation

This subsection provides a detailed description of the applied modeling techniques for describing the stochastic behavior of the driving variables, i.e., hour-ahead and real-time load forecast and wind generation forecast error.

Actual Load

If actual data is available for year 2007, for a future study year $2007+i$, the actual annual load curve can be simulated as the year 2007 load multiplied by the i -th power of the annual load growth factor:

$$L_a^{2007+i} = (1 + \gamma)^i \times L_a^{2007} \quad (3.14)$$

The actual one-minute resolution load data is used for this study. The annual load growth factor i is to be set by the BA.

Hour-Ahead Load Schedule Model

The scheduled load is the one-hour block energy schedule that includes 20 minute ramps between the hours (Figure 3.12). It is calculated based on the load forecast error using the following approach. The hour-ahead load schedule $L_{ha,1hr}^{2007+i}$ is simulated based on the actual load and the expected load forecast error $\varepsilon_{L,ha}$:

$$L_{ha,1hr}^{2007+i} = \mathfrak{R}_{20} \left\{ avg_{1hr} \left(L_a^{2007+i} \right) - \varepsilon_{L,ha} \right\} \quad (3.15)$$

where $\varepsilon_{L,ha}^{\min} \leq \varepsilon_{L,ha} \leq \varepsilon_{L,ha}^{\max}$, $\varepsilon_{L,ha}^{\max} = 3\sigma_{L,ha}$ and $\varepsilon_{L,ha}^{\min} = -3\sigma_{L,ha}$, and the operator \mathfrak{R}_{20} adds 20 minute linear ramps to the block energy load schedule.

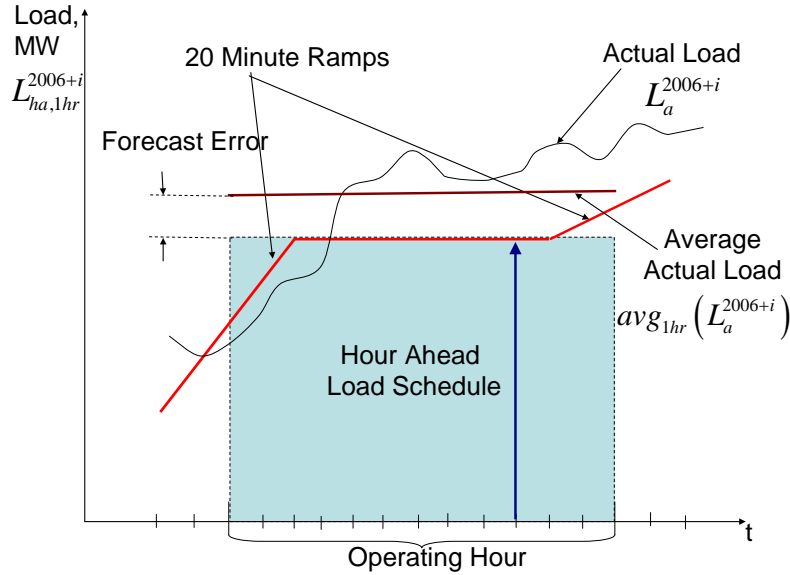


Figure 3.12. Simulated Hour-Ahead Load Schedule (Red Line)

The error is simulated using a TND random number generator based on the statistical characteristics of the load forecast error (for instance, derived from the year 2007/2008 data). The simulated error distribution applied to the hour-ahead schedule is shown in Figure 3.13.

Based on these specified values, a random number generator is used to generate values of $\varepsilon_{L,ha}$. For each operating hour, the random values of $\varepsilon_{L,ha}$ are substituted into simulated load forecast expression to produce the simulated hour-ahead load schedule. It is assumed that the load error distribution is *unbiased* for $PDF_N(\varepsilon)$, that is $\varepsilon_0 = 0$, and $\varepsilon_{L,ha}^{\min}, \varepsilon_{L,ha}^{\max}$ correspond to the minimum and maximum forecast errors specified for this study. Based on the above approach, hour-ahead load scheduling can be simulated for any season and year.

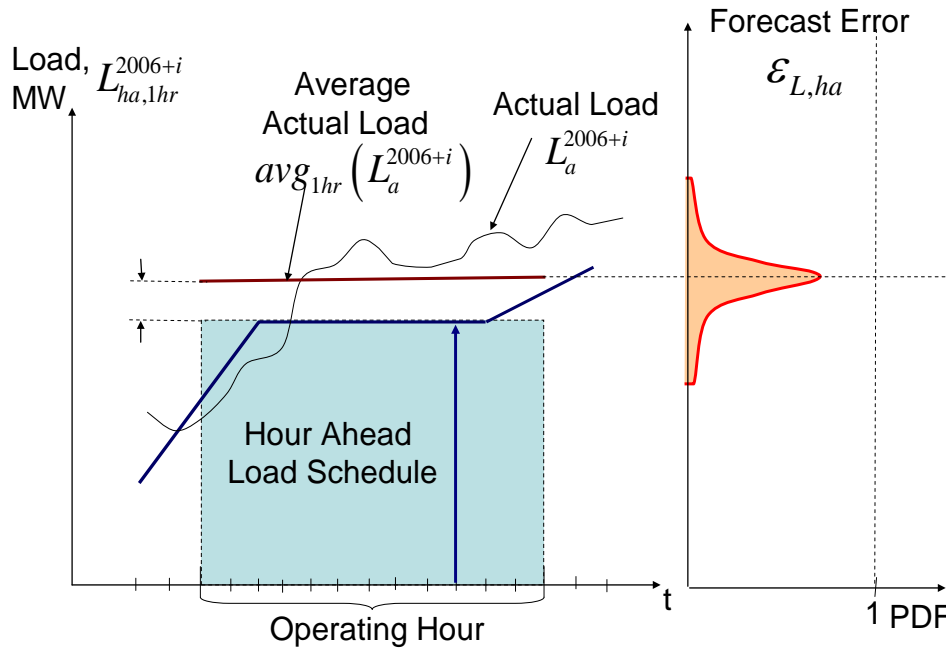


Figure 3.13. Probability Density Function (PDF) of the Load Forecast Function (Red Line)

Real-Time Load Forecast

The real-time load forecast is the average five-minute load forecast, that includes five-minute ramps between the hours (Figure 3.14). The real-time load forecast $L_{rf,5min}^{2007+i}$ is simulated based on the actual load and the expected load forecast error $\epsilon_{L,rf}$:

$$L_{rf,5min}^{2007+i} = \mathfrak{R}_5 \{ avg_{5min} L_a^{2007+i} - \epsilon_{L,rf} \} \quad (3.16)$$

where $\epsilon_{L,rf}^{\min} \leq \epsilon_{L,rf} \leq \epsilon_{L,rf}^{\max}$; and the operator \mathfrak{R}_5 adds 5-minute ramps to the block energy load schedule.

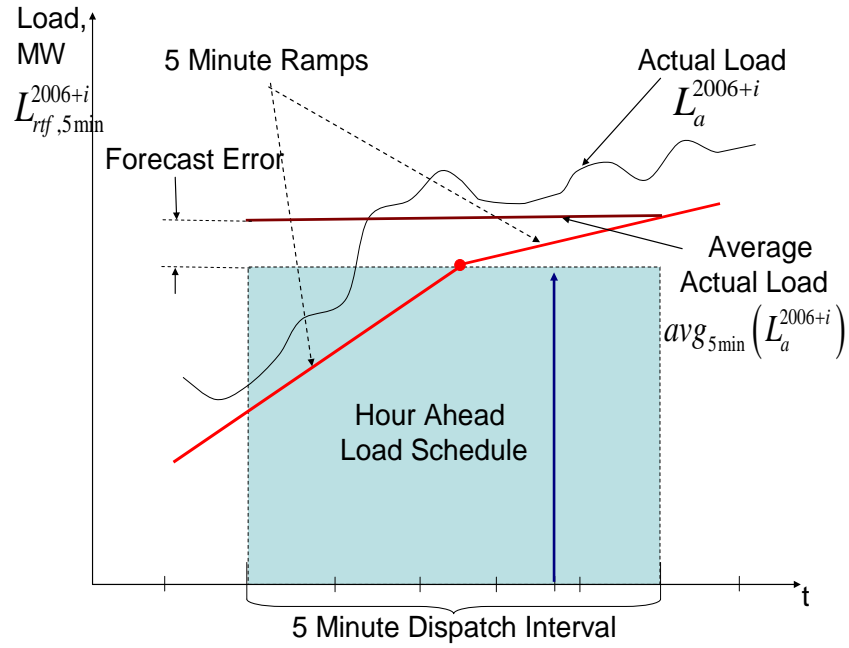


Figure 3.14. Simulated Real-Time Load Forecast (Red Line)

The error is simulated using a random number generator based on the statistical characteristics of the real-time load forecast error. Based on these specified values, a random number generator will be used to generate values of $\varepsilon_{L,rtf}$.

Wind Generation Hour-Ahead Scheduling Model

Reliable wind data are essential for a detailed wind assessment. Wind generation data was developed by combining a previous energy output scenario with the short term variability from current wind plants.

Wind generation hour-ahead schedules are simulated using the wind generation model described above and wind generation forecast error model described below. Similar to the load hour-ahead schedule and real-time load forecast models, the wind generation schedules and forecasts can be simulated for the hour-ahead scheduling and real-time dispatch time horizons as follow:

Wind generation schedule model $G_{ha,1hr}^w$ for the real-time scheduling process (hourly block energy forecast schedule) is as follows:

$$G_{ha,1hr}^{w,2007+i} = \mathfrak{R}_{20} \left\{ avg_{1hr} \left(G_a^{w,2007+i} \right) - \varepsilon_{w,ha} \cdot CAP^{w,2007+i} \right\} \quad (3.17)$$

The wind generation forecast error is expressed in % of the wind generation capacity, $CAP^{w,2007+i}$. Operator $\mathfrak{R}_{20} \{ \dots \}$ adds 20-minute ramps between the hours; $\varepsilon_{w,ha}$ is the simulated hour-ahead wind generation forecast error. This error is generated with the help of *unbiased* TND random number generator. The TND has the following characteristics:

1. Parameters $\varepsilon_{w,ha}^{\min}$, $\varepsilon_{w,ha}^{\max}$ correspond to the minimum and maximum total BAs wind generation forecast errors specified for the TND.

2. The standard deviation and autocorrelation of the hour-ahead wind generation forecast error $\sigma_{w,ha}$ is set to the seasonal values.

The truncation process is based on the following rules:

$$G_{ha,1hr}^{w,2007+i} = avg_{1hr} \left(G_a^{w,2007+i} - \varepsilon_{w,ha} \cdot CAP^{w,2007+i} \right) \quad (3.18)$$

where: $\varepsilon_{w,ha}^{\min} \leq \varepsilon_{w,ha} \leq \varepsilon_{w,ha}^{\max}$.

Wind Generation Real-Time Scheduling Model

Real-time wind generation forecast is neither provided nor included into the real-time dispatch process. It is assumed that the naïve persistence model is implicitly used. This means that for a 5-minute dispatch interval $[t, t + 5]$, the implicit real-time wind generation forecast $G_{rf,5min}^{w,2007+i}$ is assumed to be equal to the actual wind generation at the moment $t - 8$:

$$G_{rf,5min}^{w,2007+i} [t, t + 5] = G_a^w [t - 8]$$

Persistence or naïve predictor is a very simple, but yet relatively effective model to forecast wind generation near real time.

3.4.3 Power Flow Incremental Model

The power flow incremental model is used to evaluate the incremental impacts of wind power generation on congested paths and control area balance. The model allows us to simplify and speed up multi-variant evaluations of the impact of different wide area balancing approaches on the congested transmission paths. Selected base cases will be produced using the full system model. The procedure used to create the model using PowerWorld Simulator software is presented.

In WECC documents [53], [54] and in the PowerWorld base case, the term ‘Area’ is used to denote regionally aggregated elements of the electric power system. The term Area in this context is not clearly defined, however, it is assumed that documents [53], [54] provide a valid definition of uncongested contiguous regions of the transmission grid. In this context, it is preferred to use the term ‘Zone’ to avoid confusion with the term ‘Control Area’ (‘Balancing Authority’).

The full WECC system model consists of 15580 buses, 19844 branches, and 3030 generators. Twenty-one zones are defined in the system (Table 3.1). This structure corresponds to WECC area assignments [53].

In the proposed model, some zones may consist of several control areas, and some control areas may consist of several zones. It is not possible to assign each control area to a single zone at present, due to the lack of information. Figure 3.15 shows the zonal structure of the WECC system [54]. Zones are connected through congested interfaces but there is no congestion within a zone.

Table 3.1. Zonal Information

Zone Number	Zone Name
10	NEW MEXICO
11	EL PASO
14	ARIZONA
18	NEVADA
20	MEXICO-CFE
21	IMPERIALCA
22	SANDIEGO
24	SOCALIF
26	LADWP
30	PG AND E
40	NORTHWEST
50	B.C.HYDRO
52	FORTISBC
54	ALBERTA
60	IDAHO
62	MONTANA
63	WAPA U.M.
64	SIERRA
65	PACE
70	PSCOLORADO
73	WAPA R.M.

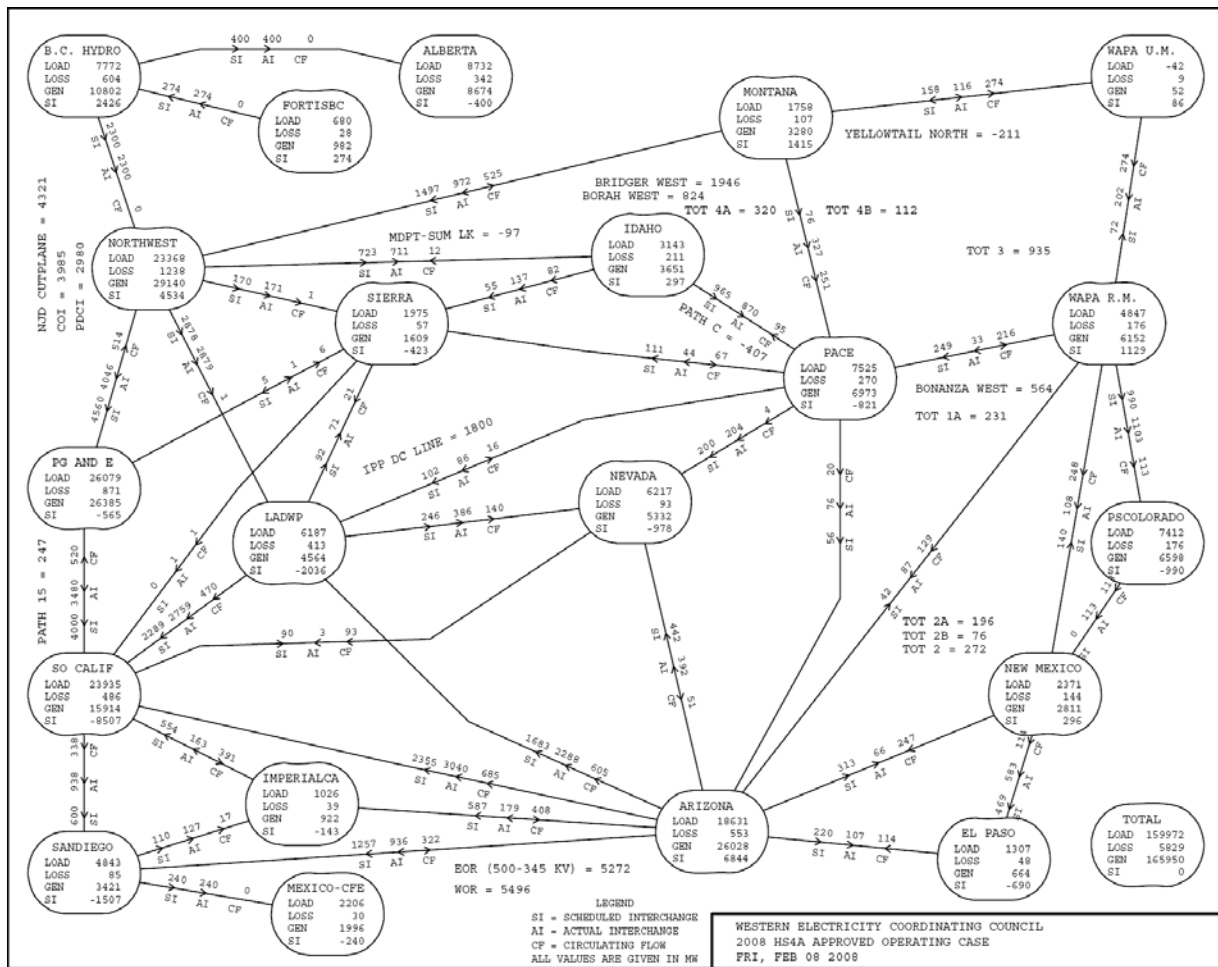


Figure 3.15. Zonal Structure of the WECC System

Figure 3.16 presents the key WECC transmission paths [57]. Information regarding operating transfer limits between zones can be found in the WECC 2008 Path Rating Catalog and other WECC official documents [51],[52].

3.4.3.1 Mathematical Definition of the Incremental Model

Incremental impact analysis has been used to find the relationship between variations of the total zonal active power generation and related active power-flow variation in selected transmission interfaces.

Active power-flow variation in the interface between the zones i and j can be calculated as:

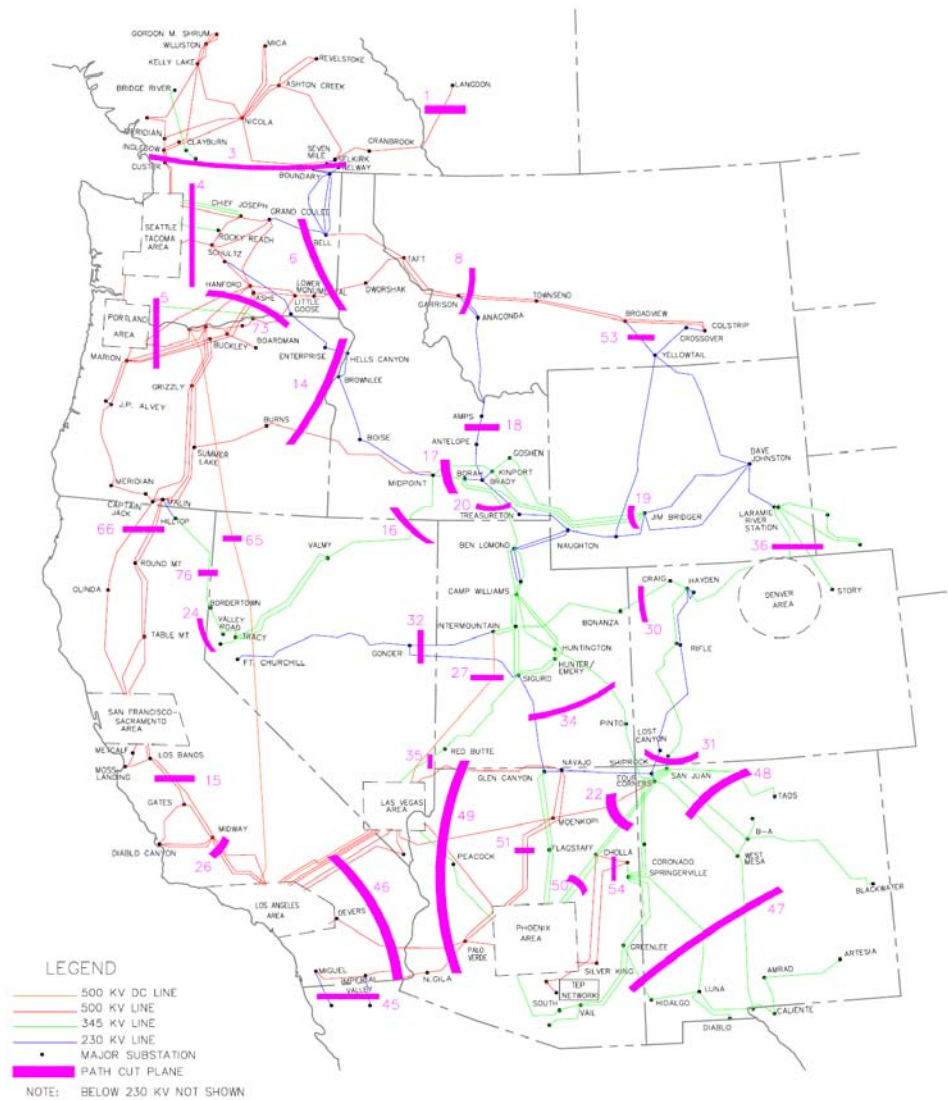
$$\Delta P_{ij} = \sum_{n=1}^N PTDF_n^{ij} \Delta P_n \quad (3.19)$$

where

N = number of zones in the system,

ΔP_n = variation of total active power generation in zone n ,

$PTDF_n^{ij} = \frac{\Delta P_{ij}}{\Delta P_n}$ = power transfer distribution factor reflecting the influence of generation in zone n on the power flow in the interface i - j .



Picture Source [57]

Figure 3.16. WECC Key Transmission Lines and Paths

3.4.3.2 Incremental Model Development Using PowerWorld Simulator

The PowerWorld Simulator software can be used to create the incremental zonal model of the WECC system. Details of the approach are given in Appendix D. A fragment of the interface PTFDs table calculated for the WECC zonal model using PowerWorld simulator is presented in Table 3.2

For example, if generation in New Mexico zone increases by 200 MW, power flow through interface New Mexico-PS Colorado will change by $200 \cdot 0.05 = 10$ MW, because the interface PTFD of New Mexico zone on New Mexico-PS Colorado interface is equal to 5%. (See Table 3.2).

Table 3.2. Interface PTDFs (%)

Name	NEW MEXICO	EL PASO	ARIZONA	NEVADA	IMPERIAL CA	SOCALIF	LADWP	PG AND E	NORTHWEST
NEW MEXICO-PSCOLORADO	5	2.2	1.4	1	1	0.9	0.5	0.5	0
NEW MEXICO-WAPA R.M.	7.8	8.1	6.3	4.3	4.3	4.1	1.7	2.1	-0.2
EL PASO-NEW MEXICO	-19.2	30.8	1.4	0.5	0.7	0.6	0.2	0.3	0.1
ARIZONA-NEW MEXICO	-69.9	-25.1	8.3	6.6	6.3	6.4	3.9	4.4	1.9
ARIZONA-EL PASO	-19.4	-72.2	2	1	1.2	1.1	0.7	0.9	0.6
ARIZONA-NEVADA	1.9	3	5.7	-44.5	4.6	3	0.8	1.7	0.7
ARIZONA-IMPERIALCA	0.7	0.8	2.1	0.7	-21.6	-0.7	-0.1	-0.3	-0.2
ARIZONA-SANDIEGO	6.7	8.2	9.6	3	-7.1	-5.3	-0.2	-1.2	-0.3
ARIZONA-SOCALIF	25.4	29	29.7	-2	-12.3	-15.8	-7.3	-11.8	-8
ARIZONA-LADWP	19.5	24	29.2	13.3	7.7	-11.2	-11	-12.5	-9.2
ARIZONA-PACE	11.8	12	10	5.1	5.9	4.9	-3	0.4	-3.6
ARIZONA-WAPA R.M.	2.4	3.1	3.2	2.2	2.2	2.1	1	1.2	0
NEVADA-SOCALIF	0.6	0.8	1.1	12.2	0	-1.7	-0.6	-1.4	-0.9
NEVADA-PACE	0.6	1.6	3.8	6.7	4	4.3	-0.8	1.4	-1.4
MEXICO-CFE-SANDIEGO	-1.3	-1.3	-1.5	-1.3	-1.3	-1.3	-1.2	-1.4	-1.4
IMPERIALCA-SANDIEGO	-0.1	-0.1	0.3	0.3	18.9	-0.1	0.1	0.1	0.1
IMPERIALCA-SOCALIF	0.1	0.3	0.8	-0.2	56.7	-1	-0.7	-0.9	-0.8
SANDIEGO-SOCALIF	3.2	4.7	6	0.1	8.7	-8.4	-3.1	-4.5	-3.6
LADWP-NEVADA	2.5	2.8	3.2	-36.4	2.9	3.3	1.3	2.3	0.9
LADWP-SOCALIF	13.8	17.7	22.1	46.8	2.3	-16.6	61.3	-17.1	-12.6
LADWP-NORTHWEST	0	0	0	0	0	0	0	0	0
LADWP-SIERRA	1	1	0.6	0.3	0.2	0	2.4	-0.9	-0.9
LADWP-PACE	-1.8	-1.9	-1.6	-1.3	-1.1	-0.9	24.9	-0.1	-0.1

Incremental model approach results were compared with the real full flow model results to validate accuracy of the incremental model approach. An example of interface power flows calculated using the full system model, estimated using the incremental model, and the estimation errors are given in Table 3.3. Table 3.3 also validates sufficiently high estimation accuracy of the incremental model for testing contingencies.

Table 3.3. Interface Power Flow Validation

Interface Name	Contingency 1			Contingency 2			Contingency 3		
	Full model, MW	Incremental model, MW	Error, MW	Full model, MW	Incremental model, MW	Error, MW	Full model, MW	Incremental model, MW	Error, MW
NEW MEXICO-PSCOLORADO	-91.1	-91.1	0	-91.2	-91.1	-0.1	-91.1	-91.1	0
NEW MEXICO-WAPA R.M.	-88.9	-88.564	-0.336	-88.3	-87.9	-0.4	-89.5	-88.9	-0.6
EL PASO-NEW MEXICO	-292.5	-292.418	-0.082	-292.5	-292.75	0.25	-292.4	-292.25	-0.15
ARIZONA-NEW MEXICO	113.3	113.958	-0.658	109.7	107.65	2.05	115.9	117.15	-1.25
ARIZONA-EL PASO	365.9	365.992	-0.092	364.2	364	0.2	366.8	367	-0.2
ARIZONA-NEVADA	440.5	440.574	-0.074	437.5	438.25	-0.75	443.6	441.75	1.85
ARIZONA-IMPERIALCA	250.5	250.436	0.064	250.7	251.1	-0.4	250.2	250.1	0.1
ARIZONA-SANDIEGO	979.1	978.854	0.246	978.1	979.85	-1.75	978.4	978.35	0.05
ARIZONA-SOCALIF	3369.9	3368.54	1.36	3387.5	3395.1	-7.6	3356.7	3355.1	1.6
ARIZONA-LADWP	2663.3	2661.956	1.344	2685.6	2692.5	-6.9	2648	2646.5	1.5
ARIZONA-PACE	-77	-76.952	-0.048	-65.4	-65	-0.4	-82.7	-83	0.3
ARIZONA-WAPA R.M.	-64.6	-64.4	-0.2	-64.6	-64.4	-0.2	-64.6	-64.4	-0.2
NEVADA-SOCALIF	67.9	67.762	0.138	70.7	70.75	-0.05	65.8	66.25	-0.45
NEVADA-PACE	196.4	196.552	-0.152	201.7	201.2	0.5	193.7	194.2	-0.5
MEXICO-CFE-SANDIEGO	-154.9	-155.048	0.148	-149.6	-150.4	0.8	-157.2	-157.4	0.2
IMPERIALCA-SANDIEGO	-87.1	-87.118	0.018	-87.4	-87.45	0.05	-87	-86.95	-0.05
IMPERIALCA-SOCALIF	191.9	191.744	0.156	194.2	194.4	-0.2	190.5	190.4	0.1

4.0 Analysis Methodologies for BA Cooperation Approaches

4.1 Area Control Error (ACE) Sharing

4.1.1 ACE Diversity Interchange (ADI)

To reduce the balancing effort, a rule-based ACE diversity interchange (ADI) approach was proposed in [43]. This rule-based ADI approach has been implemented in Western Interconnection [4]. It has been shown that this ADI implementation always benefits all participating BAs [12].

The idea of ADI is that the control effort needed to balance generation against load and interchange can be relaxed through coordination among multiple control areas [12]. Relaxed control can be achieved because of the sign diversity among area control errors (ACE). As a result of ADI, participating BAs can reduce their respective regulation burdens in real time. ADI is also expected to result in a reduction in generator control movements.

Yet, within this existing rule-based ADI approach, it is hard to effectively integrate reliability constraints (e.g., line transmission limits). As described in [4] and [12], a constant cap of 25 MW was used to limit maximum ADI adjustments and minimize the risk of congestion based on operational experience. Nonetheless, these constant caps may result in over-conservative (less efficient) and/or over-aggressive (causing congestion) operations.

4.1.2 ADI Philosophy

For different BAs, the signs of their ACEs are usually different. ACE values determine how much a balancing authority needs to move its regulating units to meet the mandatory control performance standard requirements. The diversity of the ACEs provides an opportunity for BAs to reduce their total ACEs through coordination. The ACEs with different signs can net out through ACE sharing.

In this approach, participating BAs calculate a common ACE in real time, and then share the common ACE among them based on certain algorithm. Therefore, the participating BAs are balancing against their share of common ACE, which is expected to be smaller than the sum of their individual ACEs. In the US, the ADI is based on the following principles:

- ADI never makes a BAs' ACE less effective.
- ADI moves BAs' ACE towards zero or has no effect.
- ADI never changes the ACE signs.
- ADI does not change any other BA functions.

This ADI approach has been implemented and put into operational practice by New York ISO, ISO New England, and Maritime in the Northeast US in 2002. Midwest ISO implemented the ADI in 2005, but discontinued its use in 2009 because it now operates as a single BA. In 2006-2007, Idaho Power, PacifiCorp East, PacifiCorp West and Northwest Energy formed a new ADI in the Pacific Northwest [4]. British Columbia Transmission Corporation implemented the software used by these BAs for ADI. Later on, the initiative was extended over a larger geographical region in the Western interconnection, by including Arizona Public Service, Nevada Power/Sierra Pacific Power, Public Service Company of New

Mexico, Salt River Project, Seattle City Light, Bonneville Power Administration (BPA), Public Service Colorado/Excel Energy and Glacier Wind Farm (Naturener) [48].

It has been observed that this ADI implementation benefits all participating BAs by improving their CPS2 compliance scores [12]. At the same time, some members of the NERC [21], and some studies [48], expressed concerns regarding the potential adverse transmission and frequency control performance impacts of the ADI. In particular, their concerns are: (1) possible transmission system impacts, including unauthorized and unscheduled use of transmission; (2) possible significant increases of power interchange between the participating BAs and impacts on constrained paths, and (3) inadvertent interchange accumulations and interconnection time error control impacts.

In 2008, three transmission system operators (TSO) in Germany formed an ACE sharing scheme (called shared secondary reserve¹ utilization scheme), which is similar to the ADI scheme in the USA. These TSOs include: Vattenfall Europe Transmission, E.ON Netz, and EnBW Transportnetze. Initially, the scheme included only a mutual compensation of TSOs imbalances that have opposite directions (similar to ADI). By this moment, the German scheme additionally implies that any secondary reserve resource in any BA can be activated by an optimization tool, based on their merit order, to meet the collective regulation requirement of the participating TSOs.

The latest idea is a possible step forward in developing the ADI technology to be evaluated in the USA for the future. To implement this scheme, a wide area regulation reserve market should be created. Unlike the U.S. experience, participating German TSOs indicate a reduction in the regulation reserve requirements due to the secondary reserve utilization scheme [46]. At the same time, transmission constraints are not incorporated into the shared secondary reserve utilization scheme in Germany. This is possible because of the very strong transmission network created in this country, where the congestion problems are observed very infrequently.

The ADI provides a systematic tool for the participating BAs to share their raw ACEs [4]. The resulting ADI ACE value is usually smaller than the original ACE. The smaller ACE values benefit participating BAs by reducing the size of required generation control.

To achieve the ADI benefits, a rule-based ADI approach is formulated in [4]. Figure 4.1 illustrates the existing implementation of ADI. All participating BAs send their raw ACEs to an ADI coordination center. Applying the pre-agreed rules, the ADI adjustments are calculated and sent back to each BA. Each BA adjusts its raw ACE according to the ADI adjustment to get an ADI ACE. The generation allocation is then operated according to the ADI ACE instead of the raw ACE.

The following principles were applied to make rules acceptable to all participating BAs [4]:

1. Maximize the benefits of ACE sharing.
2. For each BA, the ACE should always get better or remain unchanged through an ADI adjustment. Compared to the raw ACE, the ADI ACE should be closer to zero and not have opposite signs.
3. The benefits of ADI should be distributed ‘fairly’ to all participants.

For the rule-based ACE sharing, the risk of potential transmission system violations is mitigated by introducing a constant cap of 25 MW for ADI adjustments. One can argue that because power system operating conditions keep changing, a fixed experience-based constant cap cannot represent operational

¹ In Europe, the term “secondary reserve” has the same meaning as the term “regulation reserve” used in the United States.

conditions adequately. This cap could result in over-conservative and/or over-aggressive ADI adjustments. And this, in turn, can reduce the efficiency of ACE sharing and/or jeopardize system reliability.

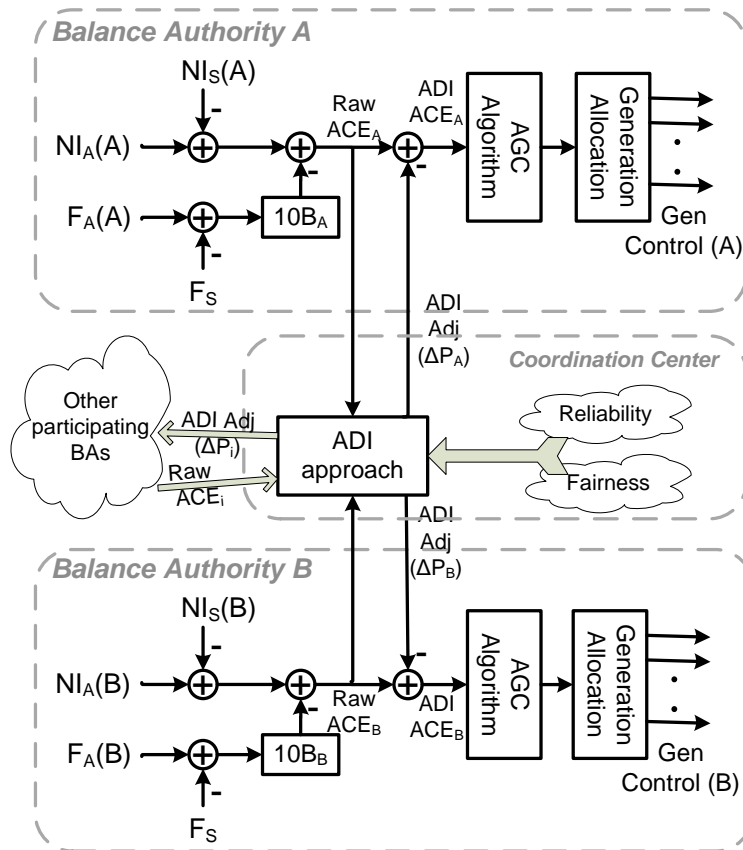


Figure 4.1. ADI Operation and ADI ACE

4.1.3 ADI Limitations

- ADI adjustment limits can be imposed to ensure fail-safe implementation (25 MW limit currently in place). This rule limits potential benefits of ADI.
- An ADI adjustment will be calculated only if there is ACE diversity (positive and negative values) among participants. More flexible strategy could still create benefits under these conditions. For example in Germany, the ADI analog allows distributing the regulation job to the participating units based on their merit order regardless their location,
- An ADI adjustment will never make ACE less effective, i.e., it will always move ACE toward zero or will have no impact. A more flexible scheme could be operating within the NERC control performance limits while maximizing resulting benefits,
- Participants have the right to ignore (suspend) ADI adjustments; suspension means that participants control to original ACE (status quo operations). This option requires participating BAs to carry reserves sufficient for their individual operation.

4.2 Dynamic Scheduling

4.2.1 Background of the Study

Dynamic transfers and pseudo-ties from one balancing authority to another are very promising mechanisms for implementing various BA consolidation methods. They can help to bring more essential ancillary services to a BA that may have their shortage. They can be also used to add more external renewable energy resources into some BAs, which may experience difficulties with meeting their RPS standard goals. At the same time, dynamic schedules could create additional system problems. All these aspects should be analyzed through studies before the actual implementation begins. This report develops methodologies for such analyses.

4.2.2 Available Options for Dynamic Transfers

As introduced in Section 2.5, dynamic transfers can be implemented in two different ways, by dynamic scheduling (DS) or by creating pseudo-ties [59]. Dynamic schedules facilitate changes in net scheduled interchange between two BAs by automating intra-hour dispatch and real time interchange adjustments within an operating hour [8]. It can also provide variable energy and ancillary services between two BAs within an operating hour. The transferred energy can be either conventional or renewable. The concept of dynamic scheduling is shown in Figure 4.2.

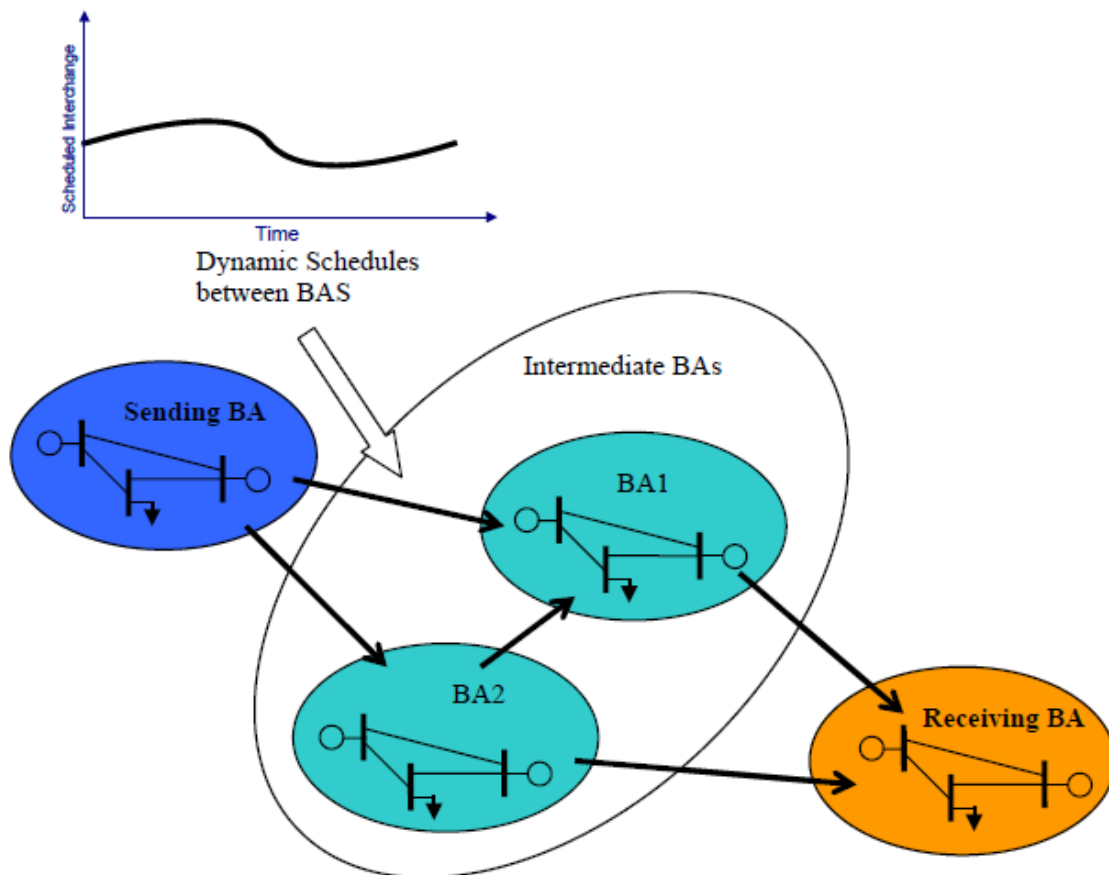


Figure 4.2. Concept of Dynamic Scheduling

Pseudo-ties are employed to transfer energy from one BA (the sending BA) where the energy resource (e.g., a pseudo generator) is located to another BA (the receiving BA) that has operational control of the resource (the pseudo generator). This external generator is considered as an internal generator that can bid in the power market of the receiving BA. But in this case, there are no physical tie lines that actually exist between this pseudo generator and the receiving BA. The concept of a pseudo tie is depicted in Figure 4.3. Additionally, the actual interchange term in the ACE equation, rather than the scheduled interchange terms is adjusted for a pseudo tie. Both of these two options have benefits for dynamically transferring energy and they need to be designed properly to meet the real time telemetry, software and hardware, communication and administration requirements, etc. The main difference between dynamic schedules and pseudo-ties are further discussed in [8].

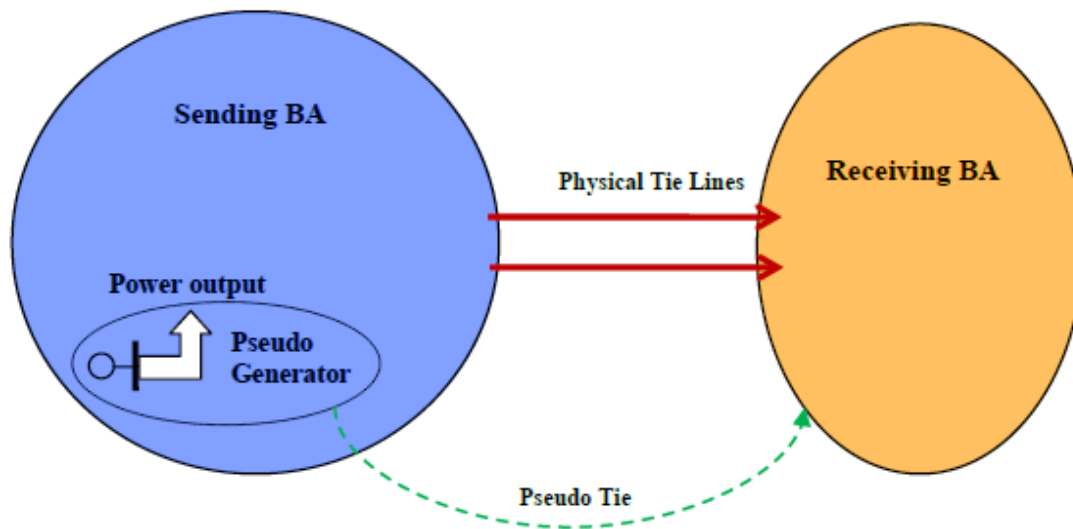


Figure 4.3. Concept of a Pseudo-Tie

4.2.3 Benefits and Main Issues

With the advent of new energy policy and the trend to increase penetration of renewable energy to a higher level, dynamic scheduling becomes a more and more promising and feasible method to achieve these goals. The potential application and benefits can be summarized as follows:

1. Serve customer loads that are located in other balancing authorities
2. Seek external support when a balancing authority is unable to meet the scheduled generation level
3. Import (or export) renewable energy to increase its penetration
4. Shift balancing burdens between different balancing authorities to provide ancillary services including load following and regulation, etc.

Various balancing authorities (e.g., California ISO and Bonneville Power Administration) in the WECC system are expressing greater interest in further expanding their existing implementation of dynamic scheduling. At the current stage, California ISO has a limited set of dynamic transfer services which is implemented on a case by case basis. Increasing the amount of intermittent resources via dynamic scheduling can effectively help to meet the new standards, but it can also incur a large influence

on the system balancing effort in real time. Among the other factors, two attributes could impact reliable operation in this regard: variability and uncertainty.

As required by FERC Order 890-B, transmission providers are obligated to provide generator imbalance services [63]. If they are unable to do so, they have to facilitate the use of dynamic scheduling for providing these ancillary services. However as for large scale application of dynamic scheduling, no standards have been formulated to instruct the implementation yet, especially for intermittent energy. As a consequence, because of the variant power flows on the tie lines, dynamic scheduling needs to be designed and carried out in a scientific way with careful coordination among the sending BA, the receiving BA and the intermediate BAs. To achieve this goal, a new study is needed to investigate the expansion of dynamic scheduling service from various aspects in order to enhance DS service and maximize benefit achievement. The following questions will be answered as the outcomes of this study:

1. What are the impacts of dynamic scheduling on the balancing services of involved balancing authorities, (e.g., the sending BA and receiving BA)?
2. What are the major constraints that limit the implementation of dynamic scheduling?
3. How to select optimal renewable resources for dynamic scheduling based on congestion management?
4. What are the negative impacts of dynamic scheduling on intermediate balancing authorities? How to compensate such effects?

4.2.4 Proposed Methodology and Outcomes

In this section, initial methodologies to evaluate the design and implementation of dynamic scheduling from various aspects are discussed. These methodologies will be tested on two separate cases. (1) Importing external energy to a BA for providing balancing services including load following and regulation to relieve BA's balancing burden due to the high penetration of wind energy. (2) Importing external renewable energy (wind and solar) to a BA in order to increase the ratio of renewable energy usage in the system.

4.2.4.1 Impact on Local Balancing Services

The application of dynamic scheduling by dynamically transferring energy will affect the balancing burdens of the sending BA and the receiving BA, based on different types of energy services. Assume that a BA would like to bring in more renewable energy from surrounding BAs in order to meet its Renewable Portfolio Standard goals. However, if a large amount of intermittent renewable energy is dynamically transferred, the BA has to prepare for a higher level of load following and regulation obligations caused by the uncertainty of wind and solar. As another example, assume that a BA would like to import ancillary services to reduce its balancing burden due to a large amount of wind penetration in its balancing area. In this case, the BA itself may not need a very high load following and regulation reserve requirement due to dynamically scheduled external ancillary services. To accurately quantify such effects, performance envelopes proposed in Chapter 2.0 can be used..

The balancing requirements can be further characterized as scheduling, load following and regulation set of requirements. They are calculated using the following equations. Examples of these curves for a real system are shown from Figure 4.4 to Figure 4.6.

- Net load = actual load – actual renewable generation + interchange schedule

- Hour ahead schedule = hourly average of net load – hour ahead forecast errors
- Load following = real time schedules – hour ahead schedules
- Regulation = net load – real time schedules

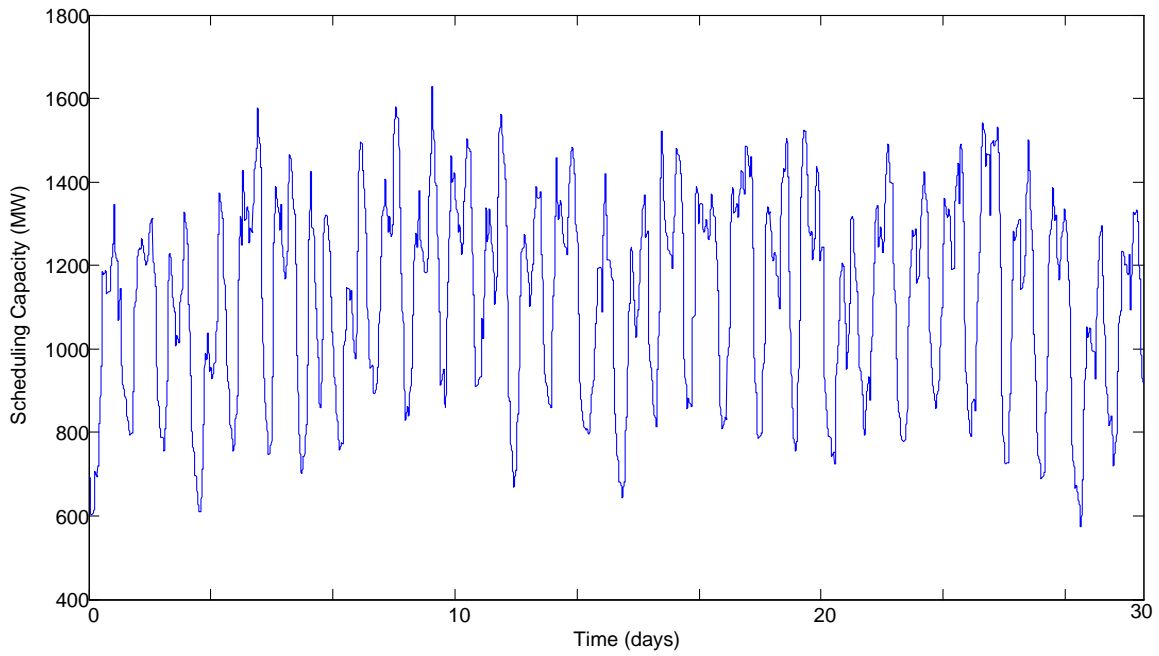


Figure 4.4. Example of 1 Hour Ahead Scheduling Curve

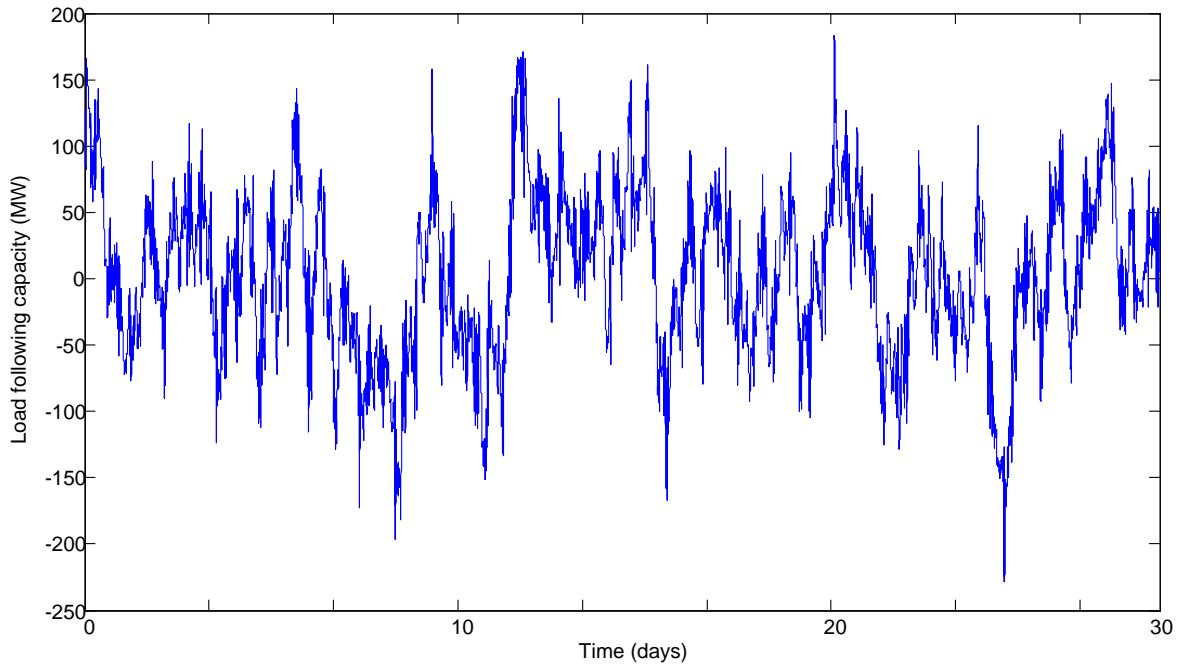


Figure 4.5. Example of Load Following Curve

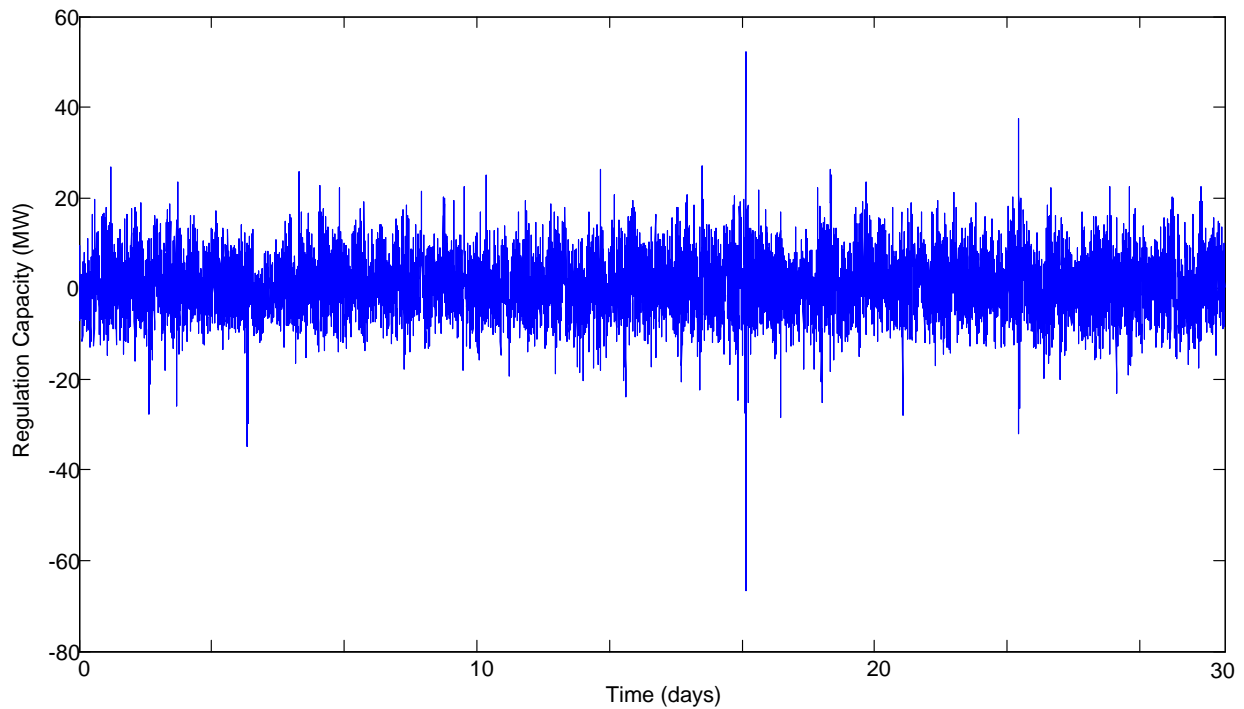


Figure 4.6. Example of Regulation Curve in a Month

For each of the above time series curves, it is further processed using the 1st and the 2nd performance envelopes. The 1st performance envelope method adopts a ‘swinging door’ algorithm to compress the time series data points and derive ramping actions that are characterized by four metrics, including ramp capacity (π), ramp duration (δ), ramp rate (ρ) and ramp energy (ϵ), shown in Figure 2.2. By projecting all the points into a 4 dimensional space determined by the four metrics, a 4 dimensional ‘probability box’ can therefore be obtained to include the majority of requirements (e.g., 95% of the points are included in the box to indicate majority of balancing requirements, the remaining points outside the box represent extreme cases, which cannot be balanced by the BA). Further rearranging all the points according to different operating hours in a period of time, the maximum and minimum ramping obligations are obtained, as shown in Figure 4.7 to Figure 4.9. Figure 4.10 shows an example of the maximum Inc/Up and minimum Dec/Down ramp rates for 24 operating hours. The other metrics in the performance envelope can be assessed in a similar way.

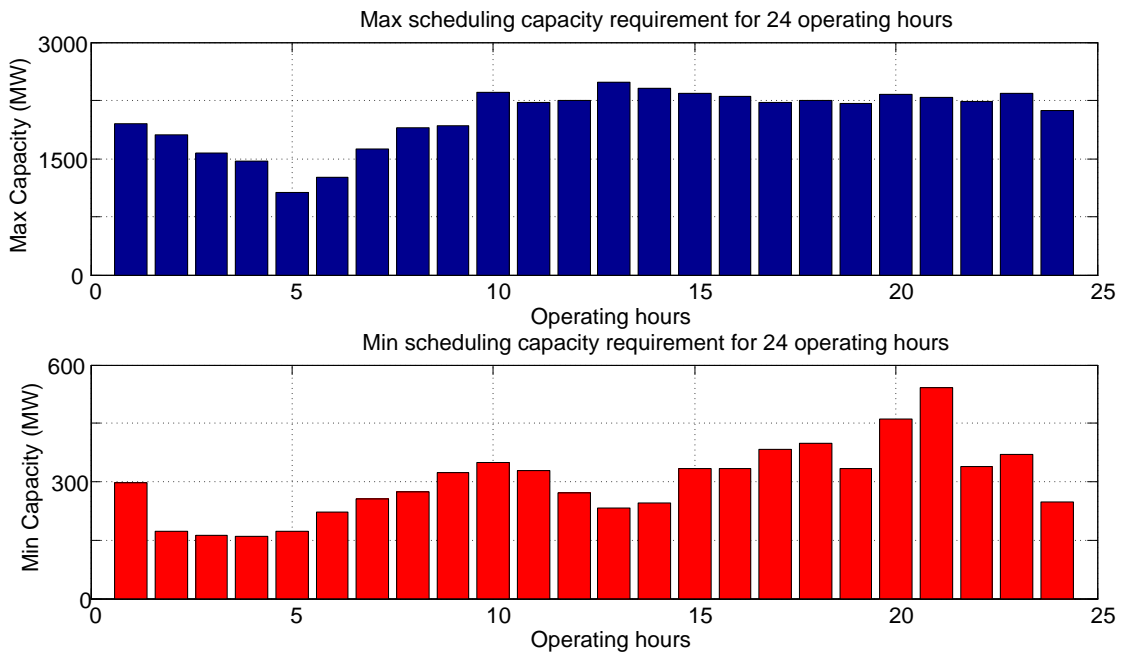


Figure 4.7. Example of the Scheduling Capacity Requirement for 24 Operating Hours

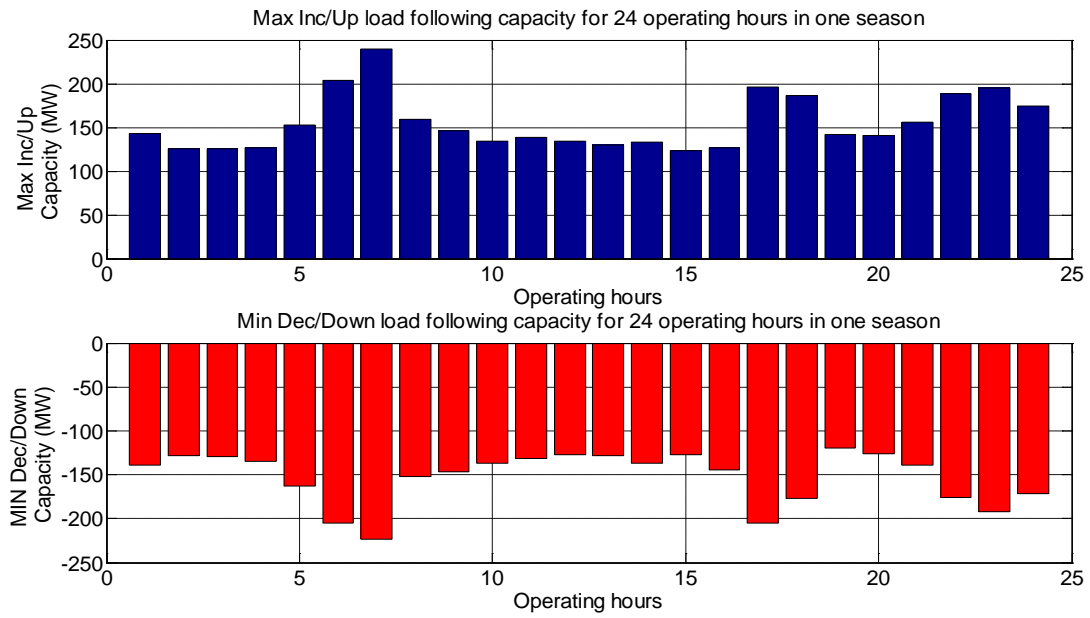


Figure 4.8. Example of Load Following Capacity for 24 Operating Hours

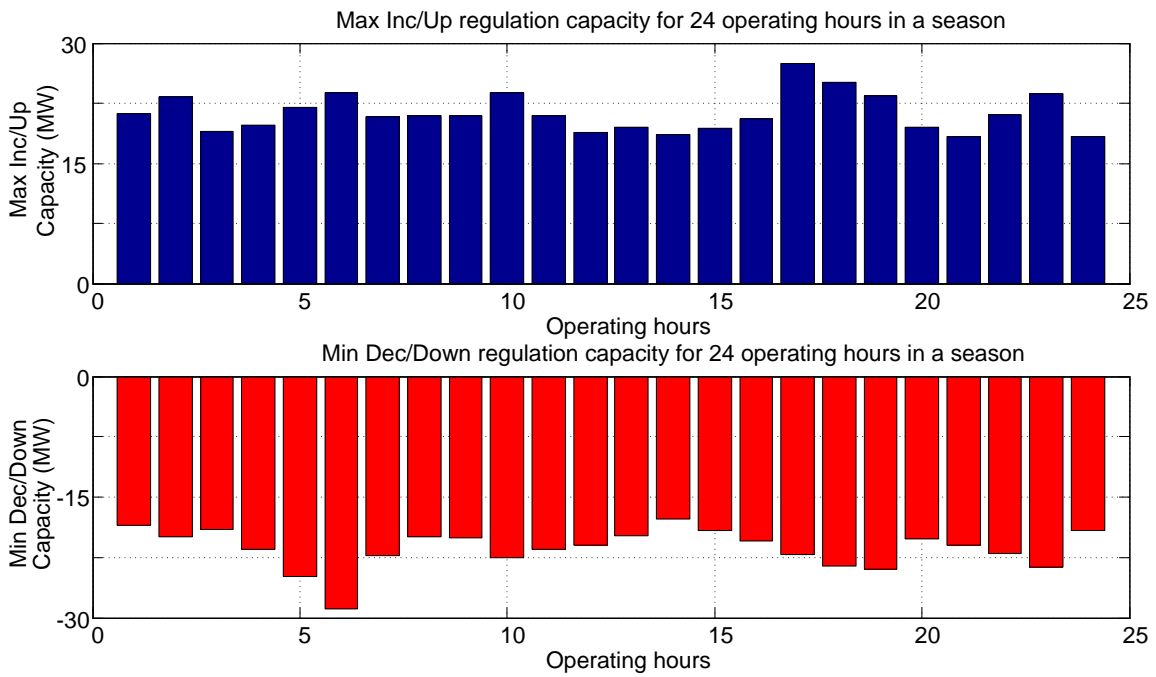


Figure 4.9. Example of Regulation Capacity for 24 Operating Hours

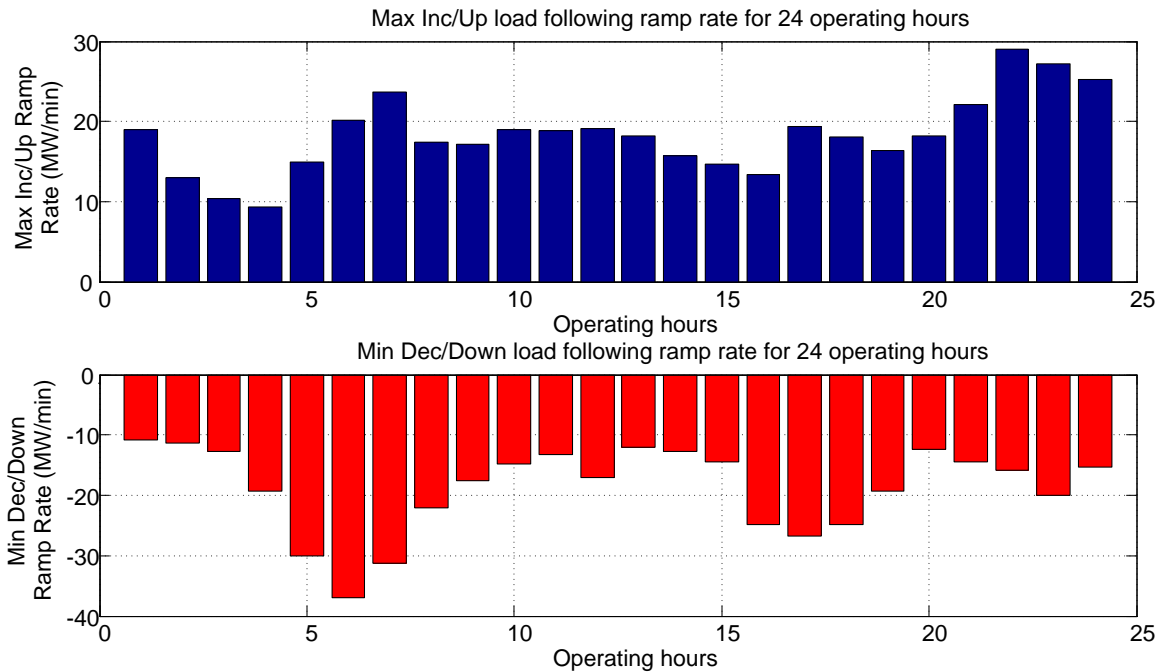


Figure 4.10. Example of Max & Min Regulation Ramp Rate for 24 Operating Hours

The 2nd performance envelope further extends the method of the 1st performance envelope using the concept of half-cycles (see Figure 2.3). Each half-cycle contains all adjacent ramp actions with the same sign of ramp rates and it is characterized by half-cycle magnitude, half-cycle duration, half-cycle ramp rate and half-cycle energy. In this way, a more comprehensive result to quantify system ramping up or ramping down can be achieved. Moreover, the 2nd performance envelope can serve as good indicator to assess equipments' wear and tear; energy storage needs, etc.

The above performance envelopes (1 and 2) will be used to compare the system capability to meet balancing requirements between the conditions with dynamic scheduling and without dynamic scheduling. PNNL's main task is to evaluate the effects of dynamic scheduling achieved by all the participating BAs in terms of the changes in scheduling, load following and regulation obligations. More specifically, this method will help different balancing authorities in estimating the exact amount of ancillary services before and after dynamic scheduling is implemented. The incurred change in balancing services will help to decide on the optimal amount of dynamic transfers.

4.2.4.2 Physical Constraints of Expanding Dynamic Scheduling

The second important task is to evaluate the constraints that limit the implementation of dynamic scheduling. Such limits include the congestion problem on critical paths and the system capability to provide ramping capacity. This subtask will help to determine the maximum amount of dynamic transfers. In this study, an incremental zonal model for the whole WECC system is used to evaluate the constraints (See Chapter 3.4.3). Given an operating point and an incremental generation change in one BA, this model provides the sensitivity information regarding the impact of this change on the congested paths. Figure 4.11 shows the structure of this incremental zonal model and how it is working. If, for example, the generation output in the Northwest Zone is increased by a certain amount, the effects of this change on power transfers can be identified by calculating power transfer distribution factors (PTDF). The green arrow on a tie line indicates a decrease in the power transfer; while a red arrow indicates an increase in power transfer compared to the initial operating condition. The length of the arrow reflects the level of change.

The main task is to take full advantage of this incremental zonal model in order to identify potential congestion problems caused by dynamic scheduling using multiple Monte Carlo runs. This analysis can include finding out the maximum allowable amount of energy that can be dynamically transferred. Insight suggestions on better coordination of dynamic schedules among multiple BAs can be addressed.

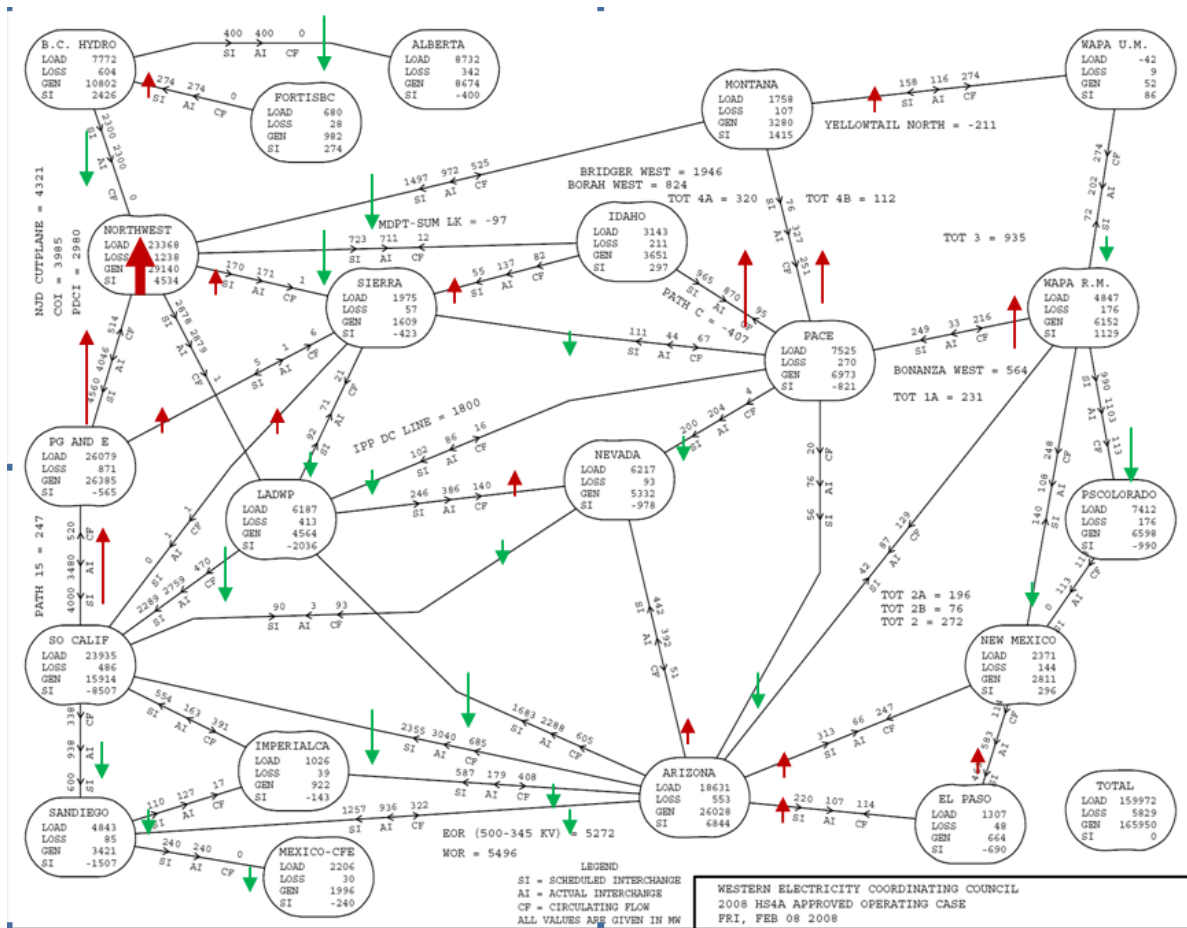


Figure 4.11. Incremental Zonal Model for WECC System

4.2.4.3 Impact on the Intermediate BAs and Compensation

Using external resources via dynamic scheduling can benefit both the receiving and sending BAs, however the impact of incurred power transfer on the intermediate transmission networks should also be considered. Although the intermediate BAs are not involved in the dynamic scheduling contract between the sending BA and the receiving BA, loop flows in the intermediate BAs can be created. The additional power transfer has little impact on the balance between local generation and local load in these BAs, it will use their transmission networks and reduce the available transfer capability. In addition, such an impact is not constant with the implementation of dynamic scheduling. Determining the amount of loop flow can help to quantify the negative impacts and design proper compensation methods. Thus, this study will also provide suggestions about how to compensate such effects, e.g., based on the Monte Carlo simulations of the amount of dynamic energy transferred using the network.

4.2.5 Example Study Scenarios

With the proposed methodologies, the following scenarios can be studied.

1. Importing ancillary services

- Dynamically import ancillary services from surrounding BAs.

- Dynamically export wind energy to surrounding BAs.
2. Importing wind energy
 - Dynamically import wind energy.

Deliverables:

3. The maximum amount of dynamic schedules that can be implemented for participating BAs without violating system security and stability constraints
4. The optimal locations of renewable resources for dynamic scheduling
5. Potential changes in the balancing effort, using the 1st and 2nd performance envelopes.
6. Study the effects of loop flows on the intermediate BAs in order to develop a methodology to compensate the negative impacts of dynamic scheduling.

4.3 Regulation and Load Following Sharing

Load following and regulation are two very important balancing services. Load following is the provision of generation dispatched to balance generation/load mismatches for certain intrahour scheduling periods. Regulation addresses power imbalances on the minute-to-minute basis. Regulation is provided by the on-line generation that is synchronized with the system and can increase or decrease its output power in response to AGC signals.

Regulation and load following sharing refers to sharing the regulation or load following services among participating balancing authorities.

4.3.1 Regulation Sharing

In this report, simulated regulation and load following signals are used for the study. The method proposed in Section 3.4 is used to separate the regulation and load following components of balancing service.

Regulation is interpreted as the difference between the actual generation requirement and the short-term five-minute dispatch shown in Figure 3.9 as the red area between the blue and green lines.

4.3.1.1 Regulation Sharing Algorithm

In this study, the regulation requirement is a derived signal based on the actual generation and total real-time generation dispatch in a BA, i.e., $REG = G_{actual} - G_{real-time}$.

A BA with a positive instantaneous regulation requirement is called “a sink BA.” A BA a negative instantaneous regulation requirement is called “a source BA”. Figure 4.12 shows an example of the source and sink BAs.

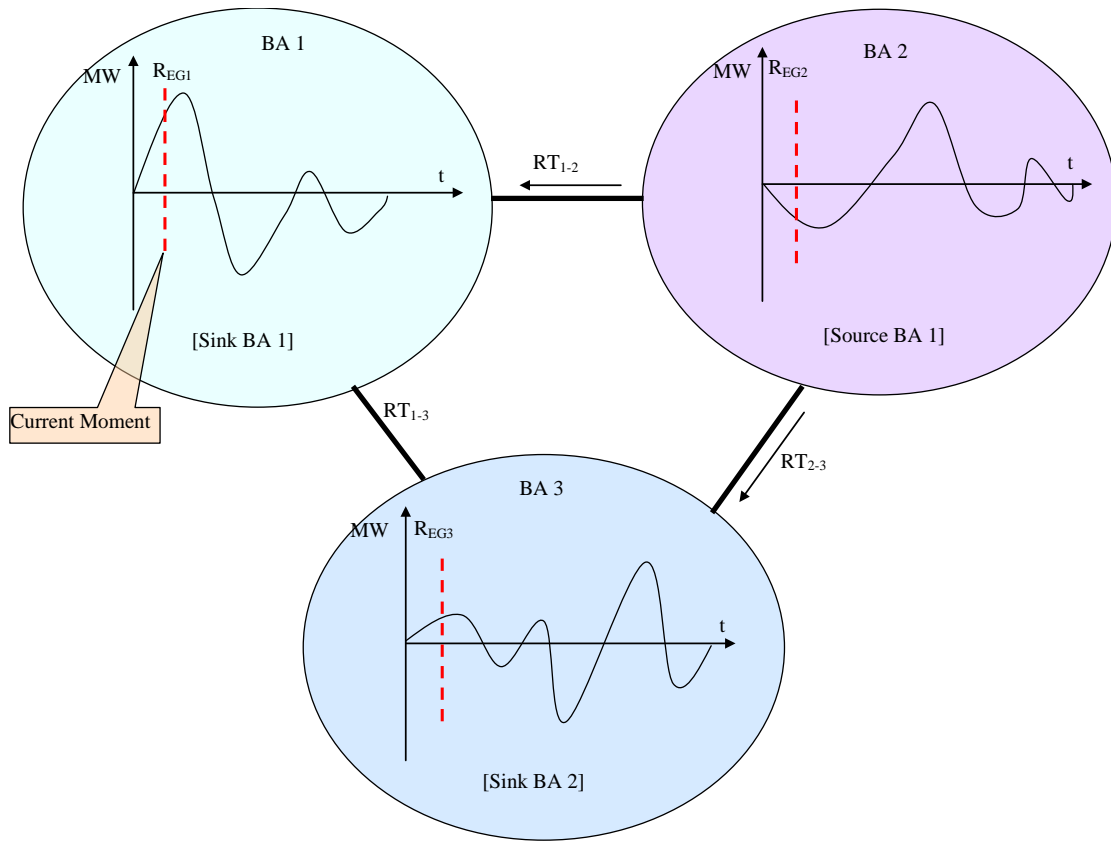


Figure 4.12. An example of Source BA and Sink BA

In the development of the regulation and load following sharing algorithms, transmission issues between BAs are ignored. A description of the proposed regulation and load following sharing algorithms is presented in Appendix C and Appendix D.

4.3.1.2 Simulation Results

Three existing BAs regulation signals are used in the simulation. Figure 4.13–Figure 4.15 show the probability distribution for the regulation capacity of the three BAs with and without regulation sharing. From these figures, one can see that the regulation sharing technology allows BAs to decrease regulation capacity requirements. Details on these simulation results are presented in Appendix C and Appendix D.

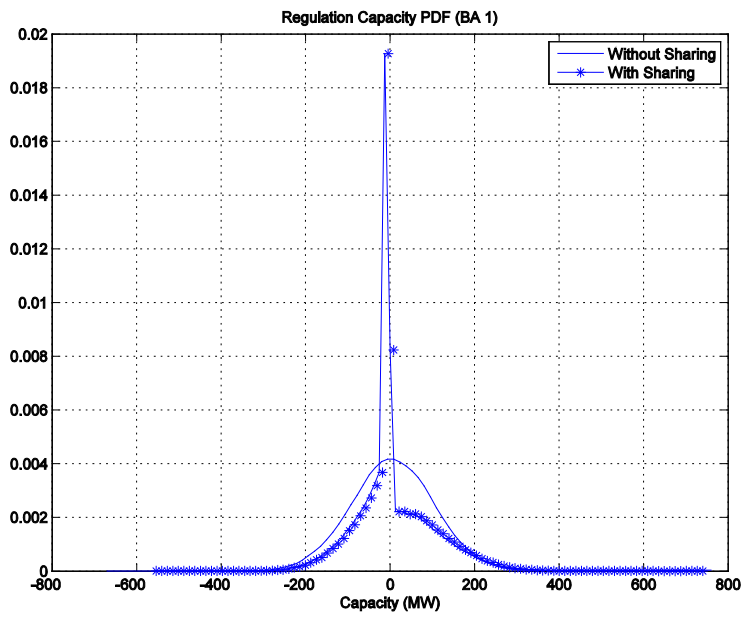


Figure 4.13. Regulation Capacity Probability Distribution Function (PDF) for BA 1 (With and Without Sharing)

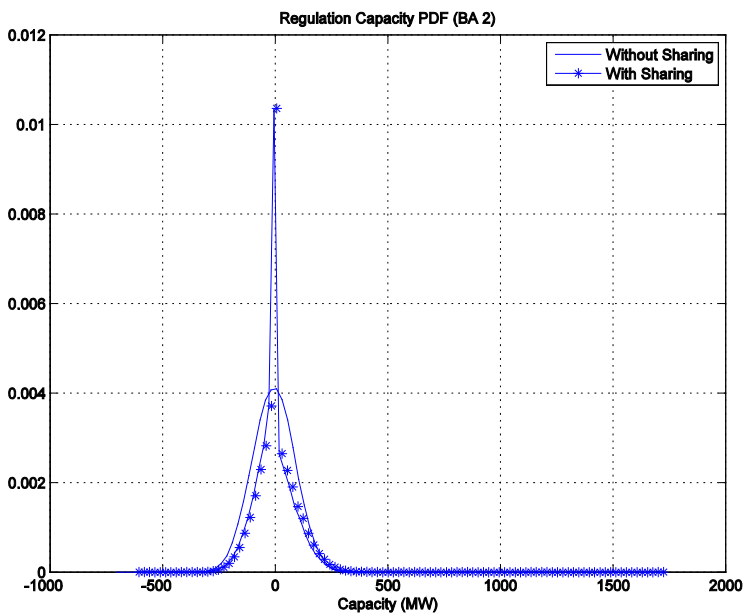


Figure 4.14. Regulation Capacity PDF for BA 2 (With and Without Sharing)

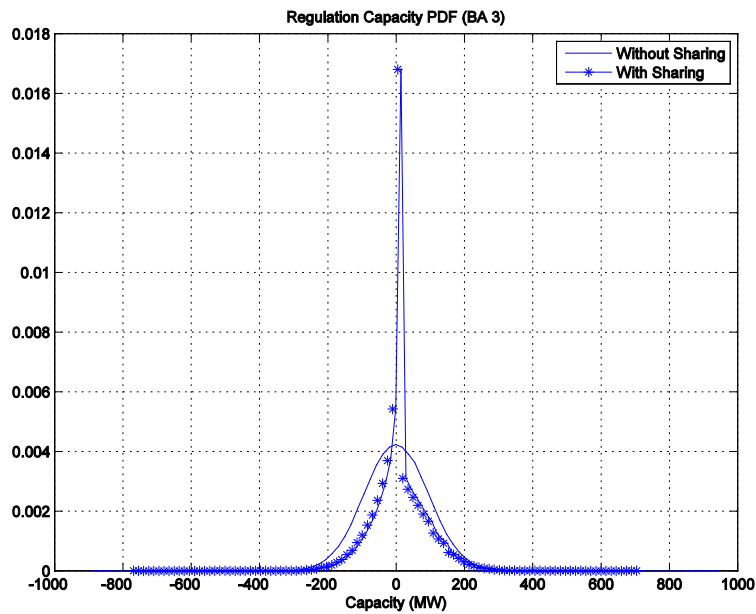


Figure 4.15. Regulation Capacity PDF for BA 3 (With and Without Sharing)

4.4 Wind Only BA

4.4.1 Wind Only BA Basic Idea

The idea of a wind-only balancing authority (BA) could help participating wind farms to join their efforts and provide a more predictable, less variable, and more dispatchable generation resource. A wind-only BA is responsible for controlling its interchange with the other balancing authorities to follow a predetermined interchange schedule. Generators participating in the wind-only BA are required to provide their own balancing reserves or purchase those services from some external resources. Wind only BAs could include wind generators distributed over a large geographical region; so they could benefit from the geographical diversity factor that minimizes the relative variability of participating resources. The balancing efforts can be reduced in conventional control areas by excluding intermittent resources which are combined into a wind-only BA. The disadvantage is that the participating wind resources will be exposed to more challenging operating conditions, and that the wind-only BA will not be benefiting from the statistical interactions between load and wind intermittency factors.

An existing example of wind-only BA is Glacier Wind Energy, the first wind-only BA in the US. Glacier Wind 1 is a 106 MW wind farm located in Cut Bank, Montana. It is operated by Constellation Energy Control and Dispatch (CECD). The project uses a sophisticated wind forecasting system and a flexible off-take (scheduling) agreement with San Diego Gas & Electric (SDG&E). Ancillary services (regulation) are purchased from Grant County PUD. The Glacier Wind BA participates in ACE Diversity Interchange (ADI), and the Northwest Power Pool reserve sharing group [34].

4.4.2 Wind Only BA Simplified Mathematical Model

Three conventional BAs and one wind generation only BA example is shown in Figure 4.16. All wind generators in the system belong to the wind only BA (Figure 4.16)

The wind only BA needs to establish a cooperation agreement with conventional generators to provide balancing services.

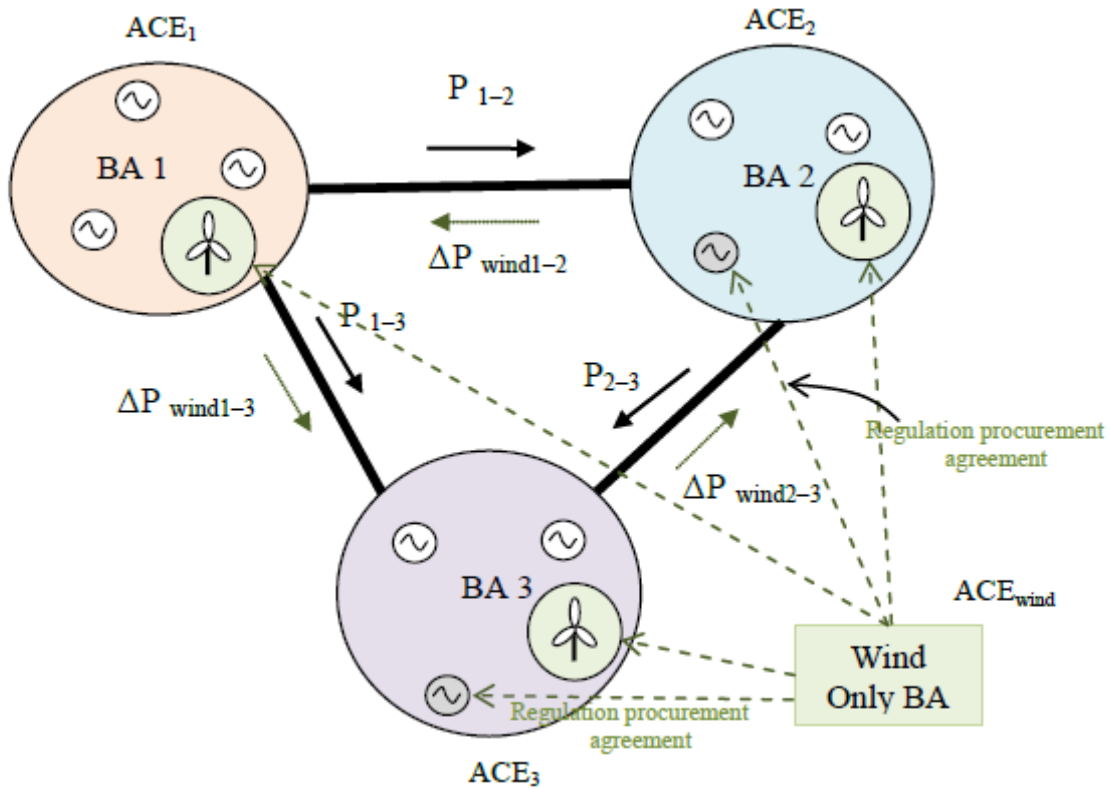


Figure 4.16. Three Conventional BAs and One Wind Generation Only BA Example

Wind only BA can procure regulation services from several suppliers and these services are limited as follow:

$$P_{reg_i}^{\min} < P_{reg_i} < P_{reg_i}^{\max}, i=1 \dots M \quad (4.1)$$

where P_{reg_i} is regulation capacity that can be procured from supplier i ;

$P_{reg_i}^{\min}, P_{reg_i}^{\max}$ are the minimum and maximum regulation limits available from supplier i ;

M is the number of regulation service suppliers;

Wind only BA balance equation:

$$\sum_{i=1}^N P_{wind_i} + \sum_{j=1}^M P_{reg_j} - I_s = 0 \quad (4.2)$$

where I_s is the interchange of the wind only BA.

Power flow through the interface between zones m and n can be expressed as follows:

$$P_{mn} = P_{mn}^0 + \sum_{i=1}^N (\Delta P_{wind_i} + P_{reg_i}) \cdot PTDF_i^{mn} \quad (4.3)$$

where: P_{mn}^0 is the initial power flow in the interface $m-n$;

ΔP_{wind_i} is the wind generation variation from the schedule

$PTDF_i^{mn}$ is the coefficient of influence (power transfer distribution factor) of the area i on the interface $m-n$.

Here we suppose that there are no power flow deviations in the interfaces caused by conventional BAs (conventional BAs are following the schedule)

Interface power flow constrains are applied to the interface power flows as follow:

$$P_{mn}^{Lim-} < P_{mn} < P_{mn}^{Lim+}, \quad (4.4)$$

where P_{mn}^{Lim-} and P_{mn}^{Lim+} are the transmission limits of the interface $m-n$;

The total cost of regulation services procurement should be optimized:

$$\sum_{i=1}^N Cost_i \cdot \int_{T1}^{T2} P_{reg_i} \cdot dt \longrightarrow \min \quad (4.5)$$

where $Cost_i$ is the regulation energy cost (\$/MWh) provided from supplier I for the time interval $[T1, T2]$; and subjected to constrains (4.2) and (4.4)

4.5 BA Consolidation

The objective of BA consolidation is to propose and evaluate key technical metrics in order to demonstrate the potential gains that would accrue by consolidating all the balancing authorities within a large geographical area and by operating them as a single consolidated BA (CBA).

4.5.1 The Concept of BA Consolidation

The consolidation of individual BAs is the integration of two or more BAs into a single consolidated balancing authority (CBA). The CBA will provide the necessary infrastructure to facilitate the intra-zonal transfers (formerly BA to BA schedules). These transfers are initiated by the allocation of wide area regulation, load following and scheduling requirements. Transmission owners would provide Available Transfer Capability (ATC) Information so that intra-zonal transfers would not exceed security constraints. Ultimately, transmission owners would provide loading and line ratings so that the CBA can calculate security constraints.

The existing BA assets will be made available to the CBA, but other market mechanisms may emerge as an alternative subject to the interested market participants and stakeholders within the CBA footprint. Such markets may provide an effective valuation of resources and may facilitate features such as 10 minute scheduling and dispatch intervals for quick access to transmission and generation resources for regulation, load following, balancing, and redispatch.

Individual zones (former BA) may still balance generation and load within its zone, but the CBA would provide intra-zonal capability for sharing resources subject only to transmission loading constraints. Resources for provision of ancillary services will be provided by asset owners within the existing BAs. The CBA will be the provider of last resort for ancillary services.

4.5.2 Motivation for BA Consolidation

With the rapid changes in the power industry, the motivations for individual BAs to consolidate into a larger single BA are becoming more viable. Some of these motivations can be summarized as follows:

1. The expected high penetration of renewable energy in the next decade would make it expensive for individual BAs to manage the net load variability if not aggregated over large geographic areas.
2. With new reliability standards enforced by NERC and WECC, individual BAs are exposed to liabilities that might be lessened through improved consolidated operations.
3. Congestion on the existing system, recognized as a problem years ago, continues to grow with new loads, new generators and changes in the pattern of transactions. While new transmission facilities will help, they are years away and construction projects cannot be as responsive to new and changing conditions.
4. Individual BAs are spending a lot of time and effort working on resolving balancing area boundary issues. The solutions often entail more contracts, more policies and more procedures at the many interfaces between the many existing balancing areas.
5. Several recent reports from the power industry identified the following problems associated with the operation of individual BAs:
 - a. Control area operators do not have a broad view of the system
 - b. Control areas do not have the authority or mechanisms to achieve maximum efficiency on a system-wide basis
 - c. Independent decisions by individual control areas can lead to impacts on other control areas
 - d. Transmission system no longer has flexibility sufficient to allow control areas to operate as independently (a “one utility” viewpoint may allow for more efficient/effective operation).
 - e. Difficulty managing unscheduled flows on the transmission system, leading to reliability risks
 - f. Difficulty reconciling physically available Transmission capacity with that available on a contractual basis, resulting in potentially inefficient use of available transmission and generation capacity

4.5.3 Benefits of BA Consolidation

The potential benefits of BA consolidation are by leveraging the diversity associated with wind outputs with existing loads, and available flexibility of existing generators, across large geographic regions. Numerous short and long term benefits for the BA consolidation can be identified. The consolidated BA with much wider geographical boundary results in significantly lower scheduling, load

following and regulation requirements compared to the sum carried by the individual balancing areas. These savings could be realized immediately by reallocating regulation reserve requirements to the balancing areas and reduced operational burden. In addition, BA consolidation has more ramping capability and less need-on a per unit basis-for this capability. This benefit - which follows the same rationale for creating reserve sharing pools to reduce individual BAs contingency reserve requirements - make it attractive to balance over large electrical footprints. The variability of wind penetration up to 20% of annual energy can be managed with existing balancing resources in a consolidated BA. Enforcement of mandatory reliability standards is forcing system operators in many ways. Individual balancing areas are exposed to liabilities that might be lessened though improved consolidated operations. Consolidation would transfer the obligation for compliance and reduce the cost of reliability compliance, possibly reduce liabilities and could also provide benefits for uniform infrastructure, maintenance and replacement programs. A single consolidated balancing authority can provide significant benefits in reliability without requiring structured energy markets.

The relative benefits of consolidation will depend on how the forecast for load and wind generation will be performed on the consolidated BA. For a consistent forecast error statistics, a savings in load following and regulation reserve requirements in terms of energy, ramping capacity and ramp rate is expected to yield a substantial economic benefit for a consolidated BA. An example of the saving in the load following incremental and decremental capacity requirements for over one-hour intervals is shown in Figure 4.17. The saving is determined by calculating the difference between the sums of requirements for all individual BAs versus the consolidated BA. On the left side are the expected incremental and decremental capacity values for 3 BAs stacked on one another in different colors for 24 operating hours of a day for a certain season. On the right side are the sums of expected incremental and decremental capacity values for the 3 BAs, and those for the consolidated BA side-by-side in different colors.

Many system operators recognize that there will be a certain improvement in efficiencies and reliability with the operation of consolidating balancing areas. This is achieved through the optimal use of capability in the regional system by an operator with broader visibility and control of the system. Reliability would be enhanced if the system operators operating worldview extended beyond the interchange meters that define their control area.

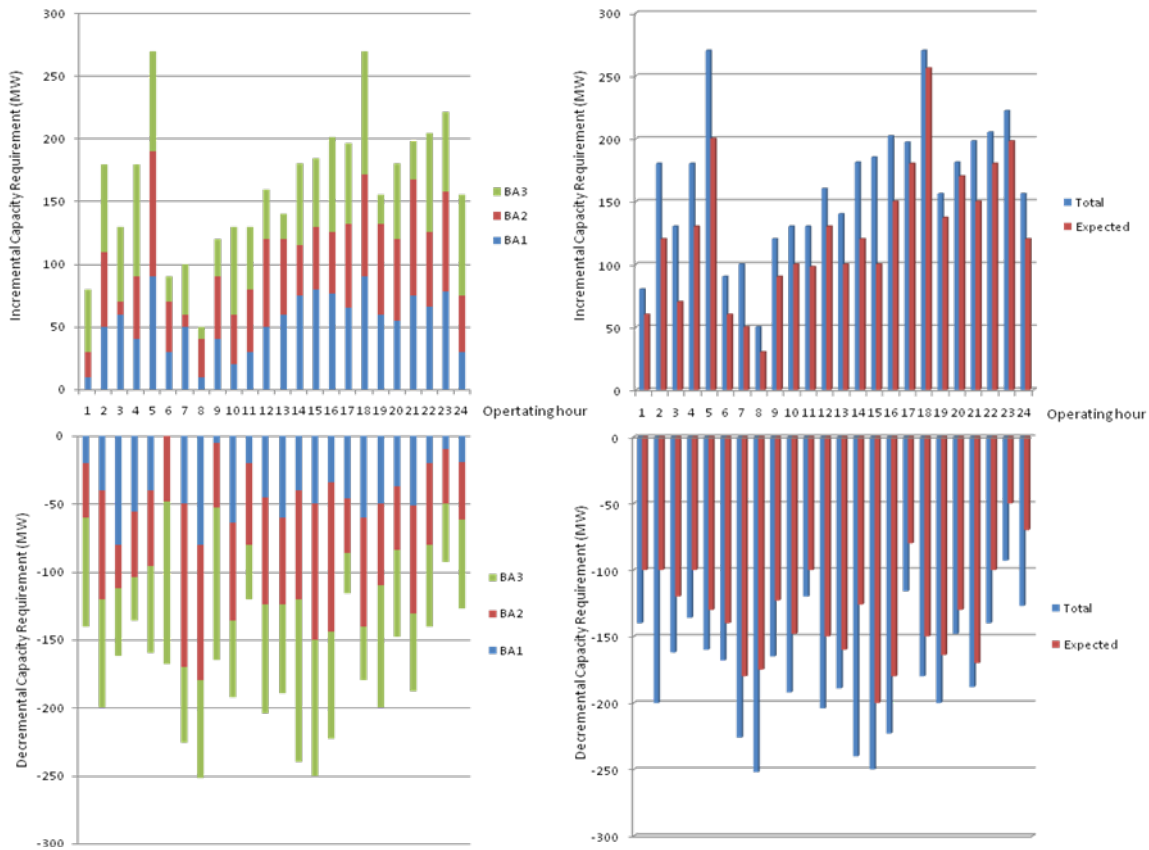


Figure 4.17. An Example of Results Comparison for Load Following Incremental/Decremental Capacity Requirement (Individual BAs vs. CBA)

4.5.4 Case Study

The objective of this study is to investigate the consolidation benefits of a group of balancing areas. Representative data at one minute resolution for load, wind power production and interchange is being used for the study.

4.5.4.1 Evaluation Metrics

A set of metrics used to quantify the benefits of BA consolidation have been introduced in this study. The set is defined by “the first performance envelope” (defined in Section 2.1.5), which represents the BA balancing operations, hence it includes capacity, ramp rate, ramp duration, and energy of ramps requirement for regulation, load following and scheduling.

4.5.4.2 Calculation of the Metrics

The ramping capability of various generating units can directly influence the required regulation and load following capacity. If the ramping capability is insufficient, more units and more capacity must be involved in regulation and load following to follow the ramps. Hence, a simultaneous evaluation of ramps and capacity needed for regulation and load following is necessary to determine the true requirements.

The required ramping capability can be extracted from the shape of the hour-ahead generation schedule, regulation and load following curves as shown in the Figure 4.18 to Figure 4.21.

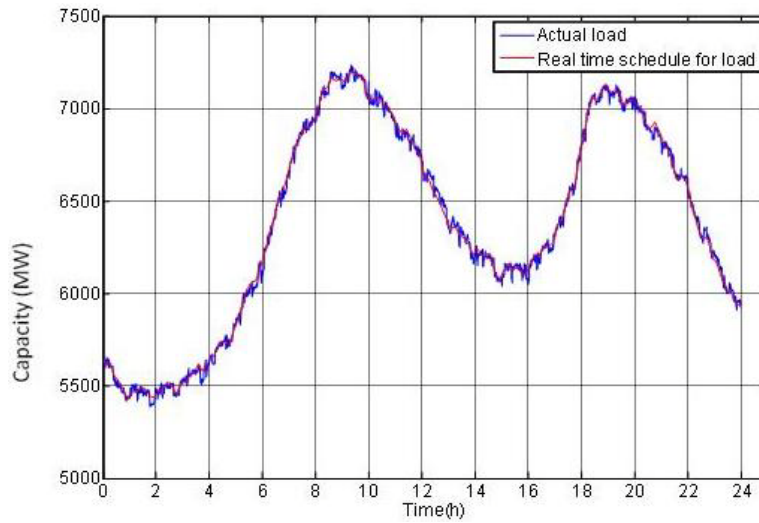


Figure 4.18. Actual load $L_{\text{actual}}(\text{min})$ and Real-Time Load Schedule $L_{\text{schedule}}(\text{min})$

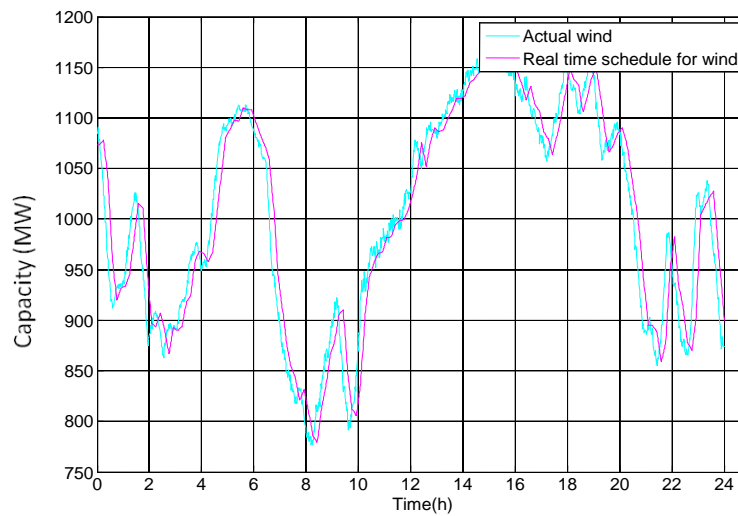


Figure 4.19. Actual Wind $W_{\text{actual}}(\text{min})$ and Real-Time Wind Schedule $W_{\text{schedule}}(\text{min})$

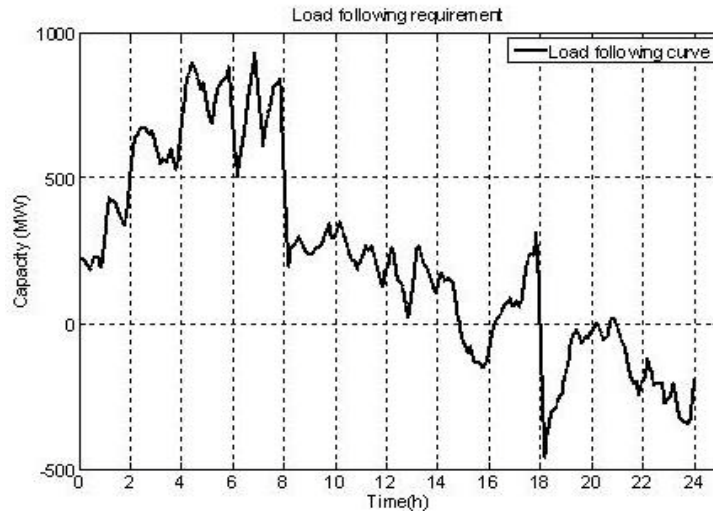


Figure 4.20. Calculated Load Following Requirements Curve

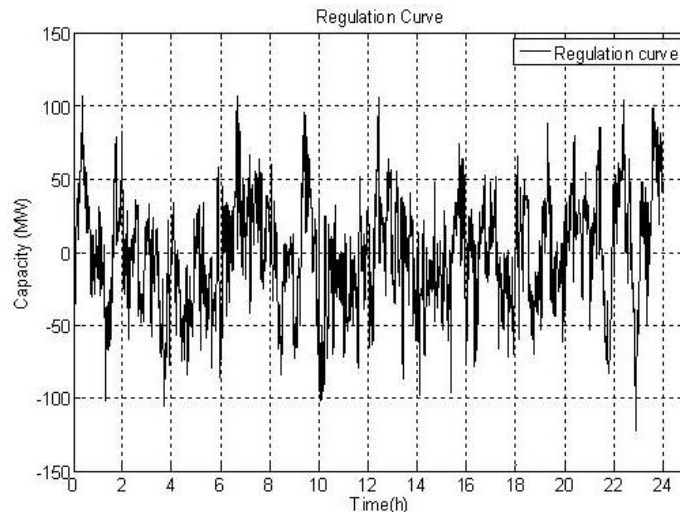


Figure 4.21. Calculated Regulation Requirement Curve

Since the curves follow a noisy, zigzag pattern, the most essential ramps required to follow these curves must be determined systematically by introducing certain tolerance band around the ramps. We propose to use the “swinging door” algorithm for this purpose. This is a proven technical solution implemented in time-series databases to compress and store time dependent datasets.

The swinging door algorithm determines which parts of the curves can be subsumed and represented by common ramps. Each ramp rate corresponds to a ‘swinging window’, and all the points within a swinging window are assigned the same ramp rate.

The end result of the swinging door algorithm application to the regulation, load following, and hour-ahead schedules is that each operating point is characterized by: capacity, ramp rate, ramp duration, and energy requirements needed at each operating point on the curve. The physical significance of these quantities is explained below:

- a. The incremental capacity has a positive sign that means, it is an extra capacity needed over the scheduled capacity (above the zero MW line in the load following and regulation curves). The

decremental capacity has a negative sign that means a lower capacity needed comparing to the scheduled capacity (under the zero MW line in the load following and regulation curves).

- b. A ramp rate has a positive sign if the last point in the swing door has higher capacity requirements than the first point, i.e., generating units need to be moved up. A ramp rate has a negative sign if the last point in the swing door has lower capacity requirements than the first point, i.e., generating units need to be moved down.
- c. Each minute in the hour-ahead schedule, load following, or regulation curves is characterized by four parameters: capacity, ramp rate, ramp duration, and energy. The all these parameters determined along a curve of interest form the first performance envelope for this curve.
- d. As is the case with any methodology that is based on random number generators, in this case generation of forecast errors, we do not rely on a single realization of a forecast error time series, rather, the previous steps are repeated 20 times (Monte Carlo simulation) with a different set of time series forecast errors for each run; and four parameters are evaluated for each of the three curves generated in each run of the 20 simulations.
- e. Note: As a result of this, we generate a dataset that is subjected to further analysis. The total number of points generated equals to about 252 million (60 minutes *24 hours *8760 day* 20 runs.)
- f. System operators are not required to balance against each point along the generation requirement curve. Therefore, certain percentage of points could be left not completely balanced. The first performance metric obtained in step ‘e’ is pruned to eliminate up to say 5% points that can be considered as statistical outliers, i.e., those below and above certain threshold requirements are not considered for further analysis. This would mean that we are not going to balance against certain percentage of extreme situations where the components of the performance envelope exceed certain values.
- g. For each hour in a day within the season, the maximum incremental and decremental capacity, and ramp rate requirements for each of the three curves are calculated. This is achieved by comparing all the points within the bounding box. The results for scheduling capacity (maximum and minimum) are shown in Figure 4.22 for the whole summer season.

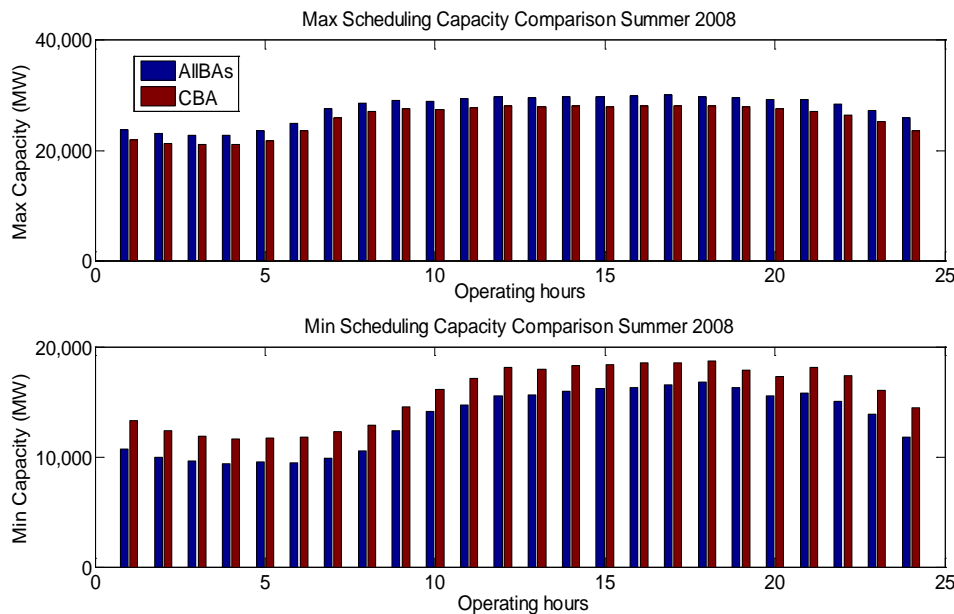


Figure 4.22. Min/Max Capacity Requirement Comparison for Scheduling

The relative benefits of consolidation will depend on how the forecast for load and wind generation will be performed on the consolidated BA. To investigate the results' sensitivity to the hour-ahead load and wind forecast errors, three different scenarios (worst cases) were considered as given in Table 4.1. Preliminary results for savings in the MW capacity, ramp rate and energy for load following and regulation are given in the following, Figure 4.23 to Figure 4.32.

Table 4.1. Analyzed Scenarios in the Study Case

Statistics		Scenario 1	Scenario 2	Scenario 3
Hour-ahead load forecast error	Mean error	0%	0%	0%
	Standard deviation	1%	2%	2.5%
	Auto correlation	0.9	0.9	0.9
Hour-ahead wind forecast error	Mean error	0%	0%	0%
	Standard deviation	4%	7%	12%
	Auto correlation	0.6	0.6	0.6

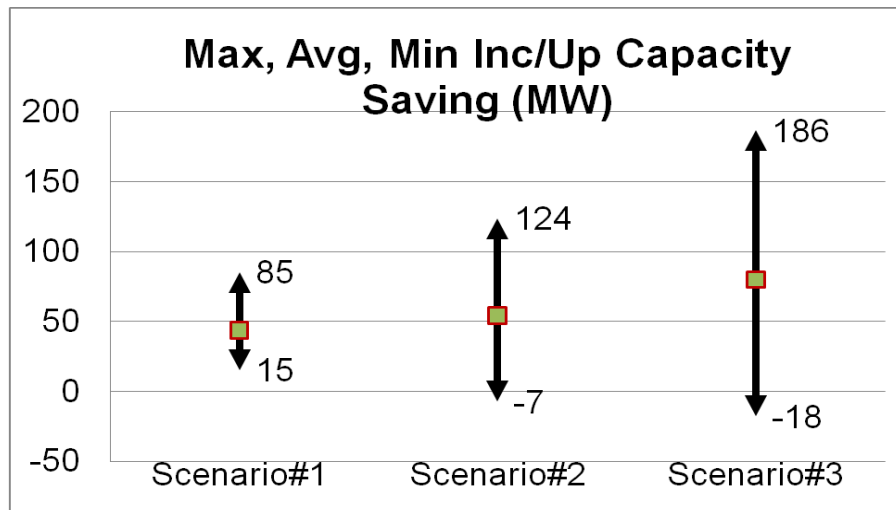


Figure 4.23. Incremental Capacity Saving Comparison for Load Following

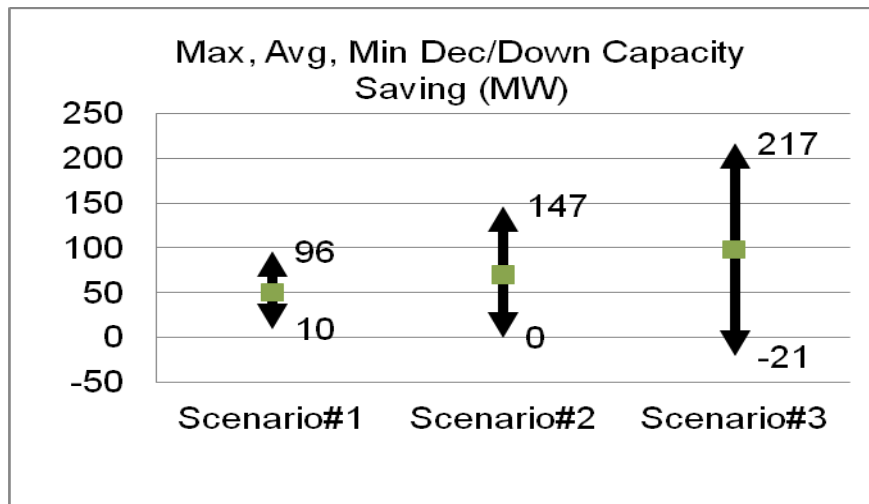


Figure 4.24. Decremental Capacity Saving Comparison for Load Following

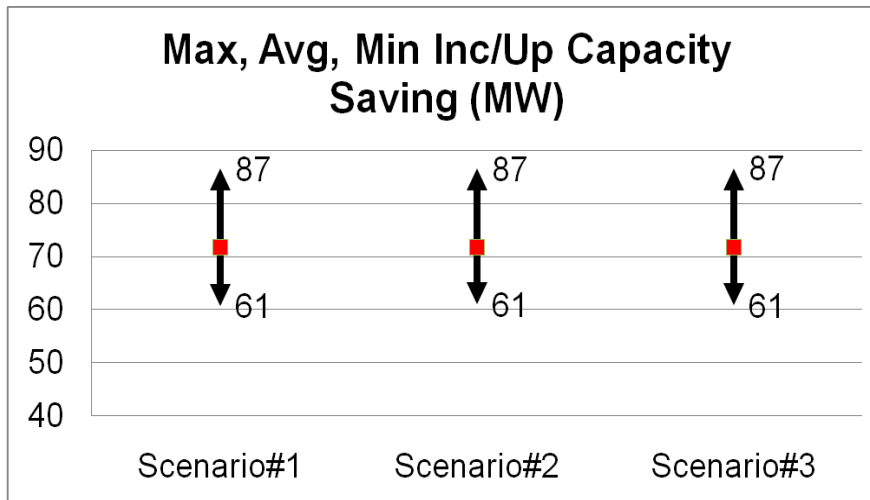


Figure 4.25. Incremental Capacity Saving Comparison for Regulation

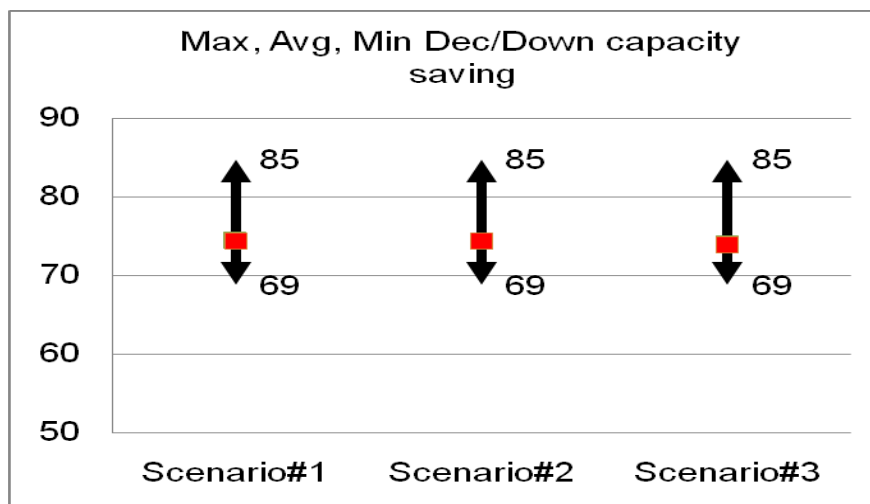


Figure 4.26. Decremental Capacity Saving Comparison for Regulation

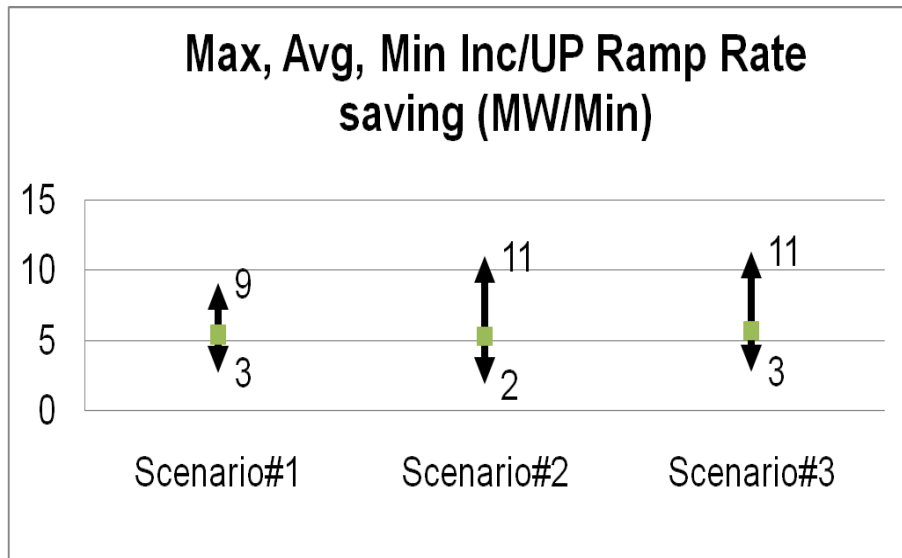


Figure 4.27. Ramp Rate Saving Comparison for Inc/Up Load Following

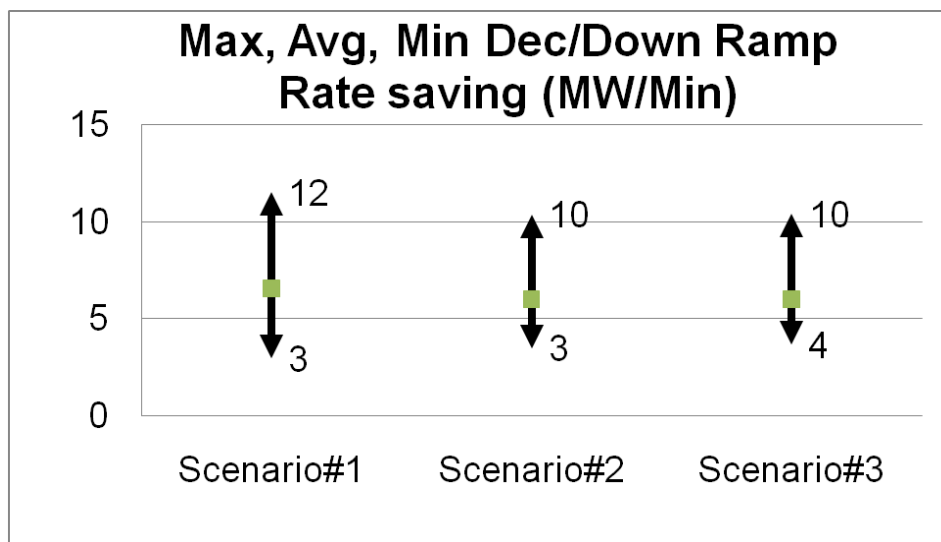


Figure 4.28. Ramp Rate Saving Comparison for Dec/Down Load Following

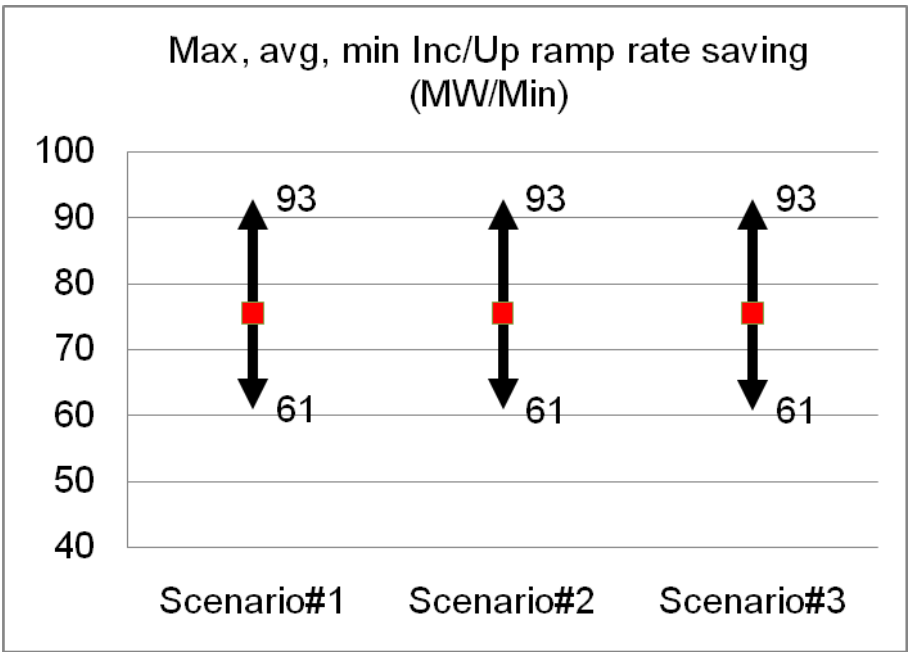


Figure 4.29. Ramp Rate Saving Comparison for Inc/Up Regulation

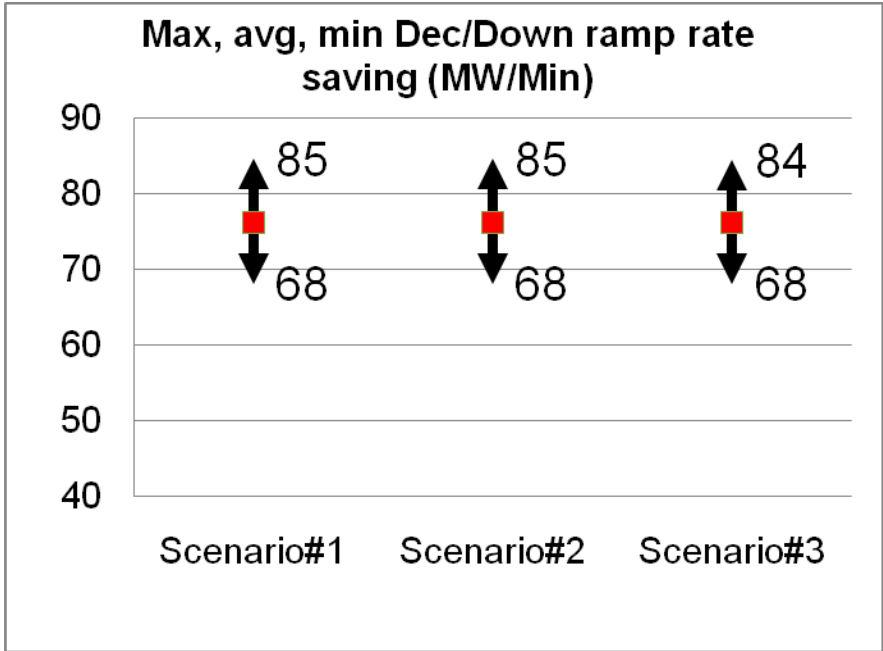


Figure 4.30. Ramp Rate Saving Comparison for Dec/Down Regulation

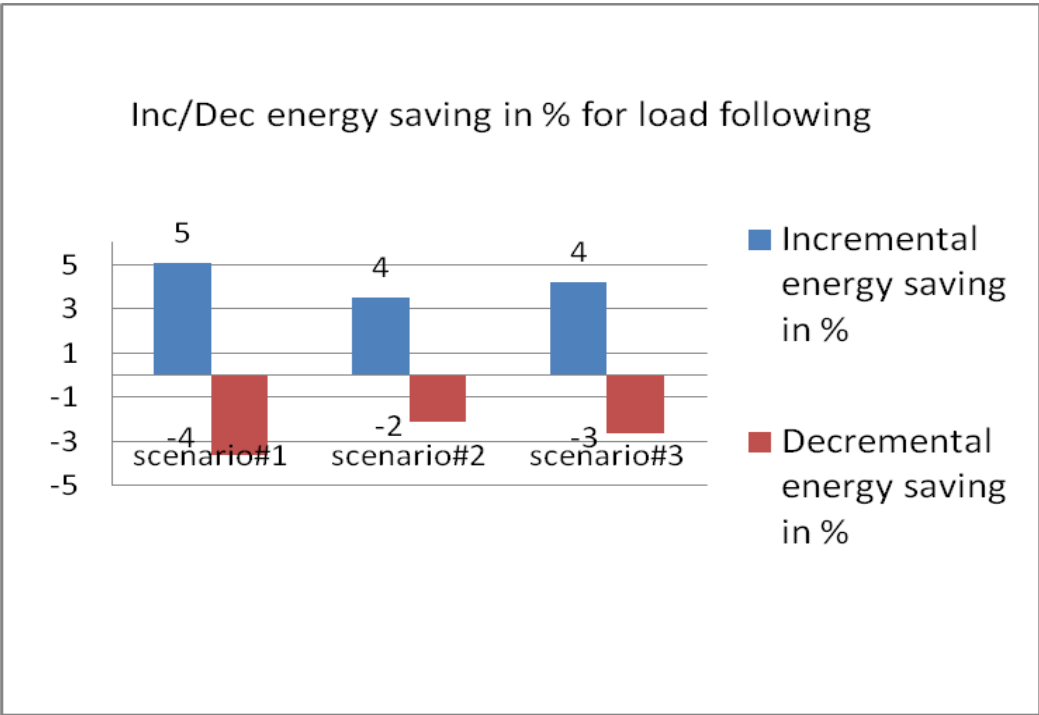


Figure 4.31. Percentage Energy Saving Comparison for Load Following

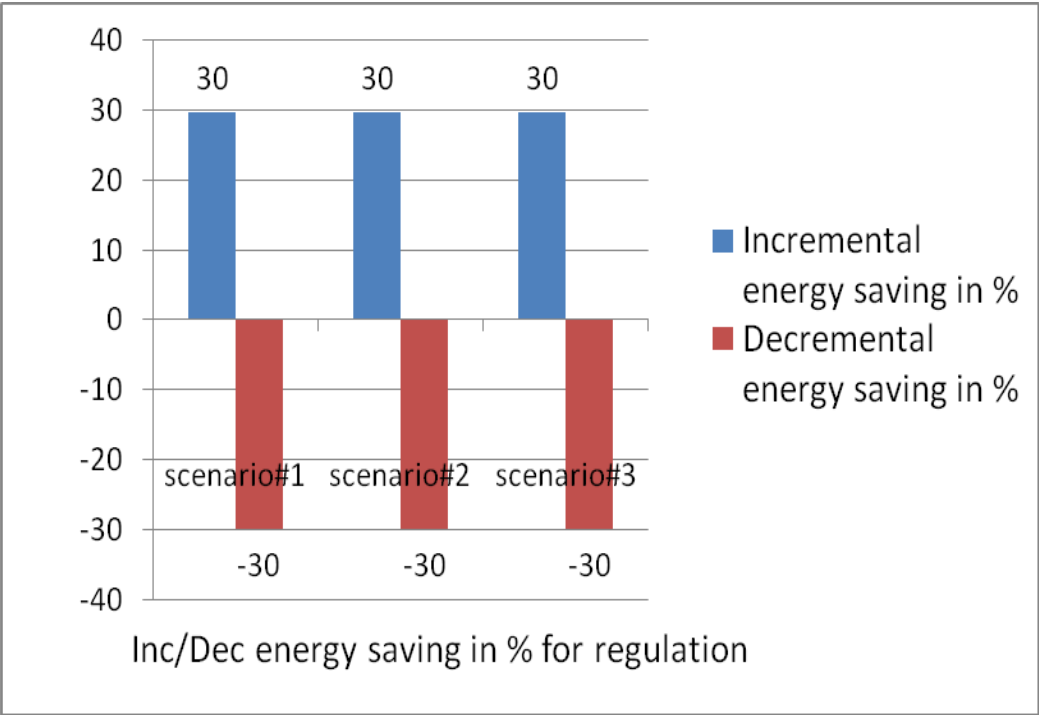


Figure 4.32. Percentage Energy Saving Comparison for Regulation

4.5.5 Future Work:

The comparison for the savings in MW capacity, ramp rate and energy for regulation and load following makes it evident that BA consolidation has proven benefits. The forecast statistics considered indicates worst case scenarios. The regulation signals to online generating units comprise of shorter duration ramps and lesser ramp rates. The regulation energy requirement diminishes by almost 30% while load following energy diminishes by 4% at a maximum. Improved forecast error statistics for the consolidated BA probably can benefit the load following energy saving too. These investigations can be extended to a real and large geographical system with several balancing areas. Improved methods can be adopted for load and wind forecast errors evaluation. The analysis to quantify the operational savings and reduced burden on market operations for such system may yield a valuable insight to the benefits of BA consolidation.

5.0 Development and Evaluation on Some New BA Cooperation Approaches

5.1 Advanced ADI Methodology

To overcome limitations of the conventional ADI, the authors propose two improved approaches for ADI.

Detailed mathematical model of conventional ADI is given in Appendix B. A constant cap of 25 MW as described in [4] and [12] has been used to restrict maximum ADI adjustments and minimize the risk of congestion. Nonetheless, these constant caps may result in over-conservative (i.e., less efficient) and/or over-aggressive (causing congestion) operation. Thus, within the existing ADI approaches, it is desirable to integrate reliability constraints, such as transmission capacity limits.

Figure 5.1 depicts the ACE adjustments calculated using real statistical data provided by California ISO (CAISO) and Bonneville Power Administration (BPA). One can see that the adjustment values can exceed the 25 MW limit applied to the conventional ADI. Thus, the 25 MW limit now in use in the WECC ADI reduces potential benefits from the ACE sharing technology

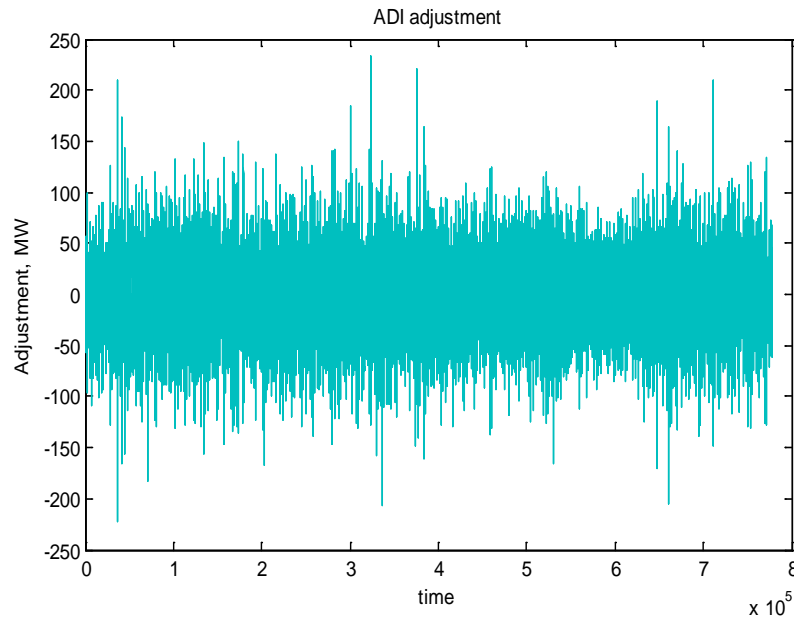


Figure 5.1. ACE Adjustments

To address this issue, the authors propose to incorporate the transmission system constraints directly into the ADI algorithm, and by addressing the congestion problem using an optimization approach. Otherwise, the proposed method adopts the same ACE sharing principles as the existing ADI algorithm.

The authors proposed two improved approaches. First is based on linear optimization technique. The second uses two-stage linear programming method. Both approaches include the transmission congestion model based on a linearized approximation of the power flow equations (see Section 3.4.3 for the details on power flow incremental model). The incremental power flow model could be periodically updated using the state estimation results.

Mathematical models of the proposed approaches, as well as details of simulation results are given in Appendix B. Simulations have been done for two test systems: 4-machine model and IEEE 30 bus test power system.

Moreover simulations using real system data were performed. The CAISO and BPA year 2006 data were used. The data set used included the following information:

- CAISO ACE
- BPA ACE
- California–Oregon Intertie (COI) actual power flow
- COI interchange schedule
- COI power flow limit

The COI is the major transmission path connecting BPA and the CAISO systems. COI is used mostly to transfer power from BPA to the CAISO, but at times reverse flows also occur. The COI power transfer limit is about 4,800 MW from BPA to CAISO and about 4,000 MW from the CAISO to BPA [52].

Four scenarios were considered in the study:

- No ADI
- Conventional ADI with 25MW adjustment limits
- Conventional ADI without limits
- Proposed ADI with the congestion model.

BPA and the CAISO regulating energy requirements for different scenarios are presented in Figure 5.2 through Figure 5.3. It can be seen that the ADI methodology reduces the energy needed for regulation. Moreover, by eliminating the 25MW limit applied to ADI adjustments, one could essentially increase the ADI efficiency and bring more benefits to the ADI participants.

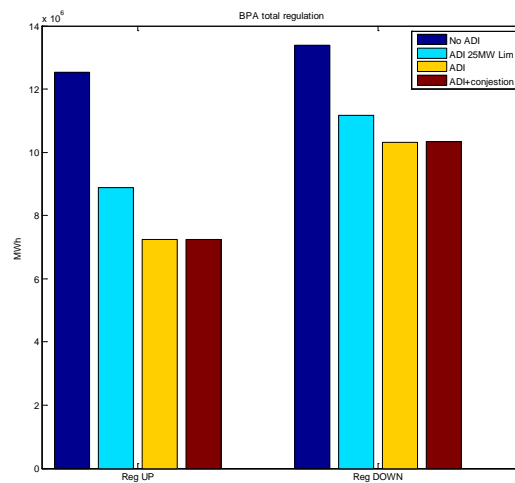


Figure 5.2. BPA Regulating Energy (Up and Down): Without ADI, ADI With 25MW Limit, ADI, ADI With Congestion Model

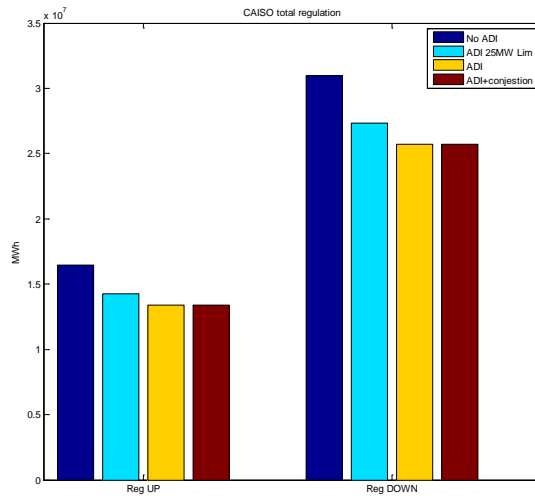


Figure 5.3. CAISO Regulating Energy (Up and Down): Without ADI, ADI With 25MW Limit, ADI, ADI With Congestion Model

Ramping requirements analysis was performed according to the methodology given in Section 9.0A.2. As a result of this analysis, a performance envelope containing information on ramping requirements (ramp and capacity) was obtained (see Section 2.1.5.1). Two scenarios were considered: (1) a scenario, without ADI; (2) a scenario, where the advanced ADI is used.

Figure 5.4 and Figure 5.5 show the distribution of ACE signals for the BPA and the CAISO BAs respectively. It is evident that the ADI reduces the spread of ACE distribution and thus decreases the regulation capacity requirements. As shown, the congestion limit, once introduced, does not affect the ADI performance when compared to the full size ADI without congestion. Ramp rate requirements distribution for the BPA and the CAISO BAs are presented in Figure 5.6–Figure 5.7. As shown, the ADI reduces the ramping requirements for both BAs.

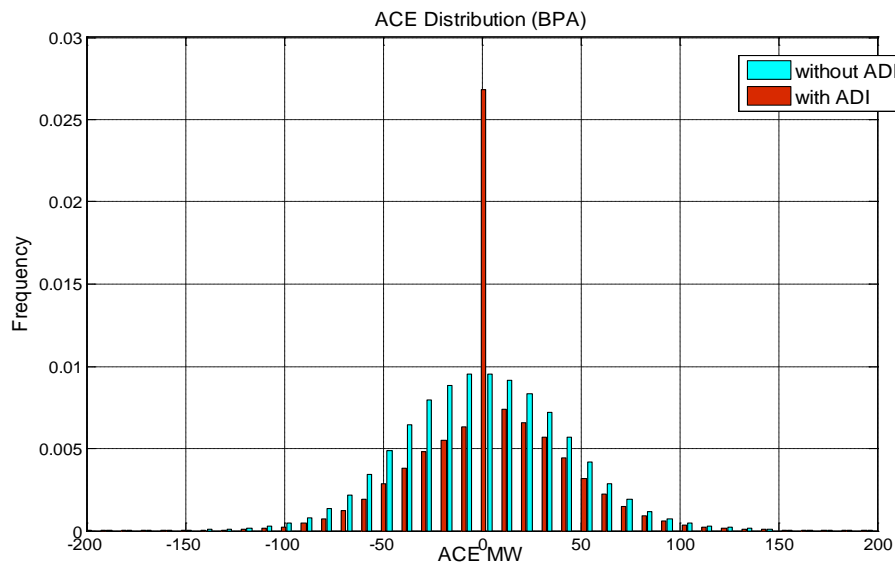


Figure 5.4. BPA ACE Distribution: With ADI, Without ADI

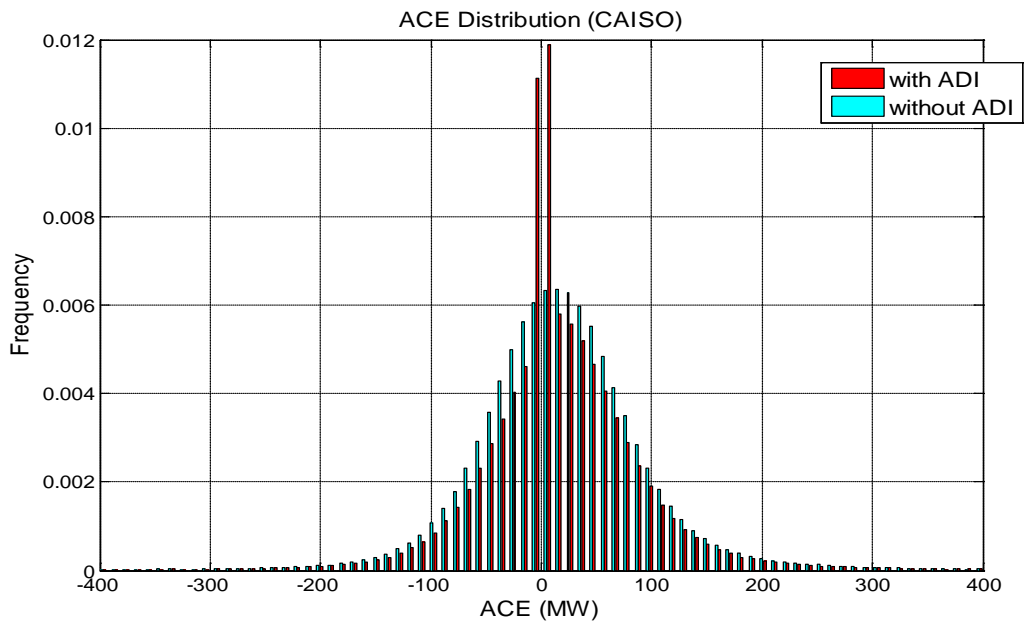


Figure 5.5. CAISO ACE Distribution: With ADI, Without ADI

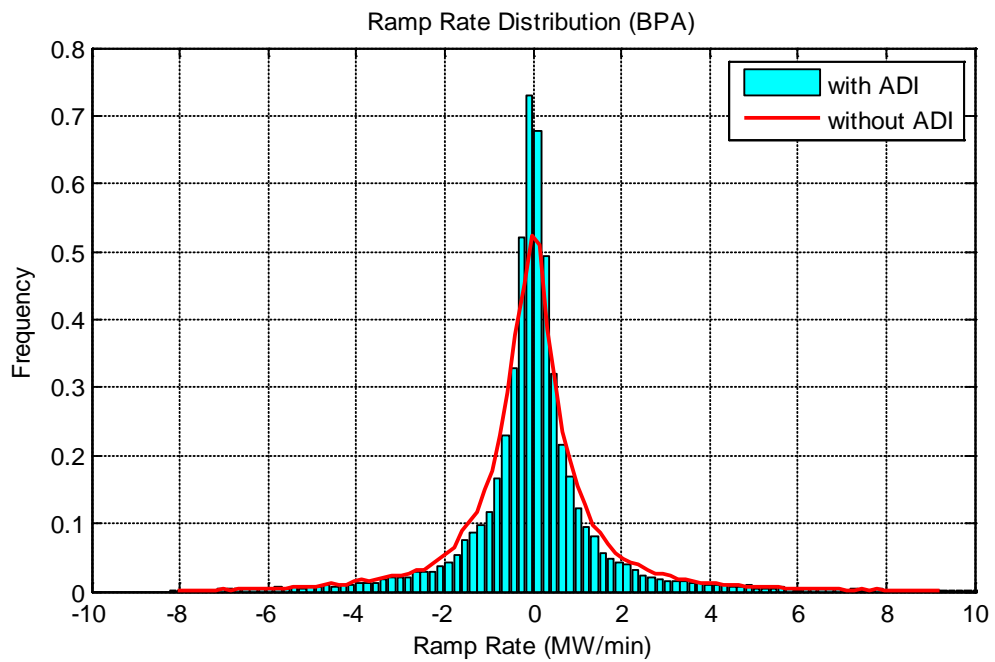


Figure 5.6. BPA Ramp Rate Requirements Distribution: With ADI, Without ADI

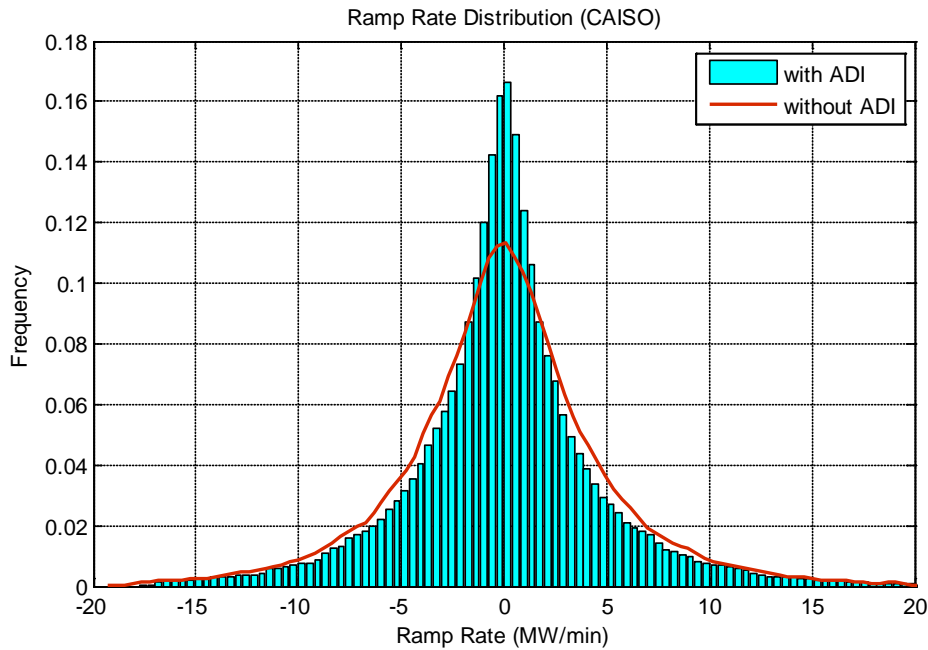


Figure 5.7. CAISO Ramp Rate Requirements Distribution: With ADI, Without ADI

Thus, the proposed new advanced ADI methodology is capable to enhance the performance of the conventional ADI by incorporating congestion model. Study results have shown that the advanced ADI methodology can improve the performance of existing ADI technology, reduce the required capacity, ramping and energy requirements needed for the BA balancing purposes.

5.2 Virtual Energy Storage to Partially Mitigate Unscheduled Interchange Caused by Wind Power

Each balancing authority (BA) in a grid conforms to a schedule that sets forth how much capacity will be allowed to pass through the area at given times of the day. These schedules are normally set a day in advance. However, a certain amount of energy will normally pass through over and above the scheduled amount. This unscheduled energy transfer is referred to as inadvertent interchange (see Section 3.3.3), and less is normally considered better. Wind generation is variable and non-dispatchable source of energy. It causes additional unscheduled deviation of electric generation and complicates the problem of system balancing. For instance, BAs need to procure more regulation capacity to meet CPS requirements. Due to the lack of fast response units and because of slow units are not capable to follow the fast ramping events more units and more capacity must be involved in regulation process.

To promote large-scaled wind power penetration, advanced techniques were proposed, e.g., energy storage, BA collaboration and more accurate wind forecasting. A fast-response storage device with appropriate duration holds great promise in that it is very effective in mitigating varieties of wind power. The benefit of energy storage can be more efficiently utilized when they operate in parallel with conventional regulation resources. In this way, energy storage only responds to a filtered area control error signal. However, despite advancements in technologies, capital costs of energy storages are still very high.

A more advanced concept, referred to as “virtual energy storage” in Figure 5.8, is proposed as BA collaboration under evaluation or developed. By allowing the periodic energy exchanged between BAs,

this scheme takes advantages of diversity of wind power in different geographic areas. The oscillating power represents the resources remotely providing ancillary service and it benefits both provider and receiver. The cost of a virtual energy storage is zero while the benefit of this concept include less amount of regulation that can be procured (lower regulation service cost), and decreased area control errors.

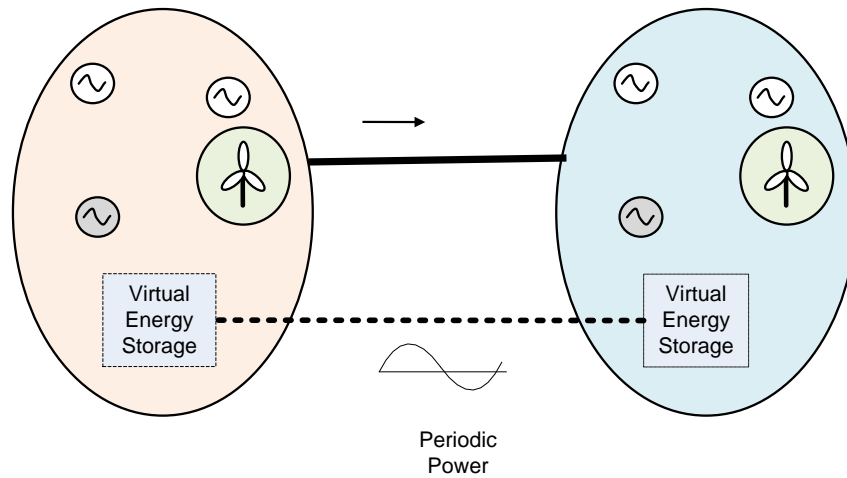


Figure 5.8. Illustration of Virtual Energy Storage Concept

This chapter explains the basic principle behind virtual energy storage, its performance evaluation and technical implications.

5.2.1 Background and Basic Principle

Area control error (ACE) plays a vital role in power system generation control to balance expected and unexpected variations in system load and interchange. ACE is defined as the active power control error for a BA. ACE values determine how much a BA needs to move its regulating units to meet the mandatory control performance standard requirements. The power system control objective is to minimize its area control error (ACE) in the extent sufficient to comply with the North American Electric Reliability Corporation (NERC) Control Performance Standards (CPS). Therefore, the “ideal” regulation/load following signal is the signal that opposes deviations of ACE from zero when they exceed certain thresholds:

$$\begin{aligned}
 -ACE &= -(I_a - I_s) + 10B(F_a - F_s) \\
 &\approx -(G_a - L_a) \rightarrow \min
 \end{aligned}
 \tag{5.1}$$

where subscript a denotes actual, s denotes schedule, I stands for interchange between control areas, F stands for system frequency, and B is the system frequency bias (MW/0.1 Hz, a negative value). G_a is the actual generation and L_a is the actual load within the control area.

NERC has established the requirements on the deviations of ACE to enhance the reliability of interconnection of power systems. To be in compliance with these reliability standards, adequate generation or other resources (e.g., energy storage) have to be procured to mitigate the deviations. Due to its slow response, the large amount of conventional generation must be reserved for ancillary services. Compared to the conventional generation, a fast-response storage device with appropriate duration is

more effective for regulation service. However, depending on technologies, capital costs of energy storages are very high. Thus, utilities are still looking for effective and affordable means to help them meet these reliability standards.

The proposed approach, referred to as “virtual energy storage”, is a significant advancement in improving reliability while saving cost. Essentially, BAs are free to exchange periodic power between them. The scheduled interchange is the constant schedule superposed with the periodic ones. This scheme takes advantages of diversity of wind power in different geographic areas. The oscillating power represents the resources remotely providing ancillary service and it benefits both provider and receiver. Since the energy of periodic power fluctuates around zero, each BA acts as virtual energy storage to others. The cost of a “virtual” energy storage is virtually zero while the benefit of this concept include less amount of regulation that can be procured (lower regulation service cost), and decreased area control errors.

5.2.2 Performance Evaluation

The performance of the virtual energy storage is demonstrated on the COI transmission corridor. The COI is the major transmission path connecting BPA and the CAISO systems. COI is used mostly to transfer power from BPA to the CAISO, but at times reverse flows also occur. The COI power transfer limit is about 4,800 MW from BPA to CAISO and about 4,000 MW from the CAISO to BPA. Figure 5.9 shows the scheduled COI power (red), the actual COI power (blue) and the COI power deviation from the scheduled (green) that were measured each 4 seconds on the selected days in 2006. The deviation has a biased 65 MW, with a maximum value of 868 MW and a minimum value of -763 MW.

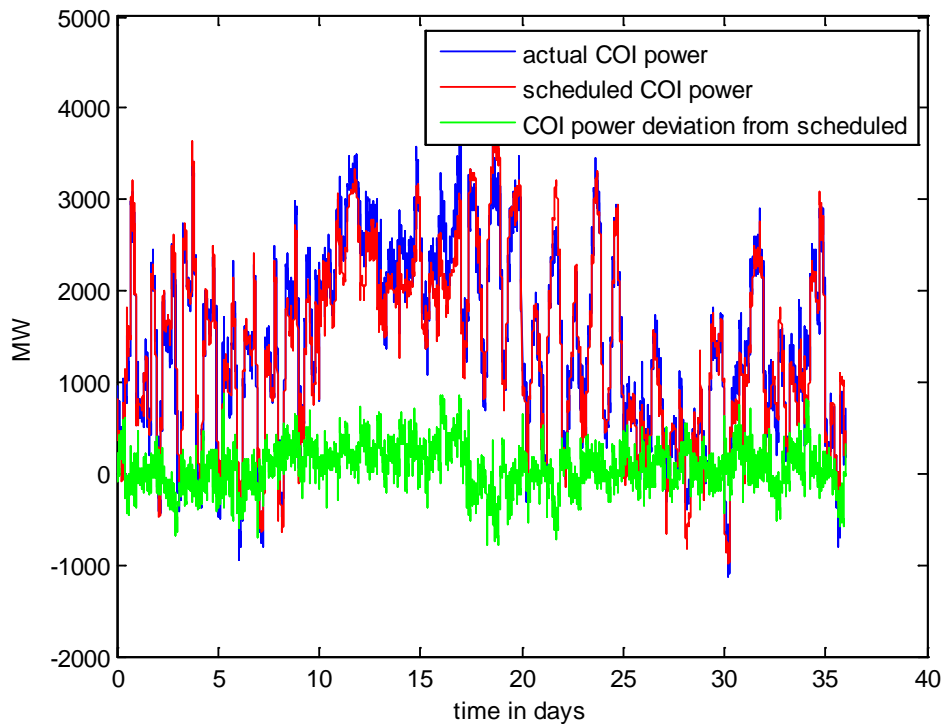


Figure 5.9. COI Power Deviation from Scheduled

A band-pass filter was applied to the COI power deviation to eliminate DC component and high-frequency components. The characteristic of the band-pass filter is shown in Figure 5.10.

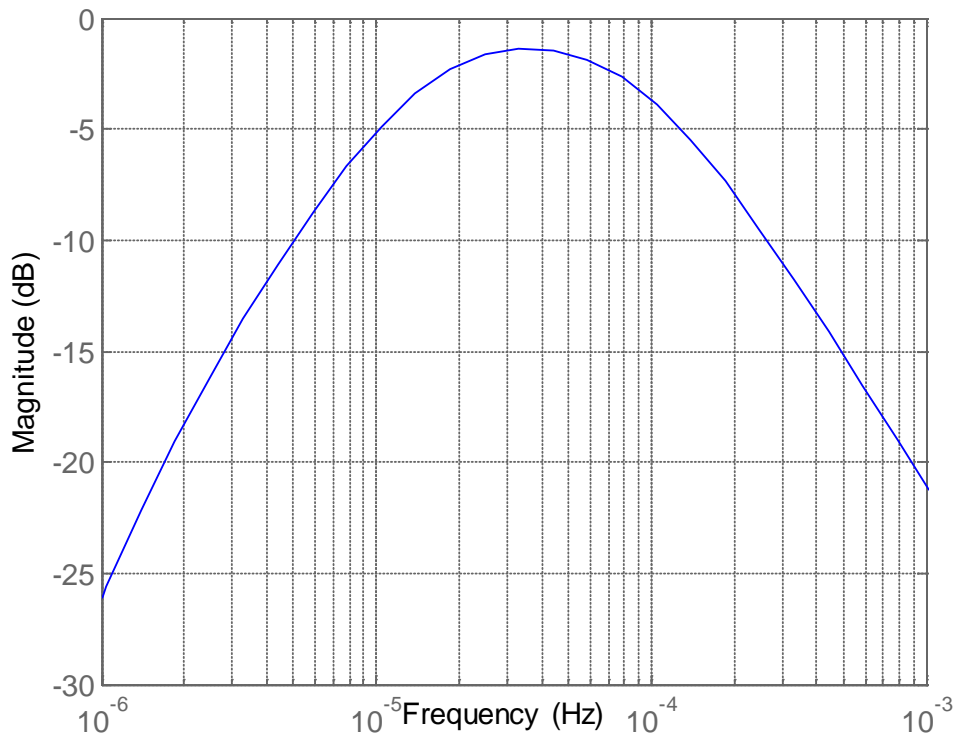
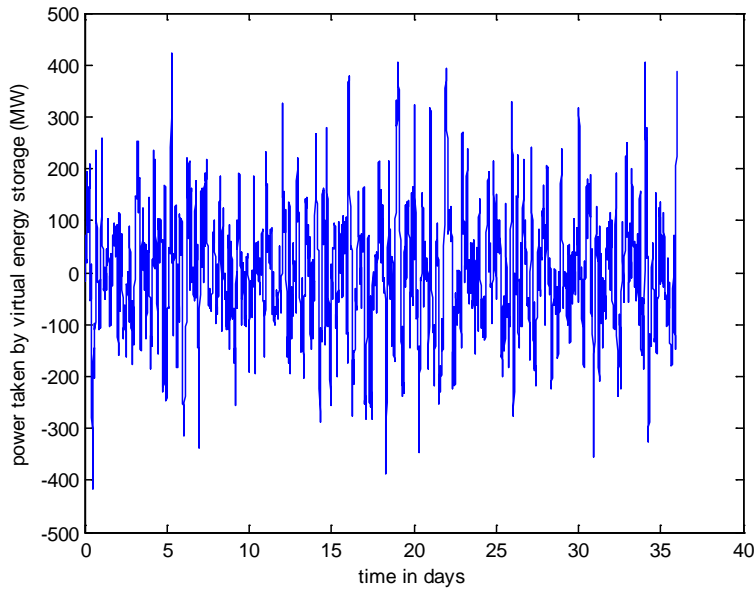
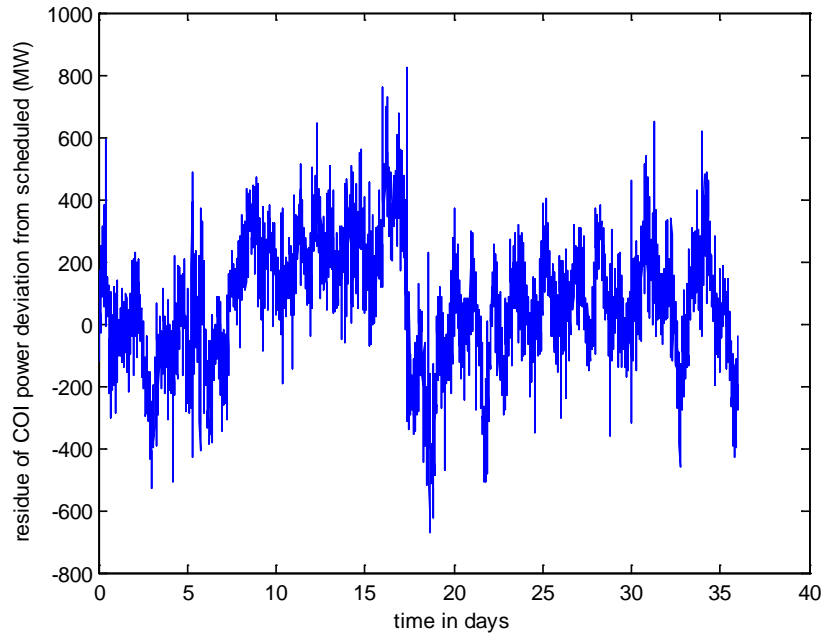


Figure 5.10. Characteristics of the Band-Pass Filter

The filtered result of the COI power deviation is shown in Figure 5.11 (a), and the residue (COI power deviation – filtered power) is shown in Figure 5.11 (b). It implies that the oscillatory exchanges embedded in the filtered power flow between BPA and CAISO, but the magnitude and frequency of the oscillations change over time.



(a) filtered power



(b) residue

Figure 5.11. Filtered Power and Residue of COI Power Deviation

The characteristics of the COI power deviation and its residue are summarized in Table 5.1. The stand deviation is decreased from 227.93 MW to 189.27 MW by removing the filtered power from COI power deviation. This leads to a decreased area control error, which requires less primary resources for regulation.

Table 5.1. Statistics of COI Power Deviation, Filtered Power and Residue

	Mean (MW)	Maximum (MW)	Minimum (MW)	Standard deviation (MW)
COI power deviation from scheduled	65.31	868.05	-763.15	227.93
Power taken by virtual energy storage	-0.7633	422.70	-415.43	116.61
Residue of COI power deviation from scheduled	66.07	822.77	-672.15	189.27

The characteristics of the COI power deviation and its residue are also shown in Figure 5.12. Compared with the unfiltered power deviation, the shape of the residue changes as its tail part shrinks and it becomes more concentrated on the central part.

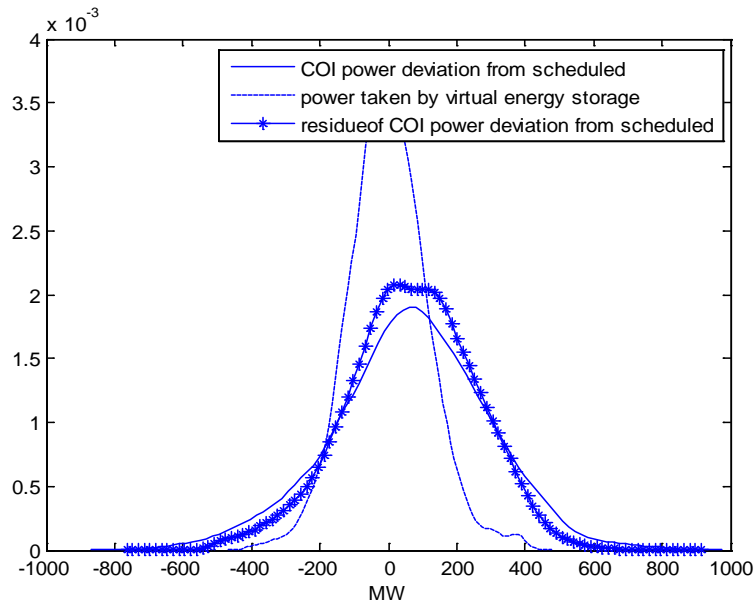


Figure 5.12. Histogram of COI Power Deviation, Filtered Power and Residue

An adaptive filter can be used to predict the future value of the filter COI power deviation based on the history information. LMS (least mean square) filter is preferred due to its simple structure and the good convergence performance. The five-minute-ahead prediction from LMS filter can yield a good match to the filtered COI power, as shown in Figure 5.13. This prediction is successful due to the slowly varying nature of the predicated signal (high frequency component in the filtered COI power deviation has been removed by the band-pass filter). If this prediction is performed in real-time with the tolerant errors, conventional generators can be adjusted ahead of time to match the variations in loads. Therefore, regulation will become more efficient.

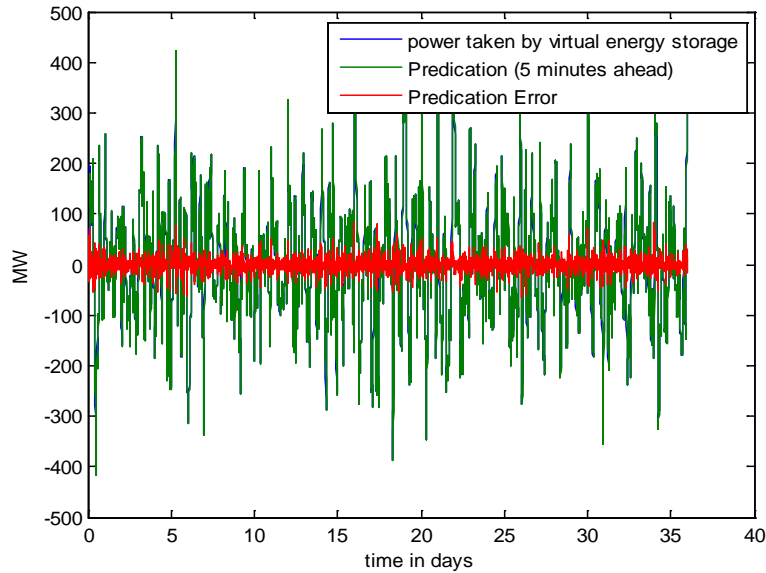


Figure 5.13. Predication of Filtered COI Power Deviation by LMS Filter

When the filtered COI power deviation is positive, the virtual energy storage is charged. In contrary, when the filter COI power deviation is negative, the virtual energy storage is discharged. The size of the virtual energy storage (2500 MWh in this case) can be determined by charge profile of virtual energy storage (see Figure 5.14).

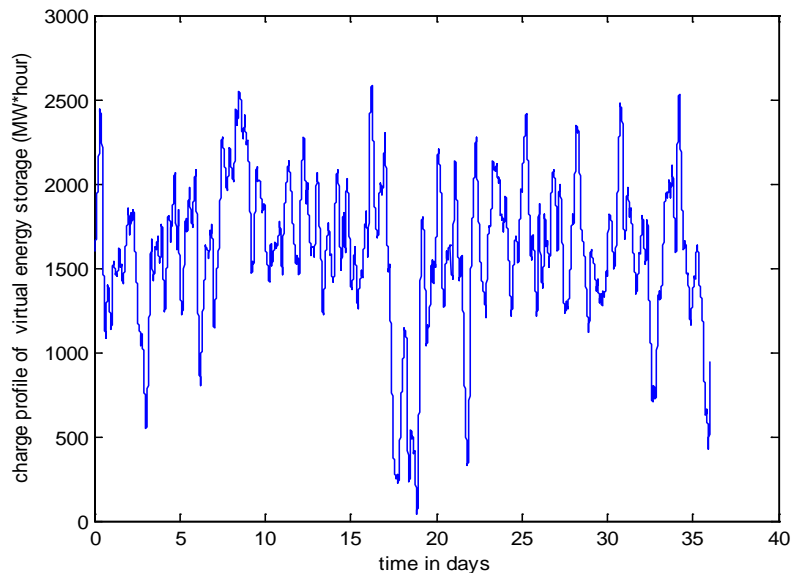


Figure 5.14. Charge Profile of Virtual Energy Storage

5.2.3 Technical and Operation Implications

As discussed, the use of virtual energy storage can significantly reduce the requirement of regulation capacity. However, its implementation requires a different operating philosophy of power systems. There are several technical or operation aspects worthwhile discussing.

5.2.3.1 Obey Transmission Constraints

Any interchange arrangement should not compromise reliability and security of power systems. Traditionally, the security conditions on the scheduled interchanges for large power systems are expressed as nomograms. This represents the maximum transfer capability of path flows, which is also known as transmission constraint. The actual power flow (usually time-invariant during the scheduling interval) is determined based on the economical principle with the security constraint satisfied. If the new scheme is in place, the actual power flow becomes the sum of the periodic power and the time-invariant scheduled power. Therefore, in case of inadequate security margin reserved ahead, there is a risk of violation of transmission constraints. To circumvent this problem, the interchange schedule has to be operated in less efficient way, leading to higher operation cost. This consequence should be weighted against the benefits obtained from virtual energy storage.

5.2.3.2 On-Peak and Off-Peak Hours Energy Exchange

As noted, although the periodic power varies in frequency and magnitude, its energy oscillates around zero (or close to zero). This zero-energy property makes virtual energy storage concept very attractive because BAs can absorb energy over the half cycle of operation interval while inject almost the same amount of energy over other half cycle. If market mechanism is not involved, the net revenue or profit incurred between BAs will be not significant. However, if the power is priced at the real-time market, the cost of exchanged periodic power becomes different for different BAs. Some of them may make profit while others pay for this ancillary service resulting from virtual energy storage scheme. Agreements should be arranged prior to execution of this approach.

5.2.3.3 Elimination of Loop Flows

The success of virtual energy storage concept depends largely on the presence of periodic power, which has been verified by the example illustrated above. However, this periodic power should exclude loop flow that may practically appear in interconnected power systems. Loop flow is defined as the power flow circulated in the ring-structure of power systems, as shown in Figure 5.15. Without loss of generality, assume that the positive loop flow is in the arrow direction.

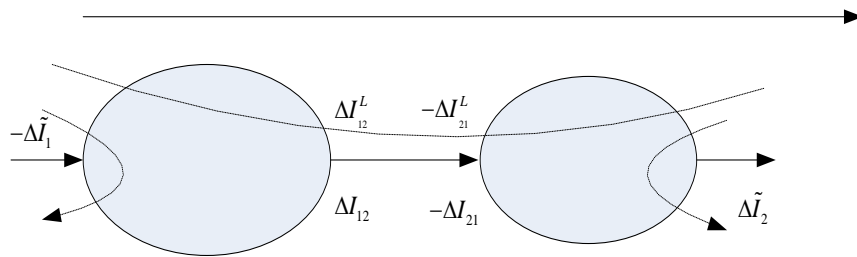


Figure 5.15. Illustration of Loop Flow

ΔI_{12} , and $-\Delta I_{21}$ are the power flows along the tie lines connecting BA1 and BA2.

ΔI_{12}^L , and $-\Delta I_{21}^L$ are the loop flows along the tie lines connecting BA1 and BA2.

$$\Delta \tilde{I}_1 = f(\Delta I_{12}^L) \quad (5.2)$$

$$\Delta \tilde{I}_2 = f(\Delta I_{21}^L) \quad (5.3)$$

Net loop flow for BA1

$$\Delta I_1 = -\Delta \tilde{I}_1 + \Delta I_{12} \quad (5.4)$$

Net loop flow for BA2

$$\Delta I_2 = \Delta \tilde{I}_2 - \Delta I_{21} \quad (5.5)$$

The rules of determining loop flow are as follows.

```
If  $\Delta \tilde{I}_1 > 0$ 
  If  $\Delta I_{12} > 0$ 
     $LF_1 = \min(\Delta \tilde{I}_1, \Delta I_{12})$ 
  End
  If  $\Delta I_{12} \leq 0$ 
     $LF_1 = 0$  (BA1 sink)
  End
End
```

```
If  $\Delta \tilde{I}_1 < 0$ 
  If  $\Delta I_{12} > 0$ 
     $LF_1 = 0$  (BA1 source)
  End
  If  $\Delta I_{12} \leq 0$ 
     $LF_1 = \min(-\Delta \tilde{I}_1, -\Delta I_{12})$ 
  End
End
```

```
If  $\Delta \tilde{I}_{21} > 0$ 
  If  $\Delta \tilde{I}_2 > 0$ 
     $LF_2 = \min(\Delta \tilde{I}_2, \Delta I_{21})$ 
  End
  If  $\Delta \tilde{I}_2 \leq 0$ 
     $LF_2 = 0$  (BA2 sink)
  End
End
```

```

If  $\Delta\tilde{I}_{21} < 0$ 
    If  $\Delta\tilde{I}_2 > 0$ 
         $LF_2 = 0$  (BA2 source)
    End
    If  $\Delta\tilde{I}_2 \leq 0$ 
         $LF_2 = \min(-\Delta\tilde{I}_2, -\Delta I_{21})$ 
    End
End

```

It is an important task to ensure that loop flow is removed before virtual energy storage concept is applied.

5.2.4 Summary

Virtual energy storage is a novel concept to un-compensate for the periodic energy exchanged between BAs to minimize the burden on regulation process. It can result in tremendous saving in the procured regulation capacity at no cost. The following algorithms and approaches of virtual energy storage have been developed to investigate its technical feasibility and evaluating its performance.

1. Periodic power exchange can be identified by a band-pass filter. Preliminary simulation results performed on the transferred power between CAISO and BPA (2006) have confirmed presence of cycling power component. Its magnitude is significant as it oscillates between -400MW and 400MW.
2. Impact of eliminating periodic power by virtual energy storage over Area Control Error (ACE) was investigated. By removing this power off from compensation requirement, the histogram of ACE becomes more concentrated on the central part as stand deviation reduces from 227.93MW to 189.27 MW.
3. Despite the fact that periodic power is non-stationary, it can be predicted with very satisfactory accuracy by an adaptive filter (LMS) 5-minute ahead of time. If this prediction is performed in real-time, conventional generators can be adjusted ahead of time to match the variations in loads or wind to achieve more efficient regulation.

There are several technical or operation implications that can be subject of future work.

1. Obey transmission constraints
2. On-peak and off-peak hours energy exchange
3. Elimination of loop flows

6.0 Extreme Event Analysis

6.1 Objective of the Analysis

Growth in the demand and changes in the load and wind pattern may create major bottlenecks in the delivery of electric energy. Electric power systems are usually designed to operate under stable load and wind patterns. These design assumptions are strained by tail events (large imbalance between generation and load) happening due to unfortunate combinations of load and wind forecast errors. These extreme events are very difficult to predict so most of the times they are unexpected. They have been practically observed in the ERCOT and BPA service areas in the US as well as in Germany in Europe.

Tail events due to the forecast error extremes can impact the power system infrastructure from two main avenues. First one is the sudden and very significant power imbalances and the second one is sudden increases of power flows on the system critical paths. The magnitude of power imbalances and incremental power flows can reach to several thousand megawatts in case of an extreme of wind and load forecast errors occurring at the same time. The system operators do not have special reserves to mitigate these events.

With the increasing penetration of intermittent energy resources like wind, it is necessary to quantify the impacts of likely changes in the statistics of load and wind forecast errors on the operating reserve requirements and transmission line congestion for a look-ahead period of few hours. This can warn system operators of the possibility of happening tail events during those hours. Sharing the variability of the wind and load forecast errors across a broader region provides a natural aggregation impact; it results in reduction of required operating reserves while may increase congestion on the transmission interfaces.

This preliminary study based on the wind forecast errors levels, attempts to evaluate the expectancy of occurrences of these tail events using two balancing area example and relates with the operating reserve requirements and transmission congestion. Having this information, a detailed study for a large geographical region with many balancing areas including wind and load forecast errors can be carried out. As a result, these balancing areas could be better prepared to address the tail events by exploring different reserve options, wide area control coordination, new operating procedures and remedial actions.

6.2 Impact on Operating Reserve

The calculation of operating reserve to attain an expected level of power system generation adequacy to a given confidence level has been known for many years. However in the presence of wind generation, the calculation of required operating reserve has not been standardized. A methodology for setting required operating reserve is proposed and illustrated using wind forecast error levels. The approach uses the statistics of the extreme to identify how many times and to what extent generation margin is scheduled adequately in the presence of wind generation resources.

6.2.1 Introduction to Gumbel's Theory

The application of the Gumbel's theory is considered here in the occurrences of extreme values in the difference between actual wind generation power and forecast wind generation available [19],[20]. When the forecast exceeds the actual available wind power, there is an impact on the adequacy of total generation available. In particular, if the actual wind energy is less than forecast, there may be insufficient generation margin to comply with usual operating norms.

If one views ξ as error in wind power forecasts, a random process, it is natural to ask about extreme values of ξ . An ‘exceedance’ is a case in which a random variable sample ξ_1 exceeds (e.g., is greater than) all previously observed samples. For the errors in an ensemble of measurements,

$$\xi_1 \geq \xi_2 \geq \dots \geq \xi_n \quad (6.1)$$

The question is that when and with what probability would the ‘all time high’ ξ_1 be exceeded in future measurements. This number of exceedences is x which is a random variable.

6.2.2 Probability Model for Wind Forecast Error Exceedences

Given the ranking of past measurements of wind forecast errors shown in $\xi_1 \geq \xi_2 \geq \dots \geq \xi_n$ (6.1), Gumbel shows that for N future samples of wind forecast error, the random variable x (an integer) is defined as the number of times in the future that ξ_m is exceeded – that is, if $m = 1$, then how many times in the future will ξ_1 be exceeded, and if $m = 2$ how many times will ξ_2 be exceeded. As suggested by Gumbel, no assumption is used on the probability function of ξ_i but the concept of Bernoulli trials is used to obtain the probability density function of the random integer x .

$$f_x(n, m, N, x) = \frac{m \binom{n}{m} \binom{N}{x}}{(N+n) \binom{n+N-1}{m+x-1}} \quad (6.2)$$

where the Bernoulli combinatorial is

$$\binom{n}{m} = \frac{n!}{(n-m)!m!}$$

Equation $f_x(n, m, N, x) = \frac{m \binom{n}{m} \binom{N}{x}}{(N+n) \binom{n+N-1}{m+x-1}}$ (6.2) is the probability density of random

variable x – and since x is an integer, f_x is evaluated only at integer values of x (as well as integer values of

n , m , and N). With $f_x(n, m, N, x) = \frac{m \binom{n}{m} \binom{N}{x}}{(N+n) \binom{n+N-1}{m+x-1}}$ (6.2) in view, the expectation (i.e.,

mean) of x ,

$$E(x) = \sum_{x=1}^N x f_x(n, m, N, x) \quad (6.3)$$

Gumbel shows that the expectation of the number of exceedences in the next N samples is simply

$$E(x) = \frac{mN}{n+1} \quad (6.4)$$

As per Gumbel, it is also possible to manipulate $f_x(n, m, N, x) = \frac{m \binom{n}{m} \binom{N}{x}}{(N+n) \binom{n+N-1}{m+x-1}}$ (6.2) to

find the variance of x as,

$$\sigma_x^2 = \frac{nN(N+n+1)}{(n+1)^2(n+2)} \quad (6.5)$$

Since $f_x(n, m, N, x) = \frac{m \binom{n}{m} \binom{N}{x}}{(N+n) \binom{n+N-1}{m+x-1}}$ (6.2) shows the probability of occurrence, then

$1-f_x$ is the probability of not occurring and therefore the ‘return time’ $T(x)$, expected to achieve at least one exceedance is

$$T(x) = \frac{1}{1-f_x(x)} \quad (6.6)$$

6.2.3 Application to Wind Forecasts

The foregoing is now applied to a balancing area to examine the impact of extremes in wind power forecasts. Figure 6.1 shows wind generation data for a typical balancing authority for 5 minute intervals.

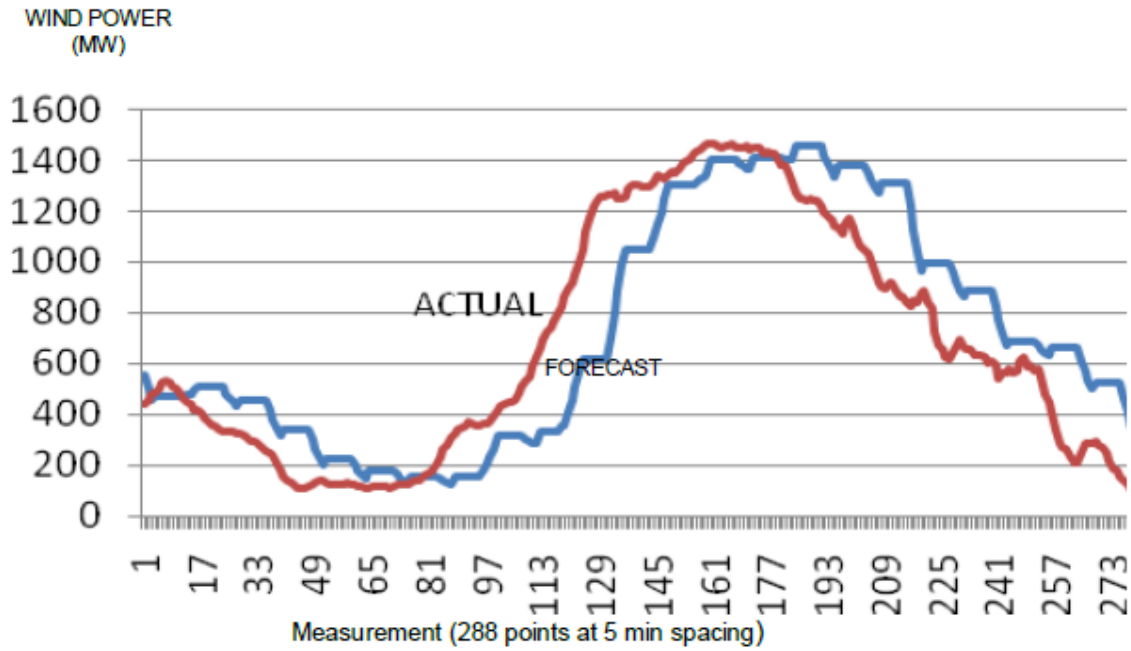


Figure 6.1. Wind Power Forecast and Actual Wind Power Values, for One Day, in 5 Minute Intervals

In Figure 6.2 the largest positive value of error is sample 1; the most negative value is sample 288. Positive error denotes that actual wind generation is more than forecast.

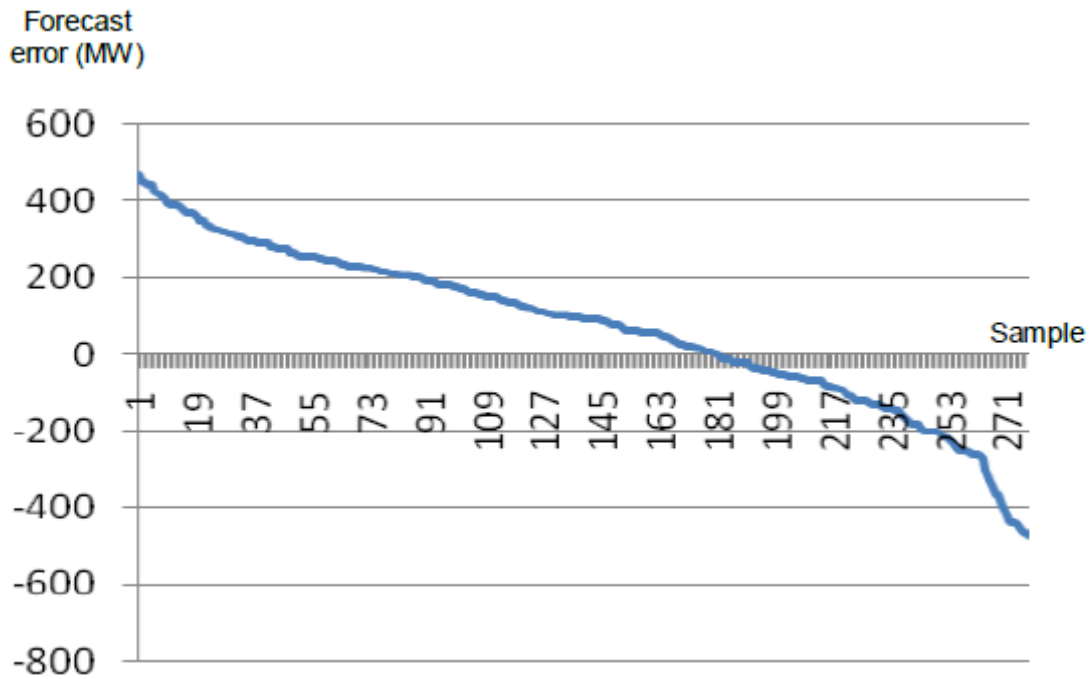


Figure 6.2. Ranked Wind Power Forecast Error ξ for a Day at 5 Minute Intervals

6.2.4 Implications on Reserve Margin Calculations

The implications of the previous sections can be brought to bear on the operating calculation. Equation (5.4) for the expectation and the values of $x_i(1), x_i(2), \dots, x_i(m)$ (exceedance levels) are to be used to obtain a plot of x_i vs. $E(x)$ where x is the number of exceedances of $x_i(m)$. Such a plot is the expected number of times in N future cases that the past $x_i(1), x_i(2), \dots$ will be exceeded. N time 5 min is the time span of the study into the future and so this is the time period for which the study is carried out. That is the generation margin (GM) is calculated $5N$ minutes into the future. For a GM in the next 30 minutes, $N = 6$. This can be expanded out to a calculation for a week or a quarter of a year (or even a year).

In Figure 6.3 which is a plot of exceedance level in MW versus expected number of exceedances in the next $5N$ minutes. The leftmost graph is $N=3$, next to the right is $N=6, \dots, 15$; the rightmost is $N=15$. If operating reserve is added to the system, the vertical scale shifts upward. As an example, for an addition of 100 MW reserve for the next 30 min, use the $N=6$ graph and shift the vertical axis so that 400 MW becomes 300 MW.

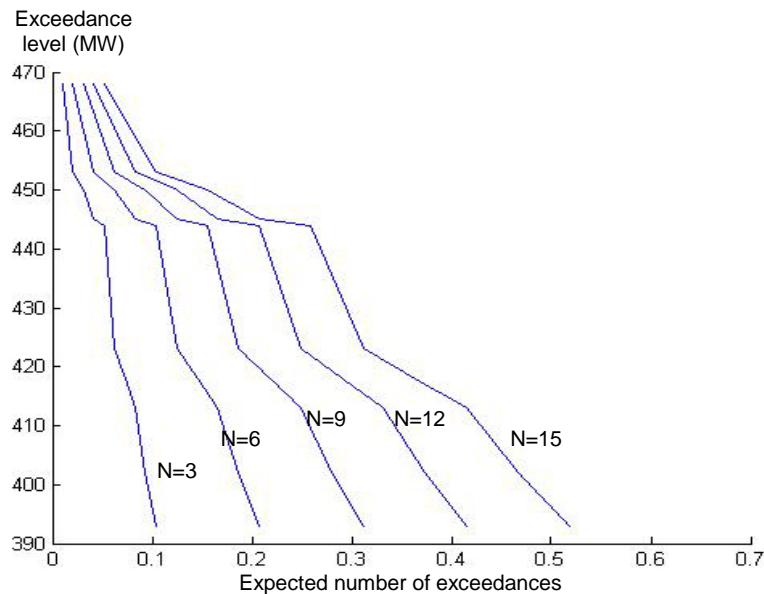


Figure 6.3. Exceedance Level Versus Expected Number of Exceedances in the Next $5N$ Minutes

6.3 Impact on the Transmission Congestion

It is imperative to maintain the reliability of the system in the case of extreme events of wind and load. Setting generation margin based on the statistics of extreme events and coordinating high proportion of wind generation and load in neighboring balancing authority areas attempt to resolve generation imbalance issues. The transmission congestion problem gets elevated especially in case the coordinating balancing areas have extreme events at the same time. Based on the historical data for the wind forecast errors of the two balancing areas, an evaluation of the transmission congestion problem for a future time line is presented in terms of incremental tie-line power flow. The problem of transmission congestion presented for two balancing areas sharing the wind forecast errors can be extended to a network of coordinated balancing authorities.

6.3.1 The Problem:

Using a superposition principle for the tie-line power flow as a result of extreme events of wind forecast errors in the balancing areas, the problem of transmission congestion can be illustrated as in Figure 6.4 for two balancing areas connected through a tie line 1-2.

In the Figure 6.4 $\Delta P1$ and $\Delta P2$ are the extreme wind forecast errors for BA1 and BA2 respectively having same expectancy of occurrence in specified future time-periods. These extreme events can be assumed to be shared as follows:

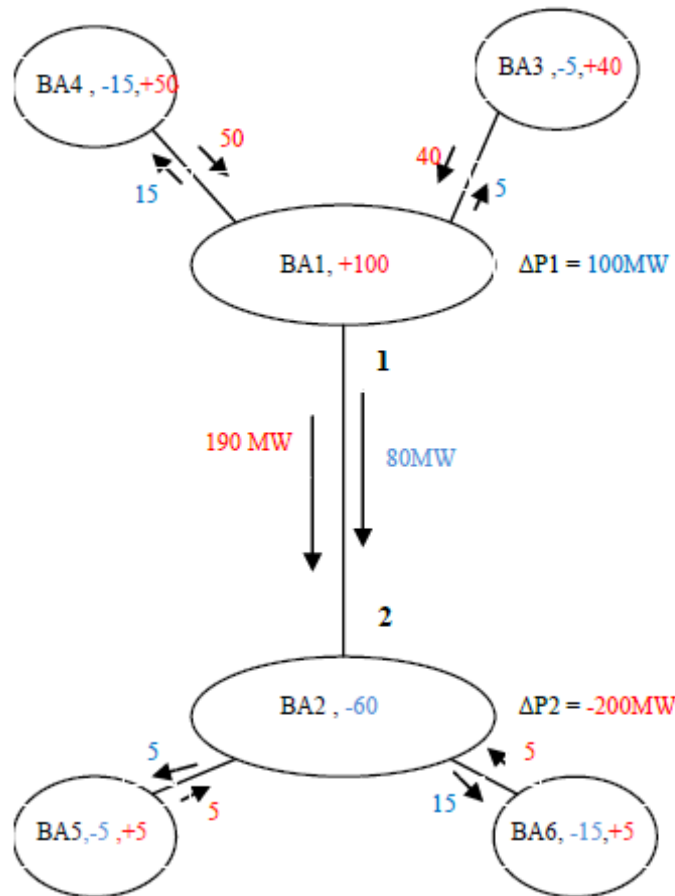


Figure 6.4. Problem of Transmission Congestion and Extreme Wind Forecast Errors

1. BA1 has a positive forecast error of $\Delta P1 = +100\text{MW}$ which can feed the deficiency of 60 MW of BA2, 15 MW of BA6 and 5 MW of BA5.
2. BA2 has a negative forecast error of $\Delta P2 = -200\text{MW}$ which can be supplied by additional generation of 100 MW from BA1, 40 MW from BA3, 50 MW from BA4 (making 190 MW) , 5MW each from BA5 and BA6.
3. The power transfer from one BA to the other BA is restricted by Zonal PTDFs.

As a result the tie-line 1-2 has a total additional loading of $190+80=270\text{MW}$. It may cause transmission congestion if addition of this incremental power flow to the existing power flow of the line exceeds its loading limits.

6.3.2 Methodology to Estimate Congestion in Case of Extreme Events

The methodology to estimate the congestion for these extreme events happening in near future is given below.

6.3.2.1 Methodology 1

Forecast Errors and Their Distribution:

Determine forecast errors for load and wind from the historical measurements for the balancing areas and rank them. Separate out positive and negative forecast errors.

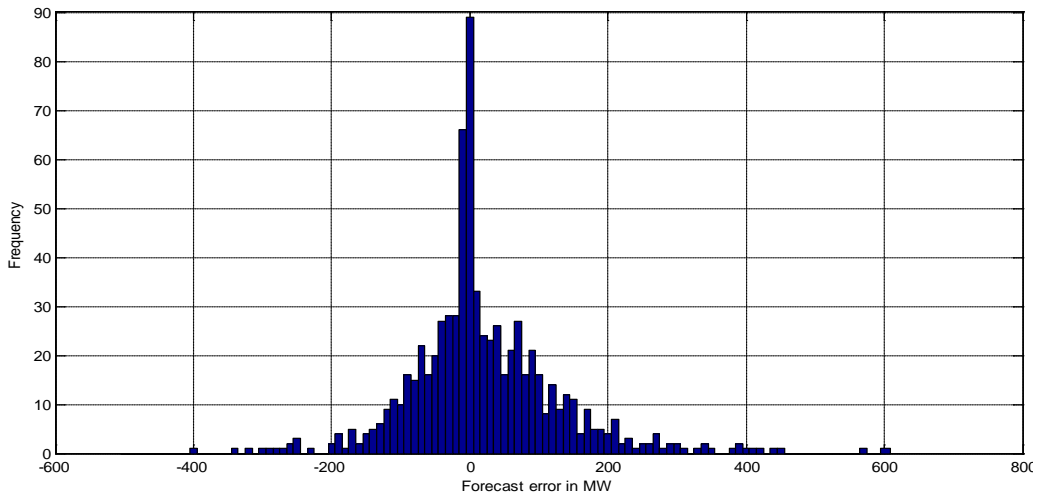


Figure 6.5. Forecast Error Histogram for a Month

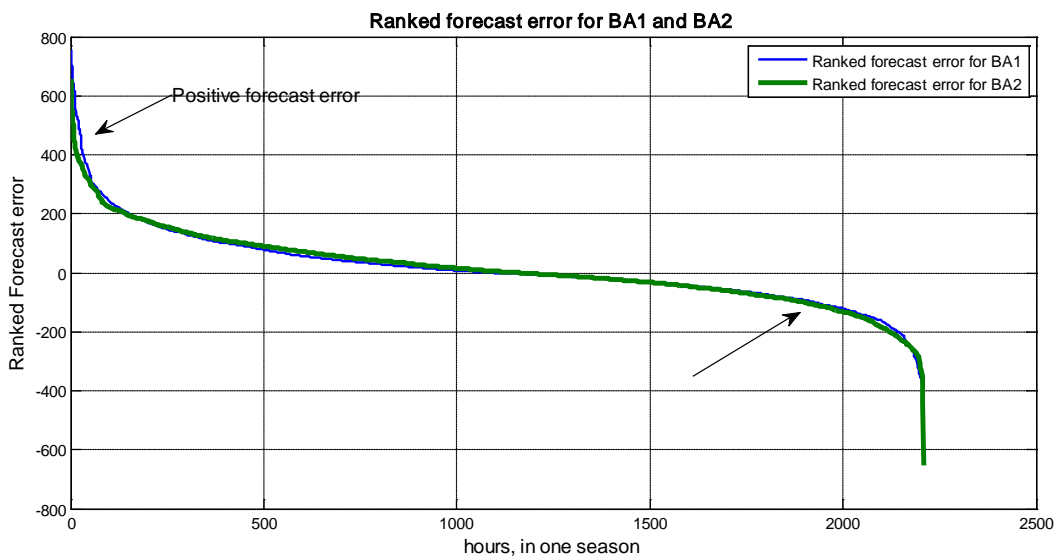


Figure 6.6. Ranked Forecast Error

Expectancy of Occurrence of Extreme Forecast Errors Using Gumbel's Theory:

As Gumbel shows that the expectation of the number of exceedences in the next N samples is simply

$$E(x) = \frac{mN}{n+1}$$

The expectancy of occurrence of extreme positive and extreme negative forecast errors in next 30 hours for both the BAs is calculated separately. Based on the defined problem, following is the exceedance level (extreme) vs. expectation of occurrence of the extreme in two different balancing areas. A positive forecast error is a generation increment and a negative forecast error is considered as a generation decrement. The expectation is calculated for next 30 hours in the future.

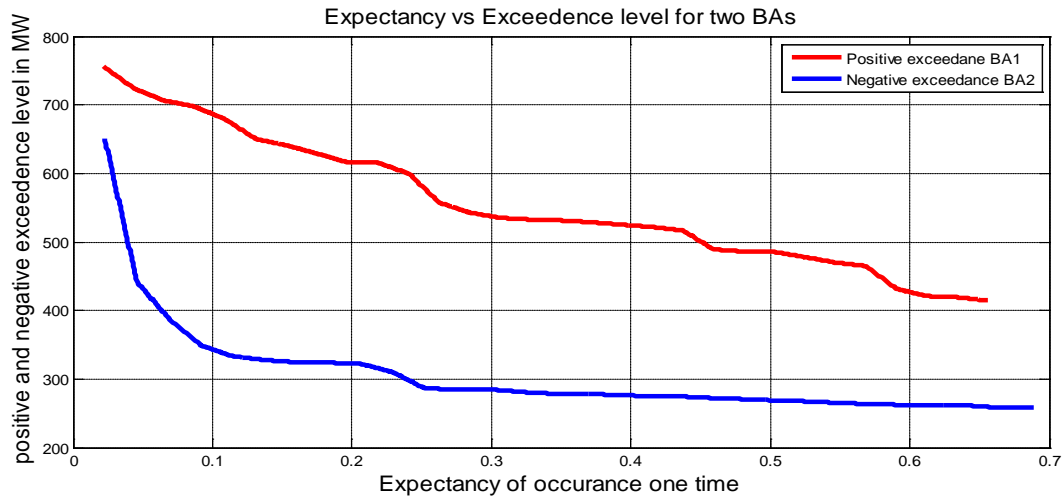


Figure 6.7. Expectancy vs. Exceedance Level of Forecast for Two BAs in Next 30 Hours

For an expectation of $E_j=0.2$, assume that BA1 has forecast error extreme (exceedance level) of $\Delta P_1 = +615$ MW (generation increment) while BA2 has $\Delta P_2 = -320$ MW (generation decrement)

Power Transfer Distribution Factor (PTDF) and Incremental Power Flow:

Different balancing areas and transmission paths would participate based on the power transfer distribution factor (PTDF) to adjust for the increment/decrement in generation ΔP_1 and ΔP_2 in two BAs. A PTDF value shows the incremental impact which a power transfer from a specified source to a specified sink would have upon each power system element. Thus, PTDF shows the incremental impact on the line flows. Details on power flow incremental model are given in Section 3.4.3.

Active power-flow change in the transmission path between the BA_i and BA_j according to **Error! Reference source not found.** can be calculated as:

$$\Delta P_{ij} = \sum_{n=1}^N PTDF_n^{ij} \Delta P_n \quad (6.7)$$

where: N = Number of zones/balancing areas in the system, ($N = 2$ for this problem)

ΔP_n = Variation of total active power generation in BA_n due to extreme forecast error

$PTDF_n^{ij}$ = Power transfer distribution factor reflecting the influence of extreme forecast error in

BA_n on the power flow in the interface i-j.

a. Two BA study

Table 6.1. Zonal PTDF for the Balancing Areas (shown RED)

Balancing area	PTDF
BA1	$PTDF_1^2 = -0.9$
BA2	$PTDF_2^1 = -0.8$

The zonal PTDF restricts the power that can be transferred from one zone to the other zone (Table 6.2)

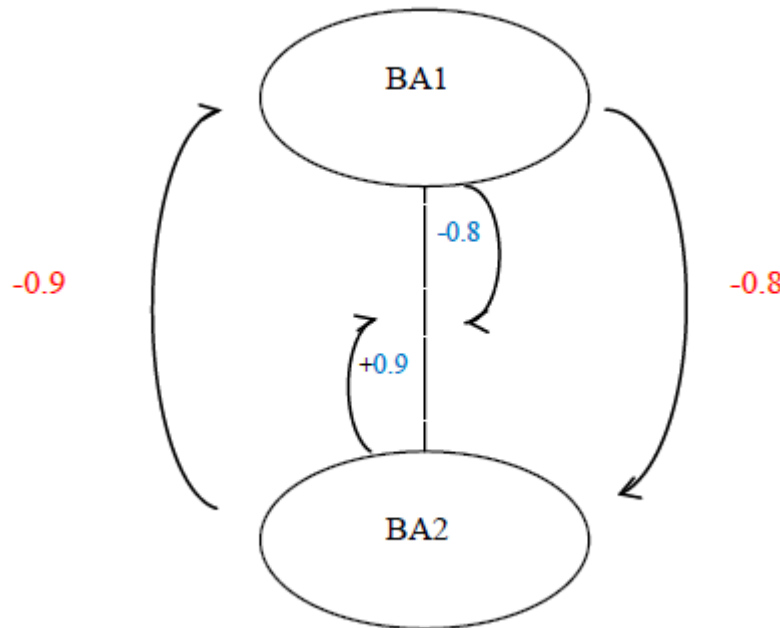


Figure 6.8. Zonal and Interface PTDFs

Table 6.2. Interface PTDF for the Transmission Path 1-2 Joining BA1 and BA2 (Shown BLUE)

Balancing area	PTDF
BA1	$PTDF_1^{12} = -0.8$
BA2	$PTDF_2^{12} = +0.9$

There may be more than one transmission lines connected to each BA and PTDF for each would be required to know to watch the congestion for those lines due to extreme forecast errors. The Change in power flow on the transmission interface between BA1 and BA2 for one expectation E_j is given by equation (3.19) elaborated as:

$$\Delta P_{12} = PTDF_1^{12} \Delta P_1 + PTDF_2^{12} \Delta P_2 \quad (6.8)$$

$$\Delta P_{12} = -0.8 * 615 + 0.9 * (-320) = -780MW \quad (6.9)$$

The incremental power flow of 780 MW on the tie-line 1-2 over and above the existing power flow can create transmission congestion on the line 1-2 if the net power flow exceeds line loading limits.

a. Multiple BA study

Similar study can be carried out for multiple BAs connected through different tie-lines. Assume that PTDF for different interfaces connected to each BA are as shown in Table 6.3.

Table 6.3. PTDFs for Different Interfaces Connected to BAs

Interface→				
Balancing area↓	1	2	3	4
BA1	0.1	0.2	0.9	0.8
BA2	0.1	0.8	0.1	-0.3
BA3	0.9	-0.7	-0.8	-0.4

It is evident from the table that transmission lines 2, 3 and 4 need to be examined for the congestion in case of incremental power flow due to extreme forecast errors in three BAs.

Transmission Congestion and Expectation of Occurrence of Extreme Forecast Error:

Net power flow in the transmission path m-n can be calculated according to the incremental power flow model (3.19) as:

$$P_{mn} = P_{mn}^0 + \sum_{i=1}^N PTDF_i^{mn} \cdot \Delta P_i \quad (6.10)$$

Where: P_{mn} is the power flow in the transmission path between BA_m and BA_n

P_{mn}^0 is the initial power flow in the transmission path m-n

$PTDF_i^{mn}$ is the coefficient of influence (power transfer distribution factor) of the BA_i on the transmission path m-n.

a. Two BA study

For different expectations E_m , each BA would have different change in generation ΔP_1 and ΔP_2 , respectively. As a result, Net power flow on the transmission line 1-2 according to

$$P_{mn} = P_{mn}^0 + \sum_{i=1}^N PTDF_i^{mn} \cdot \Delta P_i \quad (6.10) \quad P_{mn} = P_{mn}^0 + \sum_{i=1}^N PTDF_i^{mn} \cdot \Delta P_i \quad (6.10 \text{ is:})$$

$$P_{12} = P_{12}^0 + \Delta P_1 \cdot PTDF_1^{12} + \Delta P_2 \cdot PTDF_2^{12} \quad (6.11)$$

where P_{12}^0 is the base-case power flow on the transmission line 1-2. Calculation of incremental power flow on the transmission interface between BA1 and BA2 for different expectations E_m would lead to a plot of incremental power flow vs. expectancy of occurrence of extreme forecast error as is shown in Figure 6.9.

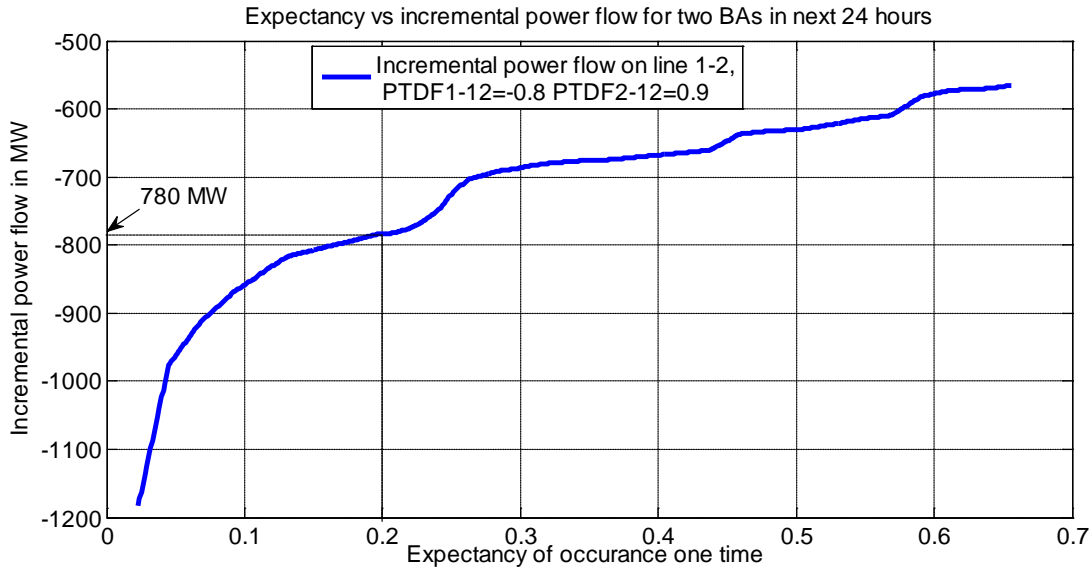


Figure 6.9. Incremental Power Flow – Methodology 1

The limit of incremental power flow for any interface when exceeded, results in the congestion on the transmission path. This analysis projects that the congestion can occur on the transmission lines in case of extreme forecast errors in different balancing areas and simultaneously gives an expectation of occurrence of this congestion. The analysis can be extended to see the congestion in various transmission lines in future based on past extreme events of forecast errors.

6.3.2.2 Methodology 2

The methodology 1 is based on the assumption of simultaneous occurrence of positive forecast error in one BA and negative forecast error in the other BA. This is an extreme case. A more practical analysis is based on the methodology 2 where forecast errors occur randomly. The steps to determine transmission congestion are as follows:

1. Determine forecast errors for each BA for each hour (ΔP_1 and ΔP_2)
2. Determine incremental power flow on line 1-2 based on PTDF of each BA for line 1-2 and rank it (Figure 6.10).
3. Determine the expectancy of positive and negative extremes of the incremental power flow for the future 30 hours (Figure 6.11).

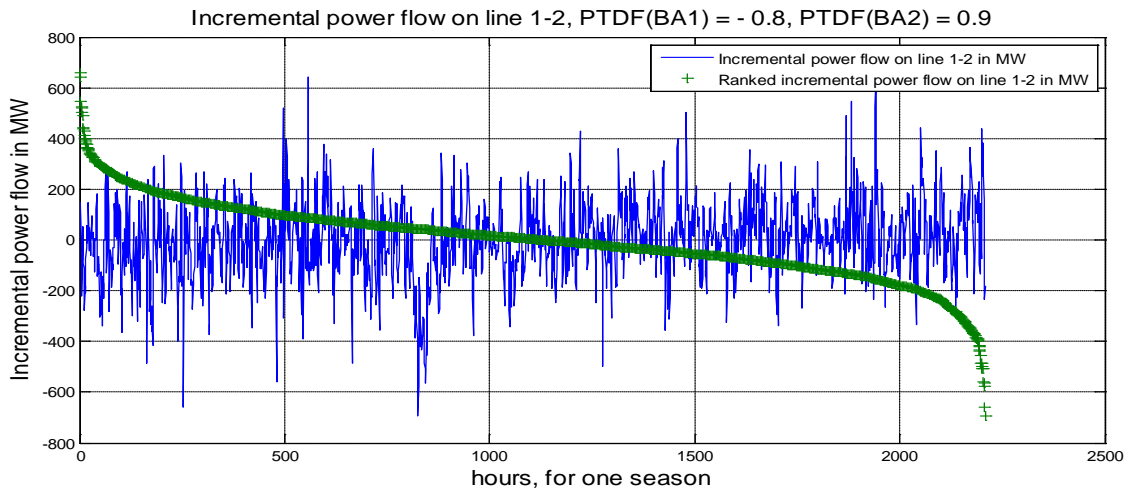


Figure 6.10. Hourly Instantaneous Incremental Power Flow and Hourly Ranked Incremental Power Flow

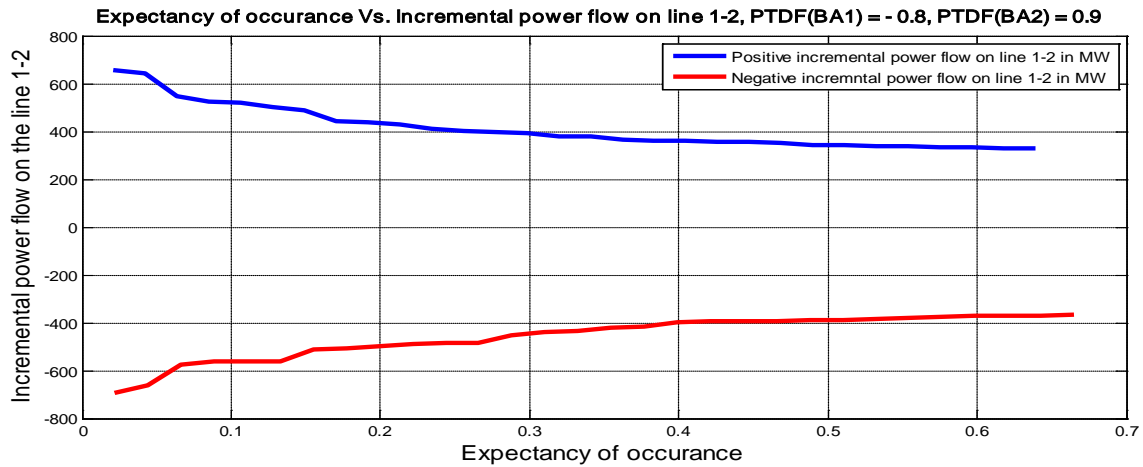


Figure 6.11. Incremental Power Flow – Methodology 2

6.3.2.3 Comparison of Methodology 1 and Methodology 2

In the methodology 1 the magnitude of incremental power flow is too large causing more congestion as it is assumed that the extremes occur at the same time, the magnitude of incremental power flow is too large causing more congestion. For the $E_1=0.2$, $\Delta P_{12} = - 780$ MW. For the same expectancy of occurrence in the methodology 2, $\Delta P_{12} = - 490$ MW or $+415$ MW. The methodology 2 results are based on the random occurrence of extreme forecast errors in the balancing areas.

It is clearly evident that a line with a loading limit of 2000 MW will foresee congestion regardless of the methodology used for the extreme events.

6.4 Future work on the Extreme Events

- The study needs to be performed on multiple balancing areas considering more transmission interfaces into account for the congestion analysis as a result of extreme forecast errors.
- Zonal PTDFs are required to be taken into account with real system data for a more realistic study.

7.0 Conclusions and Future Work

With high level wind penetration, the variability of wind power will pose significant challenges for power system operation in both economic and reliability perspectives. BA consolidation and cooperation helps manage the variability by allowing BAs to work as a team. By sharing resource and averaging out the variability, the virtual BA concept helps improve efficiency and reliability of power system operations. The following approaches were proposed and studied:

- ACE diversity interchange (ADI);
- BA Consolidation;
- Dynamic scheduling.
- Regulation and load following sharing;
- Wind only BA;

The following methods and algorithm were developed:

- New metrics (performance envelopes) were developed to evaluate the potential benefits and drawbacks of BAs coordination
- New advanced ADI approaches based on linear optimization and dynamic programming techniques
- Incremental model of the WECC system
- Method for extreme event prediction using Gumbel's theory

Through extensive studies, the proposed methods and algorithms are examined. The benefits and limitation of the proposed methods are revealed. The study results show significant economic and/or reliability benefits of BA coordination and consolidation in power system operation.

This report provides a guideline to help industry select a suitable coordination or consolidation method, which fits its specific needs. The study results have been adopted by industry to guide the several BA consolidation and coordination applications (e.g., Northwest utilities consolidation).

At the next phase of the project, it is proposed to:

- Continue developing and extending advanced ADI approach;
- Continue developing and extending wind only BA approach ;
- Developing BA consolidation approach;
- Studying the problem of inadvertent interchange;
- Developing the approach of dynamic scheduling;
- Studying the problem of extreme events;
- Perform complex simulation using real statistical data;
- Provide support in building an industrial demonstration project;

With extended study efforts, it is expected that the proposed methods become mature for industrial application. By providing mitigation solutions to manage variability of wind generation, it is expected that the study will facilitate the high level penetration of renewable generation.

8.0 Summary of Project Contributions

The work pursues the following objectives:

- To introduce the concept of virtual BA by exploring new strategies for BAs collaboration to overcome the challenges of high penetration of renewable energy that is expected within the next decade.
- To develop innovative analytical methods to simulate the operation of BAs under the proposed new strategies.
- To implement some of the proposed methods in a form tools that can determine the operational requirements for individual BAs and the new consolidated BA under different strategies.
- To use the developed tools to perform few case studies on BAs within the WECC to evaluate and compare the advantages and disadvantage of each proposed strategy.
- To recommend a road map for future cooperation between BAs.

The main outcomes presented in this report are summarized in the following points:

- Two sets of metrics to quantify the benefits of BA collaboration have been introduced. Each set of metrics is defined by a certain performance envelope.
 - The first performance envelope represents BA balancing operation, hence it includes capacity, ramp rate, ramp duration, and energy requirement for regulation, load following and scheduling.
 - The second performance envelope represents the cycling of generating and storage units within the BA to perform the needed balancing operations. It reflects the nature of using such units to meet the variation of load and the output of intermittent generation resources.
- A methodology for building an incremental power flow model has been developed. It has been used to evaluate the impact of various wide area wind integration options. It is also used in investigating transmission congestions that can limit BA cooperation. The method has been implemented and validated with WECC models.
- A developed method for evaluating the power system security region has been applied to quantify the transmission system congestion with better accuracy. That results in improving the usage of transmission system and minimizing the congestion cost under different wide area wind integration options.
- Several strategies for BAs collaboration have been investigated such as ACE diversity interchange (*ADI*), wind only BA, BA consolidation, dynamic scheduling, and regulation and load following sharing.
- Two methods to optimize the advanced ACE diversity interchange (*ADI*) have been developed. These methods show improved performance compared with the current *ADI* method used in the western interconnection.
- An analytical method has been developed to assess the benefits of the consolidation of individual BAs. The method used the developed tools to determine the savings in regulation, load following and scheduling requirements for the consolidated BA in comparison with individual BAs.
- A preliminary approach for dynamic scheduling implementation is given. The main concept is to connect external wind farms to specific balancing authorities and to provide ancillary services from external resources.

- An optimization method for regulation and load following sharing amongst individual BAs has been developed.
- A method for evaluating the benefits of creating a wind only BA has been investigated. A wind-only BA is responsible for controlling the interchange of its control area with the other balancing authorities to follow a pre-determined interchange schedule.
- An extreme event analysis method is developed to evaluate the expectation, of an extreme event in the future and its impact on the operating reserves and transmission congestion. The developed method is a result of collaboration with professors Gerald Heydt and Vijay Vittal of Arizona State University.
- A procedure for loop flow analysis has been developed to be able to estimate the unplanned additional power transfers caused by VGs as well as by BA cooperation options used.
- Two methodologies for cycling analysis have been proposed. The methodologies will help to evaluate the impacts of VGs and BA consolidation options on conventional generators, evaluate the need in flexible generation resources and energy storage.
- The virtual energy storage concept was proposed and proven through experiments. The concept creates an opportunity to detect, predict, and use the unplanned randomly occurring cyclic exchanges of energy between BAs as a virtual energy storage naturally existing in the system. By using this idea, participating BA could reduce their cycling balancing requirement without investing in additional generation or energy storage.
- The methodologies and tools developed in this study are currently applied to other on-going and off-spring projects such as:
 - Several WECC BAs, such as BPA who has joined the current ADI program, show strong interest in the optimized ADI method and are going to evaluate it. In particular, BPA is helping test the method by providing field measurement data.
 - Investigation of consolidation benefits in terms of the savings in regulation, load following, and scheduling requirements for a group of BAs.
 - A study on the needed energy storage capacity in all three interconnections in US to minimize the cycling of generating units.
 - Several BAs such as “Constellation Energy” show interest in the developed approach for wind only BA. Current intention is to incorporate this analysis in the next phase of the study.
 - The methodology of regulation and load following sharing has been applied in two PNNL’s projects with BPA and California Energy Commission.
 - Work is underway to start a project with BPA on dynamic scheduling. The objective is to develop a methodology for quantifying the benefits of using dynamic scheduling. The California ISO has also expressed interest in using the results of this study.
 - A larger-scale study to investigate potential collaboration between more than thirty WECC BAs to overcome transmission congestion problems and to be able to meet the challenges associated with the rapid growth of wind energy that is expected to reach a penetration level of 20% within a decade.

Overall, the research reported in this report is an initial attempt to pave the road for further investigation to the issues of wide area BA. The innovative tools developed make it possible to compare between different BA collaboration strategies. Consequently, the benefits of BA consolidation can be quantified and recognized.

9.0 References

- [1] Alsac O, and B Stott. May 1974. "Optimal load flow with steady-state security." *IEEE Transactions on Power Apparatus and System* 93(3):745-751.
- [2] B. Ernst, U. Schreier, F. Berster, C. Scholz, H.-P. Erbring, S. Schlunke, J. H. Pease and Y. V. Makarov, "Large Scale Wind and Solar Integration in Germany," Final PNNL Report PNNL, Pacific Northwest National Laboratory, Richland, WA, February 2010.
- [3] BPA – Bonneville Power Administration. August 21, 2008. *Request for Information - Generation Inputs and/or Load Interruption Services*. Accessed Feb, 2010 at http://www.bpa.gov/corporate/ratecase/2008/2010_BPA_Rate_case/Docs/RFI%20document082108_FINAL%20POSTED.pdf (undated webpage).
- [4] British Columbia Transmission Corporation. November 1, 2006. *ACE Diversity Interchange*. Idaho Power Company, NorthWestern Energy, PacifiCorp. Amended and Restated June 15, 2007. Accessed Feb, 2010 at http://nttg.biz/site/index.php?option=com_docman&task=doc_download&gid=196&Itemid=31 (undated webpage).
- [5] CAISO – California Independent System Operator. 2006. *Market Redesign and Technology Update Tutorial for Market Participants*. Accessed Dec, 2009 at <http://www.caiso.com/docs/2005/09/22/2005092212224714566.pdf>
- [6] CAISO – California Independent System Operator. April 1, 2009. *DA Market Process Flowchart*. Accessed Feb, 2010 at www.caiso.com/2381/238172b0e8e0.pdf (undated webpage).
- [7] CAISO – California Independent System Operator. April 1, 2009. *Real-Time Timelines*. Accessed Feb, 2010 at www.caiso.com/2381/238173d91c290.pdf (undated webpage).
- [8] CAISO – California Independent System Operator. *Dynamic Transfer Issue Paper*. Accessed Feb, 2010 at <http://www.caiso.com/2476/2476ecfa5f550.pdf>.
- [9] CAISO – California Independent System Operator. June 2, 2004. *Automatic Generation Control (AGC)/ Regulation due ISO*. Accessed Feb, 2010 at <http://www.caiso.com/docs/09003a6080/1b/23/09003a60801b2389.pdf> (undated webpage).
- [10] Cohn N. May 1982. "Decomposition of Time Deviation and Inadvertent Interchange on Interconnected Systems. Part II: Utilization of Components for Performance Evaluation and Corrective Control." *IEEE Transactions on Power Apparatus and Systems* 101(5):1152-1169.
- [11] Cohn N. May 1982. "Decomposition of Time Deviation and Inadvertent Interchange on Interconnected Systems. Part I: Identification, Separation and Measurement of Components." *IEEE Transactions on Power Apparatus and Systems* 101(5):1144-1151.
- [12] ColumbiaGrid. January 1, 2008. *Report on ACE Diversity Interchange*. Accessed Feb, 2010 at <http://www.columbiagrid.org/download.cfm?DVID=436> (undated webpage).

- [13] Ehnberg, JSG, and MHJ Bollen. February 2005. "Simulation of Global Solar Radiation Based on Cloud Observations." *Solar Energy*. 78(2):157-162.
- [14] Eiselt HA, and C-L Sandblom. 2007. *Linear Programming and its Application*. Springer-Verlag, Berlin Heidelberg.
- [15] European Transmission System Operators. January 15, 2007. "European Wind Integration Study (EWIS) Towards a Successful Integration of Wind Power into European Electricity Grids." Accessed Feb, 2010 at <http://www.wind-integration.eu/downloads/library/EWIS-phase-I-final-report.pdf> (undated webpage).
- [16] Feliachia A, and D Rerkpreedapong. February 2005. "NERC compliant load frequency control design using fuzzy rules." *Electric Power System Research* 73:101-106.
- [17] Ferrero RW, SM Shahidehpour, and VC Ramesh. August 1997. "Transaction analysis in deregulated power systems using game theory." *IEEE Transactions on Power Systems* 12(3):1340-1347.
- [18] Goggin M., "MISO Coordinated Regional Grid Operations Good for Wind", Wind Energy Weekly, 9 January 2009. Available: www.awea.org/newsroom/pdf/MISO_090109.pdf.
- [19] Gumbel EJ. 1958. *Statistics of Extremes*. Columbia University Press, New York.
- [20] Gumbel EJ. February 1954 "Statistical Theory of Extreme Values and Some Practical Applications." *National Bureau of Standards, Applied Mathematics Series*
- [21] Hils D. March 12, 2009. "Implementation Requirements for ACE Diversity Interchange", A letter to NERC Operating Committee Chair, Duke Energy, March 12, 2009.
- [22] Hjort U. 1995. *Computer Intensive Statistical Methods: Validation, Model Selection and Bootstrap*. Chapman & Hall, London.
- [23] IESO - Independent Electricity System Operator. May 14, 2008. *Wind Forecast Error Impacts on Efficiency* Accessed Feb, 2010 at <http://www.theimo.com/imoweb/pubs/consult/windpower/wpsc-20080514-Item3.pdf> (undated webpage).
- [24] Jaleelit N, and L VanSlyckt L. August 1999. "NERC's New Control Performance Standards." *IEEE Transactions on Power System*. 14(3):1092-1099.
- [25] Kirby B, and E Hirst. January 2000. Customer-specific metrics for the regulation and load-following ancillary services. ORNL/CON-474, Oak Ridge National Laboratory, Oak Ridge, Tennessee.
- [26] Kirby B, and E Hirst. January 2001. Using Five-Minute Data to Allocate Load-Following and Regulation Requirements Among Individual Customers. ORNL/TM-2001/13, Oak Ridge National Laboratory, Oak Ridge, Tennessee.
- [27] Kirby B. and Milligan M. "Facilitating Wind Development: The Importance of Electric Industry Structure". *The Electricity Journal*. Vol. 21, April 2008, p. 40-54.

- [28] Kundur, P. 1994. *Power System Stability and Control*. McGraw-Hill, Inc., New York, p 813.
- [29] M. Mizumori and B. Nickell, “Balancing Authority Proliferation,” RPIC Meeting, WECC, November 13, 2008. [Online.] Available: http://www.wecc.biz/committees/BOD/RPIC/111308/Lists/Agendas/1/7_BA%20Proliferation.pdf.
- [30] Makarov Y, B Yang, J DeSteele, C Lu, C Miller, P Nyeng, J Ma, D Hammerstorm, and V Viswanathan. June 2008. *Wide-Area Energy Storage and Management System to Balance Intermittent Resources in the Bonneville Power Administration and California ISO Control Areas*, PNNL Project Report, Prepared for the Bonneville Power Administration under Contract BPA 00028087 / PNNL 52946, June 2008.
- [31] Makarov Y. V., Hawkins D. L., Leuze E., and Vidov J., “California ISO Wind Generation Forecasting Service Design And Experience”, Proc. of the 2002 AWEA Windpower Conference, Portland, Oregon, June 2-5, 2002.
- [32] Makarov YV, C Loutan, J Ma, and P De Mello. May 2009. “Operational impacts of wind Generation on California Power Systems.” *IEEE Transactions on Power Systems* 24(2):1039-1050.
- [33] Milligan M. and Kirby B., “Analysis of Sub-Hourly Ramping Impacts of Wind Energy and Balancing Area Size,” Proc. WindPower 2008, Houston, Texas, June 1-4, 2008. Available: www.nrel.gov/wind/pdfs/43434.pdf.
- [34] Mizumori M, and B Nickell. “Balancing Authority Proliferation”, Presentation at the RPIC Meeting, WECC, November 13th, 2008. Available, www.wecc.biz/documents/meetings/board/RPIC/2008/November/7_BA%20Proliferation.pdf
- [35] Mizumori M. and Nickell B., “Balancing Area Applications in the Western Interconnection”. Western Electricity Coordinating Council, Salt Lake City, Utah. Available at: <http://www.wecc.biz/documents/meetings/board/2008/December/BA%20Application%20whitepaper.pdf>
- [36] NERC- North American Electric Reliability Corporation. “Reliability Standards: Resource and Demand Balancing,” NERC. Accessed Jan, 2010 at: <http://www.nerc.com/page.php?cid=2|20> (undated webpage).
- [37] NERC- North American Electric Reliability Corporation. Standard BAL-006-1 — Inadvertent Interchange. Available at: <http://www.nerc.com/files/BAL-006-1.pdf>
- [38] NERC/WECC Minimum Operating Reliability Standards. Standard BAL-STD-002-1 — Disturbance Control Performance. Western Electricity Coordinating Council, Salt Lake City, Utah. Available at: http://www.wecc.biz/Documents/2006/Standards/BAL-STD-002-1_ORSTF_Version_Approved_by_MIC_October_2006.pdf

- [39] Nielsen L, L Prahm, R Berkowicz, and K Conradsen. 1981. “Net incoming radiation estimated from hourly global radiation and/or cloud observations.” *International Journal of Climatology* 1(3):255-272.
- [40] North American Electric Reliability Council (NERC), Policy 1—Generation Control and Performance, in Operating Manual, Oct 8, 2002.
- [41] North Pacific. *Glossary of Electric Utility Terms*. Accessed Feb, 2010 at http://www.north-pacific.ca/Glossary/inadvertent_energy_balancing.html
- [42] NPCC - Northwest Power and Conservation Council. March 2007. *Northwest Wind Integration Action Plan*. Portland, Oregon. Accessed Feb, 2009 at <http://www.uwig.org/NWWindIntegrationActionPlanFinal.pdf> (undated webpage).
- [43] Oneal AR. May 1995. “A Simple method for improving control area performance: area control error (ACE) diversity interchange ADI.” *IEEE Transactions on Power Systems* 10(2):1071-1076.
- [44] Piwko R., Clark K, Freeman L., Jordan G., Miller N., “Western Wind and Solar Integration Study”, GE Energy Subcontract Report, National Renewable Laboratory, February 2010. Available at: <http://wind.nrel.gov/public/WWIS/>.
- [45] PowerWorld Corporation. September 26, 2007. PowerWorld Simulator Version 13 User’s Guide. PowerWorld Corporation, Champaign, Illinois. Available at www.powerworld.com
- [46] Schlunke S., “System Balancing at VE Transmission”, Presentation, Vattenfall Europe – Transmission, Berlin, October 2009.
- [47] Shahidehpour M, H Yamin, and Z Li. 2002. *Market Operations in Electric Power Systems – Forecasting, Scheduling and Risk Management*. John Wiley & Sons, Inc., New York, page 287.
- [48] SPP - Southwest Power Pool. ACE Diversity Interchange Program, SPP MOPC Pre-meeting Informational Seminar presentation, April 14, 2009. Available at: <http://www.spp.org/publications/SPP%20ADI%20Implementation%20for%20MOPC%20041409.pdf>.
- [49] U.S. Department of Energy, Energy Efficiency and Renewable Energy, “States with Renewable Portfolio Standards” , July 2008. Accessed Jan, 2010 at: http://apps1.eere.energy.gov/states/maps/renewable_portfolio_states.cfm.
- [50] U.S. Department of Energy, Energy Efficiency and Renewable Energy, “20% Wind Energy by 2030 Increasing Wind Energy’s Contribution to U.S. Electricity Supply”, DOE/GO-102008-2567 , July 2008. Accessed Jan, 2010 at: <http://www1.eere.energy.gov/windandhydro/pdfs/41869.pdf>.
- [51] WECC – Western Electricity Coordinating Council, Operating Transfer Capability Policy Committee. October 31, 2008. Approved 2008 - 2009 Winter Operating Transfer Capability (OTC) Limits. Western Electricity Coordinating Council, Salt Lake City, Utah. Available at

- [http://www.wecc.biz/documents/library/OTC/2008-2009%20Winter%20Operating%20Transfer%20Capability%20\(OTC\)%20Limits%20\(2\)%20\(3\).pdf](http://www.wecc.biz/documents/library/OTC/2008-2009%20Winter%20Operating%20Transfer%20Capability%20(OTC)%20Limits%20(2)%20(3).pdf)
- [52] WECC – Western Electricity Coordinating Council, Technical Studies Subcommittee. January 2008. *WECC 2008 Path Rating Catalog*. Western Electricity Coordinating Council, Salt Lake City, Utah.
- [53] WECC – Western Electricity Coordinating Council. July 2007. *WECC Data Preparation Procedural Manual for Power Flow and Stability Studies, Rev. 5.0*. Western Electricity Coordinating Council, Salt Lake City, Utah. Accessed Dec, 2009 at <http://www.wecc.biz/documents/library/SRWG/dppm5.0.pdf>
- [54] WECC – Western Electricity Coordinating Council. *WECC Zonal Model*. Western Electricity Coordinating Council, Salt Lake City, Utah. Accessed Dec, 2009 at www.wecc.biz .
- [55] WECC – Western Electricity Coordinating Council. December 2006. *WECC White Paper on the Proposed NERC Balance Resources and Demand Standards*. Accessed Feb 2009 at <http://www.wecc.biz/Documents/2007/News/WECC%20White%20Paper%20on%20the%20BRD%20Standards-Dec2006-v3.pdf> (undated webpage).
- [56] WECC – Western Electricity Coordinating Council. Minimum Operating Reliability Criteria. Standard BAL-XXX-1-WECC — Frequency Response Performance. Western Electricity Coordinating Council, Salt Lake City, Utah. Accessed October 2009 at: <http://www.wecc.biz/Standards/WECC%20Criteria/BAL-00X-1%20Frequency%20Response%20Performance.pdf>
- [57] WECC – Western Electricity Coordinating Council. October 25, 2005. *WECC Reliability Coordination Center Requirements: Request for Information and Pricing (RFIP)*. Western Electricity Coordinating Council, Salt Lake City, Utah. Accessed Nov, 2009 at http://www.wecc.biz/documents/2005/News/WECC_RCC_RFIP_10-25-05.pdf (undated webpage).
- [58] WECC – Western Electricity Coordinating Council. WECC Frequency Responsive Reserve Report. Western Electricity Coordinating Council, Salt Lake City, Utah.
- [59] WECC – Western Electricity Coordinating Council. *WECC Reference Document for Dynamically Scheduled Remote Generation & Load*. Western Electricity Coordinating Council, Salt Lake City, Utah. Accessed Dec, 2009 at <http://www.wecc.biz/committees/StandingCommittees/OC/ISAS/Shared%20Documents/Dynamic%20Scheduled%20Remote%20Generation%20and%20Load.pdf> (undated webpage).
- [60] Wood A, and B Wollenberg. 1996. *Power Generation, Operation, and Control*. 2nd ed. Wiley, New York p 349.
- [61] Zack JW. *PIRP Solar Forecasting* PIRP Workshop, California ISO, Folsom, CA, April 16, 2007. Available at: [wepex.net/1bbf/1bbfe85215620.pdf](http://www.wepex.net/1bbf/1bbfe85215620.pdf).

- [62] Zimmerman R. D. and Carlos E. Murillo-Sánchez, *MATPOWER A MATLAB™ Power System Simulation Package User's Manual*, 1997-2007 Power Systems Engineering Research Center (PSERC), School of Electrical Engineering, Cornell University, Ithaca, NY 14853. Available at: <http://www.pserc.cornell.edu/matpower/>.
- [63] FERC – Federal Energy Regulation Commission “Preventing Undue Discrimination and Preference in Transmission Service”, FERC Order 890-B, June 23, 2008 Accessed Dec, 2009 at www.ferc.gov/whats-new/comm-meet/2008/061908/e-1.pdf

Appendix A

Balancing Reserve Needs Calculation Methodology

Appendix A

Balancing Reserve Needs Calculation Methodology

A.1 Scheduling, Regulation and Load Following Analysis Methodology

The methodology developed in this work to analyze the wind generation impacts is based on a mathematical model of the actual scheduling, real time dispatch, and regulation processes and their timelines. Minute-to-minute variations and statistical interactions of the system parameters involved in these processes are depicted with sufficient details to provide a robust and accurate assessment of the additional capacity, ramp rate and ramp duration requirements that the regulation and load following systems are expected to face under different BA consolidation options.

A.1.1 System Generation Requirements

Supply and demand in a power grid must always remain balanced. In real-time, generators under automatic generation control are adjusted to match any variation in demand. Generally the variations in generation and demand are difficult to predict, therefore, the system dispatchers need appropriate automatic response and reserves to deal with rapid and slow variations from a few minutes to several hours.

A.1.2 Generation Schedule

Hour-ahead schedules are hourly block energy schedules including the 20-minute ramps between hours (Figure A.1). Hour-ahead schedules can be provided before the actual beginning of an operating hour. The load forecast used for the hour-ahead scheduling process is also provided before the beginning of an operating hour.

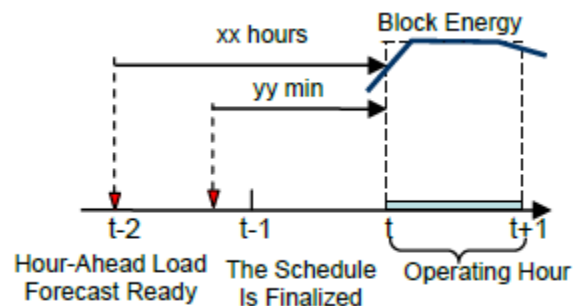


Figure A.1. Hour-Ahead Timeline

A.1.3 Load Following for Real Time Dispatch

Load following is an instructed deviation from schedule caused by the real-time dispatch. The desired changes of generation are determined in real-time for each 5-minute dispatch interval.

Figure A.2 illustrates how the generators in a control area are scheduled and dispatched.

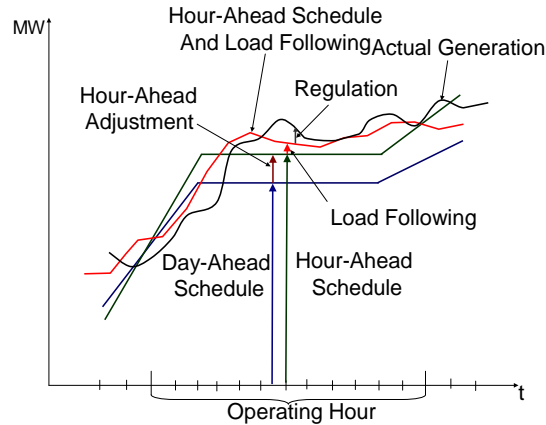


Figure A.2. Control Area Scheduling and Dispatching

The real-time dispatch is conducted by using, for example, 5-minute interval for economic dispatch (Figure A.3). The desired changes of generation are determined in real-time for each 5-minute dispatch interval several minutes before the actual beginning of the interval. System information used for that purpose is dated back also several minutes before the beginning of the interval. Units start to move toward the new set point before the interval begins. Units are required to reach the set point in the middle of the interval (e.g., 2.5 minutes after its beginning). The units may ramp by sequential segments, that is, the ramp is not necessarily constant.

For wind generation, the schedules are wind forecasts provided by a forecast service provider. Scheduling errors and variability of wind generation are balanced in real time by the BAs.

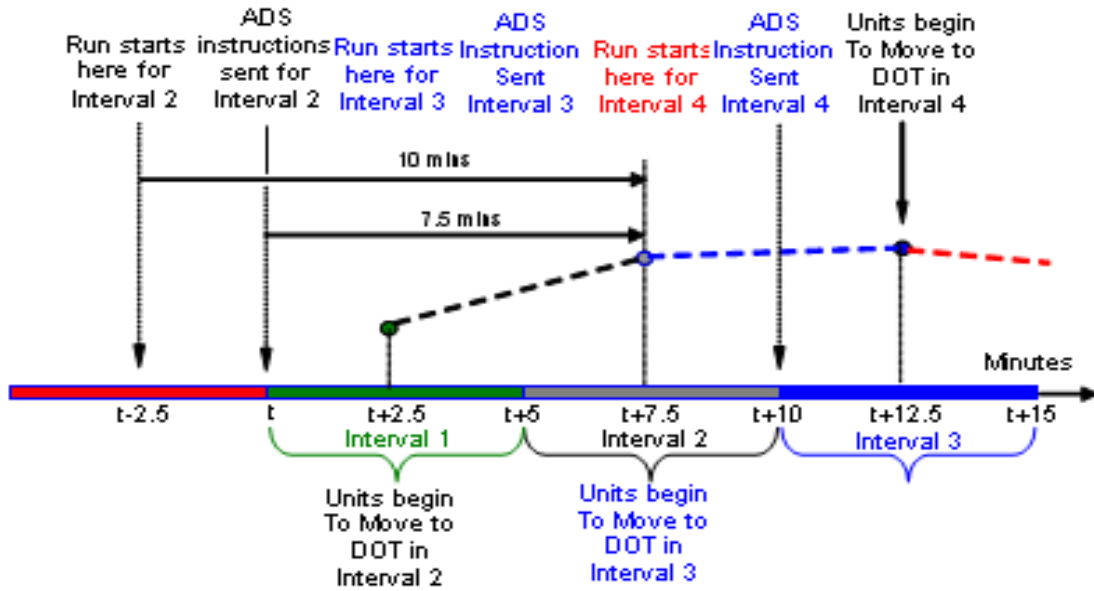


Figure A.3. An Example of the Real Time Dispatch Timeline (California ISO)

A.2 Assessment of Ramping Requirements

The regulating unit ramping capability can directly influence the required regulation and load following capacity. If the ramping capability is insufficient, more units and more capacity must be involved in regulation to follow the ramps. Hence, a simultaneous evaluation is necessary to determine the true requirements.

The required ramping capability can be derived from the shape of the regulation/load following curve. This derivation needs to be done in a scientific way. The “swinging door” algorithm was proposed for this purpose [32]. This is a proven technical solution implemented in the PI Historian and widely used to compress and store time dependent datasets.

Figure A.4 demonstrates the idea of the “swinging door” approach. A point is classified as a “turning point” whenever for the next point in the sequence any intermediate point falls out of the admissible accuracy range $\pm\epsilon_{\Delta G}$. For instance, for point 3, one can see that point 2 stays inside the window $abcd$. For point 4, both points 2 and 3 stay within the window $abef$. But for point 5, point 4 goes beyond the window, and therefore point 4 is marked as a turning point.

Based on this analysis, we conclude that points 1, 2, and 3 correspond to the different magnitudes of the regulation signal, π_1 , π_2 and π_3 , whereas the ramping requirement at all these points is the same, ρ_{1-3} (see Figure A.5) The swinging window algorithm also helps to determine the ramp duration δ .

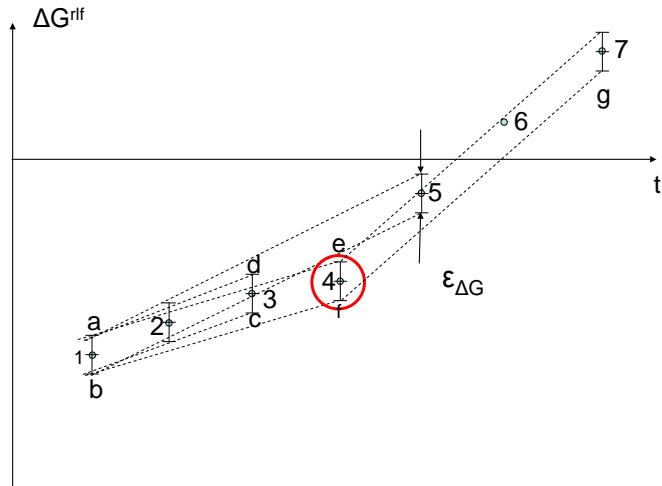


Figure A.4. The Idea of "Swinging Door" Algorithm

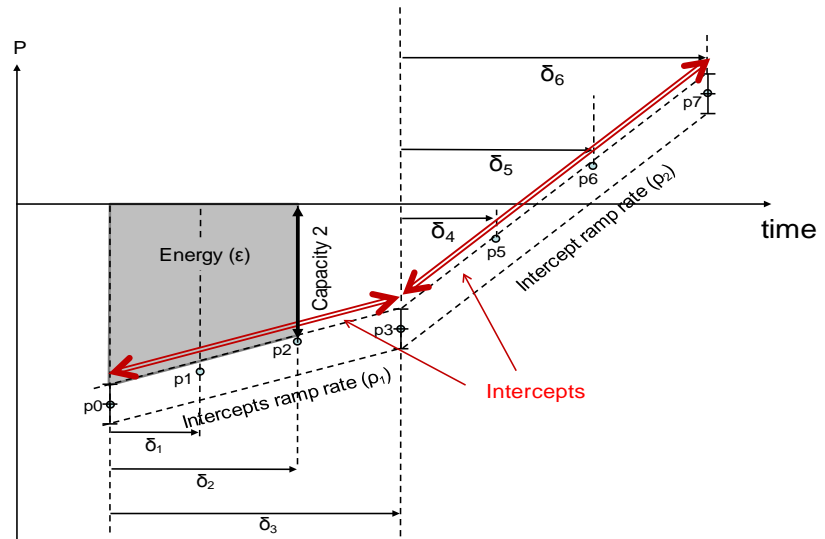


Figure A.5. "Swinging Door" Algorithm – Obtaining Regulation, Ramps, and Their Duration

With first performance envelopes the performance envelope analysis to evaluate potential benefits of BA coordination or consolidation can be undertaken.

To illustrate the idea of this approach, any three of the four dimensions can be chosen and plotted in a three-dimensional space. For example, Figure A.6 illustrates a plot of three dimensions (C, π, δ) associated with each first performance envelope. Such three dimensional plots can be applied to all other combinations as well, such as $C-\pi-\delta, C-\pi-\rho, C-\delta-\rho,$ and $\pi-\delta-\rho$ (π : capacity, δ : ramp duration; ρ : ramp rate; C : energy), but the actual analysis is conducted in the four-dimensional space

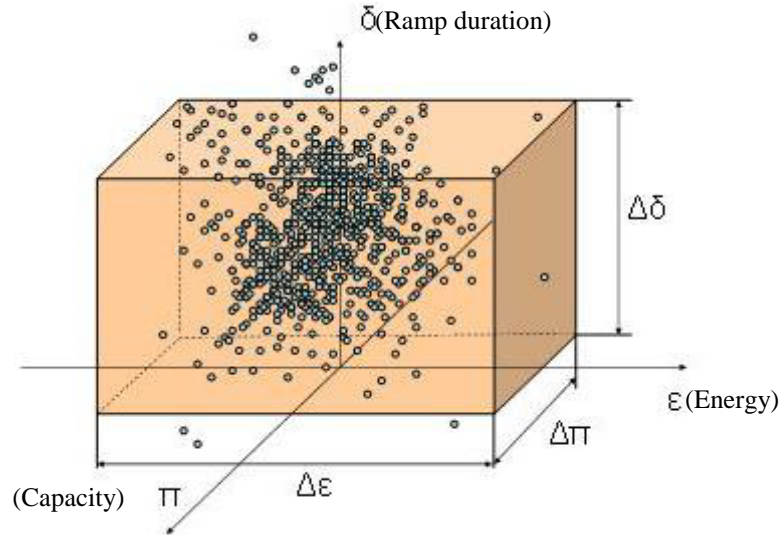


Figure A.6. Graphical Representation of (C , π , δ) Dimensions in a First Performance Envelope

The plot shown in Figure A.6 then facilitates the following steps.

- a. First, choose some percentile threshold, say $P\%$. This means that $P\%$ of all conditions will fall within the first performance envelope.
- b. For a particular BA, and each performance envelope (including net load, load following, and regulation) to be estimated for that BA, construct a bounding box such that $P\%$ of all the points in the plot are within that box as shown in Figure A.6. Some percentage of the points, $100 - P\%$, will be left outside the box. This would mean that we are not going to balance against certain percentage of extreme situations where the components of the performance envelope exceed certain values. We then determine the dimensions of the bounding box, for instance, $\Delta\pi$, $\Delta\delta$ and $\Delta\epsilon$ also shown in Figure A.6. These dimensions reflect the capacity, ramp, ramp duration, and energy requirements needed for each type of service (that is, for the net energy, load following, and regulation services).
- c. With the same $P\%$ threshold, we construct similar bounding boxes (performance envelopes) and determine their dimensions for each estimated first performance envelope of the consolidated (coordinated) system that including two or several BAs.
 - It is then expected that the dimensions of the bounding box in 'c' will be smaller than the sum of the corresponding dimensions of all bounding boxes calculated in 'b' for each net load/load following/regulation performance envelope.

A.3 Assessment of Cycling Requirements

For each balancing area, the detailed load following/regulation curve during a specific period of time (e.g., minute by minute data throughout 1 year) can be obtained. The “swinging door” algorithm (introduced in section 2.1.5.1) is first applied to calculate the 4 features (magnitude, ramp, duration and energy) of all the half-cycles in this curve. These features are then projected into a 4-dimensional space for statistical analysis. Note that if the ramp value is calculated using the simple model between magnitude and duration ($\text{Ramp} = \text{Magnitude}/\text{Duration}$), the dimension of ramp in this space can be eliminated because it is a dependent value. In this case, all the half-cycles can then be represented by a point in a 3 dimensional space. The next step is to define a basic unit (called a “mini-bin”) in this space that includes points with sufficient similarity to represent the same ramp requirements (see Figure A.7). There may be many “mini-bins” for a particular curve because ramp requirements can differ significantly

throughout a year. Some of them may contain a large number of points, which represent very frequent ramp actions in this BA; while others may have few or none points, representing rare ramp actions (Figure A.8). Therefore, counting the number of points falling into each mini-bin will provide the frequency for the corresponding ramping requirement.

For the obtained mini-bins with non-zero frequency values, a “big box” can be determined to include most of mini-bins (e.g., 95%) in the space. Some of the mini-bins are outside the big box. The probability of being outside the box is given by

$$p_{out} = \frac{N_{out}}{N_{out} + N_{in}} \quad (\text{A.1})$$

If a mini-bin lies outside the box, the regulation/load following requirements are not met. We will require that this probability must be below certain minimum probability, p_{min} . The purpose is to find the position of the wall of the probability box that corresponds to a given p_{min} . Defining the size of a mini-bin and the big box are two important tasks to solve

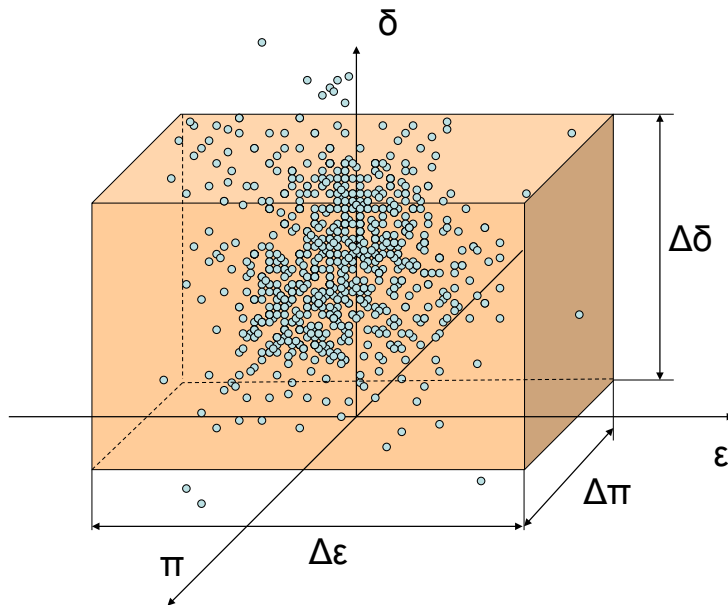


Figure A.7. Projecting Similar Half-Cycles in One 3-Dimensional “Mini-Bin”

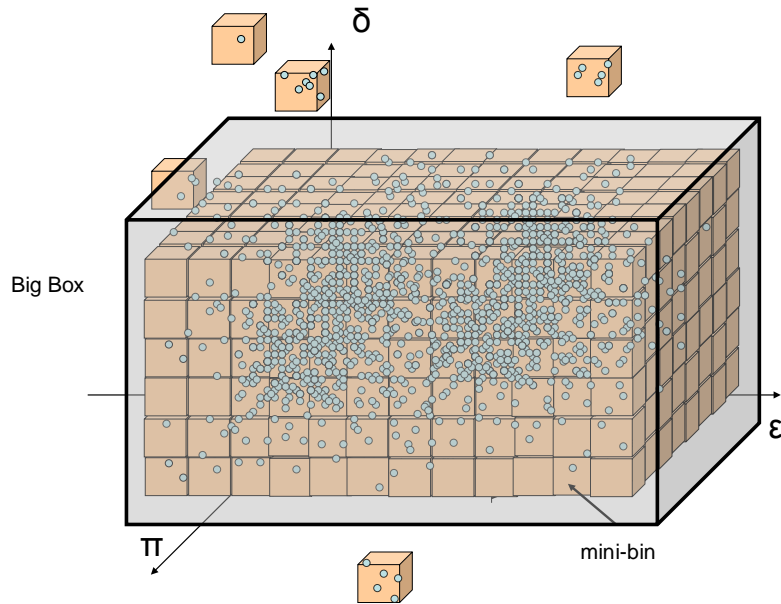


Figure A.8. Projecting All Half-Cycles in the 3D Space, Using Mini-Bins to Capture Similar Points

Furthermore, if the cost for providing every ramp requirement (each mini-bin) in each BA can also be provided, the annual economical cost for all ramping requirements will be determined. Since consolidated BA can significantly reduce the amount and frequency of load following/regulation requirements compared to the existing individual BAs, the saved cost per year will provide a direct way to quantify the benefit of consolidated BA especially with increasing wind penetration in the system.

The 3 dimensional space can further be reduced to 2D space if the energy of half-cycle is calculated directly from the magnitude and ramp of a half-cycle (e.g., $\text{energy} = 1/2 * \text{magnitude} * \text{duration}$). In this case, a 3D histogram can be built to provide a more straightforward view. The 3rd dimension is the frequency value. One of such examples is shown in Figure A.9. This histogram will indicate what are the ramp requirements that mostly occur in each BA.

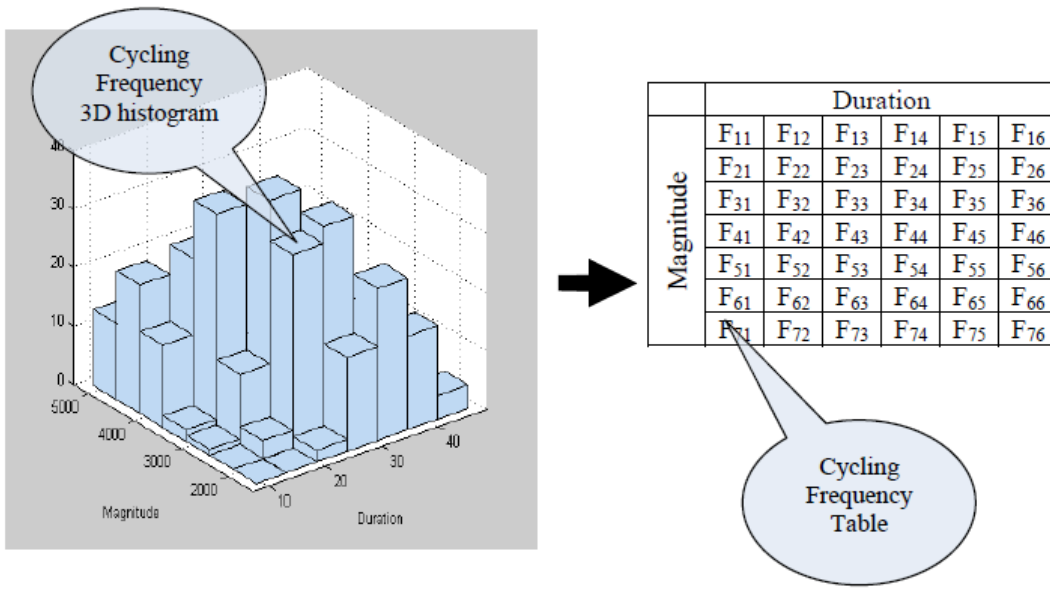


Figure A.9. Cycling Frequency Analysis

Appendix B

ACE Diversity Interchange

Appendix B

ACE Diversity Interchange

B.1 ADI Mathematical Model

At the first step, the total ADI ACE can be calculated as:

$$ACE_{\Sigma} = \sum_{i=1}^N ACE_i \quad (B.1)$$

where: ACE_i is the raw ACE of the BA i ;

N is the number of BAs.

At the next step, the sign of the net ACE is determined:

$$sign(ACE_{\Sigma}) = \begin{cases} 1 & \text{if } ACE_{\Sigma} > 0 \\ 0 & ACE_{\Sigma} = 0 \\ -1 & ACE_{\Sigma} < 0 \end{cases} \quad (B.2)$$

Similarly, the sign of the raw ACE is for each BA

$$sign(ACE_i) = \begin{cases} 1 & \text{if } ACE_i > 0 \\ 0 & ACE_i = 0 \\ -1 & ACE_i < 0 \end{cases} \quad (B.3)$$

At the following step, the signs of a minority group (MinG) and a majority group (MajG) are defined using the following principles:

- If the sign of the net ACE is positive or 0, the majority group includes BAs with positive ACEs and the minority group includes BAs with negative ACEs.
- If the sign of the net ACE is negative, the majority group includes BAs with negative ACEs and the minority group includes BAs with positive ACEs.

$$\begin{cases} \text{if } sign(ACE_{\Sigma}) = 1 \text{ then } MajG \text{ is positive}(+) \text{ and } MinG \text{ is negative}(-) \\ \text{if } sign(ACE_{\Sigma}) = -1 \text{ then } MajG \text{ is negative}(-) \text{ and } MinG \text{ is positive}(+) \end{cases} \quad (B.4)$$

The ACE adjustment for the minority group is calculated as:

$$Adj_{\Sigma}^{MinG} = -ACE_{\Sigma}^{MinG}, \quad (B.5)$$

where: $ACE_{\Sigma}^{MinG} = \sum_{\substack{i=1 \\ i \in MinG}}^N ACE_i$

ACE adjustment for BAs that belong to the minority group is calculated as follows:

$$Adj_i = -ACE_i, i = 1 \dots N$$

$$i \in MinG \quad (B.6)$$

Thus, the adjusted ACE for the minority group becomes zero, as well as individual ACEs for all BAs in this group:

$$ACE_{new\Sigma}^{MinG} = 0 \quad (B.7)$$

The adjusted ACE of the majority group is equal to net ACE:

$$ACE_{new\Sigma}^{MajG} = ACE_{\Sigma} \quad (B.8)$$

There are several methods of calculating ACE adjustment in the majority group. The equal share method is in use at the moment. Alternative allocation methods are also under discussion in the literature.

“Equal Share Method”

To be ‘fair’ to all participants, the equal share method proposes that ACE benefits be shared evenly among all the participants. Accordingly, the ACE adjustment for a BA that belongs to the majority group is:

$$Adj_i = -\frac{Adj_{\Sigma}^{MinG}}{N_{MajG}}, i = 1 \dots N$$

$$i \in MajG \quad (B.9)$$

where: N_{MajG} is the number of BAs in the majority group.

Based on the ADI principles, an ADI adjustment should not change the sign of ACE, therefore, the following correction is made for the BAs, where the adjustment could change the ACE sign:

$$if |Adj_i| > |ACE_i| then Adj_i = -ACE_i, i = 1 \dots N, i \in MajG \quad (B.10)$$

The residual ACE quantity, created by correction(B.10), is distributed among the remaining BAs in the majority group as:

$$Adj_j^{updated} = Adj_j + \frac{|Adj_i - ACE_i|}{N_{MajG} - N_0}, j = 1 \dots N, j \neq i$$

$$j \in MajG \quad (B.11)$$

where: N_0 is the number of BAs for which the correction (B.10) is applied.

“Alternative Allocation Method”

According to the alternative allocation method, the ACE adjustment of a BA that belongs to the majority group is:

$$Adj_i = -Adj_{\Sigma}^{MinG} \cdot k_i, i = 1 \dots N$$

$$i \in MajG \tag{B.12}$$

where: $k_i = \frac{ACE_i}{ACE_{\Sigma}^{MajG}}, i = 1 \dots N, i \in MajG$ is the coefficient reflecting the ACE_i in the majority group's total ACE.

B.2 Advanced ADI

Advanced ADI - Option 1

The main drawback of a conventional ADI is that the existing ADI algorithms do not include a transmission network congestion model. To prevent possible transmission violations, which could result from the ACE sharing methodology, a 25 MW limit on ACE adjustments is used.

In this report, the authors propose an improved approach, which includes the transmission congestion model based on a linearized approximation of the power flow equations. The model could be periodically updated using the state estimation results. To explain the idea behind the model, let us consider an example of a power system consisting of 3 BAs given in Figure B.1.

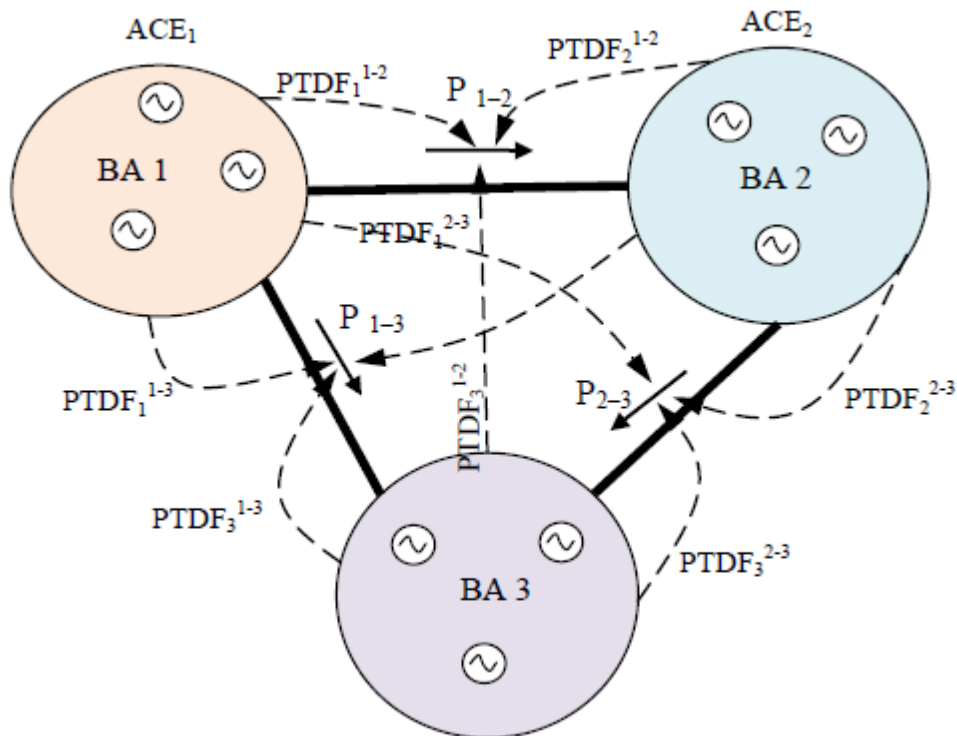


Figure B.1. Three BAs Example

Total (net) ACE can be calculated according to (B.1) as:

$$ACE_{\Sigma} = \sum_{i=1}^N ACE_i = ACE_1 + ACE_2 + ACE_3$$

where: ACE_i is the raw ACE of the BA i ;

N is the number of BA.

The total ACE can be distributed among these BAs, using the following formula:

$$ACE_i^{New} = ACE_{\Sigma} \cdot k_i \quad (B.13)$$

where: ACE_i^{New} is an updated ACE value for BA i ;

k_i is the sharing factor of BA i .

The k factors could be selected using different strategies. One of the possible strategies is to choose these factors in proportion with the BA's size. In section IIC, this selection is done based on the current values of ACE. The selected factors should satisfy the following condition:

$$\sum_{i=1}^N k_i = 1 \quad (B.14)$$

For the example shown in Figure B.1, the power variation in each BA caused by the ACE sharing, according to (B.13) can be calculated using the following expressions:

$$\Delta P_i \approx ACE_i^{New} = ACE_{\Sigma} \cdot k_i, i = 1, \dots, 3$$

The next step checks for possible transmission limit violations. The following inequalities can be used:

$$P_{mn} = P_{mn}^0 + \sum \Delta P_i \cdot PTDF_i^{mn} < P_{mn}^{Lim} \quad (B.15)$$

Where: P_{mn} is the power flow in the interface between BA m and n after ACE adjustments are applied;

P_{mn}^0 is the initial power flow in the interface $m-n$;

P_{mn}^{Lim} is the transmission limit of the interface $m-n$;

$PTDF_i^{mn}$ is power transfer distribution factor reflecting the impact of imbalances in BA i on the interface $m-n$. (see Chapter 3.4.3 for details). For the congestion problems inside the BAs, a similar model could be used.

Equation (B.15) can be rewritten in the matrix form:

$$[P] = [P^0] + [PTDF] \cdot [\Delta P] < [P_{lim}] \quad (\text{B.16})$$

For the example presented in Figure B.1 the transmission limits checking according to (B.16) can be written as:

$$\begin{cases} P_{12} = P_{12}^0 + \Delta P_1 \cdot PTDF_1^{12} + \Delta P_2 \cdot PTDF_2^{12} + \Delta P_3 \cdot PTDF_3^{12} < P_{12}^{Lim} \\ P_{23} = P_{23}^0 + \Delta P_1 \cdot PTDF_1^{23} + \Delta P_2 \cdot PTDF_2^{23} + \Delta P_3 \cdot PTDF_3^{23} < P_{23}^{Lim} \\ P_{13} = P_{13}^0 + \Delta P_1 \cdot PTDF_1^{13} + \Delta P_2 \cdot PTDF_2^{13} + \Delta P_3 \cdot PTDF_3^{13} < P_{13}^{Lim} \end{cases}$$

If one or several transmission limits would be violated by ACE adjustments, $P_{mn} > P_{mn}^{Lim}$, then the active power generation $P_i = P_i^0 + \Delta P_i$ must be corrected by the amount of ΔP_i^{corr} to avoid these violations. The following optimization procedure is formulated to find the correction:

$$\sum_{i=1}^N (\Delta P_i^{corr})^2 \longrightarrow \min \quad (\text{B.17})$$

subjected to

$$\begin{cases} \sum_{i=1}^N \Delta P_i^{corr} = 0 \\ P_{mn}^{corr} = P_{mn} + \sum \Delta P_i^{corr} \cdot PTDF_i^{mn} < P_{mn}^{Lim} \end{cases} \quad (\text{B.18})$$

The procedure ensures a minimum correction for the updated ACE, ACE_i^{New} that allows avoiding violations on the transmission paths.

Finally, the corrected ACE (the output of the proposed advanced ADI algorithm) is:

$$ACE_i^{ADI} \approx \Delta P_i + \Delta P_i^{corr} \quad (\text{B.19})$$

For the example shown in Figure B.1 the optimization task according to (B.17) and (B.18) can be formulated as:

$$\begin{aligned} & (\Delta P_1^{corr})^2 + (\Delta P_2^{corr})^2 + (\Delta P_3^{corr})^2 \longrightarrow \min \\ & \begin{cases} \Delta P_1^{corr} + \Delta P_2^{corr} + \Delta P_3^{corr} = 0 \\ P_{12}^{corr} = P_{12} + \Delta P_1^{corr} \cdot PTDF_1^{12} + \Delta P_2^{corr} \cdot PTDF_2^{12} + \Delta P_3^{corr} \cdot PTDF_3^{12} < P_{12}^{Lim} \\ P_{23}^{corr} = P_{23} + \Delta P_1^{corr} \cdot PTDF_1^{23} + \Delta P_2^{corr} \cdot PTDF_2^{23} + \Delta P_3^{corr} \cdot PTDF_3^{23} < P_{23}^{Lim} \\ P_{13}^{corr} = P_{13} + \Delta P_1^{corr} \cdot PTDF_1^{13} + \Delta P_2^{corr} \cdot PTDF_2^{13} + \Delta P_3^{corr} \cdot PTDF_3^{13} < P_{13}^{Lim} \end{cases} \end{aligned}$$

The corrected ACEs, according to (B.19) will be:

$$ACE_1^{ADI} \approx \Delta P_1 + \Delta P_1^{corr}; ACE_{21}^{ADI} \approx \Delta P_2 + \Delta P_2^{corr}; ACE_3^{ADI} \approx \Delta P_3 + \Delta P_3^{corr}$$

Advanced ADI - Option 2

To achieve maximum benefits of ACE sharing, the lumped ADI ACE should be minimized.

Objective Function

The objective function of step 1 is set up as follows:

$$\min_{\Delta P_i} \{ z_1(\Delta P_i) \} \quad (B.20)$$

$$z_1(\Delta P_i) = \sum_{i=1}^N |ADI - ACE_i| = \sum_{i=1}^N |ACE_i - \Delta P_i| \quad (B.21)$$

Here, ΔP_i is the ADI adjustment for BA i . It is a variable to be determined by a Linear Programming (LP) solver. N is the number of participating BAs. ACE_i is the raw ACE for BA i . It is a constant sent to coordination center from BA i . According to Figure 4.1,

$$ADI - ACE_i = ACE_i - \Delta P_i \quad (B.22)$$

The objective function z_1 maximizes ADI benefits. In other words, it minimizes the required balancing effort. Note that the absolute values are used to accumulate total ACE values. Despite of the use of absolute values of adjusted ACEs, (B.21) can be converted to a linear function so that step 1 can be solved using a LP solver. The conversion procedure is described in subsection C.

Constraints

Net ADI adjustment constraint

ACEs can only be shared. ACEs cannot be simply created and taken out. Thus, the sum of all ADI adjustments should always be 0.

$$\sum_{i=1}^N \Delta P_i = 0 \quad (B.23)$$

“No negative ACE impact” constraints

One of the design principles used in the current ADI is that ADI adjustments should never make any participants' ACE worse. In the proposed LP ADI method, this requirement can be enforced through the following constraint:

$$0 \leq \Delta P_i \leq ACE_i \quad \text{for } sign(ACE_i) = 1 \quad (B.24)$$

$$ACE_i \leq \Delta P_i \leq 0 \quad \text{for } sign(ACE_i) = -1 \quad (B.25)$$

$$\Delta P_i = 0 \quad \text{for } sign(ACE_i) = 0 \quad (B.26)$$

where: $sign(\bullet)$ function is defined in (B.3)

It can be observed that, with this constraint, the sign of resulting ADI_ACE_i never goes opposite to that of ACE_i . The amplitude of resulting ADI_ACE_i is smaller or equal to that of ACE_i .

Transmission limits constraints:

$$S_{mn}^{-Lim} \leq S_{mn}^0 + \sum_{i=1}^N (ACE_i - \Delta P_i) \cdot PTDF_i^{mn} \leq S_{mn}^{+Lim} \quad (B.27)$$

Here, $S_{mn}^{-Lim}, S_{mn}^{+Lim}$ (MVA) are the line limits in positive and negative directions, respectively. S_{mn}^0 is the current power flow on transmission line mn . $PTDF_i^{mn}$ is the power transfer distribution factor (see Chapter 3.4.3 for details), which is the power flow changes on path mn caused by unit regulation changes in BA i . $PTDF_i^{mn}$ can be calculated using power flow simulation based on state estimation results. In this study, an AC power flow is used to calculate $PTDF_i^{mn}$.

Note that the (n-1) contingency analysis (CA) can also be enforced using a similar approach, if needed.

ACE Capacity Constraints

$$ACE_i^{-Lim} \leq ACE_i - \Delta P_i \leq ACE_i^{+Lim} \quad (B.28)$$

With this constraint, the adjusted ACE shall not exceed the capacity limits (i.e., ACE_i^{-Lim} and ACE_i^{+Lim} .) in both directions.

ACE Ramping Rate Constraints

$$Ramp_i^{-Lim} \leq ACE_i - \Delta P_i - ADI_ACE_i^{past} \leq Ramp_i^{+Lim} \quad (B.29)$$

$ADI_ACE_i^{past}$ is the ADI ACE of the immediate past control cycle. This constraint makes sure that the ADI ACE will not exceed the ramping capability of generation (i.e., $Ramp_i^{-Lim}, Ramp_i^{+Lim}$).

Discussion

Equation (B.21) can be converted to a linear function so that step 1 can be solved using a LP solver. With the constraints defined in (B.24) - (B.26), the ADI ACE and the raw ACE should never be of an opposite sign. Thus,

$$\begin{aligned} z_1(\Delta P_i) &= \sum_{i=1}^N |ADI_ACE_i| \\ &= \sum_{i=1}^N \text{sign}(ADI_ACE_i) \cdot (ADI_ACE_i) \\ &= \sum_{i=1}^N \text{sign}(ACE_i) \cdot (ACE_i - \Delta P_i) \end{aligned} \quad (B.30)$$

With (B.30), the objective function of (B.21) is converted into a linear function. Therefore, the objective function for step 1 fits into a LP problem.

To summarize for step 1, (B.30) is set up as an objective function to minimize generation control. Equations (B.24) - (B.26) ensures that there is no degradation of ACE performance for any individual BA. Transmission limits are enforced through (B.27). ACE capacity and ramping constraints can be enforced through Equation (B.28) and (B.29). Note that both the objective function and constraints are linear. Thus, LP solver can be used to solve the LP problem. Also note that post LP analysis can be applied to identify the influence of parameters on the objective function through sensitivity analysis. Bound constraints can be identified for future planning.

If a unique solution is achieved in step 1, the LP ADI method stops and provides the unique ADI adjustment as the solution. There is no need to go to step 2. But, multiple solutions might occur under some circumstances. This is known as the dual degenerate phenomenon in linear programming [14]. Under such a condition, there are multiple feasible optimal solutions. They all result in the same optimal objective value in (B.21) and satisfy the reliability constraints (B.23) - (B.29). To choose one fair solution, which is acceptable to all participants, step 2 of LP ADI is proposed to make ADI benefits distributed impartially among participating BAs (such as equal saving split).

Step 2: Impartial ADI Benefits Distribution.

Step 2 is only needed when step 1 has multiple solutions. The objective of step 2 is to choose one solution from these multiple solutions, which is ‘fair’ to all participants.

To make sure that the solution for step 2 is one of multiple solutions from step 1, an additional constraint is added. Denote the resulting optimal value of (B.21) (or equivalently (B.30)) from step 1 as z_1^* . Note that z_1^* is a constant derived from LP solution of step 1. The constraint is constructed as

$$\sum_{i=1}^N \text{sign}(ACE_i) \cdot (ACE_i - \Delta P_i) \leq z_1^* \quad (\text{B.31})$$

The constraints for step 2 include all the constraints of step 1 and the above constraint. By comparing (B.30) and (B.31), one can observe that (B.31) makes sure that the solution for step 2 will be one of step 1 solutions [14].

The objective of step 1 is to reduce total generation control. The objective of step 2 is to pursue business ‘fairness’. In [4], two allocation methods (i.e., equal share, and prorated shared) are proposed. It is difficult to judge which one is fairer, because fairness is subjective.

In this section, the authors propose a LP approach to achieve fairness. An example objective function is proposed, which hopefully can be considered ‘fair’. If not, the readers can construct their own objective function using the proposed approach.

To achieve business fairness, an objective function of step 2 is proposed as

$$z_2(\Delta P_j^+, \Delta P_k^-) = \sum_{j=1}^{N^+} |\Delta P_j^+ - \Delta \bar{P}_j^+| + \sum_{k=1}^{N^-} |\Delta P_k^- - \Delta \bar{P}_k^-| \quad (\text{B.32})$$

$$\min_{\Delta P_j^+, \Delta P_k^-} \{ z_2(\Delta P_j^+, \Delta P_k^-) \}$$

Where ΔP_j^+ are LP ADI adjustments for the BAs with positive ACE, i.e., $sign(ACE_j)=1$; and N^+ is the number of BAs with positive ACEs. Similarly, ΔP_k^- are LP ADI adjustments for the control areas with negative ACE, i.e., $sign(ACE_j)=-1$; and N^- is the number of BAs with negative ACEs.

$$\Delta \bar{P}_j^+ = \frac{1}{N^+} \sum_{j=1}^{N^+} \Delta P_j^+ \text{ is the mean value.} \quad (\text{B.33})$$

$$\Delta \bar{P}_k^- = \frac{1}{N^-} \sum_{k=1}^{N^-} \Delta P_k^- \text{ is the mean value.} \quad (\text{B.34})$$

The objective is to minimize the deviation of the ADI ACE benefits among BAs.

Despite the appearance of the objective function in(B.32), the objective function with absolute value can be reformulated into a LP format by introducing intermediate variables [14]. To be self contained, the reformulation procedure is described as follows.

Define two groups of non-negative intermediate variables

$$d_j^+, d_j^- \geq 0, \quad j=1, \dots, N^+ \quad (\text{B.35})$$

such that

$$d_j^+ - d_j^- = \Delta P_j^+ - \Delta \bar{P}_j^+ \quad (\text{B.36})$$

and

$$d_j^+ + d_j^- = |\Delta P_j^+ - \Delta \bar{P}_j^+| \quad (\text{B.37})$$

Similarly, define

$$d_k^+, d_k^- \geq 0, \quad k=1, \dots, N^- \quad (\text{B.38})$$

such that

$$d_k^+ - d_k^- = \Delta P_k^- - \Delta \bar{P}_k^- \quad (\text{B.39})$$

and

$$d_k^+ + d_k^- = |\Delta P_k^- - \Delta \bar{P}_k^-| \quad (\text{B.40})$$

With the introduced intermediate variables, the objective function of step 2 can be reformulated into

$$z_2 = \min \left\{ \sum_{j=1}^{N^+} (d_j^+ + d_j^-) + \sum_{k=1}^{N^-} (d_k^+ + d_k^-) \right\} \quad (\text{B.41})$$

The variables to be determined are

$$d_j^+, d_j^-, \Delta P_j^+, \Delta P_j^-, \quad j=1, \dots, N^+$$

$$d_k^+, d_k^-, \Delta P_k^+, \Delta P_k^-, \quad k=1, \dots, N^-$$

$\Delta\bar{P}_i^+$ and $\Delta\bar{P}_i^-$.

The constraints are

- Equation (B.31) for including the analysis results from step 1;
- Equation (B.23) - (B.26), (B.27) - (B.29) for including constraints in step 1;
- Equation (B.33) - (B.36), (B.38), (B.39), (B.40) for introducing intermediate variables.

This is a typical LP problem and can be solved using a LP solver.

Note that the final solution of step 2 is a ‘fair’ optimal solution. The solution was endorsed by the objective function of both optimization steps. The objective function of step 1 is dominant, which is enforced through (B.31) in step 2. The objective function of step 2 is supplementary, which is to enhance the business fairness.

Authors also tried several other candidate objective functions for step 2. Two examples are

4. using relative deviation values;
5. taking out the bound ΔP_j^+ and ΔP_k^- .

They all make some ‘fairness’ sense and can be implemented using the proposed LP approach. It is up to ADI participants to choose a ‘fair’ objective function. To avoid confusion, the details are not described in this report.

B.3 Implementing Security Region Constrains into ADI Algorithm

The hyper-planes (in the power transfer space) approximating security conditions are calculated off-line, and can be described in multidimensional space as

$$\begin{aligned} n_{11}P_{12} + n_{12}P_{13} + n_{13}P_{23} &< L_1 \\ n_{21}P_{12} + n_{22}P_{13} + n_{23}P_{23} &< L_2 \\ n_{31}P_{12} + n_{32}P_{13} + n_{33}P_{23} &< L_3 \end{aligned} \tag{B.42}$$

or in matrix form

$$[N][P] < [L] \tag{B.43}$$

Power flow in the interface m-n can be calculated according to the following equation:

$$P_{mn} = P_{mn}^0 + \sum_{i=1}^N PTDF_i^{mn} \cdot \Delta P_i \tag{B.44}$$

where: P_{mn} is the power flow in the interface between BA m and n;

P_{mn}^0 is the initial power flow in the interface m–n ;

$PTDF_i^{mn}$ is the coefficient of influence (power transfer distribution factor) of the BA i on the interface $m-n$.

Equation in the matrix form is:

$$[P] = [P^0] + [PTDF] \cdot [\Delta P] \quad (B.45)$$

For the example in Figure B.1 the power flows are:

$$\begin{cases} P_{12} = P_{12}^0 + \Delta P_1 \cdot PTDF_1^{12} + \Delta P_2 \cdot PTDF_2^{12} + \Delta P_3 \cdot PTDF_3^{12} \\ P_{23} = P_{23}^0 + \Delta P_1 \cdot PTDF_1^{23} + \Delta P_2 \cdot PTDF_2^{23} + \Delta P_3 \cdot PTDF_3^{23} \\ P_{13} = P_{13}^0 + \Delta P_1 \cdot PTDF_1^{13} + \Delta P_2 \cdot PTDF_2^{13} + \Delta P_3 \cdot PTDF_3^{13} \end{cases} \quad (B.46)$$

Substitute (B.45) into (B.43)

$$[N][P^0] + [N][PTDF][\Delta P] < [L] \quad (B.47)$$

According to the matrix property: $A(BC)=(AB)C$ we can rewrite (B.47) as:

$$[A] + [B][\Delta P] < [L], \quad (B.48)$$

where: $[A] = [N][P^0]$;

$$[B] = [N][PTDF].$$

B.4 ADI Simulation Using Test Systems

In this section, simulations are performed to show the properties of the proposed advanced ADI approach. Comparison is made with the conventional ADI approach. To make the comparison straightforward, the 25 MW limits are not enforced for the conventional ADI. Also, the following two constraints are not enforced:

- ACE capacity constraints described by Equation (B.28);
- ACE ramping rate constraints described by Equation(B.29).

The focus is placed on the influence of transmission limit constraints as in (B.27). AC power flow models are used for comparison. AC power flow is solved using MATPOWER [62]. MATLAB® function '*linprog.m*' from the optimization toolbox was used as the LP solver. When there are multiple solutions for step 1, this LP solver only gives one of the solutions. Two case studies are performed on a PC computer with dual core CPU 3.0 GHz, and 4 GB RAM. MATLAB®, version R2008a is used.

Case I: 3 BAs and 4 Machine Model:

In this study case, it is assumed that three BAs (i.e., area A, B and C), participate ADI for sharing ACE.

Assume that the raw ACEs for area A, B, and C are -40MW, -46MW, and 60 MW, respectively. Initially, the transmission limit constraints are ignored. Both rule-based ADI and LP ADI are applied. For the proposed LP ADI approach, there are multiple solutions for step 1. Thus, step 2 is executed to choose the fairest solution. Resulting ACEs are summarized in (B.28). It can be observed that

- The proposed LP ADI results in exactly the same ADI ACE (after step 2) as those from the rule-based ADI, when the transmission limit constraints are ignored.
- The magnitudes of ADI ACEs are smaller than the raw ACEs for each area.
- The signs of ADI ACE never turn opposite to those of the raw ACEs.

In Table B.1, the resulting values of z_1 as in (B.21) and z_2 as in (B.32) are listed for each approaches. It can be observed that the raw ACE has the largest z_1 , which indicates lowest efficiency. Step 1 of the proposed LP ADI has a larger z_2 than step 2, which indicates that the deviation of the ADI ACE benefits is reduced through step 2. Note also that through step 2, z_1 remained the same as that of step 1. This indicates that step 2 retains the efficiency from step 1 through (B.31).

Next, the focus is on how transmission limits influence the ADI ACE. Assume that the three BAs are connected by a power grid, as in Figure B.2. This is a classical model structure used in [28]. In this report, G2, G3 and G4 are used to simulate the regulation generators for BA A, B and C, respectively. G1 is used to simulate other generations of the grid, which do not participate in the ADI. Bus 1 is the swing bus.

As in [28], for the base case,

- G1: P=700 MW, Q=185 MVar, raw ACE= 0 MW;
- G2: P=700 MW, Q=235 MVar, raw ACE=-40 MW;
- G3: P=719 MW, Q=176 MVar, raw ACE=-46 MW;
- G4: P=700 MW, Q=202 MVar, raw ACE= 60 MW;
- Bus 7: PL=967 MW, QL=100 MVar, Qc=200 MVar;
- Bus 9: PL=1,767 MW, QL=100 MVar, Qc=350 Mvar.

There are 400 MW and 12 MVar, (400.5 MVA) flowing through the long tie lines from bus 7 through 8 to 9 in the base case. Suppose that each transmission line between bus 7 and 8 has a transmission limit of 200 MVA. Two transmission lines provide total capacity of 400 MVA. These transmission limits are then enforced through transmission limit constraints defined by (B.27). The proposed LP ADI is solved and results are summarized in the last two rows of Table B.1 and

Table B.2.

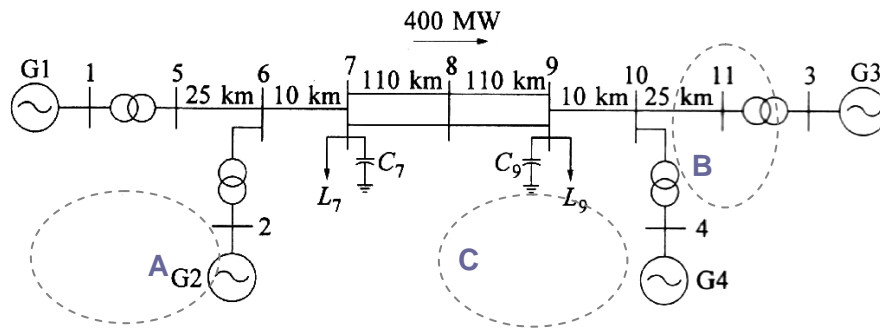


Figure B.2. The Four Machine Model. (The plot is from [11] with permission.)

Table B.1. The Resulting ACE from Different Approaches for the Three BA Case

Areas	A	B	C
Raw ACE (MW)	-40.0	-46.0	60.0
Rule-based ADI ACE (MW)	-10.0	-16.0	0.0
LP ADI ACE from Step 1 (MW)	-20.9	-5.1	0.0
LP ADI ACE from Step 2 (MW)	-10.0	-16.0	0.0
LP ADI ACE from Step 1 with line constraints (MW)	-22.1	-3.9	0.0
LP ADI ACE from Step 2 with line constraints (MW)	-20.3	-5.7	0.0

Table B.2. The Resulting Line Flow and Transmission Line Flows from Executing Aces for Three BA Case

Operations	$ S_{7,8}^1 $ (MVA)	$S_{7,8}^{+Lim}$ (MVA)	z_1 (MW)	z_2 (MW)
From raw ACE	189	200	146	0.0
From rule-based ADI	205	200	26	0.0
From step 1 LP ADI	200	200	26	21.9
From step 2 LP ADI	205	200	26	0.0
From step 1 LP ADI with line limit constraints	199	200	26	24.3
From step 2 LP ADI with line limit constraints	200	200	26	20.7

To execute AGC, active power of G2, G3, and G4 are adjusted according to ACEs. AC power flow is solved. The resulting power flow (MVA) of $|S_{7,8}^1|$ is summarized in Table II. $|S_{7,8}^1|$ is the magnitude of complex power, which flows through 1st line from bus 7 to bus 8. It can be observed that the operation based on raw ACE will not result in any violation. The two ADI ACEs, which ignored the transmission limits, have line flow exceeding the line limits by 5 MW. Thus, those two ADI ACEs will result in the line flow violation.

The proposed LP ADI method provides a solution for managing the line flow violation by including line limit constraints. In contrast to unconstrained ADI approaches, the constrained LP ADI automatically shifts the negative ACE from area B to area A. This reduces the power flowing through the intertie between bus 7 and 8, and therefore makes the intertie power flow stay within transmission limits (as shown in

Table B.2).

The computation time for the constrained LP ADI is about 0.66 seconds. Assuming that the ACE processing cycle is 4.0 seconds, the LP ADI computation is fast enough for real time execution.

Case II: Four BAs and Modified IEEE 30-Bus System.

In this case study, the power flow model “case30.m” from MATPOWER is used [62]. It is a 30-bus 6-machine model originally from [1]. Instead of the original IEEE 30 bus, this modified model is used because it has valid transmission line limits. The topology of the system is shown in Table B.3 [17].

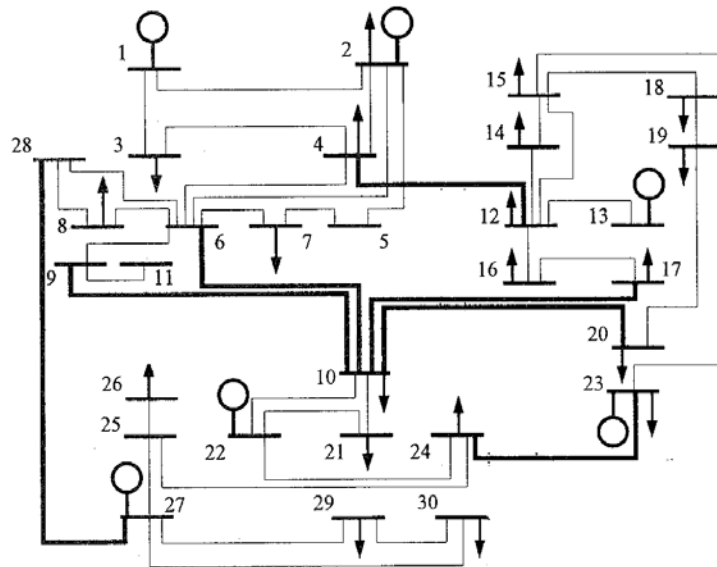
For the ADI ACE study, four areas, (i.e., A, B, C, and D,) are set up. Generator 2 (on bus 2), 3 (on bus 13), 4 (on bus 22) and 5 (on bus 27) are used to simulate respective regularization generation for BA A, B, C and D, respectively. The raw ACEs are set to be -46 MW, -40 MW, 60 MW, and 40 MW, respectively. These ACE values are same as those from [4] to facilitate comparison.

Generators 1 and 6 are used to simulate the rest of system, which does not participate in ADI.

For the base case, the following three transmission lines are identified as heavily loaded lines. Therefore, their transmission limits are enforced in the LP ADI using (B.27).

- from bus 6 to 8: limit=34.4 MVA (100% loaded);
- from bus 21 to 22: limit=32.0 MVA (95% loaded);
- from bus 15 to 23: limit=16.0 MVA (65% loaded).

The transfer limits of the rest of the lines are not enforced during the initial LP ADI calculation. But the ACE solutions are put back to all the line limit constraints to check for the violations. The violated constraints are added for the next round of LP computation until no violation is observed. This solving strategy method is called Bender cut [47].



**(The plot is from [17]with permission.)*

Figure B.3. The Modified 30-Bus Model

The simulation results are summarized in Table B.3 and Table B.4. For the constrained LP ADI approach, it has been checked that all the line power are within their limits. The top four most heavily loaded lines are

- from bus 21 to 22: limit=32.0 MVA (99.4% loaded);
- from bus 6 to 8: limit=34.4 MVA (97.0% loaded);
- from bus 15 to 23: limit=16.0 MVA (71.7% loaded);
- from bus 25 to 27: limit= 16.0 MVA (66.8% loaded).

Table B.3. The Resulting ACE from Different Approaches for the Four BA Case

Areas	A	B	C	D
Raw ACE (MW)	-46.0	-40.0	60.0	40.0
Rule-based ADI ACE (MW)	0.0	0.0	14.0	0.0
LP ADI ACE from step 1 (MW)	0.0	0.0	6.9	7.1
LP ADI ACE from step 2 (MW)	0.0	0.0	14.0	0.0
LP ADI ACE from step 1 with line constraints (MW)	0.0	0.0	0.1	13.9
LP ADI ACE from step 2 with line constraints (MW)	0.0	0.0	2.9	11.1

It can be observed that simulation results are consistent with those of case I. The results are consistent to those in [4]. In addition, the study also shows that the Bender cut method can be applied to reduce the LP problem size.

The computation time for the constrained LP ADI is about 0.58 second.

Table B.4. The Resulting Line Flow and Transmission Line Flows from Executing ACEs for Four BA Case

Operations	$ S_{21,22}^1 $ (MVA)	$S_{21,22}^{+Lim}$ (MVA)	z_1 (MW)	z_2 (MW)
From raw ACE	56.3	32.0	186	0
From rule-based ADI	34.5	32.0	14.0	12.0
From step 1 LP ADI	32.7	32.0	14.0	26.1
From step 2 LP ADI	34.5	32.0	14.0	12.0
From step 1 LP ADI with line limit constraints	31.2	32.0	14.0	39.8
From step 2 LP ADI with line limit constraints	31.8	32.0	14.0	34.3

B.5 ADI Simulation Using Real Statistical Data

Preliminary simulation using real statistical data has been performed. California Independent System Operator (CAISO) and Bonneville Power Administration (BPA) year 2006 data has been used. Studied data set includes the following information:

- CAISO ACE
- BPA ACE
- California – Oregon Intertie (COI) actual active power flow
- COI interchange schedule
- COI power flow limit

The data used for the simulations had 4 seconds resolution. Time series length is 777600 data points. Table B.4 presents CAISO and BPA ACE signals.

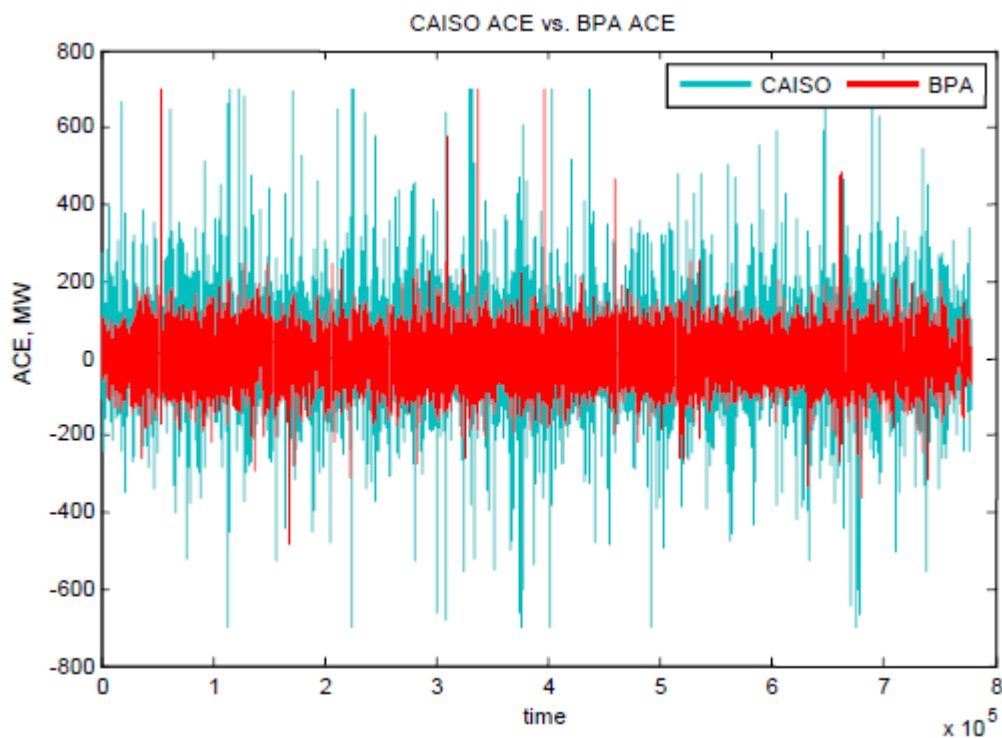


Figure B.4. BPA and CAISO ACE Signals

The COI is the major transmission path connecting BPA and the CAISO systems. COI is used mostly to transfer power from BPA to the CAISO, but at times reverse flows also occur. The COI power transfer limit is about 4,800 MW from BPA to CAISO and about 4,000 MW from the CAISO to BPA [52]. Actual power flow through COI and COI power flow limit are presented in Figure B.5. It is assumed that the positive sign of power flow corresponds to the power flow from BPA to CAISO.

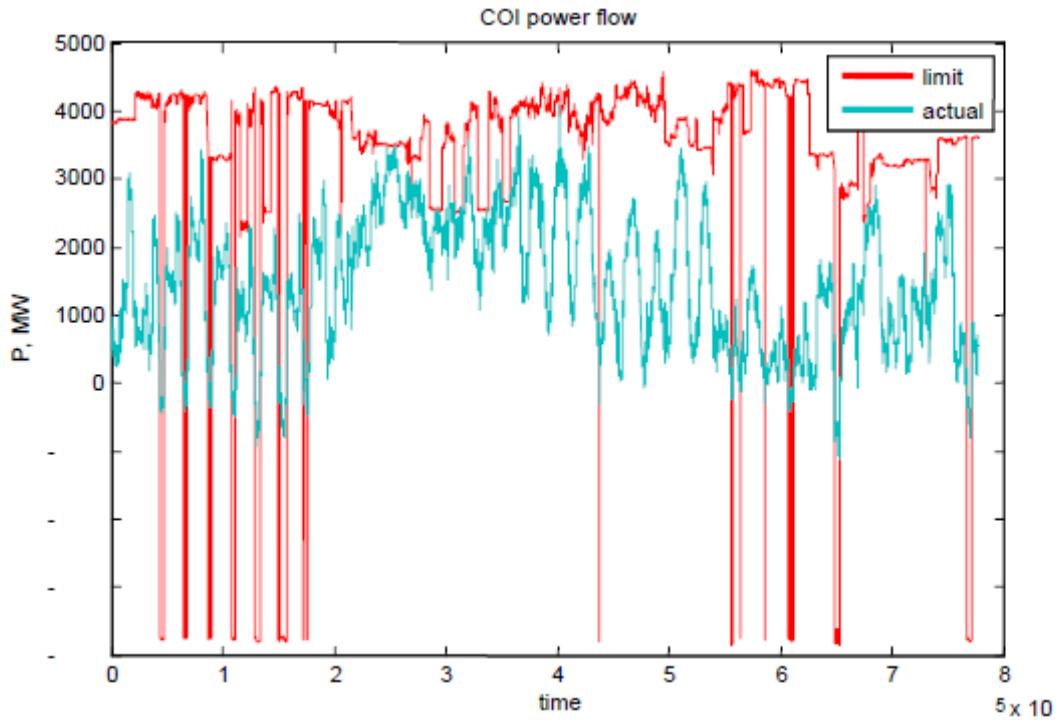


Figure B.5. COI Actual Power Flow vs. COI Power Flow Limit

According to (B.5) the ACE adjustments for the two BAs test system can be calculated using the following formula:

$$\begin{aligned}
 Adj &= 0 \text{ if } \text{sign}(ACE_{BPA}) = \text{sign}(ACE_{CAISO}) \\
 Adj &= \min(ACE_{BPA}, ACE_{CAISO}) \text{ if } \text{sign}(ACE_{BPA}) \neq \text{sign}(ACE_{CAISO})
 \end{aligned}
 \tag{B.49}$$

ACE adjustments calculate according to (B.49) are presented in Figure B.6. One can see that the adjustment values can exceed the 25 MW limit applied to the conventional ADI. Thus, the 25 MW limit that is now in use in the WECC ADI reduces potential benefits from the ACE sharing technology.

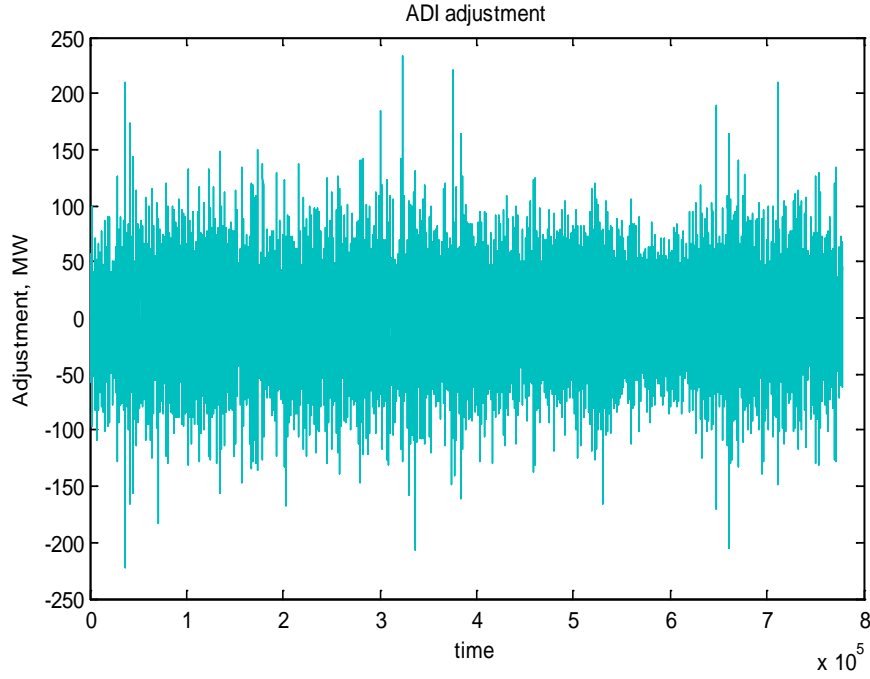


Figure B.6. ACE Adjustments

Adjusted ACE is calculated using the following equation (see Figure B.7):

$$\begin{aligned} \text{if } ACE_i > 0 \text{ then } ACE_i^{adj} &= ACE_i - |Adj| \\ \text{if } ACE_i < 0 \text{ then } ACE_i^{adj} &= ACE_i + |Adj| \end{aligned} \quad (\text{B.50})$$

Adjusted power flow through COI is:

$$\begin{aligned} \text{if } ACE_{BPA} > 0 \text{ then } P_{COI}^{adj} &= P_{COI} + |Adj| \\ \text{if } ACE_{BPA} < 0 \text{ then } P_{COI}^{adj} &= P_{COI} - |Adj| \end{aligned} \quad (\text{B.51})$$

For illustration purpose only, it is assumed that the COI power transfer distribution factors (PTDFs) for the CAISO and BPA are equal to 1. If a transmission limit is violated, the modified adjusted ACEs can be calculated as follow:

- For positive power flow (flow from BPA to CAISO) (Figure B.7)

$$\begin{aligned} \text{if } P_{COI}^{adj} > P_{COI}^{Lim(+)} \text{ then} \\ ACE_{BPA}^{adj'} &= ACE_{BPA}^{adj} + \Delta P \\ ACE_{CAISO}^{adj'} &= ACE_{CAISO}^{adj} - \Delta P \end{aligned} \quad (\text{B.52})$$

where: $\Delta P = P_{COI}^{adj} - P_{COI}^{Lim}$

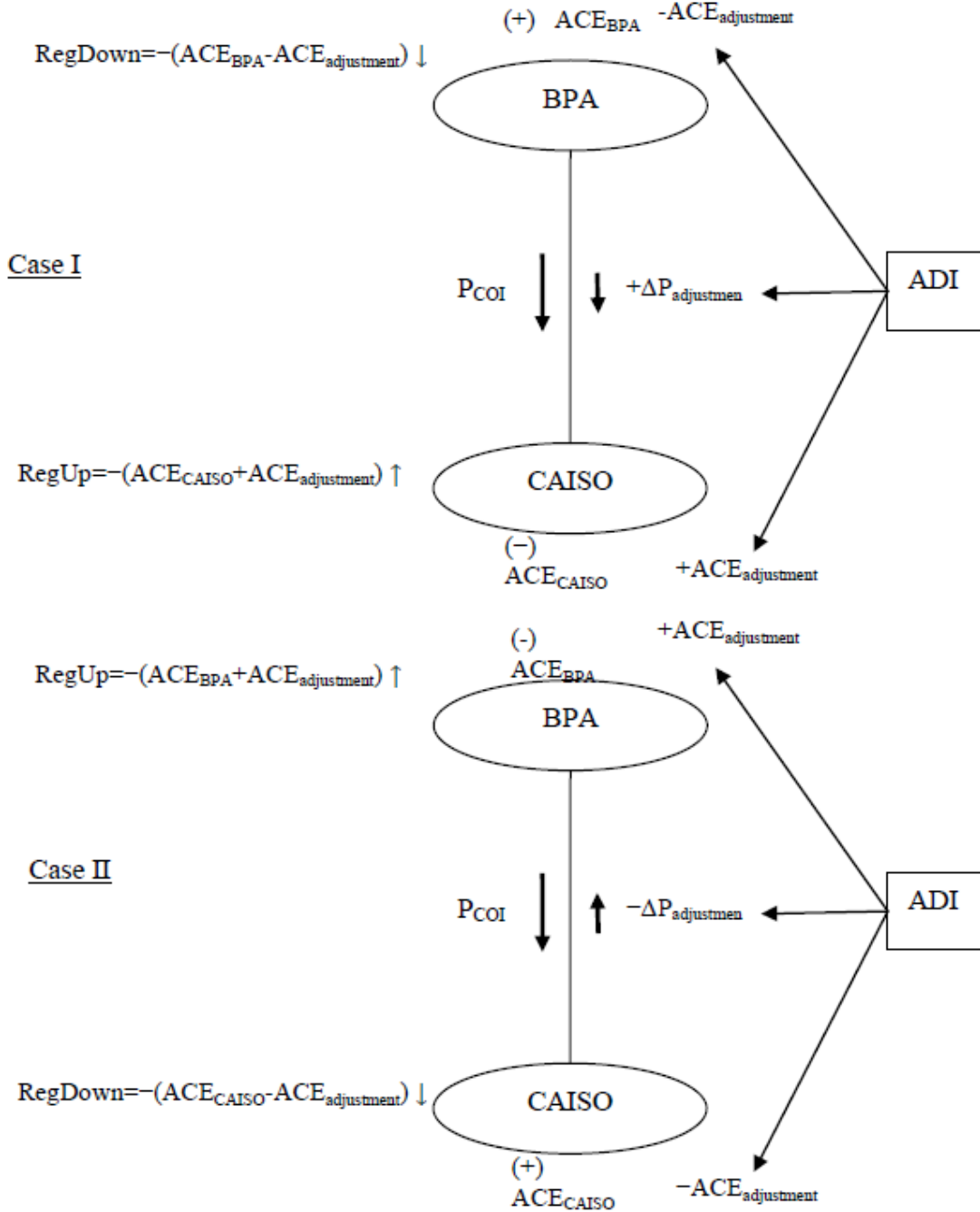


Figure B.7. BPA – CAISO ADI Illustration

- For negative power flow (flow from CAISO to BPA)

$$\begin{aligned}
 & \text{if } -P_{COI}^{adj} < P_{COI}^{Lim(-)} \text{ then} \\
 & ACE_{BPA}^{adj'} = ACE_{BPA}^{adj} - \Delta P \\
 & ACE_{CAISO}^{adj'} = ACE_{CAISO}^{adj} + \Delta P
 \end{aligned} \tag{B.53}$$

It is assumed that AGC regulation response is equal to ACE: $reg_i = -ACE_i$

Regulation Energy

The “regulation up” term corresponds to a positive regulation signal, whereas the regulation down term corresponds a to negative regulation signal:

$$\begin{aligned} reg_i &\in regup \text{ if } reg_i > 0 \\ reg_i &\in regdown \text{ if } reg_i < 0 \\ i &= 1 \dots N \end{aligned} \tag{B.54}$$

The positive and negative energy needed for regulation is calculated using the following expressions:

$$\begin{aligned} EnergyUP &= \sum_{m=1}^M regup_m \cdot \Delta t \\ EnergyDOWN &= \sum_{m=1}^M regdown_m \cdot \Delta t \end{aligned} \tag{B.55}$$

where: Δt is the time series resolution and M is the time series length.

Four scenarios are considered in the study:

- No ADI
- Conventional ADI with 25MW adjustment limit
- Conventional ADI without limits
- Proposed ADI with congestion model.

BPA and CAISO regulating energy requirements for different scenarios are presented in Figure B.8–Figure B.9. It can be seen that the ADI methodology reduces the energy needed for regulation. Moreover, by eliminating the 25 MW limit applied to ADI adjustments, one could essentially increase the ADI efficiency and bring more benefits to the ADI participants.

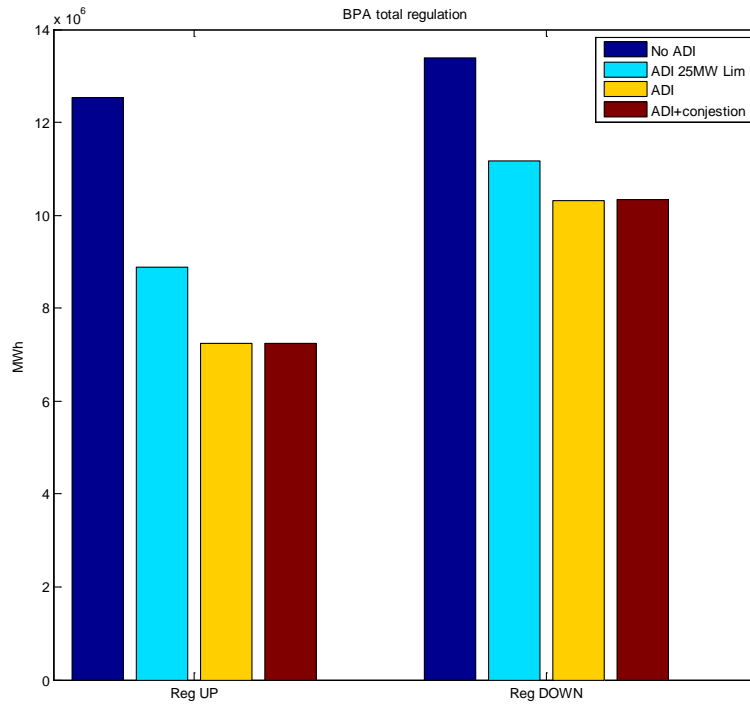


Figure B.8. BPA Regulating Energy (Up and Down): Without ADI, ADI With 25MW Limit, ADI

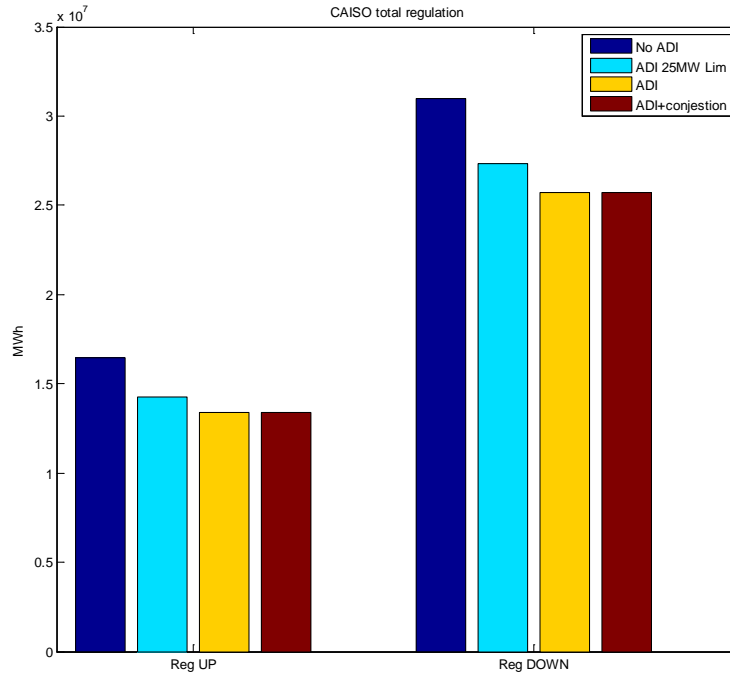


Figure B.9. CAISO Regulating Energy (Up and Down): Without ADI, ADI With 25MW Limit, ADI

Ramping Analysis

Ramping requirements analysis is performed according to the methodology presented in Section 2.1.5.1. As a result of this analysis a performance envelope containing information on ramping requirements (ramp rate/ramp duration/capacity) was received. Two scenarios are considered: 1) there is no ADI; 2) advanced ADI is used.

Figure B.10–Figure B.11 show the distribution of ACE signals for the BPA and the CAISO BAs respectively. One can see that the ADI reduces the spread of ACE distribution and thus decreases the regulation capacity requirements. As shown, the congestion limit, once introduced, does not affect the ADI performance when compared to the full size ADI without congestion.

Ramp rate requirements distribution for BPA and the CAISO BAs are presented in Figure B.12–Figure B.13. As shown, the ADI reduces the ramping requirements for both BAs.

Ramp duration distributions are shown in Figure B.14–Figure B.15. As shown, the ADI slightly increases the ramp duration requirements.

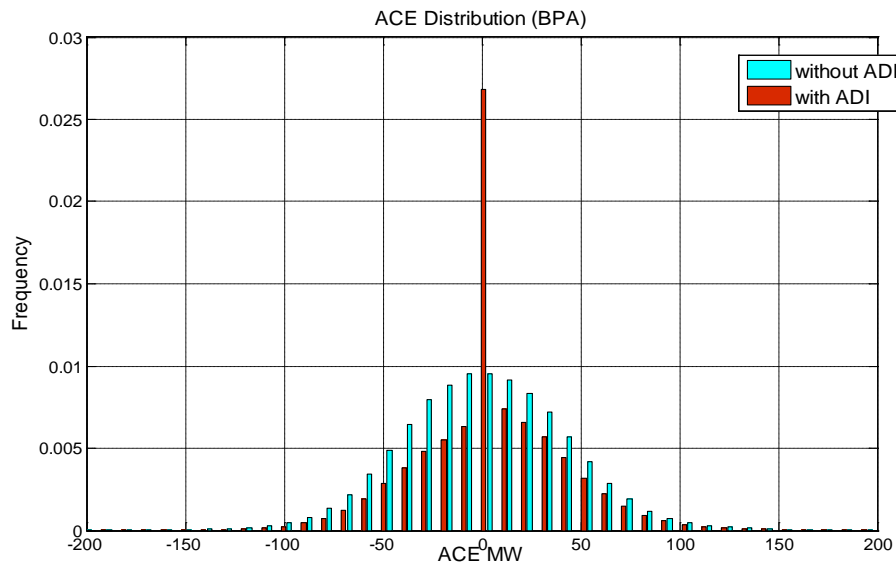


Figure B.10. BPA ACE Distribution: With ADI, Without ADI

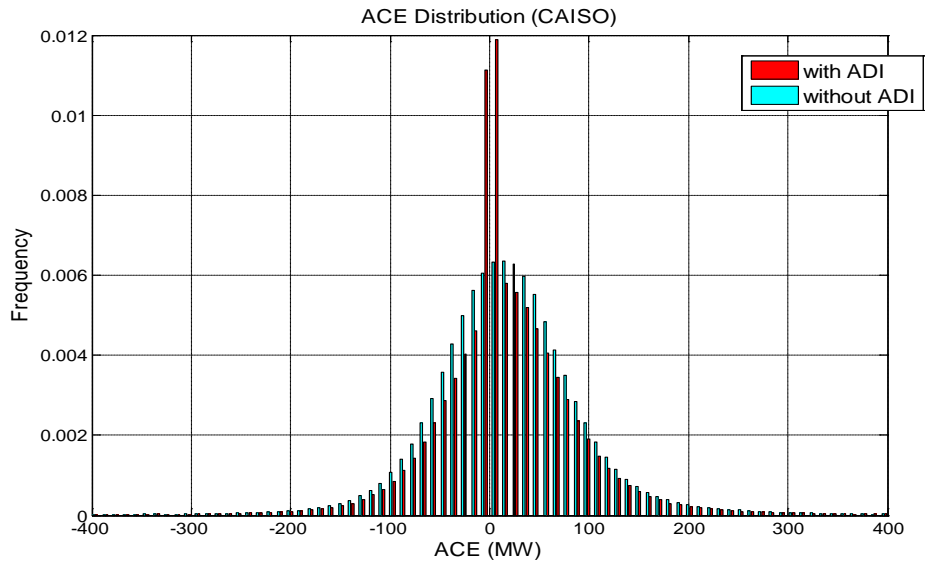


Figure B.11. CAISO ACE Distribution: With ADI, Without ADI

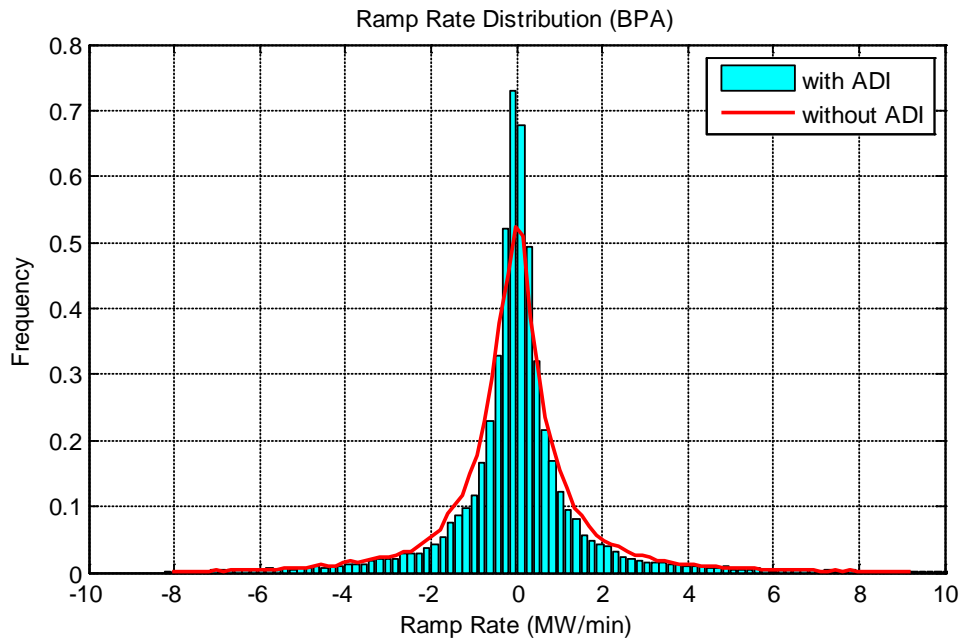


Figure B.12. BPA Ramp Rate Requirements Distribution: With ADI, Without ADI

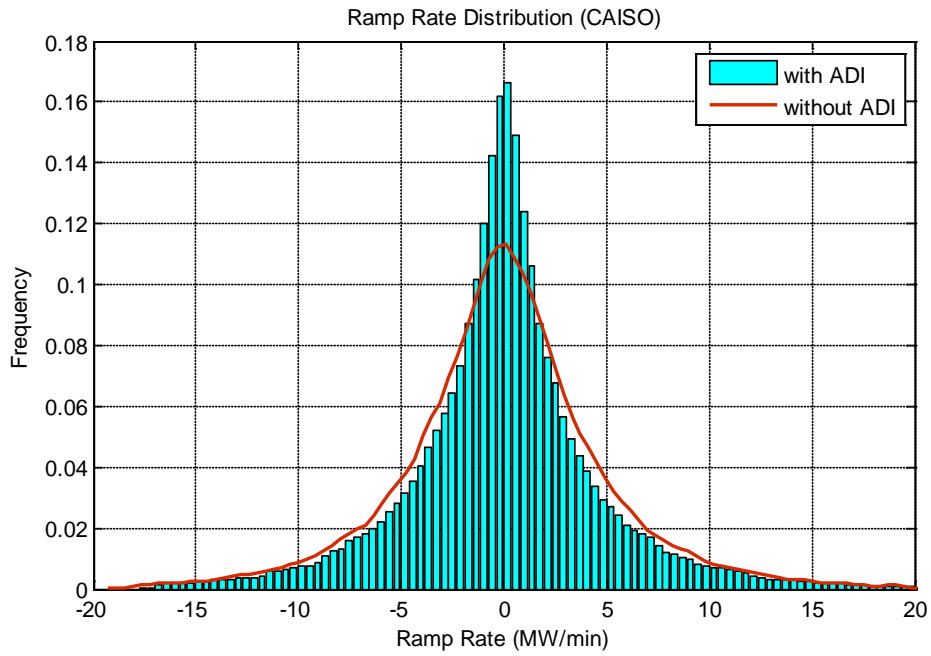


Figure B.13. CAISO Ramp Rate Requirements Distribution: With ADI, Without ADI

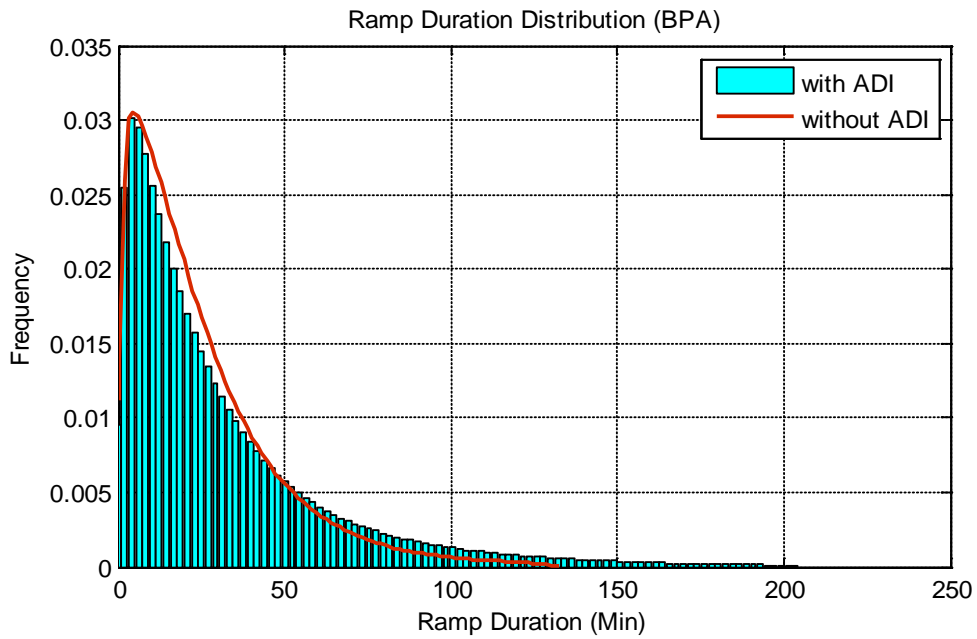


Figure B.14. BPA Ramp Duration Requirements Distribution: With ADI, Without ADI

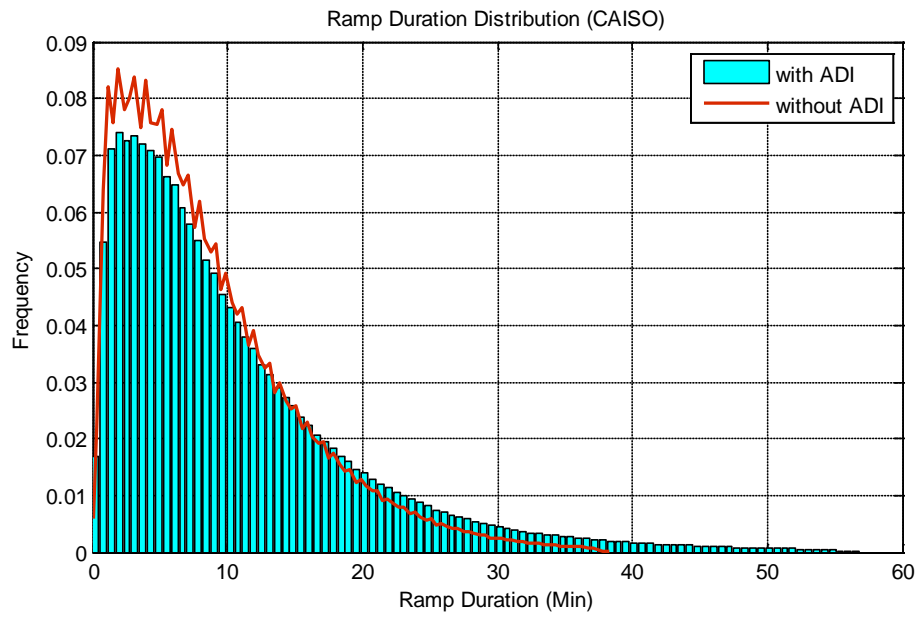


Figure B.15. CAISO Ramp Duration Requirements Distribution: With ADI, Without ADI

Appendix C

Regulation Sharing Model

Appendix C

Regulation Sharing Model

C.1 Regulation Sharing (Option I)

Input: Regulation signals REG_i ($i = 1, \dots, N$) for all N BAs, where N is the total number of the BAs; transmission limits for all inter-ties between BAs.

Step 1: //Group the sink and source BAs based on the signs of regulation signals
 FOR $i = 1, \dots, N$
 IF $REG_i > 0$ THEN
 The i -th BA belongs to {sink BA group}, of which the total number of sink BAs is m .
 ELSE
 The i -th BA belongs to {source BA group}, of which the total number of source BAs is n .
 END IF
 END FOR

Step 2: //Compare total regulation for sink and source BAs

Calculate total regulation of sink BAs: $\sum_{i=1}^m R_{EGi}, i \in \{sink\ BAs\}$.

Calculate total regulation of source BAs: $\sum_{j=1}^n R_{EGj}, j \in \{source\ BAs\}$.

IF $\left| \sum_{i=1}^m R_{EGi} \right| > \sum_{j=1}^n R_{EGj}$, THEN There are more generation than demand in the system.

IF $\left| \sum_{i=1}^m R_{EGi} \right| < \sum_{j=1}^n R_{EGj}$, THEN There are more demand than generation in the system.

Calculate total regulation of all BAs: $R_{EGt} = \sum_{i=1}^N R_{EGi}$.

Calculate average regulation of all BAs: $R_{EGa} = \frac{\sum_{i=1}^N R_{EGi}}{N}$.

Step 3: //calculate the power flow at transmission lines caused by regulation sharing

FOR $i = 1, \dots, n$ //for all the source BAs

 IF $R_{EGi} \neq 0$, THEN //if the regulation is zero in BA i , the BA cannot be a source BA

 For the i -th BA in the source BA group, find all the sink BAs directly connected to the i -th source BA, $REG_j, R_{EGj}, j \in \{1, 2, \dots, p\}$, where p is the total number of this kind of BAs

 FOR $j = 1, \dots, p$

```

IF  $R_{EGj} \neq 0$ , THEN //if the regulation is zero in BA j, the BA cannot be a sink
    //source BA
    Calculate  $\Delta R_{EGi-j} = |R_{EGi}| - |R_{EGj}|$ .
    IF  $\Delta R_{EGi-j} > 0$ , THEN //more generation in i-th BA than demand in j-th
    BA
        IF  $|R_{EGj}| > T_{i-j}$  THEN //transmission limit between i, j BAs
             $RT_{i-j} = T_{i-j}$  //power flow from i to j
        ELSE
             $RT_{i-j} = R_{EGj}$  //power flow from i to j,  $R_{EGj} > 0$ 
        END IF
         $R_{EGi} = -|\Delta R_{EGi-j}|$  //update regulation amount in BA i
         $R_{EGj} = 0$  //update regulation amount in BA j
    ELSE //more demand in i-th BA than generation in j-th BA
        IF  $|R_{EGi}| > T_{i-j}$  THEN //transmission limit between i, j BAs
             $RT_{i-j} = -T_{i-j}$  //power flow from j to i
        ELSE
             $RT_{i-j} = R_{EGi}$  //power flow from j to i,  $R_{EGi} < 0$ 
        END IF
         $R_{EGi} = 0$  //update regulation amount in BA i
         $R_{EGj} = |\Delta R_{EGi-j}|$  //update regulation amount in BA j
    END IF
END IF
END IF
END FOR // j = 1, ..., p
END IF
END FOR // i = 1, ..., n

```

Step 4: //Recalculate the modified regulation in each BA

FOR $i = 1, \dots, N$

$$R'_{EGi} = R_{EGi} + \sum_{k=1}^n RT_{i-k}, \quad k \in \{\text{other BAs directly connected to the } i\text{-th BA}\}, \text{ where}$$

$\sum_{k=1}^n RT_{i-k}$ is the total transmission between the i -th BA and other BAs directly connected to the i -th BA.

END FOR

Step 5: //evaluate the stopping criteria

//criterion 1

For all N BAs, if $R'_{EGi} < R_{EGa}$, then stop the process; otherwise go to step 2

//criterion 2

If there are no changes between two continuous attempts in step 2 - step 4, then stop the process; otherwise go to step 2

Output: Modified regulation signals REG'_i ($i = 1, \dots, N$) for all N BAs; transmission power flow (caused by regulation sharing) at all transmission lines between BAs.

The deviation between original regulation and modified regulation, i.e., $DE_REG = REG'_i - REG_i$ is the regulation needs to be transferred from/to other BAs via transmission lines. These part of regulation deviation can be provided by *dynamic scheduling process* using available generators in the source BA.

Although there is no objective function involved in the algorithm, basically, the optimization process is implicitly incorporated in the algorithm. The objective is to make the deviation of the regulation from 0 point as less as possible. Because each BA uses the same price for its regulation, then the regulation cost is directly proportion to the regulation itself.

The flow chart for regulation sharing is given in Figure C.1.

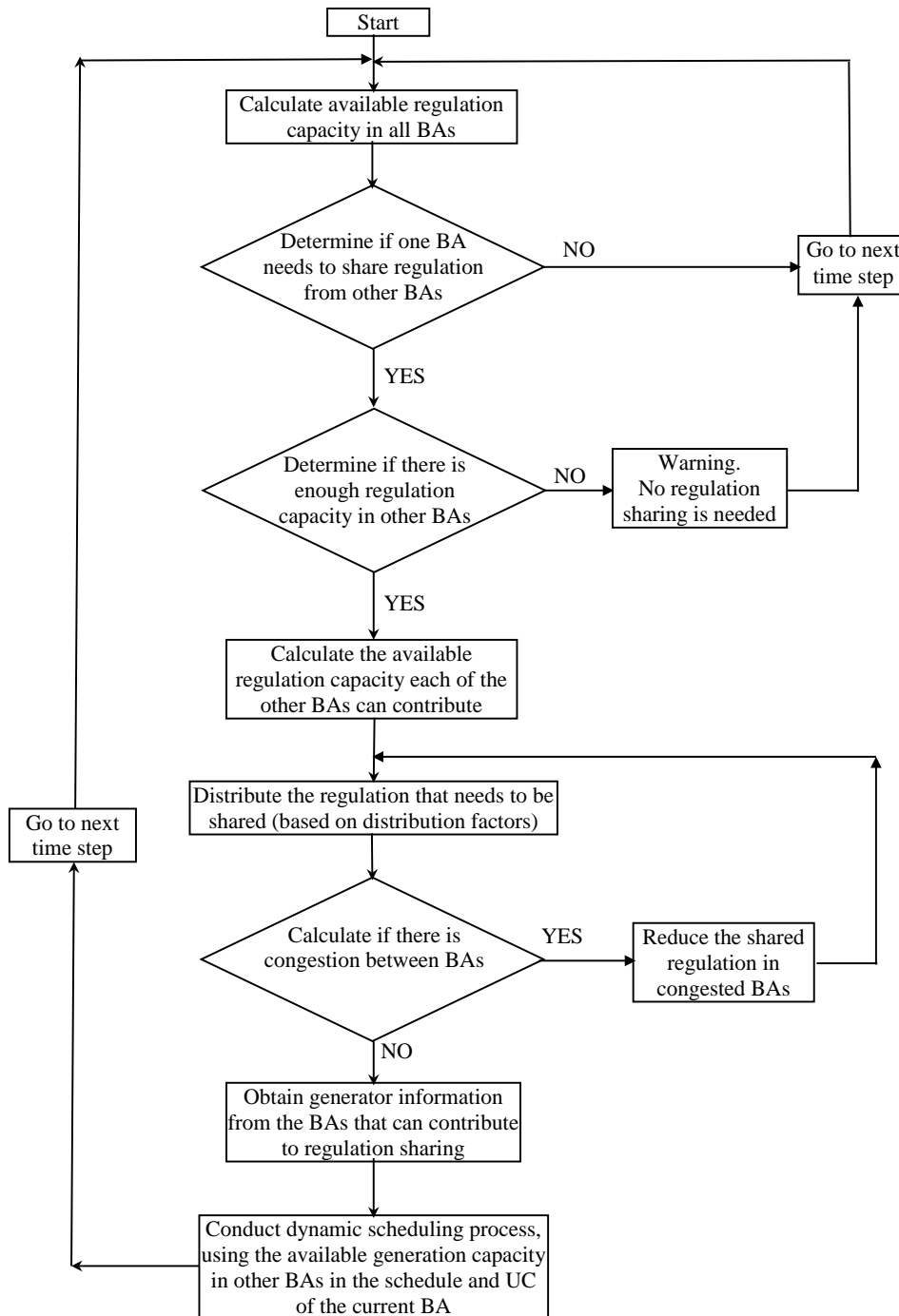


Figure C.1. Flow Chart of the Regulation Sharing

C.2 Regulation Sharing Based on Optimization (Option II)

The objective is to minimize the summation of square power of regulation up and regulation down. The constraints include transmission limit constraint and ramp rate limit constraint.

The formulation of the optimization problem is described as:

$$\min \sum_{i=1}^n (R_i^t)^2 \quad (\text{C.1})$$

$$\text{s.t.} \quad (\bar{R}_i^t - R_i^t) - (\bar{R}_j^t - R_j^t) < T_{i-j}^t \quad (i, j = 1, 2, \dots, n)$$

$$\left. \begin{array}{l} \text{if } R_i^t > R_i^{t-1} > 0 \\ \text{if } 0 > R_i^t > R_i^{t-1} \\ \text{if } R_i^{t-1} < 0, R_i^t > 0 \end{array} \right\}, \quad |R_i^t - R_i^{t-1}| < L_i^{up}$$

$$\left. \begin{array}{l} \text{if } R_i^{t-1} > R_i^t > 0 \\ \text{if } 0 > R_i^{t-1} > R_i^t \\ \text{if } R_i^{t-1} > 0, R_i^t < 0 \end{array} \right\}, \quad |R_i^t - R_i^{t-1}| < L_i^{dn}$$

where: R_i^t : the final regulation of the i -th control area at time t .

\bar{R}_i^t : the original regulation of the i -th control area at time t .

T_{i-j}^t : transmission limit between the i -th and j -th the control areas at time t .

n : total number of control areas.

L_i^{up} : regulation up ramp rate limit at the i -th control area.

L_i^{dn} : regulation down ramp rate limit at the i -th control area.

C.3 Regulation Sharing (Option III)

Regulation Signal

The regulation at the moment m can be given as:

$$\Delta G^r(m) = L_a^y(m) - L_{rf,5\min}^y(m) \quad (\text{C.2})$$

where $L_a^y(m)$ refers to actual load at moment t in the year y , $L_{rf,5\min}^y(m)$ means the real-time (5-minutues) scheduling load.

For the Balancing Authorities (BAs), the total actual load and real-time scheduling load are:

$$L_A = \sum_{i=1}^N L_{a,i}^y(m) \quad (\text{C.3})$$

and

$$L_{RTF} = \sum_{i=1}^N L_{rf,5min,i}^y(m) \quad (C.4)$$

Total (net) regulation in a group of Balancing Authorities (BAs) can be calculated by:

$$RG(m)_{\Sigma} = L_A - L_{RTF} = \sum_{i=1}^N L_{a,i}^y(m) - \sum_{i=1}^N L_{rf,5min,i}^y(m) \quad (C.5)$$

where $RG(m)_{\Sigma}$ is total the regulation of the BAs at the moment m , N is the total number of BAs.

The sign of the net regulation can be given:

$$sign[RG(m)_{\Sigma}] = \begin{cases} 1 & \text{if } RG(m)_{\Sigma} > 0 \\ 0 & \text{if } RG(m)_{\Sigma} = 0 \\ -1 & \text{if } RG(m)_{\Sigma} < 0 \end{cases} \quad (C.6)$$

The above relationship can also be given as:

$$\text{if } RG(m)_{\Sigma} > 0, \text{ then } \sum_{i=1}^N L_{a,i}^y(m) > \sum_{i=1}^N L_{rf,5min,i}^y(m);$$

$$\text{if } RG(m)_{\Sigma} = 0, \text{ then } \sum_{i=1}^N L_{a,i}^y(m) = \sum_{i=1}^N L_{rf,5min,i}^y(m);$$

$$\text{if } RG(m)_{\Sigma} < 0, \text{ then } \sum_{i=1}^N L_{a,i}^y(m) < \sum_{i=1}^N L_{rf,5min,i}^y(m).$$

The total regulation can be described as:

$$RG(m)_{\Sigma} = \sum_{i=1}^N RG(m)_i \quad (C.7)$$

where $RG(m)_i$ is the regulation in the BA i .

The sign of the raw regulation of each BA can be given:

$$sign[RG(m)_i] = \begin{cases} 1 & \text{if } RG(m)_i > 0 \\ 0 & \text{if } RG(m)_i = 0 \\ -1 & \text{if } RG(m)_i < 0 \end{cases}$$

Regulation Distribution Approaches

A few distribution methods can be used to distribute regulation among BAs.

1. Evenly distributed regulation among all BAs

The total net regulation can be evenly distributed among BAs. The final distributed regulation for each BA is:

$$RG(m)'_i = \frac{RG(m)_\Sigma}{N} \quad (C.8)$$

Then the adjusted regulation at each BA is:

$$\Delta RG(m)_i = RG(m)_i - RG(m)'_i = RG(m)_i - \frac{RG(m)_\Sigma}{N} \quad (C.9)$$

2. Based on regulation variance

The variance of each BA can be given as $\sigma_{RG,i}^2$, where $\sigma_{RG,i}$ ($i = 1, \dots, N$) is the standard deviation of the BA i . Then the final distributed regulation for each BA is:

$$RG(m)'_i = \frac{\sigma_{RG,i}^2}{\sum_{i=1}^N \sigma_{RG,i}^2} \times RG(m)_\Sigma \quad (C.10)$$

Then the adjusted regulation at each BA is:

$$\Delta RG(m)_i = RG(m)_i - RG(m)'_i = RG(m)_i - \frac{\sigma_{RG,i}^2}{\sum_{i=1}^N \sigma_{RG,i}^2} \times RG(m)_\Sigma \quad (C.11)$$

3. Based on participation factors

The participation factor of each BA can be given as p_i ($i = 1, \dots, N$). Then the final distributed regulation for each BA is:

$$RG(m)'_i = \frac{p_i}{\sum_{i=1}^N p_i} \times RG(m)_\Sigma \quad (C.12)$$

Then the adjusted regulation at each BA is:

$$\Delta RG(m)_i = RG(m)_i - RG(m)'_i = RG(m)_i - \frac{p_i}{\sum_{i=1}^N p_i} \times RG(m)_\Sigma \quad (C.13)$$

Adjust Regulation

After the adjusted regulation is computed for each BA. The deviation of regulation can be adjusted by modifying the real-time scheduling.

If $\Delta RG(m)_i > 0$, the real-time scheduling that needs to adjusted is $-\Delta RG(m)_i$, which means the real-time scheduling needs to reduce $-\Delta RG(m)_i$.

If $\Delta RG(m)_i < 0$, the real-time scheduling that needs to adjusted is $+\Delta RG(m)_i$, which means the real-time scheduling needs to increase $+\Delta RG(m)_i$.

If $\Delta RG(m)_i = 0$, the real-time scheduling does not need to be changed.

C.4 Simulation Results

The regulation and load following signals used for the simulation are shown in this section. The method proposed in [32] to separate regulation and load following is used in the simulation. 2006 actual CAISO load data is used to derive regulation and load following signals. Hour-ahead and real-time scheduling is simulated based on the method described in [32]. Figure C.2 shows the simulated regulation signal. Figure C.3 illustrates the difference in the time frame between regulation and load following signals. From Figure C.3 it is evident that the regulation has a smaller time frame compared to the load following. Figure C.4 shows the histograms of regulation.

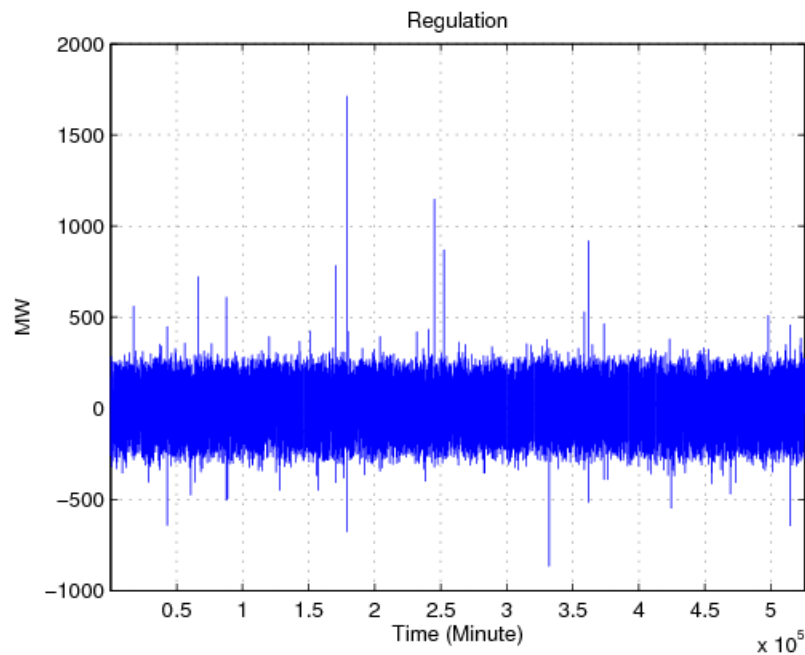


Figure C.2. Regulation Signal

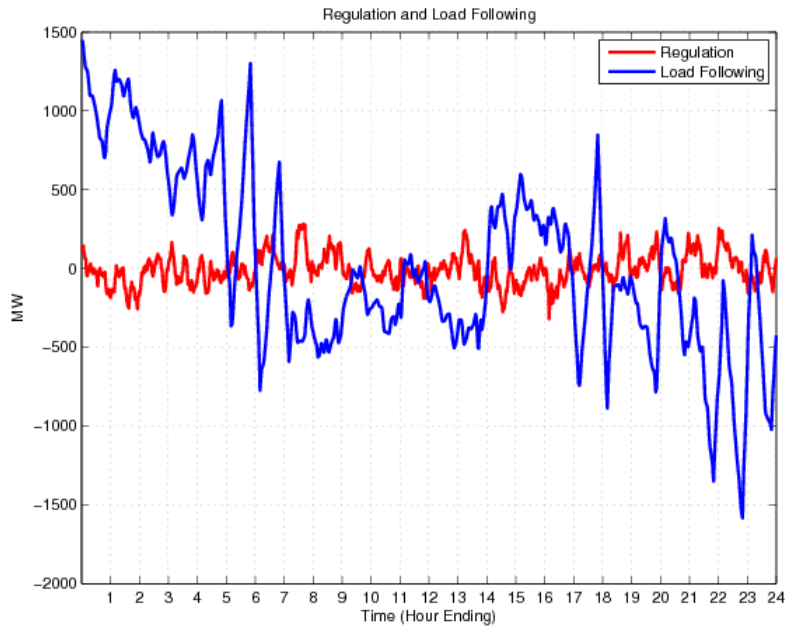


Figure C.3. Regulation and Load Following Time Frame

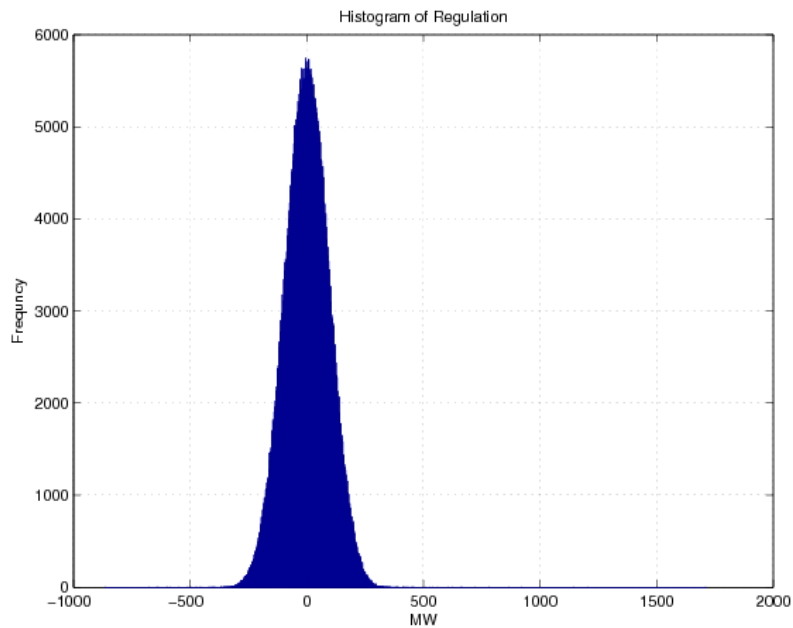


Figure C.4. Histogram of Regulation

Figure C.5 shows the regulation signals before and after applying the regulation sharing algorithm for the three BAs. Figure C.6 compares the maximum up and down regulation capacity for three BAs with and without sharing regulation. From Figure C.6 we can see, the regulation sharing algorithm reduces the maximum regulation down capacity for three BAs.

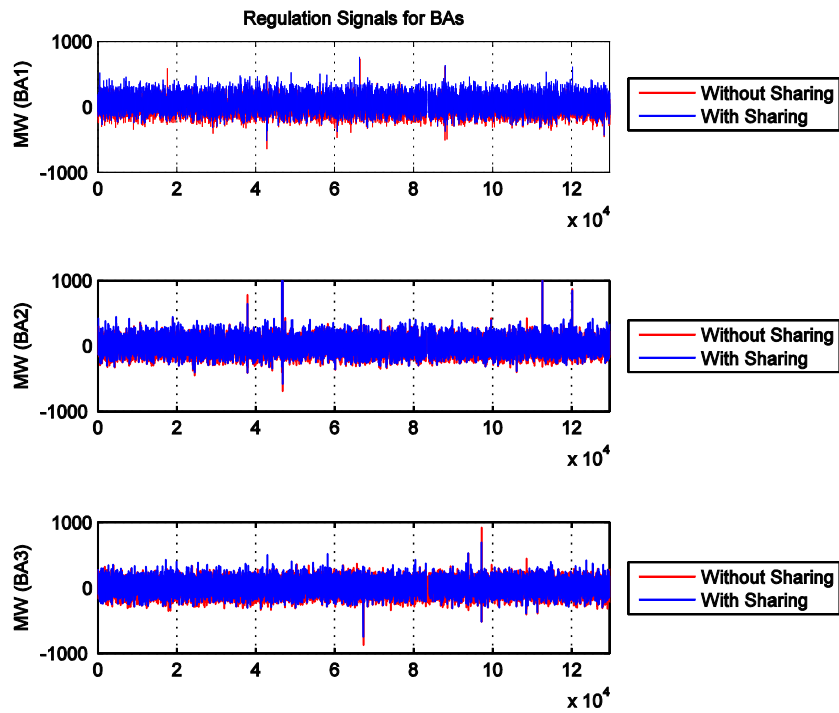


Figure C.5. Simulated Regulation Signals for Three BAs (With and Without Sharing)

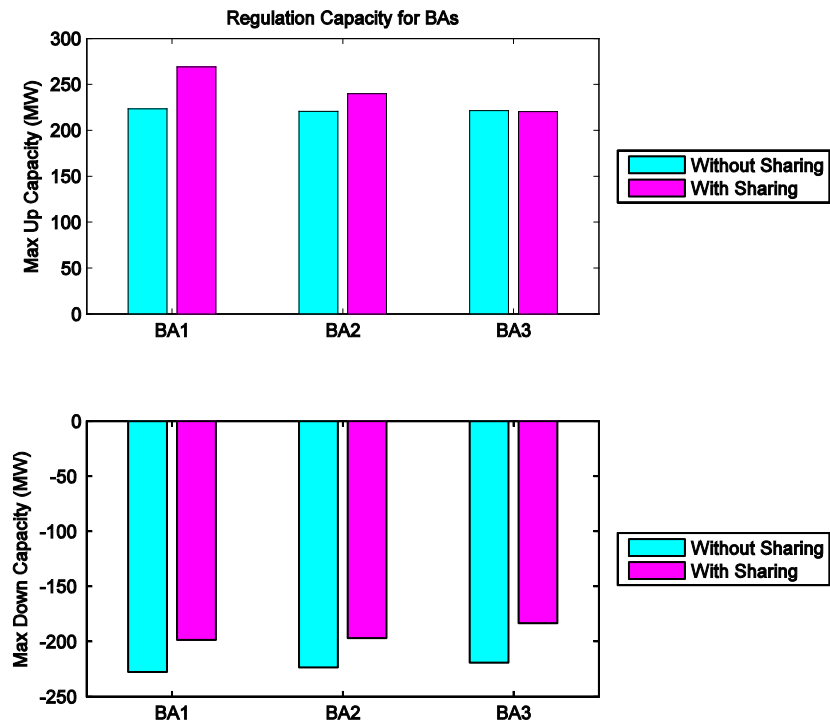


Figure C.6. Regulation Capacity (With and Without Sharing)

Figure C.7, Figure C.8 and Figure C.9 show the probability distribution for the regulation capacity of the three BAs with and without sharing regulation. From these figures we can see that the regulation sharing increase the frequency of small regulation capacity.

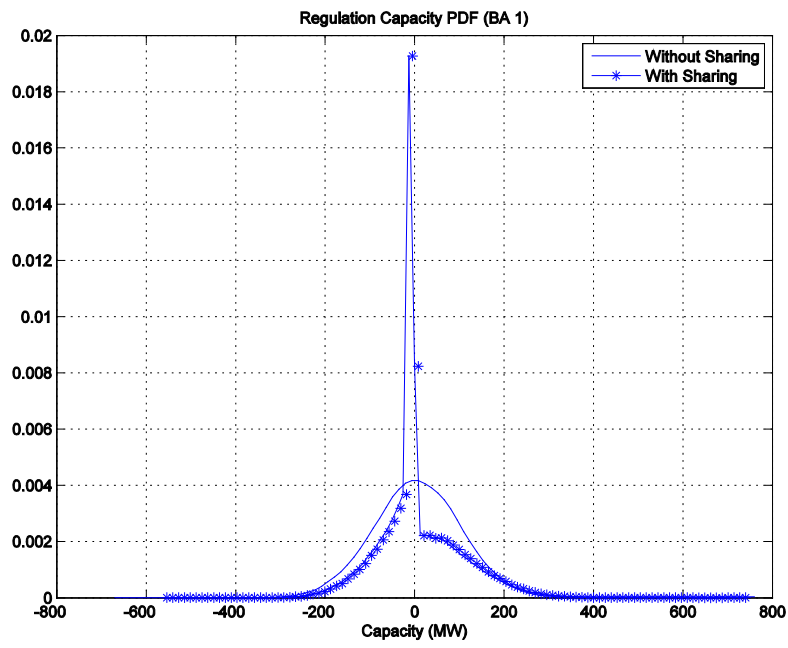


Figure C.7. Regulation Capacity Probability Distribution Function (PDF) for BA 1 (With and Without Sharing)

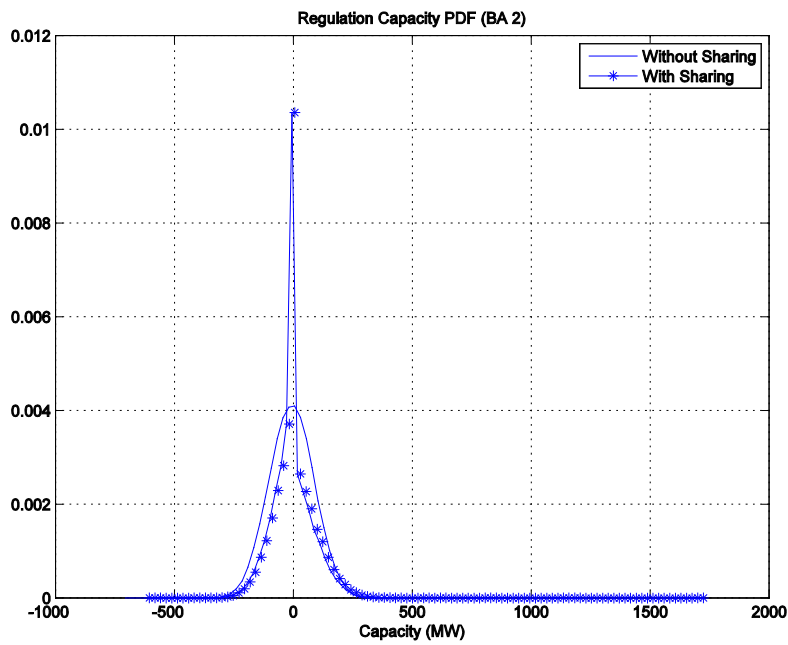


Figure C.8. Regulation Capacity PDF for BA 2 (With and Without Sharing)

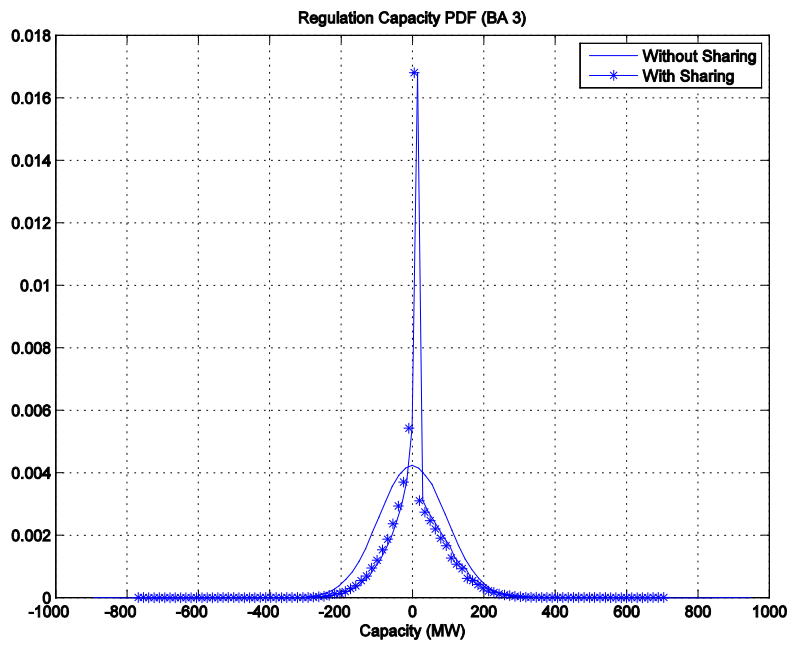


Figure C.9. Regulation Capacity PDF for BA 3 (With and Without Sharing)

Figure C.10, Figure C.11 and Figure C.12 show the probability distribution for the regulation ramp rates of the three BAs with and without sharing regulation. From these figures we can see that the regulation sharing increases the frequency of small regulation ramp rates.

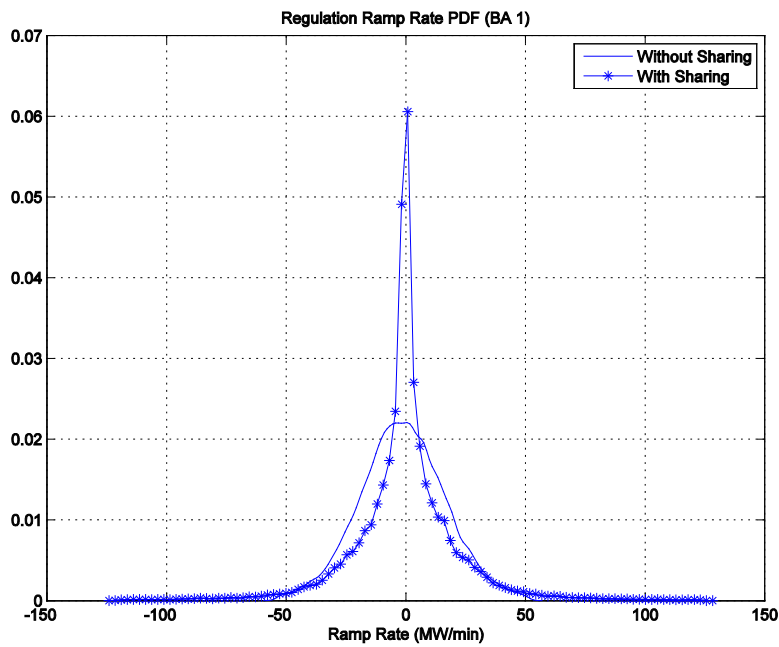


Figure C.10. Regulation Ramp Rate PDF for BA 1 (With and Without Sharing)

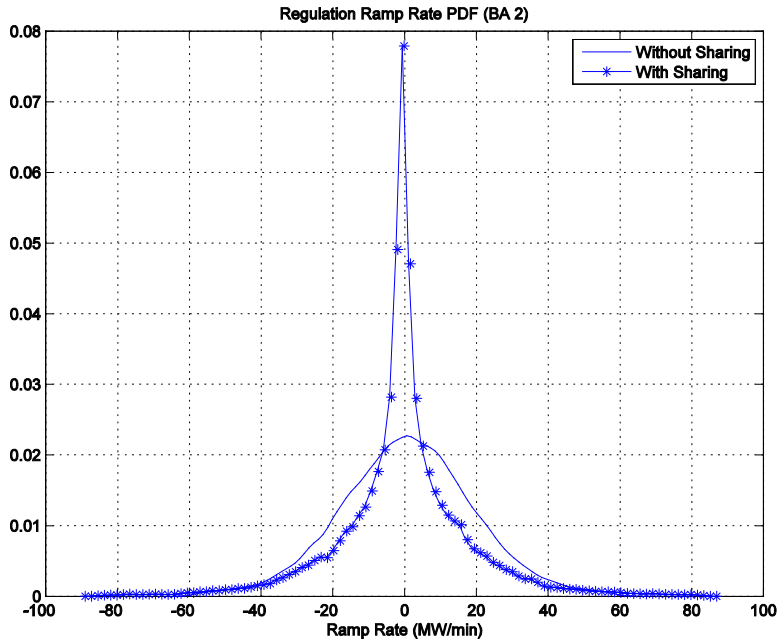


Figure C.11. Regulation Ramp Rate PDF for BA 2 (With and Without Sharing)

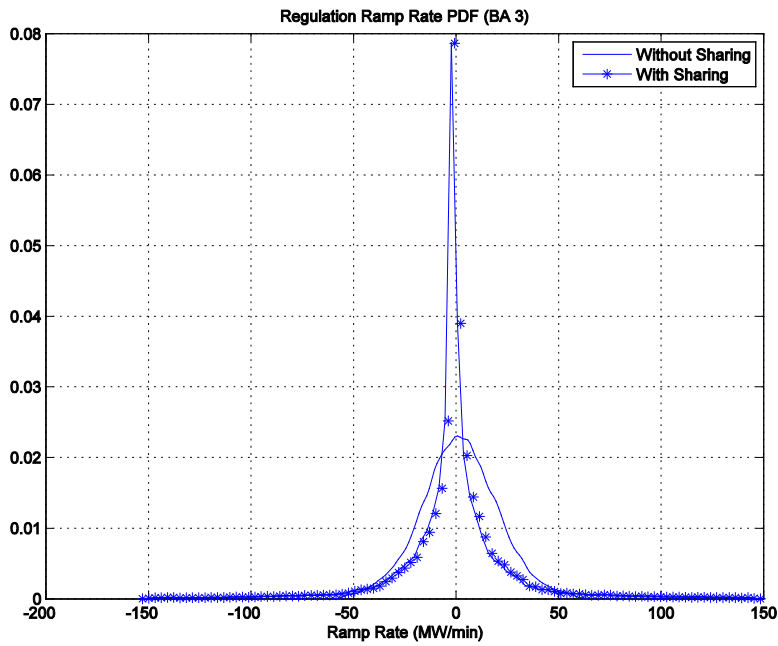


Figure C.12. Regulation Ramp Rate PDF for BA 3 (With and Without Sharing)

Figure C.13, Figure C.14 and Figure C.15 show the probability distribution for the regulation ramp duration of the three BAs with and without sharing regulation. From these figures we can see that the regulation sharing increase the frequency of shorter regulation ramp duration and increase the frequency of longer regulation ramp duration.

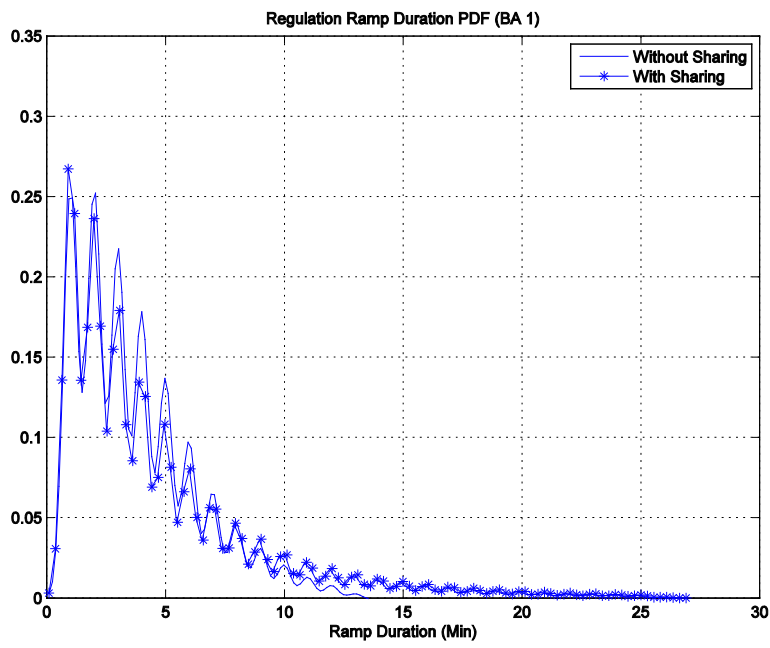


Figure C.13. Regulation Ramp Duration PDF for BA 1 (With and Without Sharing)

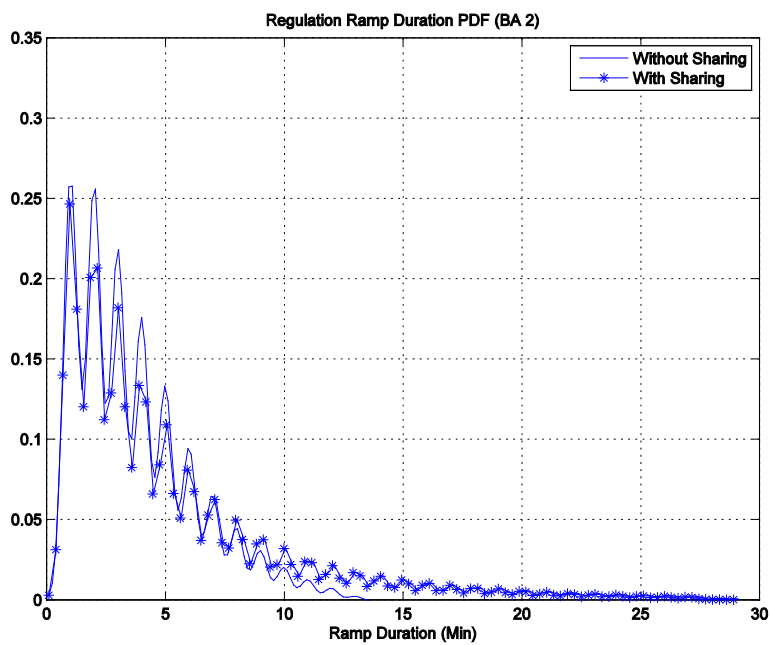


Figure C.14. Regulation Ramp Duration PDF for BA 2 (With and Without Sharing)

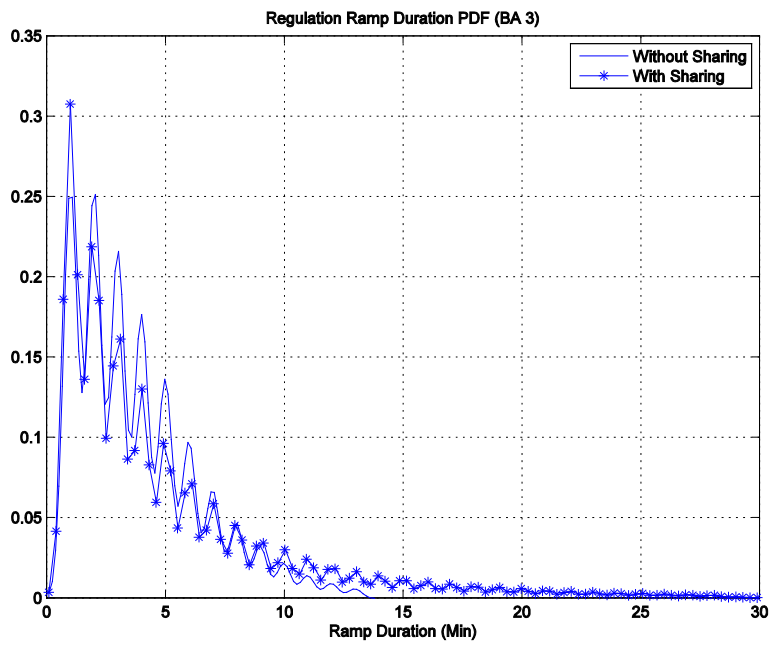


Figure C.15. Regulation Ramp Duration PDF for BA 3 (With and Without Sharing)

Appendix D

Load Following Sharing Model

Appendix D

Load Following Sharing Model

D.1 Load Following Signal

The load following at the moment m can be given as:

$$\Delta G^{lf}(m) = L_{rf,5min}^y(m) - L_{rf,1hr}^y(m)$$

where $L_{rf,5min}^y(m)$ means the real-time (5-minitues) scheduling, and $L_{rf,1hr}^y(m)$ means the hour-ahead scheduling.

For the Balancing Authorities (BAs), the total actual real-time scheduling and hour-ahead scheduling are:

$$L_{RTF} = \sum_{i=1}^N L_{rf,5min,i}^y(m) \text{ and } L_{HR} = \sum_{i=1}^N L_{rf,1hr,i}^y(m).$$

Total (net) load following in a group of Balancing Authorities (BAs) can be calculated by:

$$LF(m)_{\Sigma} = L_{RTF} - L_{HR} = \sum_{i=1}^N L_{rf,5min,i}^y(m) - \sum_{i=1}^N L_{rf,1hr,i}^y(m)$$

where $LF(m)_{\Sigma}$ is total the load following of the BAs at the moment m , N is the total number of BAs.

The sign of the net load following can be given as:

$$sign[LF(m)_{\Sigma}] = \begin{cases} 1 & \text{if } LF(m)_{\Sigma} > 0 \\ 0 & \text{if } LF(m)_{\Sigma} = 0 \\ -1 & \text{if } LF(m)_{\Sigma} < 0 \end{cases}$$

It is can also be described as:

$$\text{if } LF(m)_{\Sigma} > 0, \text{ then } \sum_{i=1}^N L_{rf,5min,i}^y(m) > \sum_{i=1}^N L_{rf,1hr,i}^y(m);$$

$$\text{if } LF(m)_{\Sigma} = 0, \text{ then } \sum_{i=1}^N L_{rf,5min,i}^y(m) = \sum_{i=1}^N L_{rf,1hr,i}^y(m);$$

$$\text{if } LF(m)_{\Sigma} < 0, \text{ then } \sum_{i=1}^N L_{rf,5min,i}^y(m) < \sum_{i=1}^N L_{rf,1hr,i}^y(m).$$

The total load following can also be described as:

$$LF(m)_\Sigma = \sum_{i=1}^N LF(m)_i$$

where $LF(m)_i$ is the load following in the BA i .

The sign of the raw load following of each BA can be given:

$$sign[LF(m)_i] = \begin{cases} 1 & \text{if } LF(m)_i > 0 \\ 0 & \text{if } LF(m)_i = 0 \\ -1 & \text{if } LF(m)_i < 0 \end{cases}$$

D.2 Load Following Distribution Approaches

A few distribution methods can be used to distribute load following among BAs.

1. Evenly distributed load following among all BAs

The total net load following can be evenly distributed among BAs. The final distributed load following for each BA is:

$$LF(m)'_i = \frac{LF(m)_\Sigma}{N}$$

Then the adjusted load following at each BA is:

$$\Delta LF(m)_i = LF(m)_i - LF(m)'_i = LF(m)_i - \frac{LF(m)_\Sigma}{N}$$

2. Based on load following variance

The variance of the load following at each BA can be given as $\sigma_{LF,i}^2$, where $\sigma_{LF,i}$ ($i = 1, \dots, N$) is the standard deviation of the BA i . Then the final distributed regulation for each BA is:

$$LF(m)'_i = \frac{\sigma_{LF,i}^2}{\sum_{i=1}^N \sigma_{LF,i}^2} \times LF(m)_\Sigma$$

Then the adjusted load following at each BA is:

$$\Delta LF(m)_i = LF(m)_i - LF(m)'_i = LF(m)_i - \frac{\sigma_{LF,i}^2}{\sum_{i=1}^N \sigma_{LF,i}^2} \times LF(m)_\Sigma$$

3. Based on participation factors

The participation factor of each BA can be given as p_i ($i = 1, \dots, N$). Then the final distribution of load the following at each BA is:

$$LF(m)'_i = \frac{p_i}{\sum_{i=1}^N p_i} \times LF(m)_\Sigma$$

Then the adjusted load following at each BA is:

$$\Delta LF(m)_i = LF(m)_i - LF(m)'_i = LF(m)_i - \frac{p_i}{\sum_{i=1}^N p_i} \times LF(m)_\Sigma$$

D.2.1 Adjust Load Following

After the adjusted load following is calculated for each BA. The deviation of load following can be adjusted by modifying the real-time scheduling and hour-ahead scheduling.

If $\Delta LF(m)_i > 0$, the real-time scheduling that needs to adjusted is $-\Delta LF(m)_i$, which means the real-time scheduling needs to reduce by $-\Delta LF(m)_i$.

If $\Delta LF(m)_i < 0$, the real-time scheduling that needs to adjusted is $+\Delta LF(m)_i$, which means the real-time scheduling needs to increase by $+\Delta LF(m)_i$.

If $\Delta LF(m)_i = 0$, the real-time scheduling does not need to be changed.

D.3 Simulation Results

Figure D.1 shows the simulated load following signal. Figure D.2 shows the histograms of load following.

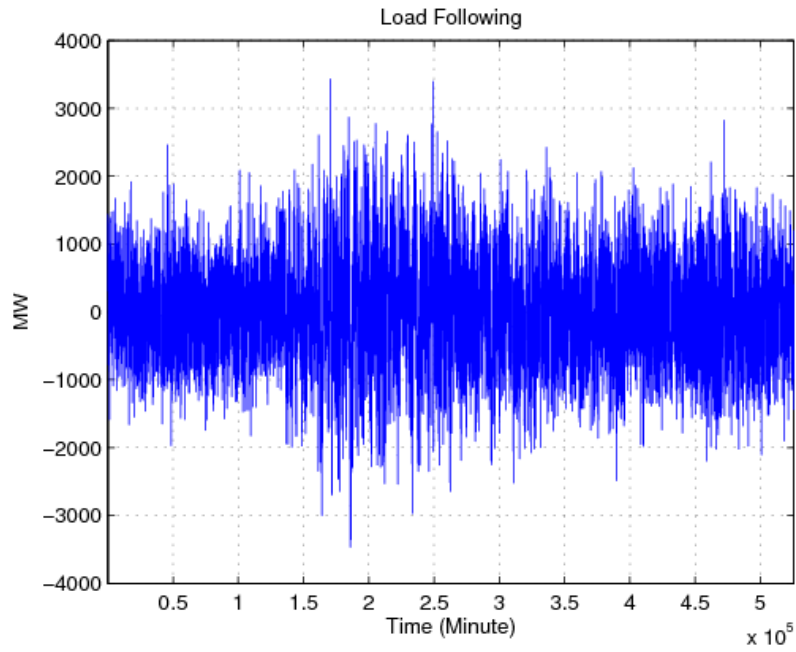


Figure D.1. Load Following Signal

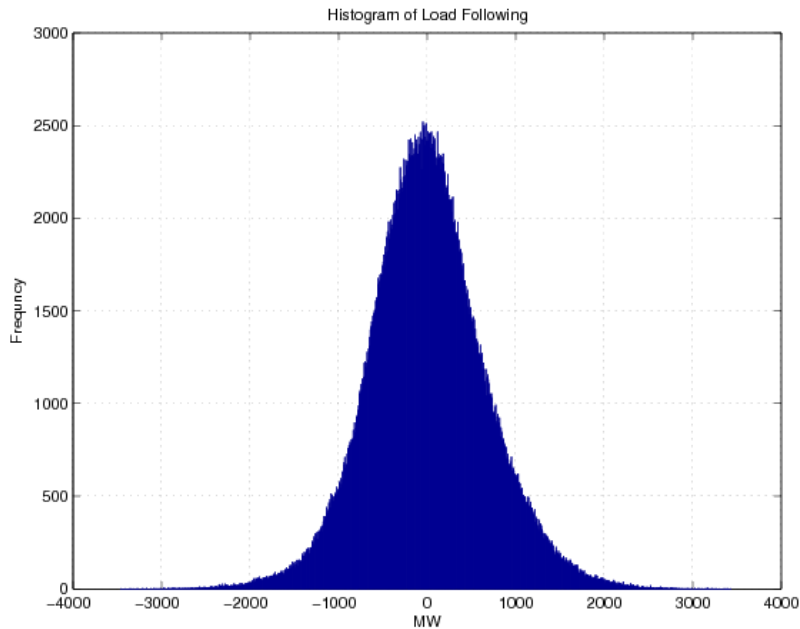


Figure D.2. Histogram of load following

Figure D.3 shows the load following signals before and after applying the load following sharing algorithm for the three BAs. Figure D.4 compares the maximum up and down load following capacity for three BAs with and without sharing regulation. From Figure D.4 it is evident that, the load following sharing algorithm reduces the maximum load following down capacity for three BAs.

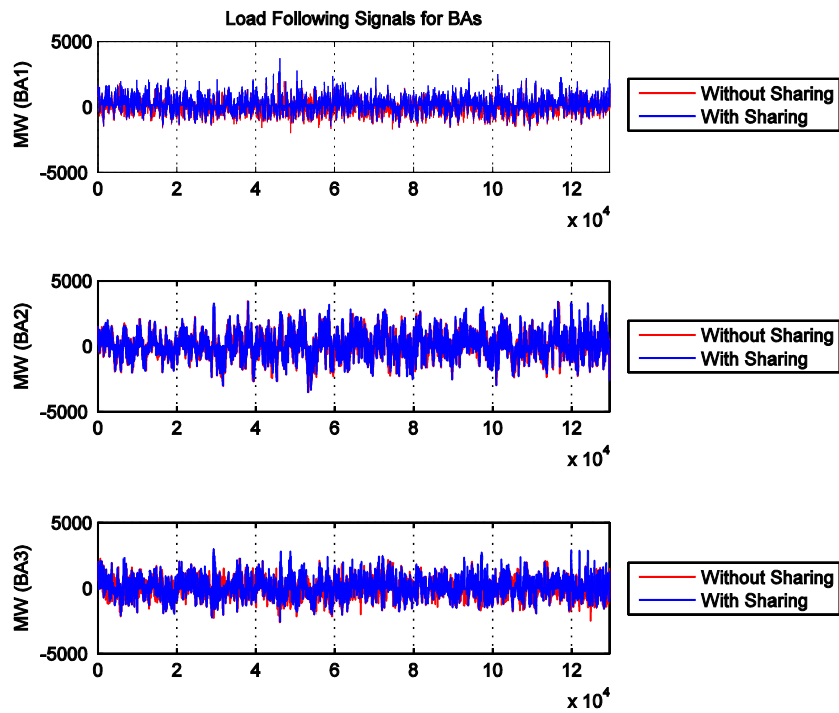


Figure D.3. Simulated Load Following Signals for Three Bas (With and Without Sharing)

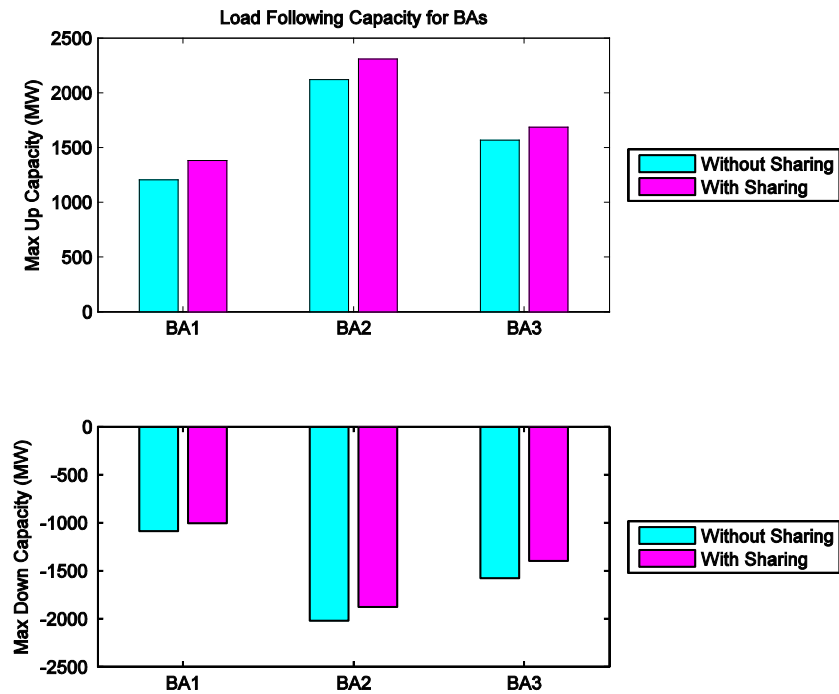


Figure D.4. Load Following Capacity for Three BAs (With and Without Sharing)

Figure D.5, Figure D.6 and Figure D.7 show the probability distribution for the load following capacity of the three BAs with and without sharing load following. From these figures we can see that the load following sharing increase the frequency of small load following capacity.

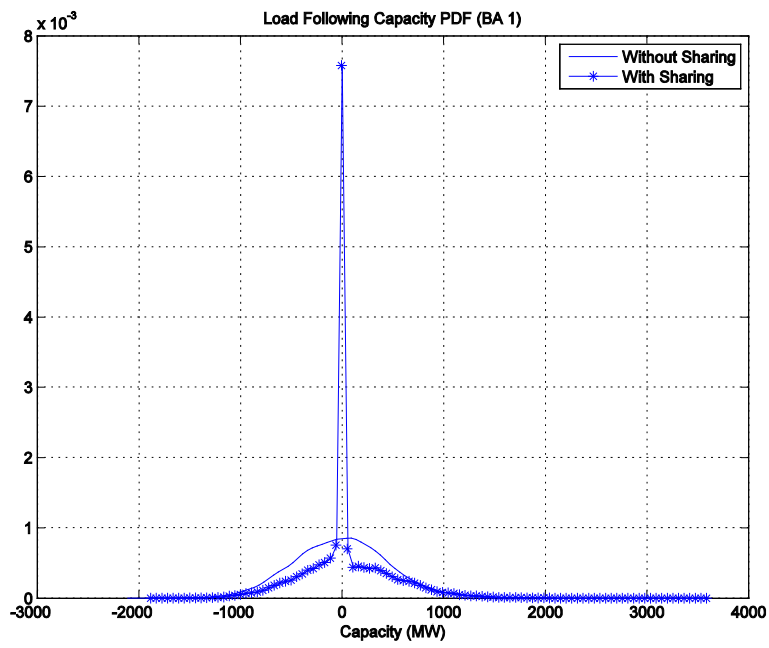


Figure D.5. Load Following Capacity PDF for BA 1 (With and Without Sharing)

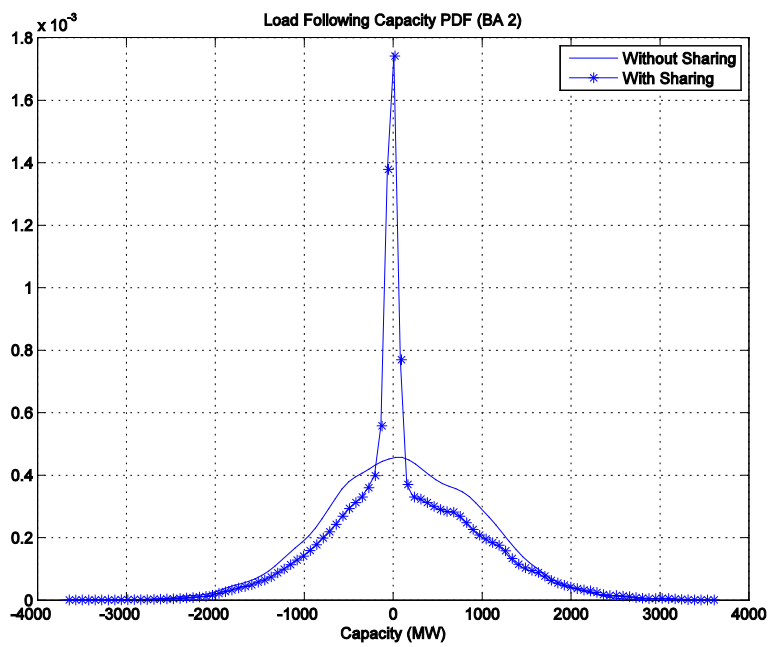


Figure D.6. Load Following Capacity PDF for BA 2 (With and Without Sharing)

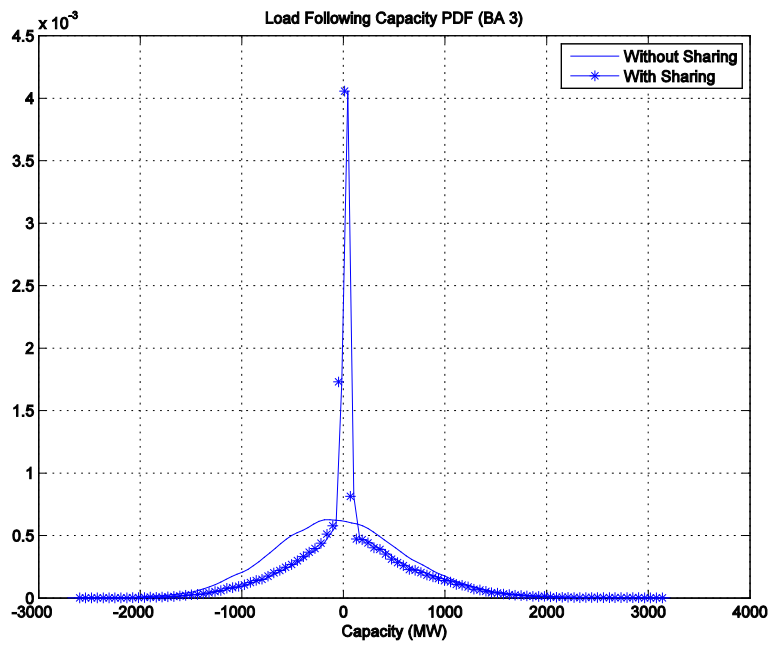


Figure D.7. Load Following Capacity PDF for BA 3 (With and Without Sharing)

Figure D.8, Figure D.9 and Figure D.10 show the probability distribution for the load following ramp rates of the three BAs with and without sharing load following. From these figures we can see that the load following sharing increase the frequency of small load following ramp rates.

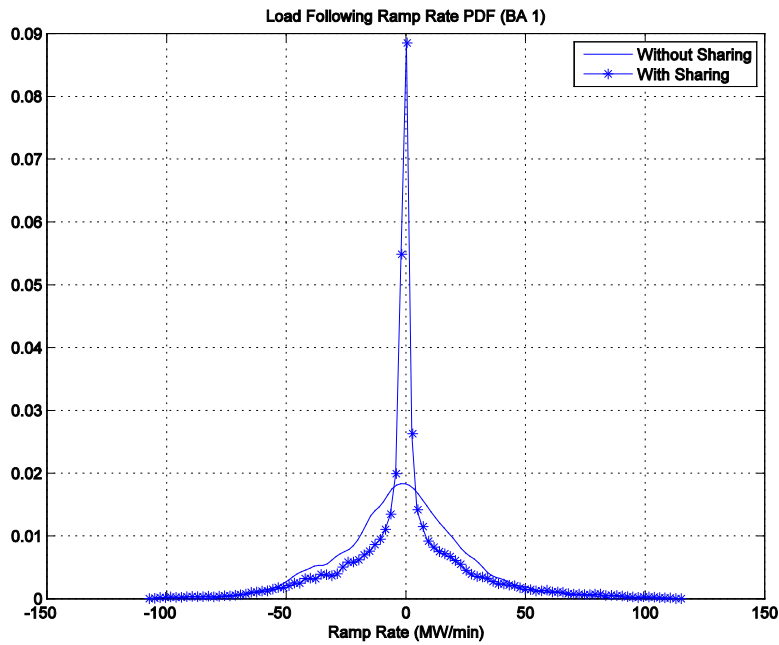


Figure D.8. Load Following Ramp Rate PDF for BA 1 (With and Without Sharing)

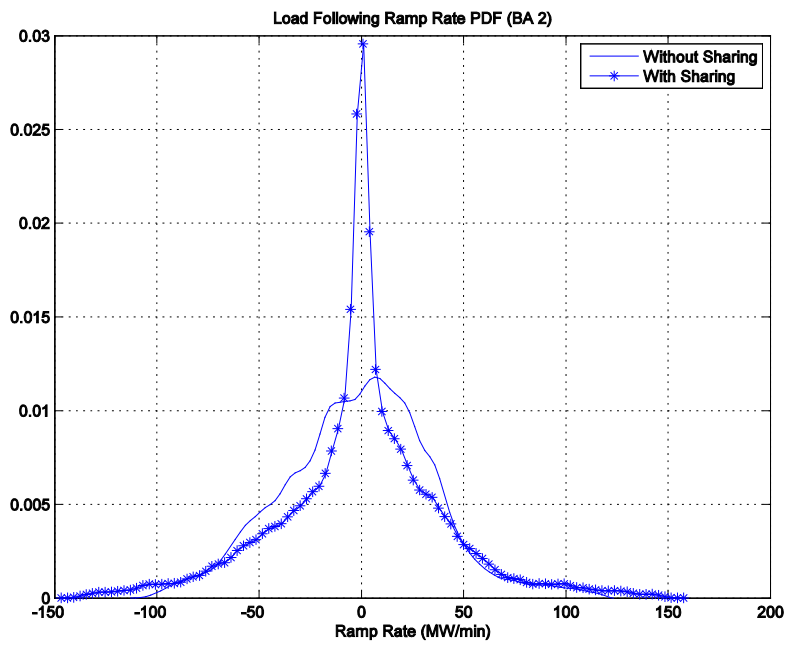


Figure D.9. Load Following Ramp Rate PDF for BA 2 (With and Without Sharing)

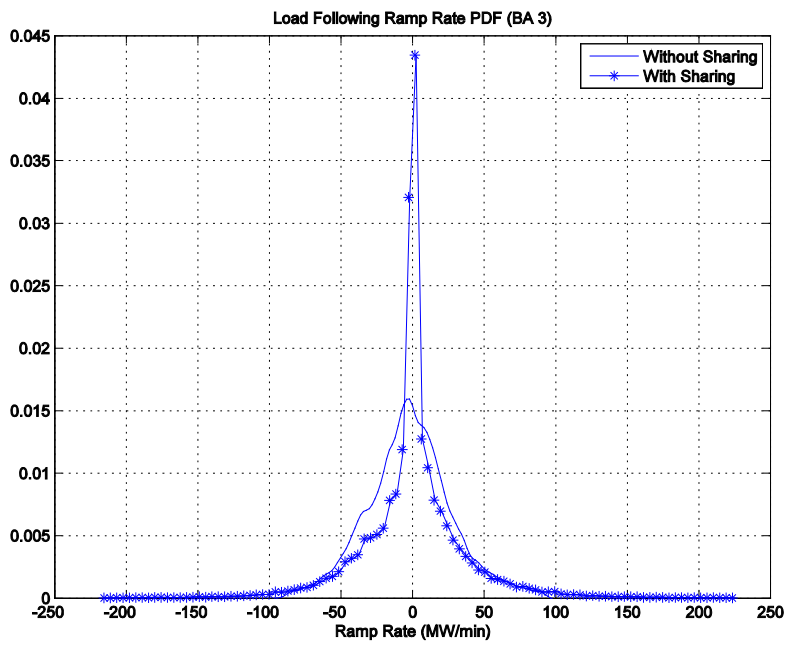


Figure D.10. Load Following Ramp Rate PDF for BA 3 (With and Without Sharing)

Figure D.11, Figure D.12 and Figure D.13 show the probability distribution for the load following ramp duration of the three BAs with and without sharing load following. From these figures we can see that the load following sharing increase the frequency of shorter load following ramp duration and increase the frequency of longer load following ramp duration.

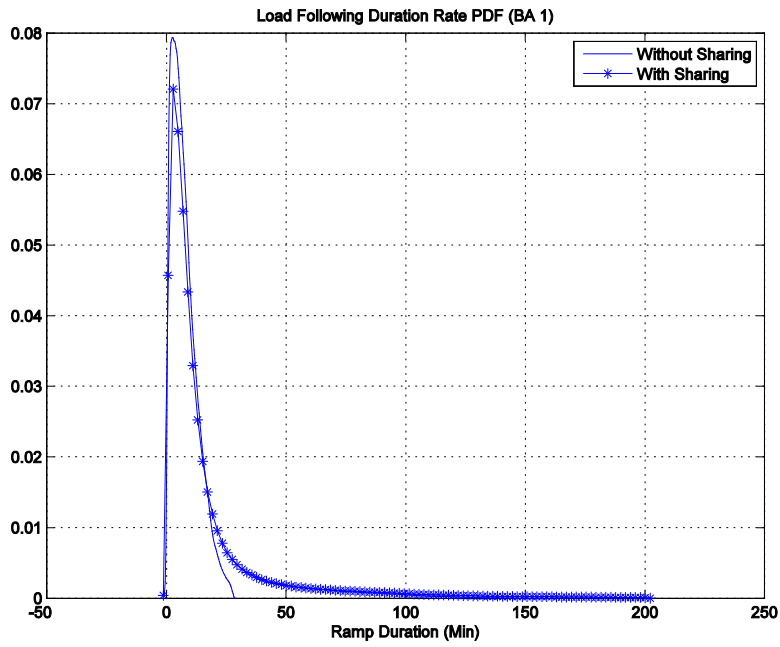


Figure D.11. Load Following Duration PDF for BA 1 (With and Without Sharing)

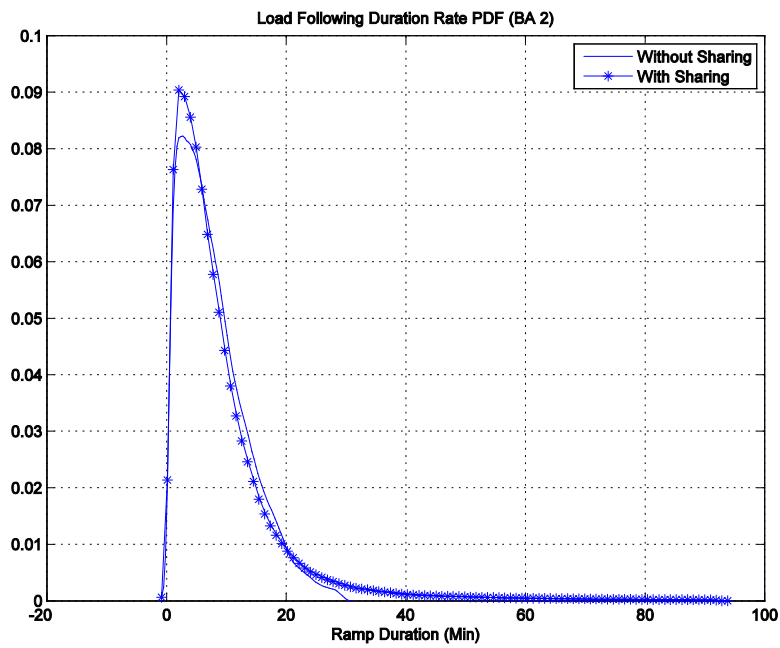


Figure D.12. Load Following Duration PDF for BA 2 (With and Without Sharing)

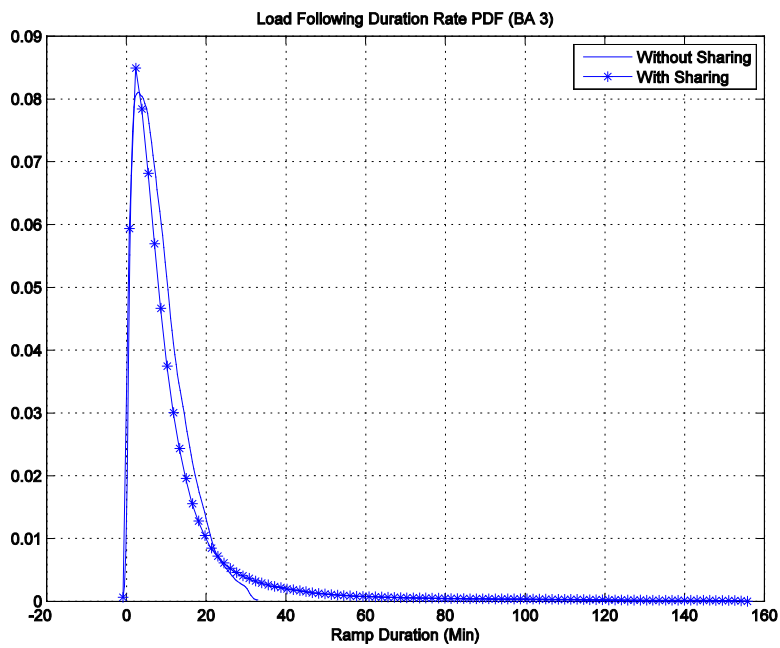


Figure D.13. Load Following Duration PDF for BA 3 (With and Without Sharing)

Appendix E

Incremental Power Flow Model

Appendix E

Incremental Power Flow Model

The PowerWorld Simulator software can be used to create the incremental zonal model of the WECC system. Details of our approach are given below. [Equation Section \(Next\)](#)

E.1 Defining Interfaces Between Zones

The first step is to define interfaces between the zones. In PowerWorld, this can be done easily using the interface auto-insertion function. In the case considered, auto insertion of tie-lines between the zones is be used. There are 242 tie lines in the system.

Table E.1 lists interfaces between the zones. Information regarding operating transfer limits between zones can be found in the WECC 2008 Path Rating Catalog and other WECC official documents [52], [51].

Table E.1. Interfaces between the WECC Zones ^(a)

Number	Name	MW Limit	Comment
1	NEW MEXICO-PSCOLORADO	558	PowerWorld
2	NEW MEXICO-WAPA R.M.	600	PowerWorld
3	EL PASO-NEW MEXICO	3700.2	PowerWorld
4	ARIZONA-NEW MEXICO	940	Path 47
5	ARIZONA-EL PASO	1656.1	PowerWorld
6	ARIZONA-NEVADA	6806.3	PowerWorld
7	ARIZONA-IMPERIALCA	480	PowerWorld
8	ARIZONA-SANDIEGO	2385	PowerWorld
9	ARIZONA-SOCALIF	8357.8	PowerWorld
10	ARIZONA-LADWP	6999.3	PowerWorld
11	ARIZONA-PACE	1412.8	PowerWorld
12	ARIZONA-WAPA R.M.	485	PowerWorld
13	NEVADA-SOCALIF	1436.4	PowerWorld
14	NEVADA-PACE	300	PowerWorld
15	MEXICO-CFE-SANDIEGO	800 / 408	Path 45
16	IMPERIALCA-SANDIEGO	351	PowerWorld
17	IMPERIALCA-SOCALIF	785.6	PowerWorld
18	SANDIEGO-SOCALIF	4000	Path 26
19	LADWP-NEVADA	3962.6	PowerWorld
20	LADWP-SOCALIF	10030	PowerWorld
21	LADWP-NORTHWEST	0	PowerWorld
22	LADWP-SIERRA	402	PowerWorld

Table E.1 (contd). Interfaces between the WECC Zones

Number	Name	MW Limit	Comment
23	LADWP-PACE	1200	PowerWorld
24	PG AND E-SOCALIF	5400	Path 15
25	PG AND E-SIERRA	369	Path 24
26	NORTHWEST-PG AND E	4800 / 3675	Path 66 (COI)
27	NORTHWEST-SIERRA	300	PowerWorld
28	B.C.HYDRO-NORTHWEST	5770.5	PowerWorld
29	B.C.HYDRO-FORTISBC	8405	PowerWorld
30	FORTISBC-NORTHWEST	509.9	PowerWorld
31	ALBERTA-B.C.HYDRO	1321.9	PowerWorld
32	IDAHO-NORTHWEST	2762	PowerWorld
33	IDAHO-SIERRA	1075.6	PowerWorld
34	IDAHO-PACE	4913.1	PowerWorld
35	MONTANA-NORTHWEST	8864.6	PowerWorld
36	MONTANA-WAPA U.M.	1459	PowerWorld
37	MONTANA-PACE	1324.6	PowerWorld
38	SIERRA-SOCALIF	65.8	PowerWorld
39	PACE-SIERRA	358.5	PowerWorld
40	PACE-WAPA R.M.	7641.6	PowerWorld
41	PSCOLORADO-WAPA R.M.	13065.6	PowerWorld
42	WAPA R.M.-WAPA U.M.	390.4	PowerWorld

(a) Table is under construction. Not all transmission limits have been indentified yet. Thus, comment 'Powerworld' means, that the transmission limit was calculated using the PowerWorld simulator

E.2 Switching Off AGC Controls (Transaction Control)¹

Each control area in the model has an automatic generation control (AGC) system. The purpose of an AGC is to ensure that the actual MW output of an area is close to the scheduled MW output of the area. (The AGC system accomplishes this goal by minimizing the Area Control Error (ACE), which is defined as follows:

$$ACE = P_{\text{actual}} - P_{\text{scheduled}} \quad (\text{E.1})$$

here frequency related issues and terms are neglected).

In PowerWorld, $P_{\text{scheduled}}$ for an area is made up of the Zone's MW Transactions and the Zone's Unspecified MW Export. The MW Transaction represents the transfer of power between two areas in the

¹In the PowerWorld Simulator base case, the WECC control area structure corresponds to the zonal structure used in this report and presented in **Figure 3.15**. It does not correspond to the control area structure of the real system; therefore we prefer to use the term 'zone'

power system [45]. In other words, if the “transaction control” is turned on, the AGC system model tries to maintain scheduled power flow between the areas (Figure E.1).

Our purpose is to evaluate wide-area balancing schemes. Because AGC functions will be simulated additionally, therefore PowerWorld AGC system model should be switched off.

System balancing is achieved using the governor power flow model (Figure E.2). Such power flow solution corresponds to primary frequency control in the power system. In the governor power flow model, unbalanced active power distributes among generators in the system according to generator participation factors, which depend on turbine governor characteristics.

PowerWorld needs following procedure for the governor power flow model:

- Case Information → Aggregation → MW transaction
 - Disable all MW transaction control
- Tools → Other → Governor power flow
 - Select “Disable automatic generation control”
 - Select “Use participation factors of individual generators”

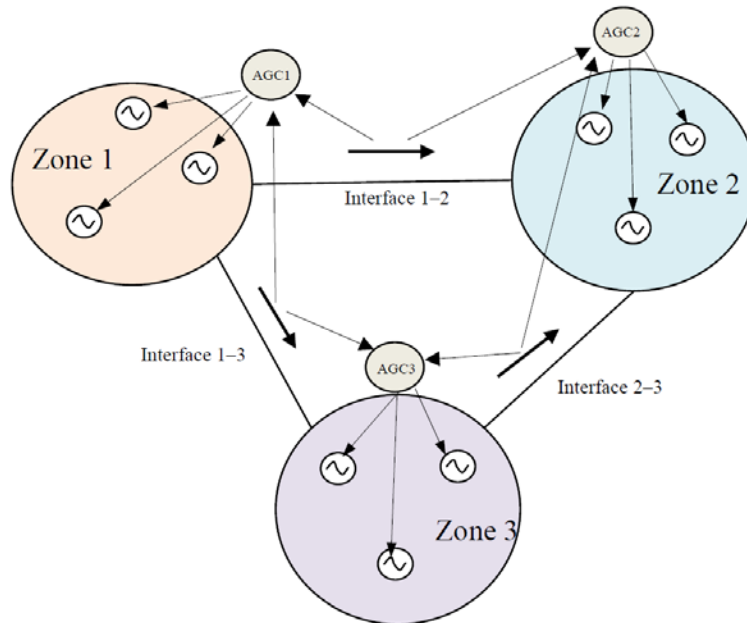


Figure E.1. AGC Power Flow Control

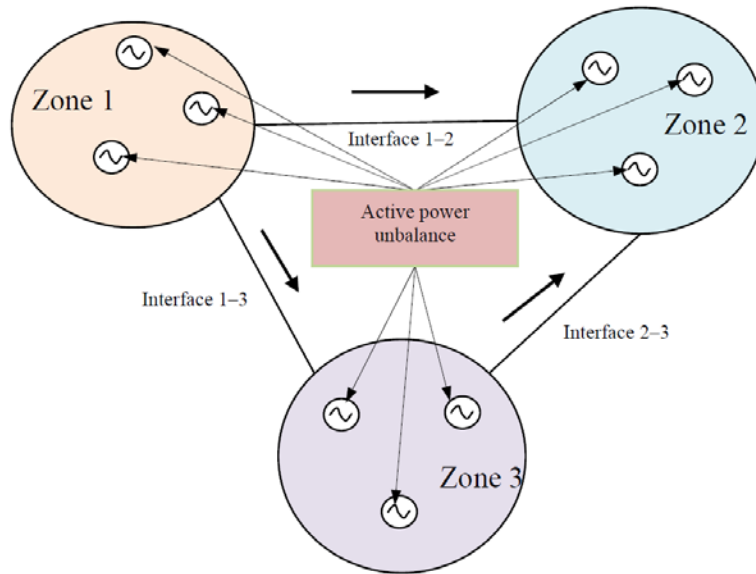


Figure E.2. Governor Power Flow Control

E.3 Create a Super Area

Power transfer distribution factors (PTDFs) can be calculated with PowerWorld Simulator software. PTDFs are the incremental distribution factors associated with power transfers between any two zones. These values provide a linearized approximation of how the flow on the transmission lines and interfaces changes in response to a transaction between the Seller and the Buyer [45].

In the case considered in the study, the Seller is a zone for which the PTDFs will be determined. The rest of the power system is the Buyer. The Buyer can be represented using Super Area (Figure E.3). The PowerWorld Simulator User's Guide gives the following definition of a super area: super areas are groups of zones whose generators are dispatched as a coordinated group [45].

PowerWorld needs following procedure for creating a super area:

- Case Information → Aggregation → Super Area
 - Inserting required zones into super area

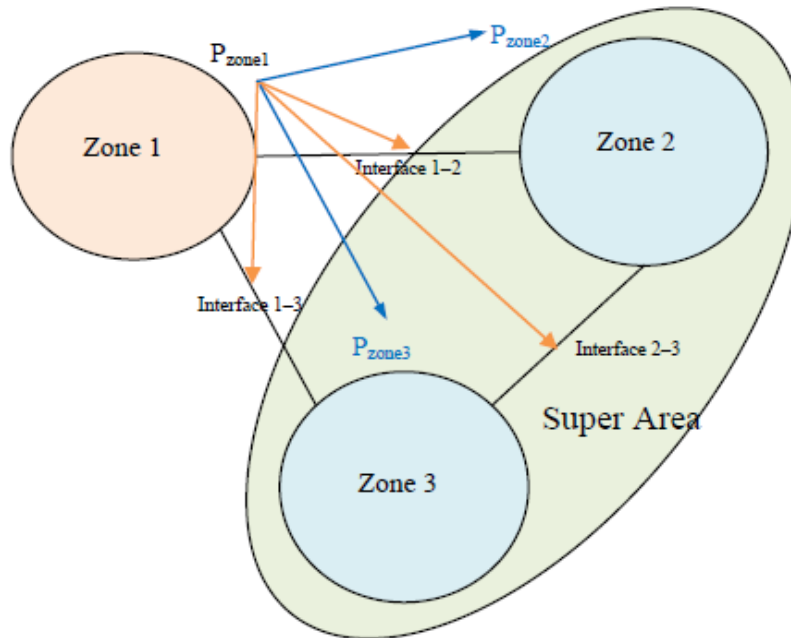


Figure E.3. Sensitivity Analysis

E.3.1 Applying Sensitivity Analysis to Calculate the PTDFs

The next step is finding the PTDFs between the studied zone and the super area. PowerWorld needs following procedure to find PTDFs:

- Tools → Sensitivities → Power Transfer Distribution Factors
- Select *Seller Type* = Area, *Seller* = Studied Area's name
 - *Buyer Type* = Super area, *Buyer* = Super area's name
 - Linear calculation method = Linearized AC
 - Then press “*Calculate PTDFs*” button.

PTDFs calculated for the WECC zonal model are presented in Table E.6–Table E.8. Interface PTDFs are shown in Table E.6 and zonal PTDFs are shown in Table E.8 respectively.

For example, if generation in New Mexico zone increases in 200 MW, power flow through interface New Mexico-PS Colorado will change in $200 \cdot 0.05 = 10$ MW, because the interface PTDF of New Mexico zone on New Mexico-PS Colorado interface is equal to 5%. (See Table E.6).

E.3.2 Validation of the Incremental Model

The results obtained using the incremental model require validation with real power flow data to evaluate the accuracy of the incremental model. Power-flow data are calculated in PowerWorld Simulator using contingency analysis.

In PowerWorld it is necessary to follow the sequence given below:

- Tools → Contingency Analysis

- Insert Contingency → Generator
- Specify number of generators in amount of active power variation
- Options → Modeling
- Select Calculation method = Full power flow
- Determine Make Up using = Generators' participation factors

Three contingencies are considered in the Northwest (Table E.2). Table E.3 presents the Northwest zone PTDFs. Variation of the active power of a single generator in the zone (Northwest) reflects not only generation changes in neighboring areas, but also other generators in the zone itself due to effects of the turbine governors. Thus, total variation of active power generation in the zone will be less than the variation of active power generation of a single generator (Table E.2). Therefore, zonal factors are introduced to take account of this difference between the variation of a single generator and total zonal generation the zonal factors is introduced.

For example if the generator RockyR03 changes the active power generation by 300 MW, the zonal total generation will be increased by only 246 MW. The zonal factor can be found as $(300-246)/300 \approx 18\%$

Table E.2. List of Contingencies

Gen Number	Gen Name	Gen Variation	Zone Variation	Zonal factor
40293	COULEE20	+100 MW	+82	18%
43047	BOARD F	- 300 MW	-246	18%
46843	ROCKYR03	+300 MW	+246	18%

Table E.3. Northwest Zonal PTDF Data

Zone Number	Zone Name	Zonal generation, MW	PTDF, %
10	NEW MEXICO	2444.72	-2.08
11	EL PASO	580.91	-0.56
14	ARIZONA	26561.08	-18.11
18	NEVADA	5057.44	-3.99
20	MEXICO-CFE	2011.43	-1.45
21	IMPERIALCA	904.35	-0.63
22	SANDIEGO	3038.79	-2.09
24	SOCALIF	14869.25	-11.99
26	LADWP	4989.62	-3.88
30	PG AND E	24707.45	-6.39
40	NORTHWEST	29203.36	100
50	B.C.HYDRO	10886.77	-7.11
52	FORTISBC	761.36	-0.73
54	ALBERTA	8436.05	-8.85
60	IDAHO	4100.24	-2.76
62	MONTANA	3163.99	-1.97
63	WAPA U.M.	47.26	-0.03
64	SIERRA	1287.42	-0.92
65	PACE	7296.55	-5.1
70	PSCOLORADO	6406.39	-5.65
73	WAPA R.M.	5832.46	-4.04

The following equation is used to calculate active power generation in zone i , if generation in the Northwest zone changes by $\Delta P_{NorthWest}$

$$P_{zone,i} = P_{zone,i}^{base\ case} + \Delta P_{NorthWest} \cdot (1 - k_{NorthWest}) \cdot PTDF_{NorthWest}^i,$$

where $k_{NorthWest}$ is the Northwest zonal factor, $P_{zone,i}^{base\ case}$ is generation in zone i in the base case, and $PTDF_{NorthWest}^i$ is the zonal PTDF.

Power flow through interface $i - j$ can be calculated as:

$$P_{i-j} = P_{i-j}^{base\ case} + \Delta P_{NorthWest} \cdot (1 - k_{NorthWest}) \cdot PTDF_{NorthWest}^{i-j},$$

where $P_{i-j}^{base\ case}$ is the interface $i - j$ power flow in the base case and $PTDF_{NorthWest}^{i-j}$ is the interface PTDF.

The zonal active power generation and the interface power flows calculated using the full system model, estimated using the incremental model, and the estimation errors are given in Table E.4 and Table E.5.

For example for contingency 1 (Coulee20 generation changes in 100 MW), total zonal generation in New Mexico can be calculated as:

$$\begin{aligned} P_{NewMexico} &= P_{NewMexico}^{base\ case} + \Delta P_{NorthWest} \cdot (1 - k_{NorthWest}) \cdot PTDF_{NorthWest}^{NewMexico} = \\ &= 2444.72 + 100 \cdot (1 - 0.18) \cdot (-0.0208) = 2443.0144 \end{aligned}$$

where $P_{NewMexico}^{base\ case} = 2444.72$ can be found in Table E.3 and $PTDF_{NorthWest}^{NewMexico} = -2.08\%$ can be found in Table E.8.

Power flow in the interface NORTHWEST-PG AND E can be calculated as:

$$\begin{aligned} P_{Northwest-PGandE} &= P_{Northwest-PGandE}^{base\ case} + \Delta P_{NorthWest} \cdot (1 - k_{NorthWest}) \cdot PTDF_{NorthWest}^{Northwest-PGandE} = \\ &= 3948 + 100 \cdot (1 - 0.18) \cdot 0.487 = 3987.934 \end{aligned}$$

where $P_{Northwest-PGandE}^{base\ case} = 3948$ and $PTDF_{NorthWest}^{Northwest-PGandE} = 48.7\%$ can be found in Table E.6.

It can be seen from Table E.4 and Table E.5 that the estimation accuracy of the incremental model is sufficiently high to be potentially used in wind integration studies.

Table E.4. Zonal Generation Validation

Zone	Contingency 1			Contingency 2			Contingency 3		
	Full model, MW	Incremental model, MW	Error, MW	Full model, MW	Incremental model, MW	Error, MW	Full model, MW	Incremental model, MW	Error, MW
NEW MEXICO	2443.25	2443.0144	0.2356	2447.24	2449.92	-2.68	2440.28	2439.52	0.76
EL PASO	580.51	580.4508	0.0592	582.08	582.31	-0.23	579.73	579.51	0.22
ARIZONA	26547.14	26546.2298	0.9102	26590.42	26606.36	-15.935	26519.09	26515.81	3.285
NEVADA	5054.37	5054.1682	0.2018	5069.36	5067.415	1.945	5048.19	5047.465	0.725
MEXICO-CFE	2010.31	2010.241	0.069	2015.76	2015.055	0.705	2008.06	2007.805	0.255
IMPERIALCA	903.86	903.8334	0.0266	906.02	905.925	0.095	902.88	902.775	0.105
SANDIEGO	3037.21	3037.0762	0.1338	3043.92	3044.015	-0.095	3034.01	3033.565	0.445
SOCALIF	14860.07	14859.4182	0.6518	14895.82	14899.23	-3.405	14841.56	14839.28	2.285
LADWP	4986.82	4986.4384	0.3816	4997.24	4999.32	-2.08	4981.19	4979.92	1.27
PG AND E	24692.43	24702.2102	-9.7802	24758.08	24723.43	34.655	24678.15	24691.48	-13.325
NORTHWEST	29289.13	29285.36	3.77	28953.79	28953.36	0.43	29460	29453.36	6.64
B.C.HYDRO	10881.5	10880.9398	0.5602	10906.82	10904.55	2.275	10871.17	10869	2.175
FORTISBC	760.81	760.7614	0.0486	763.53	763.185	0.345	759.77	759.535	0.235
ALBERTA	8429.66	8428.793	0.867	8459.74	8458.175	1.565	8418.4	8413.925	4.475
IDAHO	4098.11	4097.9768	0.1332	4108.34	4107.14	1.2	4093.84	4093.34	0.5
MONTANA	3162.47	3162.3746	0.0954	3168.77	3168.915	-0.145	3159.43	3159.065	0.365
WAPA U.M.	47.24	47.2354	0.0046	47.34	47.335	0.005	47.2	47.185	0.015
SIERRA	1286.71	1286.6656	0.0444	1290.18	1289.72	0.46	1285.28	1285.12	0.16
PACE	7292.76	7292.368	0.392	7305.41	7309.3	-3.89	7285.13	7283.8	1.33
PSCOLORADO	6402.04	6401.757	0.283	6417.26	6420.515	-3.255	6393.65	6392.265	1.385
WAPA R.M.	5829.36	5829.1472	0.2128	5842.71	5842.56	0.15	5823.1	5822.36	0.74

Table E.5. Interface Power Flow Validation

Interface Name	PTD F	Contingency 1			Contingency 2			Contingency 3		
		Full model, MW	Incremental model, MW	Error, MW	Full model, MW	Incremental model, MW	Error, MW	Full model, MW	Incremental model, MW	Error, MW
NEW MEXICO-PSCOLORADO	0	-91.1	-91.1	0	-91.2	-91.1	-0.1	-91.1	-91.1	0
NEW MEXICO-WAPA R.M.	-0.2	-88.9	-88.564	-0.336	-88.3	-87.9	-0.4	-89.5	-88.9	-0.6
EL PASO-NEW MEXICO	0.1	-292.5	-292.418	-0.082	-292.5	-292.75	0.25	-292.4	-292.25	-0.15
ARIZONA-NEW MEXICO	1.9	113.3	113.958	-0.658	109.7	107.65	2.05	115.9	117.15	-1.25
ARIZONA-EL PASO	0.6	365.9	365.992	-0.092	364.2	364	0.2	366.8	367	-0.2
ARIZONA-NEVADA	0.7	440.5	440.574	-0.074	437.5	438.25	-0.75	443.6	441.75	1.85
ARIZONA-IMPERIALCA	-0.2	250.5	250.436	0.064	250.7	251.1	-0.4	250.2	250.1	0.1
ARIZONA-SANDIEGO	-0.3	979.1	978.854	0.246	978.1	979.85	-1.75	978.4	978.35	0.05
ARIZONA-SOCALIF	-8	3369.9	3368.54	1.36	3387.5	3395.1	-7.6	3356.7	3355.1	1.6
ARIZONA-LADWP	-9.2	2663.3	2661.956	1.344	2685.6	2692.5	-6.9	2648	2646.5	1.5
ARIZONA-PACE	-3.6	-77	-76.952	-0.048	-65.4	-65	-0.4	-82.7	-83	0.3
ARIZONA-WAPA R.M.	0	-64.6	-64.4	-0.2	-64.6	-64.4	-0.2	-64.6	-64.4	-0.2
NEVADA-SOCALIF	-0.9	67.9	67.762	0.138	70.7	70.75	-0.05	65.8	66.25	-0.45
NEVADA-PACE	-1.4	196.4	196.552	-0.152	201.7	201.2	0.5	193.7	194.2	-0.5
MEXICO-CFE-SANDIEGO	-1.4	-154.9	-155.048	0.148	-149.6	-150.4	0.8	-157.2	-157.4	0.2
IMPERIALCA-SANDIEGO	0.1	-87.1	-87.118	0.018	-87.4	-87.45	0.05	-87	-86.95	-0.05
IMPERIALCA-SOCALIF	-0.8	191.9	191.744	0.156	194.2	194.4	-0.2	190.5	190.4	0.1

Table E.5 (contd). Interface Power Flow Validation

Interface Name	PTD F	Contingency 1			Contingency 2			Contingency 3		
		Full model, MW	Incremental model, MW	Error, MW	Full model, MW	Incremental model, MW	Error, MW	Full model, MW	Incremental model, MW	Error, MW
SANDIEGO-SOCALIF	-3.6	-963.9	-964.352	0.452	-953.4	-952.4	-1	-969.8	-970.4	0.6
LADWP-NEVADA	0.9	388.7	388.938	-0.238	385.2	385.95	-0.75	387	390.45	-3.45
LADWP-SOCALIF	-12.6	3428.2	3426.168	2.032	3462.7	3468	-5.3	3411	3405	6
LADWP-NORTHWEST	0	-2979.7	-2979.7	0	-2979.7	-2979.7	0	-2979.7	-2979.7	0
LADWP-SIERRA	-0.9	96.7	96.562	0.138	98.8	99.55	-0.75	95.6	95.05	0.55
LADWP-PACE	-0.1	-199.8	-199.782	-0.018	-201.1	-199.45	-1.65	-200.4	-199.95	-0.45
PG AND E-SOCALIF	37.9	2312	2317.078	-5.078	2209.3	2191.25	18.05	2370.4	2380.75	-10.35
PG AND E-SIERRA	0.2	11.8	12.064	-0.264	11.9	11.4	0.5	12.6	12.4	0.2
NORTHWEST-PG AND E	48.7	3992	3987.934	4.066	3808.9	3826.25	-17.35	4073.7	4069.75	3.95
NORTHWEST-SIERRA	0.8	270.4	270.556	-0.156	268.3	267.9	0.4	269.2	271.9	-2.7
B.C.HYDRO- NORTHWEST	-15.1	2300.1	2298.118	1.982	2351.6	2348.25	3.35	2279.5	2272.75	6.75
B.C.HYDRO- FORTISBC	0.6	-124.9	-124.908	0.008	-127.4	-126.9	-0.5	-124	-123.9	-0.1
FORTISBC- NORTHWEST	0	0	0	0	0	0	0	0	0	0
ALBERTA- B.C.HYDRO	-8.4	-400.9	-402.088	1.188	-372.9	-374.2	1.3	-411.8	-416.2	4.4
IDAHO-NORTHWEST	-16.9	-388.8	-390.058	1.258	-336.6	-333.95	-2.65	-417.5	-418.45	0.95
IDAHO-SIERRA	1.9	211.9	211.758	0.142	205.4	205.45	-0.05	216.2	214.95	1.25
IDAHO-PACE	12	800.1	801.34	-1.24	765	761.5	3.5	819.2	821.5	-2.3
MONTANA- NORTHWEST	-11	977.5	978.18	-0.68	1007.9	1014.7	-6.8	958.8	959.7	-0.9
MONTANA-WAPA U.M.	2	91.1	91.04	0.06	85.7	84.4	1.3	94.6	94.4	0.2
MONTANA-PACE	7	277.4	276.94	0.46	259.3	253.7	5.6	289	288.7	0.3
SIERRA-SOCALIF	0.1	-1.7	-1.718	0.018	-2.2	-2.05	-0.15	-1.5	-1.55	0.05
PACE-SIERRA	-0.9	82.6	82.562	0.038	84.8	85.55	-0.75	81.5	81.05	0.45
PACE-WAPA R.M.	9.2	-8.8	-8.356	-0.444	-35.6	-38.9	3.3	5.6	7.1	-1.5
PSCOLORADO-WAPA R.M.	-5.8	-1251.9	-1252.356	0.456	-1236.4	-1233.1	-3.3	-1260.9	-1262.1	1.2
WAPA R.M.-WAPA U.M.	-1.9	-176.1	-175.958	-0.142	-170.9	-169.65	-1.25	-179.4	-179.15	-0.25

Table E.6. Interface PTFDs,(%)

Name	NEW MEXICO	EL PASO	ARIZONA	NEVADA	MEXICO-CFE	IMPERIALCA	SAN DIEGO	SOCALIF	LADWP	PG AND E	NORTHWEST
NEW MEXICO-PSCOLORADO	5	2.2	1.4	1	1	1	1	0.9	0.5	0.5	0
NEW MEXICO-WAPA R.M.	7.8	8.1	6.3	4.3	4.4	4.3	4.3	4.1	1.7	2.1	-0.2
EL PASO-NEW MEXICO	-19.2	30.8	1.4	0.5	0.8	0.7	0.7	0.6	0.2	0.3	0.1
ARIZONA-NEW MEXICO	-69.9	-25.1	8.3	6.6	6.4	6.3	6.3	6.4	3.9	4.4	1.9
ARIZONA-EL PASO	-19.4	-72.2	2	1	1.3	1.2	1.2	1.1	0.7	0.9	0.6
ARIZONA-NEVADA	1.9	3	5.7	-44.5	4	4.6	3.8	3	0.8	1.7	0.7
ARIZONA-IMPERIALCA	0.7	0.8	2.1	0.7	-3.3	-21.6	-2.6	-0.7	-0.1	-0.3	-0.2
ARIZONA-SANDIEGO	6.7	8.2	9.6	3	-44	-7.1	-35.5	-5.3	-0.2	-1.2	-0.3
ARIZONA-SOCALIF	25.4	29	29.7	-2	6.1	-12.3	1.2	-15.8	-7.3	-11.8	-8
ARIZONA-LADWP	19.5	24	29.2	13.3	8	7.7	4	-11.2	-11	-12.5	-9.2
ARIZONA-PACE	11.8	12	10	5.1	6.3	5.9	6	4.9	-3	0.4	-3.6
ARIZONA-WAPA R.M.	2.4	3.1	3.2	2.2	2.3	2.2	2.3	2.1	1	1.2	0
NEVADA-SOCALIF	0.6	0.8	1.1	12.2	-0.2	0	-0.4	-1.7	-0.6	-1.4	-0.9
NEVADA-PACE	0.6	1.6	3.8	6.7	3.9	4	4	4.3	-0.8	1.4	-1.4
MEXICO-CFE-SANDIEGO	-1.3	-1.3	-1.5	-1.3	99	-1.3	-1.2	-1.3	-1.2	-1.4	-1.4
IMPERIALCA-SANDIEGO	-0.1	-0.1	0.3	0.3	-7.7	18.9	-5.7	-0.1	0.1	0.1	0.1
IMPERIALCA-SOCALIF	0.1	0.3	0.8	-0.2	3.9	56.7	2.6	-1	-0.7	-0.9	-0.8
SANDIEGO-SOCALIF	3.2	4.7	6	0.1	46.1	8.7	57.6	-8.4	-3.1	-4.5	-3.6
LADWP-NEVADA	2.5	2.8	3.2	-36.4	3.1	2.9	3.2	3.3	1.3	2.3	0.9
LADWP-SOCALIF	13.8	17.7	22.1	46.8	2.3	2.3	-1.6	-16.6	61.3	-17.1	-12.6
LADWP-NORTHWEST	0	0	0	0	0	0	0	0	0	0	0
LADWP-SIERRA	1	1	0.6	0.3	0.2	0.2	0.2	0	2.4	-0.9	-0.9
LADWP-PACE	-1.8	-1.9	-1.6	-1.3	-1.1	-1.1	-1.1	-0.9	24.9	-0.1	-0.1
PG AND E-SOCALIF	-33.5	-42	-47.2	-46.3	-49.8	-47.9	-51.4	-56.2	-39.6	47.4	37.9
PG AND E-SIERRA	-0.3	-0.3	0.1	0.2	0.3	0.3	0.3	0.5	-0.5	2.1	0.2
NORTHWEST-PG AND E	-14.7	-14.5	-23.5	-22.8	-23.1	-23.4	-23.7	-28.3	-15.3	-40.5	48.7

E.10

Table E.6. (contd) Interface PTDFs,(%)

Name	NEW MEXICO	EL PASO	ARIZONA	NEVADA	MEXICO-CFE	IMPERIALCA	SAN DIEGO	SOCALIF	LADWP	PG AND E	NORTHWEST
NORTHWEST-SIERRA	-0.4	-0.3	-0.1	0	0.1	0.1	0.1	0.2	-0.5	0.7	0.8
B.C.HYDRO-NORTHWEST	-11.3	-12.7	-15	-13.1	-12.8	-12.7	-12.9	-14.1	-13.1	-14.9	-15.1
B.C.HYDRO-FORTISBC	0.4	0.5	0.6	0.5	0.5	0.5	0.5	0.6	0.5	0.6	0.6
FORTISBC-NORTHWEST	0	0	0	0	0	0	0	0	0	0	0
ALBERTA-B.C.HYDRO	-5	-7.1	-8.3	-7.3	-7.1	-7.1	-7.2	-7.8	-7.3	-8.3	-8.4
IDAHO-NORTHWEST	8.1	7.6	4.3	2.2	1.5	1.1	1.2	-0.5	8.4	-8.5	-16.9
IDAHO-SIERRA	-0.6	-0.6	-0.7	-0.6	-0.6	-0.6	-0.6	-0.7	-1.2	-0.6	1.9
IDAHO-PACE	-9.9	-9.2	-5.9	-3.6	-2.9	-2.5	-2.6	-0.9	-9.2	7	12
MONTANA-NORTHWEST	3	2.6	1.2	0.4	0.2	0.1	0.1	-0.5	1.4	-3.2	-11
MONTANA-WAPA U.M.	-1.1	-0.9	-0.6	-0.3	-0.3	-0.3	-0.3	-0.1	-0.5	0.5	2
MONTANA-PACE	-3.7	-3.3	-2.4	-1.6	-1.5	-1.4	-1.4	-1	-2.4	0.9	7
SIERRA-SOCALIF	-0.1	-0.1	-0.1	-0.2	-0.2	-0.2	-0.2	-0.4	-0.1	0	0.1
PACE-SIERRA	1.1	1.1	0.9	0.7	0.6	0.5	0.5	0.3	0.7	-0.7	-0.9
PACE-WAPA R.M.	-8.4	-5.7	-1.6	0.9	0.3	0.6	0.6	1.8	5.7	5.8	9.2
PSCOLORADO-WAPA R.M.	1.5	-2.4	-4.1	-3.9	-3.8	-3.8	-3.8	-4.4	-4.5	-5.2	-5.8
WAPA R.M.-WAPA U.M.	1.1	0.9	0.6	0.3	0.3	0.3	0.3	0.2	0.5	-0.4	-1.9

Table E.7. Interface PTDFs,(%)

Name	BCHYDRO	FORTISBC	ALBERTA	IDAHO	MONTANA	WAPA U.M.	SIERRA	PACE	PSCOLORADO	WAPA R.M.
NEW MEXICO-PSCOLORADO	0.1	0	0	-0.5	-0.3	-0.3	-0.1	-0.9	-7	-4.4
NEW MEXICO-WAPA R.M.	0	0	-0.1	-3	-1.5	-1.3	-1.4	-5.5	-21.9	-18.9
EL PASO-NEW MEXICO	0.1	0.1	0.1	-0.3	0	0	-0.2	-0.7	-1.6	-1.2
ARIZONA-NEW MEXICO	1.9	1.8	1.9	-1.3	0.2	0.3	0.5	-3.6	-25.3	-20
ARIZONA-EL PASO	0.6	0.6	0.6	0.2	0.5	0.4	0.3	-0.2	-1.1	-0.8
ARIZONA-NEVADA	0.8	0.7	0.8	-0.8	0.5	0.4	-1.1	-3.4	-0.6	-0.5
ARIZONA-IMPERIALCA	-0.1	-0.1	-0.1	0	-0.1	-0.1	0	0.3	0.4	0.3
ARIZONA-SANDIEGO	-0.3	-0.3	-0.3	0.9	0	0	0.9	2.6	3.8	3.2
ARIZONA-SOCALIF	-7.5	-7.1	-7.6	-1.8	-5.6	-5.5	-2.2	5.3	11.6	8.6
ARIZONA-LADWP	-8.5	-8	-8.6	-3.3	-6.8	-6.6	-3.6	3.1	7.9	5.4
ARIZONA-PACE	-2.8	-2.7	-2.9	-8.8	-3.5	-3.6	-10.2	-19.3	-4.1	-4.4
ARIZONA-WAPA R.M.	0.1	0.1	0.1	-1.3	-0.6	-0.6	-0.5	-2.5	-11.8	-10.1
NEVADA-SOCALIF	-0.9	-0.8	-0.9	-0.2	-0.7	-0.7	-0.2	0.7	0.4	0.2
NEVADA-PACE	-0.9	-0.9	-1	-5.1	-1.6	-1.7	-5.9	-12.3	-5.4	-4.9
MEXICO-CFE-SANDIEGO	-1.3	-1.2	-1.3	-1.2	-1.2	-1.2	-1.2	-1.3	-1.3	-1.3
IMPERIALCA-SANDIEGO	0.1	0.1	0.1	0.1	0.1	0.1	0.1	0.1	0	0
IMPERIALCA-SOCALIF	-0.7	-0.7	-0.7	-0.5	-0.7	-0.6	-0.5	-0.4	-0.2	-0.3
SANDIEGO-SOCALIF	-3.3	-3.1	-3.4	-2	-2.8	-2.8	-2	-0.5	0.6	0
LADWP-NEVADA	1	0.9	1	-1.1	0.6	0.5	-1.6	-4.7	-0.9	-0.7
LADWP-SOCALIF	-11.7	-11	-11.8	-4.6	-9.5	-9.3	-4.3	5.1	5.8	3.3
LADWP-NORTHWEST	0	0	0	0	0	0	0	0	0	0
LADWP-SIERRA	-0.8	-0.8	-0.8	-0.1	-0.5	-0.5	-13	3.3	1.9	1.6
LADWP-PACE	-0.1	-0.1	-0.1	-0.8	-0.4	-0.4	12.1	-4.3	-2.8	-2.5
PG AND E-SOCALIF	34.8	32.9	35.1	19.4	29.5	29	18.2	0.1	-7.6	-1.4
PG AND E-SIERRA	0.3	0.3	0.3	-1.8	0	0	-21.7	-2.2	-1.3	-1.1
NORTHWEST-PG AND E	30.7	27.6	31.5	32.5	28.9	31.9	23.7	13.8	8.5	7
NORTHWEST-SIERRA	0.7	0.6	0.7	-1.1	0.4	0.4	-16	-1.7	-1	-0.8

E.12

Table E.7. (contd) Interface PTDFs,(%)

Name	BCHYDRO	FORTISBC	ALBERTA	IDAHO	MONTANA	WAPA U.M.	SIERRA	PACE	PSCOLORADO	WAPA R.M.
B.C.HYDRO-NORTHWEST	81.9	77.1	84.8	-13	-13.3	-13.1	-12.8	-13.3	-13.4	-13.2
B.C.HYDRO-FORTISBC	0.5	-97	1.5	0.5	0.6	0.6	0.5	0.6	0.6	0.6
FORTISBC-NORTHWEST	0	0	0	0	0	0	0	0	0	0
ALBERTA-B.C.HYDRO	-7.5	-7.1	94.7	-7.2	-7.2	-7.1	-7.1	-7.4	-7.4	-7.3
IDAHO-NORTHWEST	-13.9	-12.9	-14	54.1	-7.9	-7.8	30.6	30.4	20.9	18.1
IDAHO-SIERRA	1.5	1.4	1.5	4.8	1.6	1.8	-40.3	-0.1	0.5	0.6
IDAHO-PACE	9.8	9	9.8	38	3.3	3.2	9.2	-32.9	-25.1	-22.3
MONTANA-NORTHWEST	-9.8	-9.7	-10.5	4.7	74.4	76.7	1.5	9.5	15.3	16.6
MONTANA-WAPA U.M.	1.8	1.8	1.9	-0.7	6.2	-94.7	-0.2	-2.4	-4.7	-5.3
MONTANA-PACE	6.2	6.2	6.7	-5.1	15.1	17.1	-2.6	-8.6	-12.6	-13.4
SIERRA-SOCALIF	0.1	0.1	0.1	0.3	0.1	0.1	1.5	0.3	0.2	0.1
PACE-SIERRA	-0.8	-0.7	-0.8	-0.5	-0.6	-0.6	-11.1	2.3	1.2	0.9
PACE-WAPA R.M.	7.9	7.5	8.1	15.2	6.9	8.6	11.2	21.2	-58.1	-55.4
PSCOLORADO-WAPA R.M.	-5.2	-4.9	-5.3	-5.7	-5.4	-5.3	-5.2	-6.3	94.6	-9.1
WAPA R.M.-WAPA U.M.	-1.7	-1.7	-1.8	0.7	-5.9	-3.6	0.3	2.3	4.6	5.1

Table E.8. Zone PTDFs, (%)

Name	NEW MEXICO	EL PASO	ARIZONA	NEVADA	MEXICO-CFE	IMPERIALCA	SANDIEGO	SOCALIF	LADWP	PG AND E	NORTHWEST
NEW MEXICO	100	-1.75	-2.06	-1.81	-1.77	-1.75	-1.78	-1.94	-1.8	-2.06	-2.08
EL PASO	-0.36	100	-0.56	-0.49	-0.48	-0.48	-0.48	-0.53	-0.49	-0.56	-0.56
ARIZONA	-16.59	-15.31	100	-15.76	-15.42	-15.32	-15.51	-16.94	-15.75	-17.96	-18.11
NEVADA	-3.16	-3.37	-3.96	100	-3.4	-3.38	-3.42	-3.73	-3.47	-3.96	-3.99
MEXICO-CFE	-1.26	-1.23	-1.44	-1.26	100	-1.23	-1.24	-1.36	-1.26	-1.44	-1.45
IMPERIALCA	-0.56	-0.54	-0.63	-0.55	-0.54	100	-0.54	-0.59	-0.55	-0.63	-0.63
SANDIEGO	-1.9	-1.76	-2.07	-1.82	-1.78	-1.76	100	-1.95	-1.81	-2.07	-2.09
SOCALIF	-9.29	-10.13	-11.89	-10.43	-10.21	-10.14	-10.26	100	-10.42	-11.89	-11.99
LADWP	-3.04	-3.28	-3.85	-3.37	-3.3	-3.28	-3.32	-3.63	100	-3.84	-3.88
PG AND E	-20.5	-29.19	-25.71	-25.28	-28.52	-26.27	-29.58	-29.93	-26.27	100	-6.39
NORTHWEST	-18.31	-15.97	-18.75	-16.45	-16.09	-15.98	-16.18	-17.68	-16.43	-18.74	100
B.C.HYDRO	-6.8	-6.01	-7.05	-6.19	-6.05	-6.01	-6.09	-6.65	-6.18	-7.05	-7.11
FORTISBC	-0.48	-0.61	-0.72	-0.63	-0.62	-0.61	-0.62	-0.68	-0.63	-0.72	-0.73
ALBERTA	-5.26	-7.48	-8.78	-7.7	-7.53	-7.48	-7.57	-8.28	-7.69	-8.77	-8.85
IDAHO	-2.56	-2.33	-2.74	-2.4	-2.35	-2.33	-2.36	-2.58	-2.4	-2.74	-2.76
MONTANA	-1.98	-1.67	-1.96	-1.72	-1.68	-1.67	-1.69	-1.85	-1.72	-1.96	-1.97
WAPA U.M.	-0.03	-0.02	-0.03	-0.02	-0.02	-0.02	-0.02	-0.02	-0.02	-0.03	-0.03
SIERRA	-0.8	-0.78	-0.92	-0.8	-0.79	-0.78	-0.79	-0.86	-0.8	-0.92	-0.92
PACE	-4.56	-4.31	-5.06	-4.44	-4.34	-4.31	-4.37	-4.77	-4.44	-5.06	-5.1
PSCOLORADO	-4	-4.77	-5.61	-4.92	-4.81	-4.78	-4.84	-5.28	-4.91	-5.6	-5.65
WAPA R.M.	-3.64	-3.41	-4	-3.51	-3.44	-3.41	-3.45	-3.77	-3.51	-4	-4.04

E.14

Table E.9. Zone PTDFs, (%)

Name	BCHYDRO	FORTISBC	ALBERTA	IDAHO	MONTANA	WAPA U.M.	SIERRA	PACE	PSCOLORADO	WAPA R.M.
NEW MEXICO	-1.86	-1.76	-1.89	-1.79	-1.77	-1.75	-1.76	-1.82	-1.83	-1.81
EL PASO	-0.5	-0.48	-0.51	-0.48	-0.48	-0.47	-0.48	-0.49	-0.5	-0.49
ARIZONA	-16.2	-15.33	-16.46	-15.6	-15.49	-15.24	-15.35	-15.92	-15.99	-15.77
NEVADA	-3.57	-3.38	-3.63	-3.44	-3.41	-3.36	-3.38	-3.51	-3.52	-3.47
MEXICO-CFE	-1.3	-1.23	-1.32	-1.25	-1.24	-1.22	-1.23	-1.28	-1.28	-1.26
IMPERIALCA	-0.57	-0.54	-0.58	-0.55	-0.54	-0.53	-0.54	-0.56	-0.56	-0.55
SANDIEGO	-1.87	-1.77	-1.9	-1.8	-1.78	-1.76	-1.77	-1.83	-1.84	-1.82
SOCALIF	-10.72	-10.14	-10.89	-10.32	-10.25	-10.08	-10.16	-10.53	-10.59	-10.44
LADWP	-3.47	-3.28	-3.52	-3.34	-3.32	-3.26	-3.29	-3.41	-3.42	-3.37
PG AND E	7.05	7.97	6.69	-12.25	3.15	-0.19	-25.85	-14.87	-16.8	-8.99
NORTHWEST	-16.91	-15.99	-17.17	-16.27	-16.16	-15.9	-16.02	-16.61	-16.69	-16.46
B.C.HYDRO	100	-6.02	-6.46	-6.12	-6.08	-5.98	-6.03	-6.25	-6.28	-6.19
FORTISBC	-0.65	100	-0.66	-0.62	-0.62	-0.61	-0.62	-0.64	-0.64	-0.63
ALBERTA	-7.91	-7.49	100	-7.62	-7.57	-7.44	-7.5	-7.77	-7.81	-7.7
IDAHO	-2.47	-2.34	-2.51	100	-2.36	-2.32	-2.34	-2.43	-2.44	-2.4
MONTANA	-1.77	-1.67	-1.79	-1.7	100	-1.66	-1.67	-1.73	-1.74	-1.72
WAPA U.M.	-0.02	-0.02	-0.02	-0.02	-0.02	100	-0.02	-0.02	-0.02	-0.02
SIERRA	-0.83	-0.78	-0.84	-0.8	-0.79	-0.78	100	-0.81	-0.82	-0.8
PACE	-4.56	-4.32	-4.64	-4.39	-4.36	-4.29	-4.32	100	-4.51	-4.44
PSCOLORADO	-5.05	-4.78	-5.13	-4.87	-4.83	-4.75	-4.79	-4.97	100	-4.92
WAPA R.M.	-3.61	-3.41	-3.67	-3.47	-3.45	-3.39	-3.42	-3.55	-3.56	100

E.15

Appendix F

Alternative Representation of the WECC Automatic Time Error Correction Term

Appendix F

Alternative Representation of the WECC Automatic Time Error Correction Term

F.1 Parameters and Abbreviations Used

- ACE_n - Area n Control Error computed at each AGC cycle, MW.
- ACE_n^{NERC} - Area n Control Error as defined by NERC, MW.
- ACE_n^{WECC} - Area n Control Error as defined by WECC (with the ATE correction term added), MW.
- ATE_n - Automatic Time Error Correction, MW.
- B_n - Area n frequency bias setting, MW/0.1 Hz.
- B_s - Interconnection frequency bias setting, MW/0.1Hz.
- Δt - AGC cycle, Hrs; e.g., 0.00111111 Hrs (= 4 sec).
- τ - ATE correction coefficient.
- ε - Accumulated time error, seconds.
- ε_n - Accumulate time error associated with area n, seconds.
- F_a - Actual interconnection frequency at each AGC cycle, Hz.
- F_s - Scheduled interconnection frequency at each AGC cycle, Hz.
- H - Correction Period, Hrs.
- I_{an} - Actual area n net interchange at each AGC cycle, MW.
- I_n - Area n accumulated inadvertent interchange over period $P = [t - T, t)$, MWh.
- I_{mn} - Area n accumulated primary inadvertent interchange over period $P = [t - T, t)$, MWh.
- I_{sn} - Scheduled area n net interchange at each AGC cycle, MW.
- n - Analyzed control area.
- N - Number of control area in the interconnection.
- P - Interval P where the time error is accumulated, Hrs.
- t - Current moment of time.
- T - Duration of the interval P where the time error is accumulated, Hrs.
- $Y_n = B_n / B_s$ - Area n bias ratio.

F.2 Derivation of Expression for the Accumulated Time Error

The accumulated time error is calculated based on the integral deviation of the actual interconnection frequency from its scheduled value.

The instantaneous deviation of the interconnection frequency is equal to

$$\Delta F = F_a - F_s \quad (F.1)$$

This deviation constitutes the time error rate

$$R_\varepsilon = \underbrace{(F_a - F_s)}_{[Hz]=[1/sec]} \cdot \frac{1}{\underbrace{60}_{[Seconds\ of\ Deviation]}} \quad [\text{Seconds of deviation/sec}] \quad (F.2)$$

or, in different physical units,

$$R_{\varepsilon} = \underbrace{3600}_{[\text{sec/hr}]} \underbrace{(F_a - F_s)}_{[Hz]=[1/\text{sec}]} \cdot \underbrace{\frac{1}{60}}_{\substack{\text{Seconds of} \\ \text{Deviation}}} = 60(F_a - F_s) \quad [\text{Seconds of deviation/Hour}] \quad (\text{F.3})$$

By integrating the time error rate over any T-hour interval, the time error accumulated over period P:

$$\varepsilon = \int_P \underbrace{R_{\varepsilon}}_{\substack{\text{sec/hr} \\ \text{hrs}}} dt = 60 \int_P (F_a - F_s) dt \quad [\text{Seconds of deviation}] \quad (\text{F.4})$$

This is exactly the expression for the accumulated time error used by Cohn in [11]. Parameter T is an arbitrary parameter, which is not required to be, for example, equal to one hour, so the length of the accumulation interval does not change expression (F.4). The only condition of using (F.4) is to measure time in hours.

F.3 “Smooth and Continuous” Automatic Time Error Correction

The objective of this Section is to develop a simpler ‘smooth and continuous’ ATE correction algorithm (without hourly stepwise changes of the automatic time error correction requirement) that would also respect the CPS2 limits by adjusting the ATE requirements on each AGC cycle.

In this analysis, we neglect all scheduling and measurement errors and their corresponding correction term used in the NERC ACE equation as well as bilateral interchange payback and automatic time error correction (WECC) terms. We also neglect the ATE term added to the ACE equation in the past moments of time. A more detailed analysis is provided in the next Section.

This analysis is based on the logic behind the Cohn’s inadvertent interchange and time error decomposition approach [11], [10].

Area n control error:

$$\underbrace{ACE_n}_{\substack{\text{Area } n \text{ Control} \\ \text{Error}}} = \underbrace{(I_{an} - I_{sn})}_{\substack{\text{Area } n \text{ Net Interchange} \\ \text{Error}}} - 10 \underbrace{B_n}_{\substack{\text{Interconnection} \\ \text{Frequency Error}}} \underbrace{(F_a - F_s)}_{\substack{\text{Interconnection} \\ \text{Frequency Error}}} \quad (\text{F.5})$$

Accumulated ACE over period $P = [t - T, t)$, t – current time:

$$\underbrace{\int_{t-T}^t ACE_n dt}_{\substack{\text{Accumulated ACE over } P}} = \underbrace{\int_P ACE_n dt}_P = T \cdot \underbrace{avg_T ACE_n}_{\substack{\text{Average ACE}}} = \underbrace{\int_P (I_{an} - I_{sn}) dt}_{=I_n} - 10 \underbrace{B_n}_{\substack{\text{Interconnection} \\ \text{Frequency Error}}} \underbrace{\int_P (F_a - F_s) dt}_{= \varepsilon / 60} = I_n - \frac{B_n}{6} \varepsilon \quad (\text{F.6})$$

Instantaneous interconnection frequency error is expressed through the sum of ACEs of all control areas in the interconnection:

$$\sum_{n=1}^N ACE_n = \underbrace{\sum_{n=1}^N (I_{an} - I_{sn})}_{=0} - 10 \left(\underbrace{\sum_{n=1}^N B_n}_{B_s} \right) (F_a - F_s) = -10 B_s (F_a - F_s) \Rightarrow$$

$$F_a - F_s = \frac{1}{-10B_s} \sum_{n=1}^N ACE_n \quad (F.7)$$

Basic Equation linking ACE and interconnection frequency error

Using (F.6), the time error accumulated over period $P = [t - T, t)$:

$$\varepsilon = 60 \int_P (F_a - F_s) dt = -\frac{6}{B_s} \sum_{n=1}^N \int ACE_n dt = -\frac{6}{B_s} \sum_{n=1}^N \left(I_n - \frac{B_n}{6} \varepsilon \right) \Rightarrow \quad (F.8)$$

Area n contribution to the time error accumulated over period $P = [t - T, t)$ can be determined as n th component of (F.8):

$$\varepsilon_n = -\frac{6}{B_s} \left(I_n - \frac{B_n}{6} \varepsilon \right) \quad (F.9)$$

Accumulated primary inadvertent interchange:

$$ACE_n = (I_{an} - I_{sn}) - 10B_n \underbrace{(F_a - F_s)}_{= -\frac{1}{10B_s} \sum_{i=1}^N ACE_i \text{ according to (2.3)}} = (I_{an} - I_{sn}) + \underbrace{\frac{B_n}{B_s} \sum_{i=1}^N ACE_i}_{Y_n} \Rightarrow$$

$$I_n = \int_P (I_{an} - I_{sn}) dt = \int_P ACE_n dt - Y_n \sum_{i=1}^N \int_P ACE_i dt = \underbrace{(1 - Y_n) \int_P ACE_n dt}_{I_{nm}} - \underbrace{Y_n \sum_{i=1, i \neq n}^N \int_P ACE_i dt}_{I_{ni}} \Rightarrow$$

From the above equality and (F.9),

$$I_{nm} = (1 - Y_n) \int_P ACE_n dt = (1 - Y_n) \left(I_n - \frac{B_n}{6} \varepsilon \right) \quad (F.10)$$

The accumulated primary inadvertent interchange is energy. The offset term ATE_n to be added to ACE should compensate this accumulated energy within H hours:

$$I_{nm} + \Delta I_{nm} = (1 - Y_n) \int_t^{t+H} (ACE_n - ATE_n) dt = (1 - Y_n) \int_t^{t+H} ACE_n dt - \underbrace{(1 - Y_n) H \cdot ATE_n}_{\text{Compensation Energy}} \Rightarrow$$

$$(1 - Y_n) H \cdot ATE_n = I_{nm} \Rightarrow$$

$$\boxed{ATE_n = \frac{I_{nm}}{(1 - Y_n) H} = \frac{1}{H} \int_{t-T}^t ACE_n dt = \frac{T}{H} \text{avg}_T ACE_n} \quad (F.11)$$

A fundamental result here is that the ATE is proportional to the accumulated ACE as well as the average ACE observed over the period $P = [t - T, t)$.

Appendix G

Load, Wind, Solar Forecast Errors

Appendix G

Load, Wind, Solar Forecast Errors

G.1 Proof on the Correlation of the Forecast Errors

For the load forecasting errors ΔL_i of the BA, the standard deviation σ of the load forecast error for consolidated Balancing Authority (CBA) is calculated as:

$$\sigma^2(\sum_i \Delta L_i) = \sum_i \sigma_i^2(\Delta L_i) + 2 \sum_{i \neq j} [\rho_{ij} \sigma(\Delta L_i) * \sigma(\Delta L_j)] \quad (G.1)$$

where i is the BA index, ρ_{ij} is the correlation factor between any two BAs ($-1 \leq \rho_{ij} \leq 1$). The percentage standard deviation will be:

$$\sigma = \sigma_{\%} * \max(L) \quad (G.2)$$

So,

$$\begin{aligned} \sigma_{\%}^2 \left(\sum_i \Delta L_i \right) * \max^2 \left(\sum_i L_i \right) &= \sum_i \sigma_{\%}^2(\Delta L_i) * \max^2(L_i) + \\ &2 \sum_{i \neq j} \{ \rho_{ij} \sigma_{\%}(\Delta L_i) * \max(L_i) * \sigma_{\%}(\Delta L_j) * \max(L_j) \} \end{aligned} \quad (G.3)$$

Case 1: Assume 100% correlation, $\rho_{ij}=1$ and $\sigma_{\%}(\Delta L_i)=\text{constant}$, (worst scenario)

New CBA standard deviation,

$$\begin{aligned} \sigma_{\%} \left(\sum_i \Delta L_i \right) * \max \left(\sum_i L_i \right) &= \sum_i \sigma_{\%}(\Delta L_i) * \max(L_i) \\ \sigma_{\%CBA} &= \sigma_{\%}(\sum_i \Delta L_i) = \sigma_{\%}(\Delta L_i) * \frac{\sum_i \max(L_i)}{\max(\sum_i L_i)} \end{aligned} \quad (G.4)$$

For BA in the study year 2008,

$$\sum_i \max(L_i) \approx \max(\sum_i L_i) \quad (G.5)$$

Thus, in our first 3 scenario studies, it is assumed that

$$\sigma_{\%CBA} = \sigma_{\%}(\Delta L_i)$$

Therefore, the percentage standard deviation of the load forecast error of CBA equals the percentage standard deviation of the load forecast error of each participating BA.

Case 2: Assume zero correlation factor, $\rho_{ij}=0$ and $\sigma_{\%}(\Delta L_i)$ being the same for all BA. Zero correlation between BA's load forecast errors results in reduction of the CBA forecast error span due to the error diversity observed in this case.

New CBA std,

$$\sigma_{\%CBA}^2 = \sigma_{\%}^2(\sum_i \Delta L_i) = \sigma_{\%}^2(\Delta L_i) * \frac{\sum_i \max^2(L_i)}{\max^2(\sum_i L_i)} \quad (G.6)$$

$$\sigma_{\%CBA} = \sigma_{\%}(\Delta L_i) * \sqrt{\frac{\sum_i \max^2(L_i)}{\max^2(\sum_i L_i)}}$$

The last expression is used to recalculate the percentage standard deviation of the load forecast error of CBA to reflect zero correlation between BA's load forecast errors assumed in this scenario.

G.2 Truncated Normal Distribution

The Probability Density Function (PDF) of the doubly truncated normal distribution is expressed as follows.

For a random variable x, the probability density function of the normal distribution is

$$PDF_N(x) = \frac{1}{\sigma\sqrt{2\pi}} \exp\left(-\frac{(x-\mu)^2}{2\sigma^2}\right) \quad (G.7)$$

For a mean of $\mu = 0$ and a standard deviation of $\sigma = 1$, this formula simplifies to

$$\phi(x) = \frac{1}{\sqrt{2\pi}} \exp\left(-\frac{x^2}{2}\right) \quad (G.8)$$

which is known as the standard normal distribution.

Suppose the wind and solar forecast error $\varepsilon \sim N(\mu, \sigma^2)$ has a normal distribution and lies within the interval $\varepsilon \in [\varepsilon_{\min}, \varepsilon_{\max}]$, $-\infty \leq \varepsilon_{\min} < \varepsilon_{\max} \leq \infty$. Then ε has a truncation normal distribution with probability density function

$$PDF_{TND}(\varepsilon; \mu, \sigma, \varepsilon_{\min}, \varepsilon_{\max}) = \frac{\frac{1}{\sigma} \phi\left(\frac{\varepsilon - \mu}{\sigma}\right)}{\Phi\left(\frac{\varepsilon_{\max} - \mu}{\sigma}\right) - \Phi\left(\frac{\varepsilon_{\min} - \mu}{\sigma}\right)} \quad (G.9)$$

where $\phi(\cdot)$ is the probability density function of the standard normal distribution, $\Phi(\cdot)$ its cumulative distribution function, with the understanding that if $\varepsilon_{\max} = \infty$, then $\Phi\left(\frac{\varepsilon_{\max} - \mu}{\sigma}\right) = 1$. And if

$\varepsilon_{\min} = -\infty$, then $\Phi\left(\frac{\varepsilon_{\min} - \mu}{\sigma}\right) = 0$.

For the two side truncation:

$$avg(\varepsilon | \varepsilon_{\min} < \varepsilon < \varepsilon_{\max}) = \mu + \sigma \frac{\phi\left(\frac{\varepsilon_{\min} - \mu}{\sigma}\right) - \phi\left(\frac{\varepsilon_{\max} - \mu}{\sigma}\right)}{\Phi\left(\frac{\varepsilon_{\max} - \mu}{\sigma}\right) - \Phi\left(\frac{\varepsilon_{\min} - \mu}{\sigma}\right)} \quad (G.10)$$

$$std^2(\varepsilon | \varepsilon_{\min} < \varepsilon < \varepsilon_{\max}) = \sigma^2 \left[1 + \frac{\frac{\varepsilon_{\min} - \mu}{\sigma} \phi\left(\frac{\varepsilon_{\min} - \mu}{\sigma}\right) - \frac{\varepsilon_{\max} - \mu}{\sigma} \phi\left(\frac{\varepsilon_{\max} - \mu}{\sigma}\right)}{\Phi\left(\frac{\varepsilon_{\max} - \mu}{\sigma}\right) - \Phi\left(\frac{\varepsilon_{\min} - \mu}{\sigma}\right)} - \left(\frac{\phi\left(\frac{\varepsilon_{\min} - \mu}{\sigma}\right) - \phi\left(\frac{\varepsilon_{\max} - \mu}{\sigma}\right)}{\Phi\left(\frac{\varepsilon_{\max} - \mu}{\sigma}\right) - \Phi\left(\frac{\varepsilon_{\min} - \mu}{\sigma}\right)} \right)^2 \right] \quad (G.11)$$

G.3 Clearness Index (CI)

If the sky is clear, the solar radiation and the solar power production are completely predictable based on the annual and daily extraterrestrial patterns and the forecast errors are close to zero. The solar radiation and generation forecast errors are mostly caused by clouds and other factors. These factors include: clouds (depth, water or ice concentration, types of water particles or ice crystals), water vapor amount, and aerosol type and amount (column) [61].

The clearness index is an index showing to what percentage of the sky is clear. Therefore, CI can be used for solar power generation forecasting. High CI could mean higher global solar radiation (i.e., global solar radiation levels being closer to their extraterrestrial values) and lower forecast errors.

The CI for a given period is obtained by dividing the observed global radiation R_g by the extraterrestrial global irradiation R :

$$CI = R_g/R \quad (G.12)$$

where R_g is the horizontal global solar radiation, R is horizontal extraterrestrial solar radiation.

Extraterrestrial solar radiation R can be calculated using the following equation [13]:

$$R = 117.5 [h \sin(\lambda) \sin(\delta) + \cos(\lambda) \cos(\delta) \sin(h)] / \pi \quad (G.13)$$

where δ is solar declination angle (radians), λ is the latitude (radians), h is the half-day length (radians) given by the following equation:

$$h = \cos^{-1}(-\tan(\lambda) \tan(\delta)) \quad (G.14)$$

δ can be calculated as a function of the day of the year (DOY) [61]

$$\delta = \sin^{-1}[0.39785 \sin(4.689 + 0.0172 * DOY + 0.03345 \sin(6.224 + 0.0172 * DOY))] \quad (G.15)$$

In different days, the daily distributions of CI have different patterns. In [22], it is shown that the PDF of CI can have a bimodal distribution. Bimodality of the distribution in a sample is a strong indication that the distribution is not normal.

If there is a lack of the global solar radiation and extraterrestrial solar radiation profiles, the solar generation profiles in terms of actual solar generation and ideal solar generation can be used to calculate approximately the CI by:

$$CI = \frac{\text{Actual Solar Generation}}{\text{Ideal Solar Generation}} \quad (\text{G.16})$$

The ideal solar generation is the maximum power output a solar plant can reach during a day period of time. If the actual solar generation profile and ideal solar generation profile are in minute by minute resolution, the CI is calculated by:

$$CI(t) = \frac{P_a(t)}{P_{\max}(t)}, (t = 1, \dots, n) \quad (\text{G.17})$$

where $Pa(t)$ is actual solar generation at the t -th minute, and $Pmax(t)$ is the ideal solar generation at the t -th minute. $CI(t)$ is used in the real-time and hour-ahead solar generation forecast error models. The values of clearness index will be in the range of $[0, 1]$. In perfect sunny minutes, the CI is 1 (or very close to 1). In heavily cloudy minutes, the CI will be 0 (or very close to 0).

G.4 Real-time Solar Forecast Model

The following steps are applied to the new model:

1. Calculate the CI at 7.5 minutes prior to the current minute:

$$CI(t - 7.5) = \frac{P_a(t - 7.5)}{P_{\max}(t - 7.5)} \quad (\text{G.18})$$

2. Calculate the mean value of actual power generation in current 5 minute interval:

$$\bar{P}_a(t : t + 5) = \frac{\sum_{i=t}^{t+5} P_{ai}}{5} \quad (\text{G.19})$$

3. Calculate the mean value of idea (maximum) power generation in current 5 minute interval:

$$\bar{P}_{\max}(t : t + 5) = \frac{\sum_{i=t}^{t+5} P_{\max i}}{5} \quad (\text{G.20})$$

4. Real-time solar generation forecast in current 5 minute interval is calculated by:

$$f_{RT}(t : t + 5) = CI(t - 7.5) \times \bar{P}_{\max}(t : t + 5) = \frac{P_a(t - 7.5)}{P_{\max}(t - 7.5) \times \bar{P}_{\max}(t : t + 5)} \quad (\text{G.21})$$

5. Apply 5 minute ramp on the real-time solar forecast f_{RT} .

G.5 Hour-ahead Solar Forecast Error Model

The following procedure is applied to generate hour-ahead solar forecast errors:

1. Calculate hourly average CI using (1.20).
2. Assign a level number (1, 2, 3, or 4) to each hourly average CI based on its value for form a level number sequence.
3. Generate random number sequences for different CI levels (4 levels in total) based on the standard deviation for different CI levels (using Table 2.1). The TND is applied to the random number sequences.
4. Assign the generated random numbers to the hourly average CI. The level number sequence is use to select which random number sequences are used.

Distribution

**No. of
Copies**

Name
Organization
Address
City, State and ZIP Code

Organization
Address
City, State and ZIP Code
Name
Name
Name
Name
Name (#)

Name
Organization
Address
City, State and ZIP Code

**No. of
Copies**

Foreign Distribution

Name
Organization
Address
Address line 2
COUNTRY

Local Distribution

Pacific Northwest National Laboratory
Name Mailstop
Name Mailstop
Name Mailstop
Name Mailstop
Name (PDF)



Pacific Northwest
NATIONAL LABORATORY

*Proudly Operated by **Battelle** Since 1965*

902 Battelle Boulevard
P.O. Box 999
Richland, WA 99352
1-888-375-PNNL (7665)

www.pnl.gov



U.S. DEPARTMENT OF
ENERGY